UNIVERSITY OF SOUTHAMPTON

EXPRESSION AND INHIBITOR STUDIES OF Ca^{2+}-ATPases

By

MELANIE JANE LOGAN-SMITH

A thesis presented for the degree of

Doctor of Philosophy

Department of Biochemistry

University of Southampton

U.K.

March 2001

UNIVERSITY OF SOUTHAMPTON

ABSTRACT

FACULTY OF SCIENCE
DEPARTMENT OF BIOCHEMISTRY

Doctor of Philosophy

EXPRESSION AND INHIBITOR STUDIES OF Ca^{2+}-ATPases

By Melanie Jane Logan-Smith

Many compounds inhibit the function of the Ca^{2+}-ATPase of the sarcoplasmic reticulum (SERCA). These are generally hydrophobic compounds containing -OH groups. Curcumin is shown to be an inhibitor of the Ca^{2+}-ATPase. Studies of the effects of mixtures of inhibitors show that 2,5-di(propyl)-1,4-benzohydroquinone and 2,5-di(*tert*-butyl)-1,4-benzohydroquinone (BHQ) bind to the same site on the ATPase, but that the binding site for BHQ is separate from that for butylatedhydroxy toluene, ellagic acid, diethylstilbestrol (DES), curcumin and nonylphenol, and that the binding site for curcumin is separate from that for ellagic acid and DES. The presence of BHQ, DES, ellagic acid and nonylphenol increase the affinity of the ATPase for curcumin, suggesting that binding of one inhibitor results in a change in the ATPase to a conformation with higher affinity for the second inhibitor. In QT-6 cells curcumin prevents the release of calcium normally seen on addition of the Ca^{2+}-ATPase inhibitor trilobilide, suggesting that curcumin blocks the inositol sensitive calcium release channel (IP_3R). In sarcoplasmic reticulum it was shown that curcumin reduces the rate of slippage on the Ca^{2+}-ATPase and so increases calcium accumulation into SR vesicles, despite being an inhibitor of ATPase function. SERCA and SERCA-GFP have been expressed in Cos-7 cells. A chimera between SERCA and a Ca^{2+}-ATPase from *Heliothis virescens*, HVSERCA, showed higher levels of expression in Cos-7 cells than HVSERCA. SERCA and HVSERCA have been expressed in *S.cerevisiae* and comparative inhibitor studies using this system have shown that trilobilide inhibits SERCA but not HVSERCA, whereas BHQ inhibits both of these pumps.

Acknowledgements

Well folks, I got there! I wouldn't have however without the supervision from my boss Prof. A. G. Lee, who pushed, er, guided me throughout. Dr Malcolm East has helped me no end with all the molecular biology and the questions I daren't ask Tony.

Thanks also go to Dr Marc Le Maire who provided me with the Y18 SERCA1a construct, Dr Wolfram Hänsel for the curcumin analogues, Dr John Chad for the confocal help and useful discussions. Drs Lorraine Williams and Jon Pittman kindly got me started with the yeast and to Dr Mike Gore, who nearly poisoned me with an egg sandwich! Maureen and Bridget in the Biochem Office have also been really helpful and many other people in the department, thanks. All the folks at Zeneca were really good whilst I was there, and thanks must also go to my supervisor there, Dr Fergus Earley.

The Lee/East group past and present..., have...well without them I'd probably have finished in two years flat! Thanks go especially to Dr Small (and Helena),Willy, Wendy, John, the "fool" Sue and Ash (maybe my bench could have been further away though, to avoid the scientific shrapnel of this particular type of research). Thanks also to The Wilton group, Andy, Jo and Susie in particular. Many, many superb memories (except the rum filled ones for some reason).

Special thanks are reserved for all my family. Especially to my Mum and Dad who have encouraged me throughout, and to Adrian & Jane (the cocktails of whom have killed too many of my brain cells to remember!). Finally the biggest, most humungous, most whopping thanks and love is for Adam, ta Smithy, for everything.

"We must keep open minds, but not so open that our brains fall out"

Prof. S Hawkins

This is for you, Adam

CONTENTS

Chapter Three: Inhibitor Studies on SR Ca^{2+}-ATPase

PAGE

Chapter Four: Effect of Ca^{2+}-ATPase Inhibitors on Uptake and Release of Calcium

PAGE

Chapter Five: Expression of Ca^{2+}-ATPases in Cos-7 cells

Chapter Six: Expression of Ca^{2+} -ATPases in Yeast

PAGE

PAGE

List of Figures

Chapter One

Chapter Three

PAGE

Chapter Four

PAGE

Chapter Five

Chapter Six

PAGE

List of Tables and Schemes

Chapter One

Chapter Three

Chapter Four

Abbreviations

ADP	Adenosine diphosphate
ATP	Adenosine triphosphate
BCA	Bicinchoninic acid
BHT	Butylatedhydroxy toluene
BHQ	2,5-di(*tert*-butyl)-1,4-benzohydroquinone
BSA	Bovine serum albumin
Ca^{2+}-ATPase	Ca^{2+} and Mg^{2+} activated ATPase
$C_{12}E_8$	Dodecylpoly(ethyleneglycolether)
CICR	Calcium induced calcium release
cADP	cyclic adenosine diphosphate
cDNA	complementary DNA
DABCO	1,4-Diazabicyclo[2.2.2]octane
DAG	Diacylglycerol
DES	Diethylstilbestrol
DHPR	Dihydropyridine receptor
DOPC	Dioleoylphosphatidylcholine
DTT	Dithiothrietol
ECL	Enhanced chemiluminescence
EDTA	Ethylenediamine tetraacetic acid
EGTA	Ethyleneglycol-bis(β-aminoethylether)-N,N,N',N'-tetraacetic acid
ER	Endoplasmic reticulum
FCCP	Carbonyl cyanide p-(triflouromethoxy) phenylhydrazone
FITC	Fluorescein-5'-isothiocyanate
FSBA	5'-(*p*-fluorosulfonyl)-benzoyl-adenosine
GFP	Green fluorescent protein
HAD	Haloacid dehydrogenase
HEPES	N-92-(hydroxyethyl)piperazine-N'-(2-ethanesulphonic acid)
HVSERCA	*Heliothis virescens* SR Ca^{2+}-ATPase
HRP	Horseradish peroxidase
IP_3	Inositol (1,4,5)-trisphosphate
IP_6	Inostiol hexakisphosphate
IP_3R	IP_3 sensitive calcium release channel

kb	Kilobase
kDa	Kilodalton
LDH	Lactate dehydorgenase
MOPS	3-(N-morpholino)propanesulphonic acid
NADH	β-Nicotinamide adenine dinucleotide (reduced form)
NBD	4-Nitrobenzo-2-oxa-1,3-diazole
NP	Nonylphenol
OD	Optical density
OG	n-Octyl β-D-glucopyranoside
PCR	Polymerase chain reaction
PEP	Phosphoenol pyruvate
PHQ	2,5-di(propyl)-1,4-benzohydroquinone
P_I	Inorganic phosphate
PIPES	Piperazine-N,N'-bis(2-ethanesulfonic acid)
PK	Pyruvate kinase
PKC	Protein kinase C
PIPES	Piperazine-N,N'-bis(2-ethanesulfonic acid)
PLC	Phospholipase C
PMSF	Phenylmethylsulphonylfluoride
PMCA	Plasma membrane Ca^{2+}-ATPase
PBS	Phosphate buffered saline
RyR	Ryanodine receptor
SC	Synthetic complete
SDS	Sodium dodecyl sulphate
SERCA	Sarco(endo)plasmic reticulum Ca^{2+}-ATPase
SR	Sarcoplasmic reticulum
TAE	Tris – acetate EDTA buffer
Tb	Trilobilide
Tg	Thapsigargin
TNP-AMP	2',3'-o-(2,4,6-trinitrophenyl)-AMP
Tris	Tris(hydroxymethyl)aminomethane
Triton X-100	Octylphenolpoly(ethyleneglycolether)
T-tubule	Transverse tubules
TRP	Transient receptor potential

Chapter One: General Introduction

1.1. Introduction

1.1.1. Calcium – A ubiquitous messenger

Calcium is a uniquely important intracellular messenger. The reason favouring this divalent calcium ion rather than others is related to its ability to complex reversibly with proteins (Brini & Carafoli, 2000). Its high selectivity of binding permits interaction with negatively charged oxygen atoms of residues (the side chains in glutamate and aspartate) and uncharged oxygens (main chain carbonyls and the side chains in glutamine and asparagine). By co-ordinating multiple ligands calcium can cross link different segments of a protein and induce the conformational changes necessary for the function of calcium binding proteins (Clapham, 1995). Calcium has the ability to act within subcellular compartments or globally across the whole cytosol, with its effects occurring from within microseconds to hours. However, uncontrolled changes in calcium levels can have harmful effects on cell structure and function (Clapham, 1995).

Resting cytosolic levels of calcium ($[Ca^{2+}]_c$) are of the order of 0.1 μM (Brini & Carafoli, 2000) and the maintenance of very low $[Ca^{2+}]_c$ is necessary for proper function. Transient increases in calcium concentration, via the activation of extracellular calcium entry pathways and intracellular release from stores, raises $[Ca^{2+}]_c$ by 10 to 100 fold. An extensive range of cellular processes ensue including short-term contraction and secretion events, and longer-term changes such as cell motility, growth, proliferation and differentiation (Berridge *et al.*, 1998). Restoration of the resting calcium levels is important. The calcium ion cannot be metabolised like other cellular messengers and prolonged raised $[Ca^{2+}]_c$ can trigger complex cytotoxic and apoptotic responses (Clapham, 1995). The removal of calcium from the cell cytoplasm is thus important to maintain cell equilibrium. Ionic exchange by the Na^+/Ca^{2+} exchanger, and the active removal (by Ca^{2+}-ATPases) of calcium from the cytoplasm out through the plasma membrane and into internal stores completes the signalling process. With a 10 000 fold gradient between the extracellular space and the cytosol, the plasma membrane provides a crucial barrier to maintain cell

integrity. The maintenance of low $[Ca^{2+}]_c$ is thus imperative if calcium is to fulfil its role.

Calcium is actively sequestered into the endoplasmic reticulum (ER) of cells. The ER is a comprehensive membrane enclosed system that provides and regulates cellular signalling pathways. The ER serves as a readily mobilisable store of calcium and employs calcium pumps and buffer proteins to aid in the accumulation of calcium. Buffer proteins such as calsequestrin have no known function other than to store calcium. On the other hand, trigger proteins such as membrane-bound enzymes and soluble kinases, proteases and calmodulin, undergo a conformational change upon binding calcium (Clapham, 1995). The actual structure and function of the ER is influenced by cellular signals that are not yet fully understood (Putney & Pedrosa Ribeiro, 2000). When calcium levels are increased and sustained, the ER structure undergoes changes and fragments (Putney & Pedrosa Ribeiro, 2000). This could possibly be a physiological mechanism through which the calcium and protein kinase-C pathways influence and regulate ER structure (Putney & Pedrosa Ribeiro, 2000). Recently, Corbett and Mickalak (Corbett & Michalak, 2000) suggested that calcium could actually function as a signalling molecule within the ER itself, as it is known to control functions of the ER such as synthesis and secretion of proteins (Sambrook, 1990) and regulation of chaperone interactions (Corbett *et al.*, 1999).

Calcium can be rapidly mobilised for signalling purposes by entry across the plasma membrane via ligand operated calcium channels (LOCs) or voltage operated calcium channels (VOCs), or by release from the ER. The di-hydropyridine receptor (DHPR) is an example of a VOC (Section 1.1.3). The LOCs include the second messenger operated calcium channels (SMOCs), which depend on second messengers such as inositol phosphates (Berridge, 1993), cADP ribose (Clapper *et al.*, 1987; Galione & White, 1994) and calcium itself (Leung *et al.*, 1994; Berridge, 1995) to control the release from internal stores (see below). Also, the store operated calcium channels (SOCs), additionally known as calcium release activated channels (CRACs, see below), are activated by calcium (Fasolato *et al.*, 1994).

1.1.2. The IP_3 second messenger pathway (involving SMOCs)

In non-excitable cells (e.g. hepatocytes, endothelia), the inositol (1,4,5)-trisphosphate (IP_3) second messenger mediated pathway (Berridge, 1993) controls

release of calcium from the ER for signalling purposes (Figure 1.1). This release can involve two receptor coupled signalling pathways; the G protein coupled receptors and the tyrosine kinase receptors (Berridge, 1993). The G proteins are coupled to receptors consisting of 7-transmembrane helices that can be activated by a range of agonists (Berridge, 1993). Stimulation of either receptor leads to the activation of phospholipase-C (PLC). PLCs hydrolyse phosphatidylinositol 4,5-bisphosphate (PIP_2) yielding diacylglycerol (DAG) and IP_3, two-second messengers. DAG recruits and docks the cytosolic protein kinase C (PKC) onto the plasma membrane and protein phosphorylation ensues. IP_3 binds to the IP_3 receptor (IP_3R) residing in the ER, which results in calcium release from the store. Calcium release is also mediated by voltage-dependent Ca^{2+} channels in cellular stores. This applies to the excitation-contraction coupling process.

1.1.3. Excitation-contraction coupling (involving VOCs)

The contraction of fast twitch skeletal muscle is regulated by "spikes", i.e. transient changes in cytosolic calcium concentrations (Ebashi, 1991). In striated muscle cells contraction is brought about by an action potential, generated by a motor neurone (Figure 1.2). When this impulse reaches the muscle cell the sarcolemma (plasma membrane) depolarises and the action potential is propagated along the membrane via invaginations in the membrane called transverse (T) tubules. The di-hydropyridine receptor (DHPR), an L type VOC (Guo *et al.*, 1994), contained in this membrane "senses" the change in membrane potential and undergoes a change in conformation. This in turn is transmitted to the ryanodine sensitive Ca^{2+}channel in the neighbouring sarcoplasmic reticulum (Takeshima *et al.*, 1989; Mcpherson & Campbell, 1993). The sarcoplasmic reticulum (SR) lies 10 – 20 nm from the T tubule system and is a specialised form of the endoplasmic reticulum (ER) located in skeletal muscle. Each T-tubule forms a junction with two terminal cisternae regions of the SR, forming a triad junction. The membrane of the T-tubule containing the DHPR contacts with the RyR in the SR membrane of skeletal muscle, forming this junction (Leong & MacLennan, 1998). These two receptors are thus directly coupled in skeletal muscle through protein-protein interactions. The ryanodine receptor is gated by electromechanical coupling to the DHPR and consequently opens, releasing calcium through the channel (Clapham, 1995). This

calcium binds to troponin C (a calcium-sensing component), which then mediates the actions of actin and myosin. The interaction between these three components leads to a shortening of the overall myofibril length, resulting in muscle contraction. Thus contraction is brought about by a rapid rise in cytosolic calcium levels and relaxation succeeds after the rapid removal of this calcium. The SR compartments occupy approximately 1 to 5 % of the volume of mammalian skeletal muscle cells and through the release of Ca^{2+} provide a mechanism via which muscle function is regulated.

In cardiac cells, the process is slightly different (Figure 1.2, insert). Protein contact is not involved between the DHPR and the RyR. Depolarisation of the membrane opens the VOC. This lets calcium into the cell, which in turn stimulates the release of stored calcium from the SR. This is known as calcium induced calcium release (CICR). In non-muscle cells, CICR is the basis for regenerative calcium waves mediated through IP_3R (Berridge, 1993).

1.1.4. Calcium release and entry

Two well-characterised calcium channels reside in the ER/SR calcium pools namely the IP_3R and the RyR. These release channels are responsible for the initial phase of stored calcium liberation, upon agonist or electrical stimulation respectively. The IP_3R and the RyR are distantly related and share both structural and functional homologies. These are the largest ion channel proteins known (refer to (Taylor, 1998) for a recent review).

The IP_3R is a tetrameric receptor spanning the ER membrane; each subunit is ~310 kDa in size. A multigene family encodes the IP_3R and alternative splicing creates further isoform diversity. Three mammalian receptor subtypes with approximately 70 % identity exist. IP_3R1 is mainly expressed in the brain, IP_3R2 in the liver, lung, skeletal muscle spleen and testis whilst IP_3R3 is located mainly in epithelial and secretory cells. The overall expression differs from cell to cell and the presence of more than one isoform in a tissue can give rise to heterotetrameric proteins (Hirota *et al.*, 1995; Mankawa *et al.*, 1995; Wajcikiewicz *et al.*, 1995). The homo- and hetero-tetramers differ in their affinity for IP_3 (Taylor, 1998; Vanlingen *et al.*, 2001). Each subunit binds one IP_3 molecule in a negatively charged Arg/Lys rich N terminal region that can be blocked by heparin (Ghosh *et al.*, 1988). The large

central cytosolic domain modulates IP_3 binding to channel gating, with the C terminus of the receptor forming the transmembrane calcium channel. The IP_3R are regulated in many ways, by phosphorylation (Wojcikiewicz & Luo, 1998), by adenine nucleotides (Bezprozvanny & Ehrlich, 1993), by FK506 binding proteins (FKBP) (Cameron *et al.*, 1995), by immunosuppressive drugs and additionally can be desensitised by IP_3 itself (Taylor & Traynor, 1995). Calcium can also regulate the sensitivity of the IP_3R to IP_3, with the calcium binding site only becoming accessible after IP_3 binding (Joseph, 1996; Taylor, 1998).

In cardiac cells calcium entering through VOCs activate the RyR, or in skeletal muscle the electromechanical coupling of the DHPR to the RyR directly modulates the calcium release (Mcpherson & Campbell, 1993). The RyR is a tetramer of 4 subunits, ~560 kDa in size and is modulated by small molecules: Mg^{2+}, ATP, Ca^{2+}, cADP ribose and nitric oxide (Zucchi & Ronca-Testoni, 1997) and larger proteins such as calmodulin and FKBPs (Mackrill, 1999). Ruthenium red (Antoniu *et al.*, 1985; Jianjie, 1993) and ryanodine (Meissner, 1986; Michalak *et al.*, 1988; McGrew *et al.*, 1989) are specific inhibitors of this release channel. The RyR can be directly activated by calcium and at higher concentrations than those required to regulate the IP_3R (Bezprozvanny *et al.*, 1991). Whilst the RyR is non-selective for cations, it excludes all anions. Three separate genes encode the RyRs and the isoforms are differentially expressed: RyR1 in the skeletal muscle; RyR2 is the cardiac isoform; RyR3 is expressed in the brain (Stokes & Wagenknecht, 2000). The homotetramer exists in the skeletal muscle but heterotetramers, like the IP_3R may be formed. The N terminus of the RyR exists in the cytoplasm, with four transmembranous domains at the C terminus.

Differential expression of the release channels in different cell types, along with the isoform diversity and the vast array of regulatory processes introduces an undefined range of specific cellular responses, which will ultimately result in tissue specific calcium signals. It is this huge range of signals that makes calcium such a versatile signalling molecule. Furthermore the regenerative calcium signalling of these two receptors gives rise to the characteristic oscillations and waves, propagating the calcium signal (Clapham, 1995).

So, the primary release phase of calcium is from the internal stores. A secondary phase in order to maintain a prolonged elevation of calcium and to replenish stores is also implemented and this is activated upon store depletion

(Berridge, 1995; Clapham, 1995). This is known as store operated calcium entry (SOC) or capacitative calcium entry (CRAC). Putney first described this mechanism that was stimulated by IP_3, ionomycin and Ca^{2+}-ATPase inhibitors in 1986 and named the current I_{CRAC} (Putney, 1986). This phase of calcium influx occurs upon depletion of the calcium stores, which triggers calcium entry across the plasma membrane. The questions of how ER calcium store depletion is coupled with calcium entry and the components involved in this mechanism are still being answered. Substantial evidence exists regarding the protein present in the plasma membrane, through which calcium enters. A transient receptor potential (TRP) protein in the plasma membrane initially identified in *Drosophila* mutants (Hardie & Minke, 1993) has been identified in vertebrate cells and implicated in the SOC pathway. Although the experiments with over-expression of TRP are unclear due to changes in the basal plasma membrane permeability (Zhu *et al.*, 1998), Zhu *et al.* (Zhu *et al.*, 1996) transfected cells with an antisense sequence against all the known TRP proteins, and this did successfully block the capacitative calcium entry.

The exact nature of the interaction between the stores and this TRP protein are less clear. A direct docking process of the IP_3R (in the ER) with the TRP protein has been suggested, Figure 1.1 (Irvine, 1990). This is analogous to the physical coupling between the DHPR and the RyR in cardiac muscle. However, after disruption of the physical contacts between the plasma membrane and the intracellular organelles there is still a current measured (Parekh *et al.*, 2001). This could however be a calcium-activated current and not SOC (Yao *et al.*, 1999). Substances such as p450 (Alvarez *et al.*, 1991), cGMP (Xu *et al.*, 269) or calcium influx factor, CIF (Randriamampita & Tsien, 1993; Csutora *et al.*, 1999) are all possible candidates for a signalling molecule that may diffuse to the plasma membrane and activate the channels. Finally inositol phosphate mediated signalling could be involved (Irvine, 1990; Irvine, 1992; Striggow & Bohnensack.R., 1994). Inositol phosphate sensitive channels in the plasma membranes of jurkat cells (Khan *et al.*, 1992), lymphocytes (Kuno & Gardner, 1987) and rat parotid cells (Tanimura *et al.*, 2000) have been identified and this could possible be a mechanism employed by some cell types to refill intracellular stores.

1.1.5. Calcium removal

After the signalling process, the reduction of the elevated $[Ca^{2+}]_c$, back to the resting levels is critical. Calcium may be extruded across the plasma membrane into the extracellular space or it can be pumped back into the ER/SR calcium stores. In muscle cells, calcium removal brings about muscle relaxation.

For the extrusion of calcium two active processes exist in the plasma membrane. The plasma membrane Ca^{2+}-ATPase (PMCA) is a member of the P-type ATPase family (Carafoli, 1994). This is a high affinity, low capacity pump. Calmodulin modulates this pump at the C terminus and when this binding protein is not complexed PMCA has the same affinity as the Na^+/Ca^{2+} exchanger in this membrane. The Na^+/Ca^{2+} exchanger has a low affinity and a large capacity for calcium and for each calcium ion removed, three sodium ions are exchanged. This is particularly effective in excitable cells that need to eject large quantities of calcium. In muscle cells PMCA plays a minor role, with the sarco(endo)plasmic reticulum Ca^{2+}-ATPase (SERCA) pump of the P type class (see below) removing most of the cytosolic calcium aided by the exchanger.

1.2. P-type ion pumps

This group of ion pumps from eukaryotes and bacteria are so called due to the formation of a phosphorylated intermediate during their catalytic cycle (de Meis & Vianna, 1979). Their function is to facilitate the active transport of cations across membranes by utilising the chemical energy acquired from the hydrolysis of the terminal phosphate of ATP. A phosphoryl-aspartyl intermediate of the enzyme is formed during the cycle and subsequently broken down (Moller *et al.*, 1996). The protein may be described as existing in one of two conformational states, E1 and E2. It is the conformational change between these two states that is responsible for the active transport of ions (Jencks, 1989). In the case of the Ca^{2+}-ATPase, the overall process concentrates calcium in reticular stores (generating a transmembrane concentration gradient) from which it may be mobilised when required.

The P-type ATPase family of pumps have recently been analysed (Axelsen & Palmgren, 1998) and grouped into five distinct sets as shown in Table 1.1. This is based on the analysis of eight highly conserved regions (core sequences), which were

used to construct phylogenetic trees. The groups were organised according to known substrate specificity and not according to the evolutionary distance between parental species. The Ca^{2+}-ATPases group as type II and further divide into the non-calmodulin stimulated type IIA pumps, and the calmodulin stimulated type IIB pumps. The type IIA group mainly contains the SERCA type pumps but also include a plant vacuolar/plasma membrane pump, and likewise the IIB mainly contain the PMCA type pumps in addition to pumps present in the vacuolar membrane. Interestingly, the type IIA Ca^{2+}-ATPases exist in bacteria whereas the type IIB do not and the authors suggest the type IIB pumps may be the result of a more recent evolutionary event (Axelsen & Palmgren, 1998). Group V are at present, poorly characterised, having no assigned substrate specificity. In fact many of the groups contain ATPases that have not yet been fully characterised. All the P-type pumps consist of a large polypeptide chain, function via the formation of a phosphorylated intermediate and exhibit sensitivity to vanadate (Fagan & Saier, 1994). Many of these pumps have now been sequenced which facilitates analysis and comparison of their structures and specific functions.

1.2.1. The sarco (endo) plasmic reticulum Ca^{2+}-ATPase (SERCA)

The sarco(endo)plasmic reticulum Ca^{2+}-ATPase pumps constitute a family of highly homologous enzymes responsible for the sequestration of cytoplasmic calcium into cellular compartments. This is a multigene family, encoded by three distinct genes: SERCA1, 2 and 3. SERCA1 is expressed in the fast twitch skeletal muscle. Alternative splicing of the gene product yields two isoforms, SERCA1a and SERCA1b (Brandl *et al.*, 1986). The difference is the presence of an extra 7 amino acids at the C terminus of SERCA1b, which is expressed in neonatal tissue, compared to the former that is expressed in adult tissue. SERCA2 also has two isoforms: SERCA2a is expressed in slow twitch skeletal, cardiac and smooth muscle whilst SERCA2b is expressed in smooth muscle and virtually all non-muscle tissues (Lytton & MacLennan, 1988). SERCA3 (Burk *et al.*, 1989) is expressed in various tissues such as the large intestine, spleen, heart, brain and stomach. Recently, alternative splicing of SERCA3 has been documented giving the isoforms SERCA3a, 3b and 3c (Dode *et al.*, 1998).

The SR Ca^{2+}-ATPase is an asymmetrically orientated membrane protein resident in the SR. It is composed of a single 110 kDa polypeptide chain (MacLennan, 1970; Andersen, 1989), with most of the cellular mass on the cytoplasmic side of the membrane. This Ca^{2+}-ATPase, which was first isolated from skeletal muscle in 1970 by MacLennan (MacLennan, 1970), belongs to the class of P type ion motive pumps. The hydrolysis of the terminal phosphate bond of ATP provides the energy required to move cations across the membrane.

1.2.2. The reaction cycle of SERCA

The mechanism of the Ca^{2+}-ATPase can be described in terms of the E2-E1 model, originally proposed by de Meis and Vianna, in 1979 (de Meis & Vianna, 1979), shown in Figure 1.3. This is based on the assumption of two distinct functional states, E1 and E2. In the E1 conformation two high affinity Ca^{2+} binding sites exposed to the cytoplasm are present whereas in the E2 conformation the ATPase can no longer bind calcium from the cytoplasmic side. The binding of two calcium ions to E1 facilitates phosphorylation by ATP forming $E2PCa_2$, a β-aspartyl phosphate intermediate, the only phosphoenzyme intermediate with calcium bound (Myung & Jencks, 1995). The two bound calcium ions can be released from $E2PCa_2$ to the lumenal side of the membrane. Release of calcium from these gives E2P, which can then dephosphorylate and return the enzyme to the E1 conformation. ATP can only phosphorylate the ATPase when in the E1 state with two Ca^{2+} ions bound. Hence, the switch in reactivity of the ATPase between E1 and E2 is linked to the change in accessibility of the Ca^{2+} binding sites. The ATPase translocates 2 Ca^{2+} ions into the lumen of the SR for each molecule of ATP hydrolysed (Inesi *et al.*, 1980).

1.2.3. The structure of SERCA

The partial primary structure of the sarcoplasmic reticulum ATPase (SERCA) was initially determined by protein sequencing (Allen *et al.*, 1980). The entire cDNA was subsequently sequenced and the rabbit SR Ca^{2+}-ATPase fully cloned by MacLennan *et al.* in 1985 (MacLennan *et al.*, 1985). Until recently structural information on the Ca^{2+}-ATPase was restricted because suitable crystals for X-ray

diffraction were unobtainable. Toyoshima *et al.*, in 1993, initially derived valuable information regarding the structure of SERCA in the membrane from cryo-electron microscopy of tubular crystals, to 14 Å resolution (Toyoshima *et al.*, 1993). These ice embedded crystals enabled evaluation of the dimensions (total height 120 Å) and distribution of the ATPase (70% cytoplasmic, 25% membranous and 5% lumenal (Mintz & Guillain, 1997). The information was interpreted in terms of the tertiary structure model of the ATPase (Green & Stokes, 1992) giving a predicted 3 dimensional representation of the enzyme containing ten transmembrane helices (Toyoshima *et al.*, 1993), Figure 1.4 A. Hydropathy plots (MacLennan *et al.*, 1985) and crystallographic analyses (Stokes *et al.*, 1994) indicated the presence of ten transmembrane α-helices (M1-M10) with the majority of the extra-membranous mass in the cytoplasm. Antibody studies supported the concept of the 10 transmembrane α-helices model (Clarke *et al.*, 1990; Matthews *et al.*, 1990), which shows that the residues between Lys-870 and Ile-890 (the loop between transmembrane α-helix M7 and M8) were on the lumenal side of the membrane. A better 8 Å resolution structure was produced in 1998 (Zhang *et al.*, 1998). Early in 2000, Toyoshima *et al.* solved the crystal structure of SERCA to 2.6 Å, Figure 1.5 (Toyoshima *et al.*, 2000). The crystals were obtained at pH 6.0 in the presence of calcium and the detergent $C_{12}E_8$ and hence represent the $E1Ca_2$ conformation of the enzyme. This has finally permitted, after years of study, the interpretation of kinetic and mutagenic studies. Ten transmembrane α-helices are indeed present, with helix 5 (M5) ~60 Å in length looking like the central mast of the protein, extending from the lumen through to the cytoplasmic portion. The less hydrophobic stalk sections, which contain a high proportion of charged residues (particularly Glu and Asp), are represented as extension of the transmembrane helices and on M5 this is an additional 41-residue α-helix, extending into the cytosol. The secondary structure predictions (Figure 1.4 B) suggested the presence of five α-helix stalk sections connecting the transmembrane segments with the rest of the protein in the cytosol (MacLennan *et al.*, 1985), but in fact only four exist above M2 to M5 with no predicted stalk above M1 (Figure 1.6).

The cytoplasmic headpiece may be divided into three domains, designated A, N and P (Figure 1.5). The A domain (previously called the β strand domain) is the smallest domain (~16k) which has an anti-parallel β structure (Green & Stokes, 1992). This domain is almost isolated from the rest of the structure and is connected

to the transmembrane region by three long loops. The 145 residues of the A domain lie between M2 and M3 on the cytosolic side, with residues 1 to 50 before transmembrane helix M1. Trypsin cleavage at Arg-198 (indicated in Figure 1.5) is increased by calcium and blocked by phosphorylation (Andersen *et al.*, 1986). This suggests that cleavage is conformation sensitive with the domain moving during calcium transport. Török *et al.* (Torok *et al.*, 1988) stated that tryptic cleavage inhibited but did not uncouple the Ca^{2+}-ATPase. However, the results from Cao *et al.*(Cao *et al.*, 1991) showed that this was not the case.

The P (phosphorylation) domain at the centre of the cytoplasmic headpiece contains Asp-351 (shown in Figure 1.5), the residue that is phosphorylated by ATP. Initially the domains were assigned such that the P domain was followed by the N, nucleotide binding domain (Green & Stokes, 1992; Zhang *et al.*, 1998), as shown in Figure 1.4B. However, with the realisation recently that the phosphorylation domain of SERCA has homology with the haloacid dehydrogenase (HAD) superfamily the cytosolic mass was re-assigned (Aravind *et al.*, 1998). The superfamily contains the phosphorylation domains of ATPases and the catalytic domains of HADs, all of which form an aspartyl ester intermediate. This concept has aided the location of the critical residues in the P domain as predicted by sequence homology (Stokes & Green, 2000). Thus by analogy to the HADs, a typical Rossman fold structure of seven stranded parallel β sheets surrounded by 8 short α-helices is evident in the P domain. The N-terminal region starts at residue 330 and extends to residue 359 with the C-terminal end from residue 605 – 737. The N domain is inserted into the P domain, from residues 360 to 604, between the end of the first β-strand (containing Asp-351) and the first α helix of the Rossman fold.

The N domain is the largest domain (~27k) and consists of a 7 stranded antiparallel β-sheet sandwiched by 2 bundles of α-helices, linked to the phosphorylation domain by 2 loops. Lys-515, with the conserved sequence KGAPE around it can be labelled with fluorescein isothiocyanate (FITC) in an ATP protectable manner and is therefore is postulated to be the binding site for ATP (Gutierrez-Merino *et al.*, 1987). Two tenuous loops link the N domain to the P domain. These presumably give the N domain flexibility with respect to the rest of the structure which explains the fact that they are sensitive to protease digestion yielding a stable fragment (from Thr-357 to Thr-608, coloured green in Figure 1.5)

that can still bind nucleotides (Champeil *et al.*, 1998). So, it is possible that this region is a hinge, which permits large movement of the N domain.

Despite the differences in the specific functions of the P type ATPases and their species of origin, there are several highly conserved areas in their sequences (Figure 1.6). In the A domain the conserved ^{181}TGES motif is present. The conserved region at Asp-351, ^{351}DKTGTLT, is used to classify a protein as a P-type ATPase. The nucleotide-binding site in the N domain ^{515}KGAPE is found in a variety of ATPases but not in all the heavy metal transporting pumps (Moller *et al.*, 1996). The PEGL motif in M4 is a key motif and the Glu is replaced by a Cys or His in the ATPases that transport heavy metals (Moller *et al.*, 1996). The ^{601}DPPR motif is next to helix P2 in the P domain and lastly the FSBA (5'-(*p*-fluorosulfonyl)-benzoyl-adenosine) binding area above transmembrane α-helix 5 is highly conserved (Luckie *et al.*, 1992).

1.2.4. Characterisation of the SERCA pump

Since the publication of the sequence of SERCA in 1985 (MacLennan *et al.*, 1985), functional studies, site directed mutagenesis and chemical derivitisation procedures have been used to obtain a wealth of information as regards the relationship between structure and function, with respect to calcium binding and translocation.

Chemical and spectroscopic studies provide meaningful structural measurements, which aid in predicting the 3 dimensional structure of the ATPase (East *et al.*, 1992). Fluorescence energy transfer is used to obtain information regarding the distances within the protein and between the protein and the lipid bilayer. This involves labelling with two fluorescence groups at specific sites and measurement of energy transfer between the donor and acceptor fluorophores, so providing structural data (Scott, 1985). In conjunction with mutagenesis studies (Figure 1.7) key residues in the functional domains within the structure have been established.

1.2.5. Calcium binding and transport

Initially, Brandl *et al.* (Brandl *et al.*, 1986) postulated that Ca^{2+} binding occurred in the amphipathic stalk sectors of the enzyme, which contain negatively charged groups. This was based solely on the primary sequence analysis and a proposed transport mechanism whereby rotation of the stalk sectors disrupts the binding of Ca^{2+}, releasing the ions. However, single mutations of 30 nucleotides encoding Glu, Gln, Asp and Asn residues in the stalk region had no effect on ATPase activity, Figure 1.7 (Clarke *et al.*, 1989), and multiple mutations resulted in only partial loss of Ca^{2+} transport function. The effects of mutations of residues in the transmembrane region were therefore studied. Residues mutated were the acidic residues (Clarke *et al.*, 1989), proline (Vilsen *et al.*, 1989), and polar residues (Clarke *et al.*, 1990). Of 34 residues chosen for mutation, 10 resulted in the loss of calcium transport. Glu-309, Glu-771, Asn-796, Thr-799 and Asp-800 are important as their side chains provide the oxygen ligands for high affinity calcium binding as shown in the crystal structure. Mutations of these led to complete loss of calcium transport function, calcium dependent phosphorylation of the enzyme by ATP and calcium occlusion (Clarke *et al.*, 1989; Vilsen & Andersen, 1992; Andersen & Vilsen, 1994). The critical residues for calcium binding are thus located at the middle of the transmembrane region of the ATPase (Andersen, 1995b). In the structure of the ATPase in the calcium bound form, binding sites I and II, which lie 5.7 Å apart, can be seen (Figure 1.8). Site I contains oxygen ligands from amino acids in M5, M6 and M8 whereas in site II the oxygen ligands are primarily from M4. Unwinding of M4 and disruption of M6 (for Thr-799 and Asp-800) are needed to facilitate contribution of these amino acids to their relevant calcium binding sites (Toyoshima *et al.*, 2000). Asp-800 co-ordinates both calcium sites (as shown in Figure 1.8). Hydrogen bonding networks must also exist in order to stabilise the unwound helices (White & Wimley, 1999).

In the KcsA K^+ channel, a clear pathway for ion movement across the membrane can be seen (Doyle *et al.*, 1998). This is not the case for the Ca^{2+}-ATPase where no clear pathway leads from either the cytoplasmic or the lumenal side to the calcium ion binding sites. On the cytoplasmic side it is possible that helix M1 is important in the access pathway leading to the calcium binding sites since M1 is highly conserved and contains a number of acidic residues. M1 could therefore

function to channel the calcium ions toward the binding sites (Figure 1.9). Glu-58 points towards the calcium binding sites and Glu-51 and Glu-55 located at the surface could provide an input pathway for the calcium, whilst Arg-63 and Asp-59 may form an ion pair in the membrane. Glu-58 may also function to sense occupation of the sites and close off the pathway following phosphorylation so that calcium is not lost.

The actual binding of calcium is sequential and co-operative (Henderson *et al.*, 1994). Calcium binds to the first inner site, which creates a second outer site, and the second calcium ion binds (Henderson *et al.*, 1994): the second site is of higher affinity than the first, so that binding is co-operative. On phosphorylation of the ATPase, calcium is released to the lumen. The mechanism is still uncertain (Figure 1.10). The original two-site model proposed a scheme whereby a single pair of sites existed that alternated between being able to bind calcium from the cytoplasmic side in E1 and being able to bind calcium from the lumenal side in E2. If this model were correct, then binding of calcium from the lumenal side would be competitive with binding calcium from the cytoplasmic side. In fact using vesicles preloaded with calcium it was shown that the presence of lumenal calcium had no effect on the affinity of the E1 sites for calcium (Petithory & Jencks, 1988; Myung & Jencks, 1991). This might suggest that calcium was unable to bind to E2 from the lumenal side of the membrane although calcium must be able to bind to E2P since $E2PCa_2$ is an intermediate in the reaction scheme. However, if this were true then high calcium concentrations would pull the equilibrium for phosphorylation by P_i totally over to the phosphorylated form giving $E2PCa_2$. In fact experimentally only a proportion of the ATPase becomes phosphorylated even in the presence of high lumenal concentrations of calcium. Thus, E2 and E2P must both be able to bind calcium ions from the lumenal side. The most straightforward explanation of these observations is the presence of separate pairs of binding sites on the cytoplasmic and lumenal sides of the membrane, and this is the four-site model (Jencks *et al.*, 1993; Myung & Jencks, 1994). In this model calcium can bind simultaneously to the cytoplasmic and lumenal sites on the unphosphorylated ATPase (Jencks *et al.*, 1993) so that calcium binding at the lumenal sites is not competitive with that at the cytoplasmic sites. In this model four calcium ions can bind in E1 but phosphorylation of the ATPase closes the cytoplasmic sites and forces the calcium ions into the lumenal pair of sites. Calcium is therefore not released from the sites

initially bound. However, mutagenesis studies (Andersen, 1995a) show that mutations of the cytoplasmic sites affect the release of calcium and thus support a model whereby calcium is released from the sites to which it initially binds. Thus, an alternating four-site site model has been proposed. This suggests two pairs of sites do indeed exist. The cytoplasmic high affinity pair and lumenal pair are available for calcium binding in the E1 conformation. Upon phosphorylation the cytoplasmic pair of transport sites transform into low affinity sites exposed to the lumen (as in the two-site model) and the lumenal pair of sites closes; in the E2 form the transport sites are inaccessible from both sides of the membrane, with only the lumenal sites available for binding. So, the lumenal sites are not required for calcium transport but serve a regulatory role. These sites prevent a build up of large amounts of the calcium bound phosphorylated ATPase in the presence of P_i and a high concentration of lumenal calcium.

1.2.6. Phosphorylation and nucleotide binding

Several amino acid substitutions have been made in the phosphorylation and nucleotide binding domains (Figure 1.7). The segment to the C terminal side of Asp-351 that is phosphorylated by ATP (^{351}DKTGTLT^{357}) is highly conserved in the P-type ATPase family and indeed residues 352, 355, 356 and 357 are critical for calcium transport and phosphorylation (Maruyama *et al.*, 1989b). Mutations in the region around Asp-351, which is phosphorylated by ATP, gave rise to 'phosphorylation-negative' mutants whereby the enzyme did not form a phosphoenzyme intermediate (with either ATP or P_i), thus not transporting Ca^{2+} (Andersen, 1995a). ADP-sensitive mutants slow or block the transition from $E2PCa_2$ to E2P and in the presence of ADP $E2PCa_2$ may reform $E1Ca_2ATP$. The substitutions giving rise to these mutants take place in the segment extending from Asp-351 to the preceding transmembrane α-helix, M4 (Zhang *et al.*, 1995). ADP-insensitive mutants slow or block transition from E2P to $E2P_i$ and are unable to reform $E2PCa_2$. These mutations occur in the transmembrane α-helices M4, M5 and M6, and some also give rise to the calcium affinity mutants. Chemical labels have additionally been used to locate residues involved in ATP binding (Bigelow & Inesi, 1992). Analogues of ATP with reactive groups on the rings invariably label residues in the N domain and block the phosphorylation by ATP but not the back reaction

with acetyl phosphate or P_i (Stokes & Green, 2000). If the reactive group is close to the γ-phosphate then residues in the P domain are labelled and the ATPase cannot be phosphorylated by ATP or P_i (Stokes & Green, 2000). Lys-515 actually sits in the depth of the ATP binding pocket (Toyoshima *et al.*, 2000). 2',3'-O-(2,4,6-trinitrophenyl)-AMP (TNP-AMP) binds to the surface of the N domain and analogues of TNP-AMP are competitive with ATP, thus it is presumed that TNP-AMP binds to the ATP binding site (Nakomoto & Inesi, 1984). Lys-515 and Lys-492 are also close to the bound TNP-AMP and labelling studies have shown these two residues are at the active site. Mutation of Lys-515 to Ala inhibits ATP and acetyl phosphate mediated transport of calcium (Maruyama *et al.*, 1989b) and mutation of Lys-492 decreased the affinity for ATP (as did the Phe-487 mutation) but had little effect on phosphorylation by P_i or acetyl phosphate (McIntosh *et al.*, 1996). So, the nucleotide binds near to Phe-487, Lys-515 and Lys-492 in a positively charged pocket created by these residues and Arg-489 and Arg-560.

1.2.7. Domain movement

Movement of the Ca^{2+}-ATPase, both in the cytoplasm and in the transmembranous region, must occur in order to transport the two calcium ions to the lumen of the SR. Asp-351 (in the P domain), which is phosphorylated by ATP is more than 25 Å away from where the ATP binds in the N domain (Toyoshima *et al.*, 2000). So, domain closure must occur during ATP hydrolysis and indeed the two loops connecting the P and N domains are thought to be flexible. Asp-351 is close to the hinge segment TTN^{359} and is linked by a conserved KTGTL sequence; it is thought that this close link allows changes at the catalytic site to initiate domain movements. Labelling studies have helped to identify residues that relocate during movement. Two residues Lys-492 and Arg-678 (indicated in Figure 1.5), which are separated by more than 25 Å, are cross-linked by glutaraldehyde (McIntosh, 1992), in an ATP protectable manner. Phosphorescence spectroscopy of erythrosin isothiocyanate, attached to Lys-464 in the N domain, highlighted large domain movements upon calcium binding (Huang & Squier, 1998). Lys-492 and Lys-684 can both be labelled by ATP pyridoxal in the presence of calcium (shown in Figure 1.5) but only Lys-684 can be labelled in the absence of calcium (Yamamoto *et al.*, 1989), suggesting a calcium dependent change in conformation. Also, ATP binding in the presence of calcium must induce a conformational change, bringing the N

domain closer to the P domain, so that the terminal phosphate of ATP is near Asp-351, to permit phosphorylation. Interestingly, in the presence of bound calcium and TNP-AMP the structure of the ATPase is not significantly different to that in the absence of TNP-AMP (Toyoshima *et al.*, 2000). This suggests that the γ phosphate of ATP may be required to bring about the structural transformation. McIntosh and Woolley (McIntosh & Woolley, 1994) covalently linked an ATP analogue (2',3-O(2,4,6 trinitrophenyl)8-azido-ATP) to Lys-492 and this was able to slowly phosphorylate Asp-351. Hence, Lys-492 must be separated by ~14 Å from Asp-351, and must be situated close to the adenyl moiety of the nucleotide in the structure.

By comparison of the high and low resolution structures of the Ca^{2+}-ATPase, in the $E1Ca_2$ and E2P (or E2) forms respectively, the conformational change following calcium and ATP binding may be deduced (Toyoshima *et al.*, 2000). In the $E1Ca_2$ form the ATP binding site appears to be open and in the E2 form closed. The fact that trypsin cleavage in the A domain is increased by calcium suggests that calcium binding may release the A domain for movement. Indeed, a 90^0 rotation in the A domain, facilitated by movements in helices M1 to M3, brings the conserved ^{181}TGES loop into the phosphorylation site (Toyoshima *et al.*, 2000). A 20^0 rotation of the N domain partially closes the gap between the N and P domains (with a 15 – 20 Å distance still remaining between Asp-351 and the nucleotide-binding site). As previously discussed movements in the α-helices must occur if the proposed residues contribute to the calcium binding sites. Any structural changes in the P domain must be small because fluorescence energy transfer experiments between labelled residues and fluorescently labelled phospholipids show that heights of Cys-344, Cys-670 and Cys-674 relative to the membrane hardly change between the conformations E1 and E2 (Baker *et al.*, 1994). Glu-439 at the end of the N domain closest to P and Lys-515 do not move significantly either (Baker *et al.*, 1994).

The ATPase only becomes phosphorylated when two calcium ions are bound so that calcium binding in the transmembrane region of the ATPase must be transmitted in some way to the cytoplasmic domain. Similarly, phosphorylation of the ATPase in the cytoplasmic domain must result in changes at the calcium binding sites in the transmembrane domain, leading to release of calcium. The link between these two separate functions appears to be the conserved loop, L67 (Figure 1.11). L67 runs along the bottom of the P domain and connects the transmembrane α-helices M6 and M7. The position of L67 relative to the membrane surface is thought

to change between the E2 and $E1Ca_2$ conformations, being situated higher in the structure in the E2 conformation (Toyoshima *et al.*, 2000). The P1 and P2 helices in the P domain sit above L67 (Figure 1.11). Upon phosphorylation the β-sheet underneath Asp-351 could move, moving P1 and P2. P2 at the C terminal end of the N domain looks like a piston ideally placed to link N domain changes. P1 at the N terminal end of the P domain near Asp-351 could press on the loop and together P1 and P2 (in a purely mechanical manner) could form a link between the phosphorylation domain and the high affinity calcium binding sites. The movements described will alter the helix packing within the membrane, so that changes in the positions of M4 and M5 and M1 to M3 (permitting A domain movement) would occur. These changes in the α-helices would disrupt the calcium binding sites, releasing calcium to the lumen of the SR.

The fact that the Ca^{2+} binding sites, located in the transmembrane region, are distinct from the catalytic ATP binding and phosphorylation site in the cytoplasm (Andersen & Vilsen, 1995) tells us not only that significant domain movement must occur in the ATPase and that transport requires long distance communication for energy coupling (Andersen & Vilsen, 1995).

1.3. *Heliothis virescens*

The tobacco budworm, *Heliothis virescens* is a pest of the cotton crop, *Gossypium hirsutum*. There are four species of *Heliothis* that are pests: *Helicoverpa armigera, Helicoverpa zea, Helicoverpa punctigera and Heliothis virescens*. They feed on crops such as tobacco, tomato, soybean, sunflower and cotton. So, this species are capable of destruction of harvests, causing economic loss. To prevent damage to the crops, the use of insecticides is widespread. The resistance of tobacco budworm to the pyrethroid, carbamate and organophosphate insecticides (Elzen *et al.*, 1992; McCaffery, 1998) is of concern as regards the implications for the control of this pest. The natural pyrethroid insecticides were introduced in the late 1970's and have been employed greatly since. Hence, resistance developed. Synthetic pyrethroids were then developed but insects still exhibited some resistance. Genomic approaches to understand the mechanism of action of insecticide resistance are currently being carried out (Heckel *et al.*, 1997; Heckel *et al.*, 1998). Resistance is an economic problem and has major human and environmental health

implications. When resistance occurs doses of the insecticide are increased and mixtures of compounds are applied to the plants, which in turn may have synergistic effects. The use of broad-spectrum insecticides then increases, killing the natural predators. Hence the cost of loss of the crop is added to the cost of the insecticides. Although transgenic plants may be used (Giband, 1998) there is a need for development of novel insecticides.

1.4. Aims of the project

Many compounds inhibit Ca^{2+}-ATPase function yet little is known about the sites to which they bind. The presence of a single binding site with competition for binding of inhibitors could be possible. On the other hand multiple binding sites could exist, that are different for each inhibitor. The specificity of the SERCA inhibitors, the sesquiterpene lactones highlights the possibility of finding an inhibitor that would for example inhibit an insect calcium pump, but not a mammalian pump. Lockyer (Lockyer *et al.*, 1998) successfully cloned the cDNA of the *Heliothis virescens* insect Ca^{2+}-ATPase but did not achieve high-level expression of the pump. Expression in a heterologous system is needed, due to the small amount obtainable from the insect. Over-expression and isolation of functional ATPase from the tobacco budworm would permit functional studies. This in turn would allow comparative inhibitor studies with compounds that inhibit SERCA1b Ca^{2+}-ATPase.

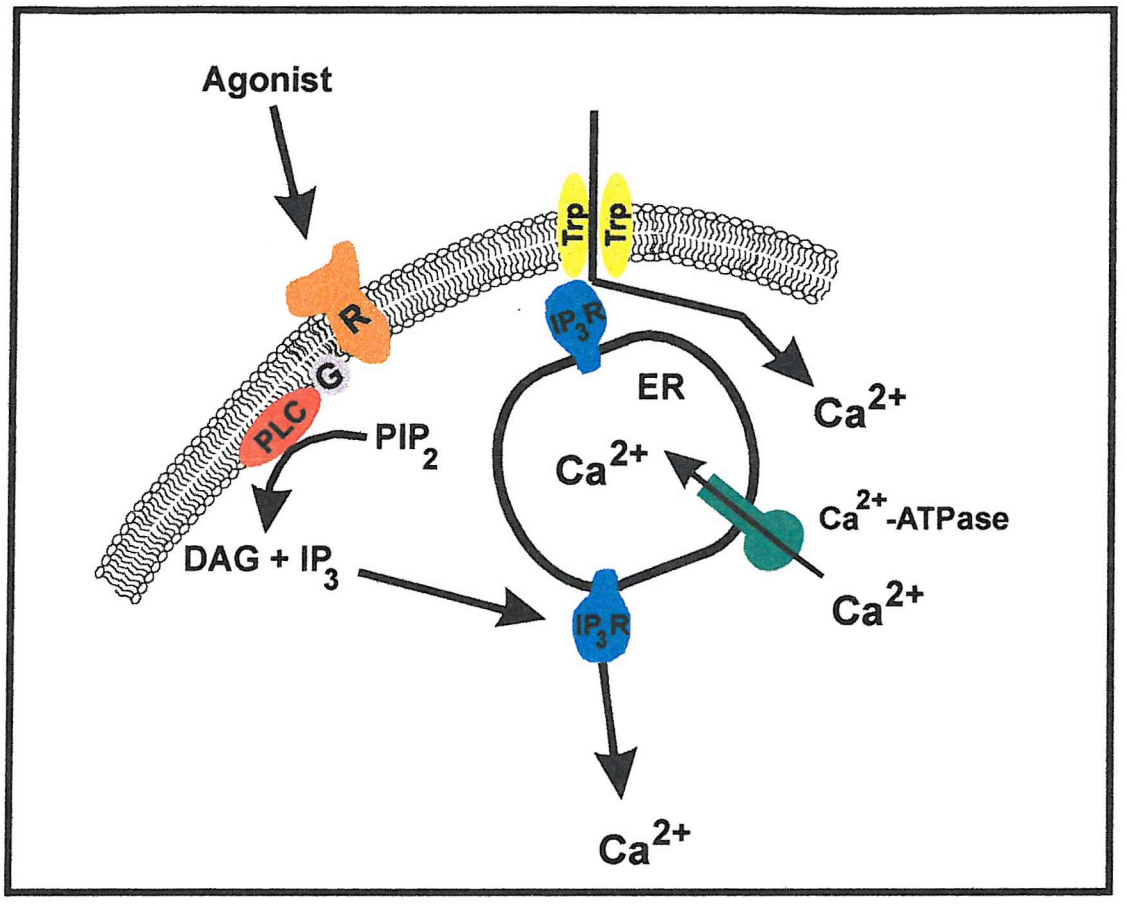

Figure 1.1. Release of calcium mediated by IP_3 and SOC

The diagram illustrates the sequence of events leading to the release of calcium from the endoplasmic reticulum (ER). Following agonist binding to the G protein linked receptor (R) in the plasma membrane, PIP_2 (a lipid in the membrane) is hydrolysed by phospholipase C (PLC), giving diacylglycerol (DAG) and IP_3. IP_3 binds to IP_3 sensitive calcium channels (IP_3R) leading to release of calcium from the ER. Upon depletion of the ER stores, calcium enters across the plasma membrane through a Trp protein. The Ca^{2+}-ATPase pumps calcium back into the ER.

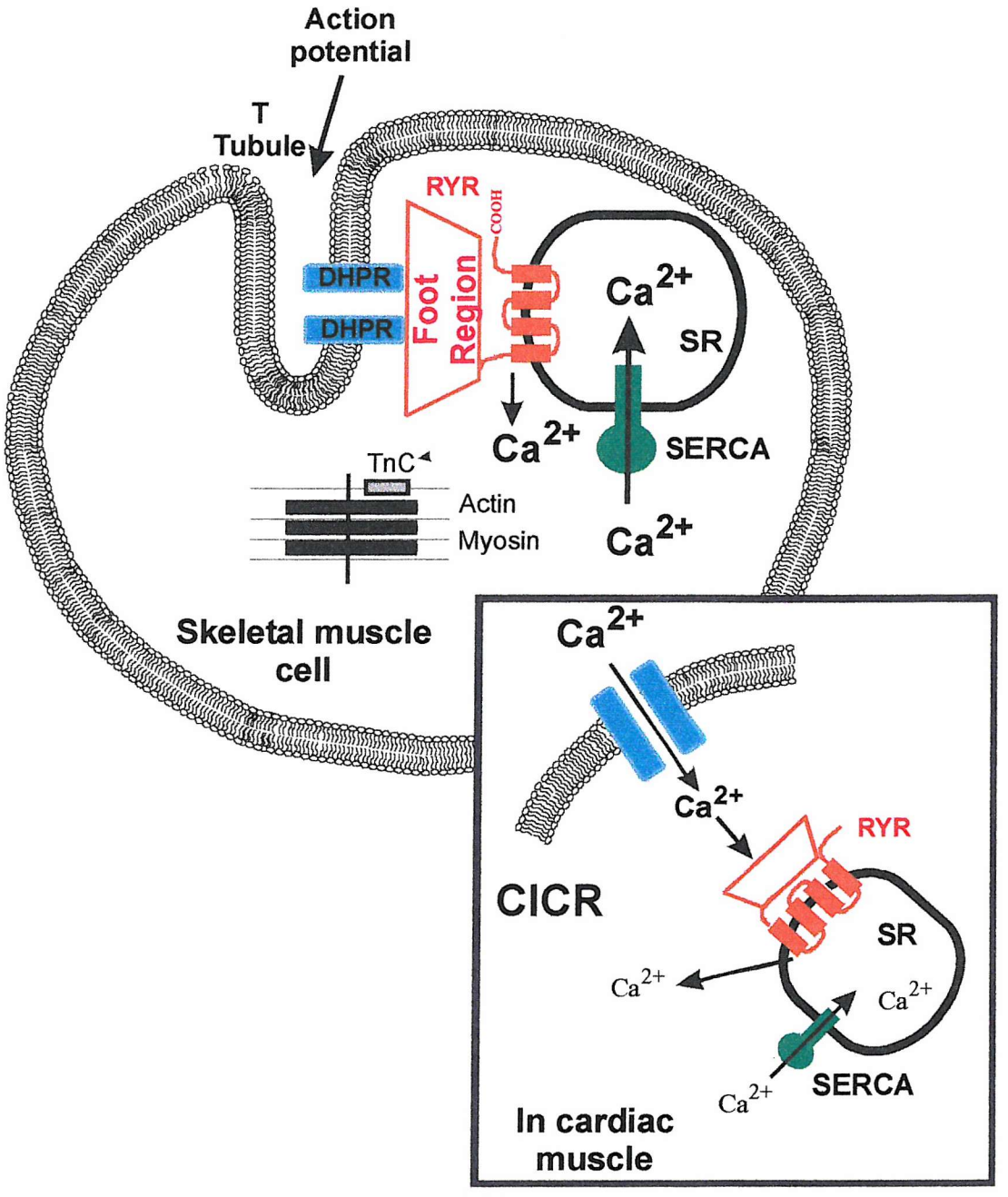

Figure 1.2. The sequence of events leading to muscle contraction

An action potential is transmitted down the T-tubule invagination in the plasma membrane of the skeletal muscle cell. The dihydropyridine receptor (DHPR) in the T tubule is directly coupled to the ryanodine receptor (RyR), in the sarcoplasmic reticulum (SR). Calcium is released through the RyR, binds to troponin C (TnC) and actin and myosin cause muscle contraction. Calcium is pumped back into the SR by the Ca^{2+}-ATPase (SERCA). The insert shows calcium induced calcium release (CICR) that occurs in cardiac muscle. Calcium enters through the plasma membrane, directly causing calcium release from the SR, via the RyR.

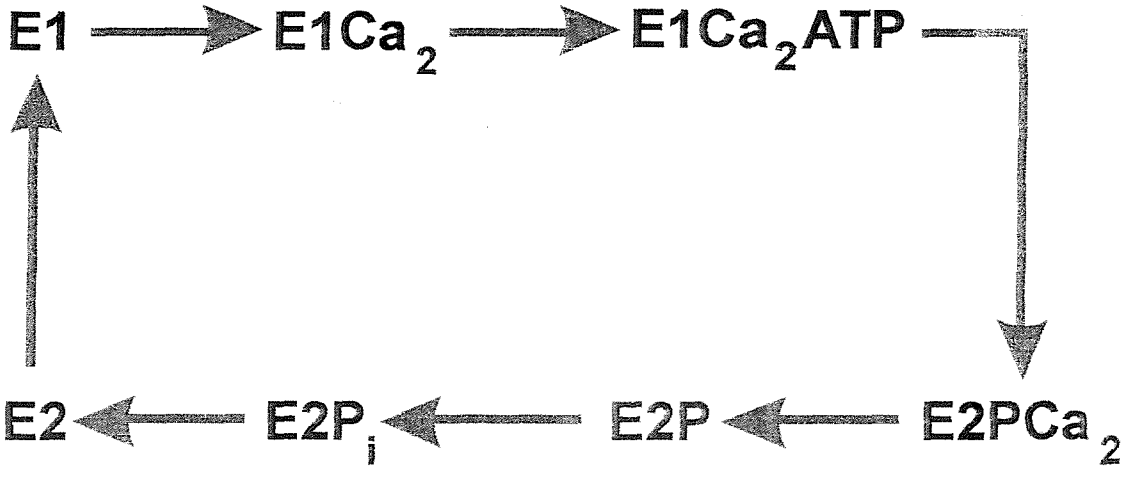

Figure 1.3. The E1-E2 reaction scheme of the Ca^{2+}-ATPase

Two Ca^{2+} ions bind sequentially to the two high affinity sites in the E1 conformation of the enzyme. ATP binds and subsequent phosphorylation occurs, with a conformation change to $E2PCa_2$. The two Ca^{2+} ions are released from the now low affinity sites and the enzyme is dephosphorylated giving E2. The Ca^{2+}-ATPase then returns to the E1 conformation.

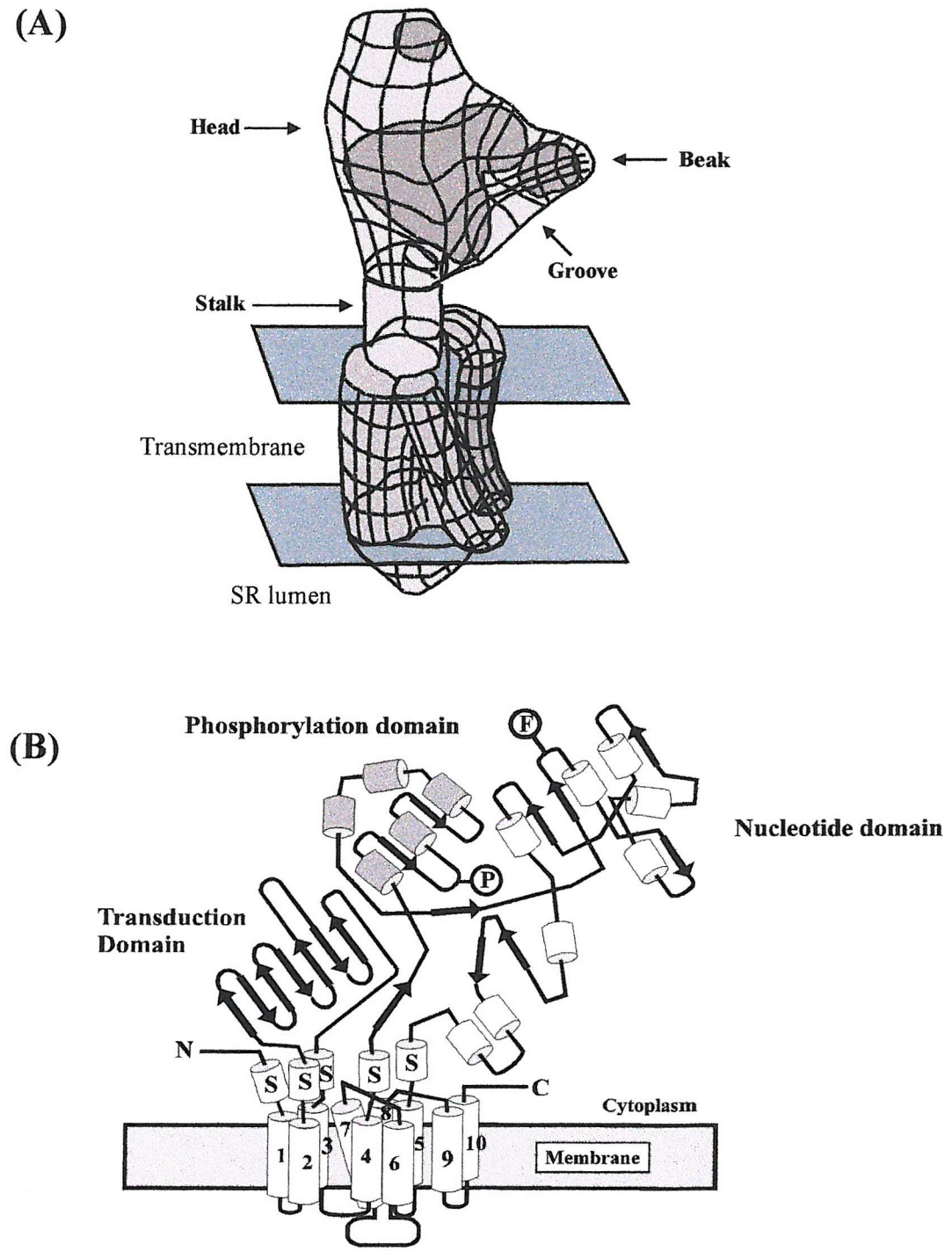

Figure 1.4. Predicted topology of the Ca^{2+}-ATPase

(A) shows the structure of the Ca^{2+}-ATPase as proposed by Toyoshima *et al.* (1993). The surfaces of the bilayer are shown by the two shadowed planes. The large cytoplasmic head of the protein is linked to the transmembrane domain by the stalk sector. (B) shows a three dimensional representation, with the previous assignment of the nucleotide binding domain at the end of the phosphorylation domain.

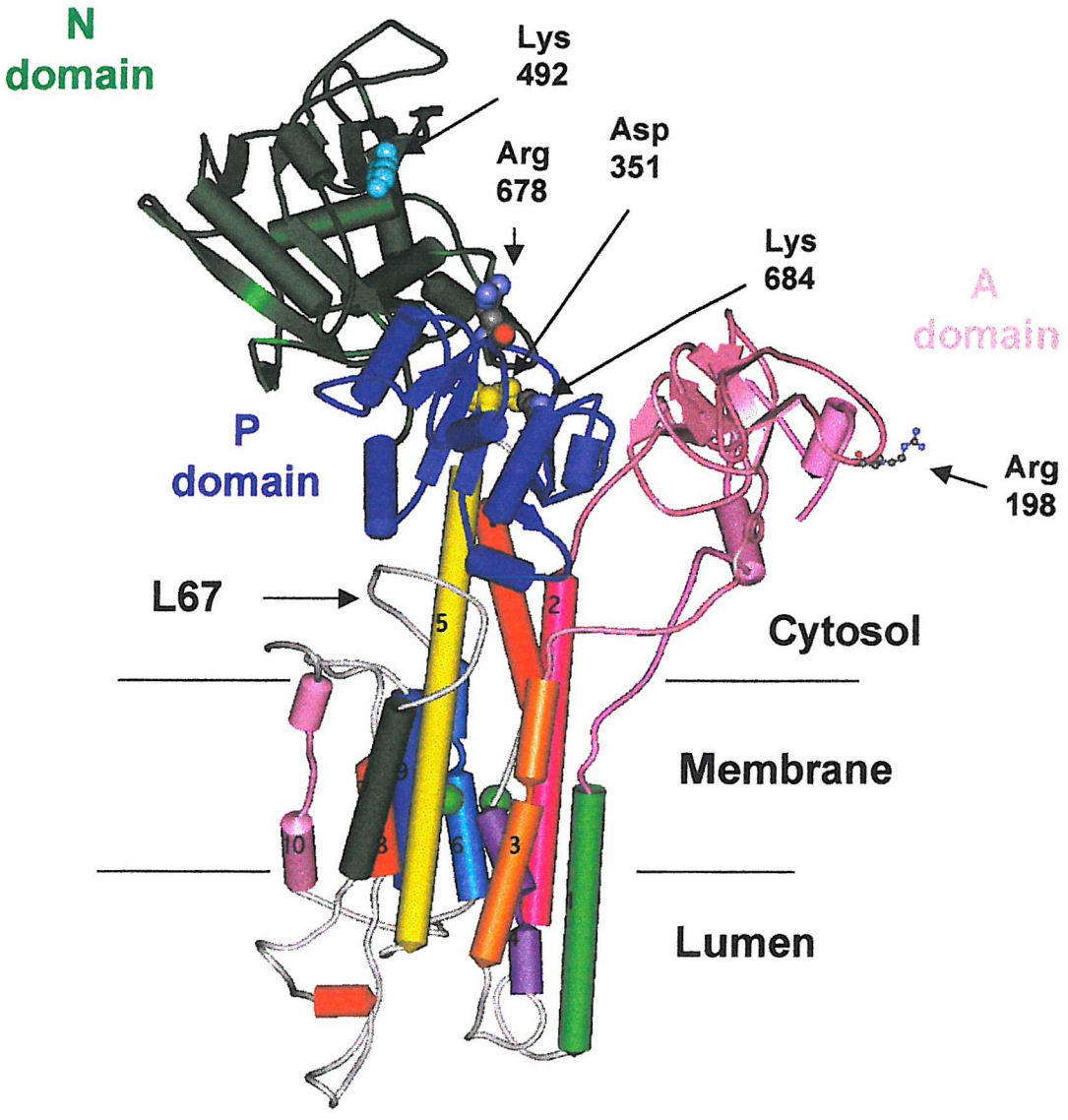

Figure 1.5. The 2.6 Å resolution structure of the Ca^{2+}-ATPase

Toyoshima *et al.* solved the crystal structure (2000). The ten transmembrane α-helices are numbered. The cytosolic mass is divided into three domains: the A domain (pink), the N domain (green) and the P domain (blue). Indicated are space-fill representations of Asp-351 (yellow), Lys-492 (light blue), Arg-678 and Lys-684, which are crosslinked to Lys-492 by glutaraldehyde and pyridoxal ATP respectively. The loop L67 connects transmembrane α-helices 6 and 7, and lies underneath the P domain.

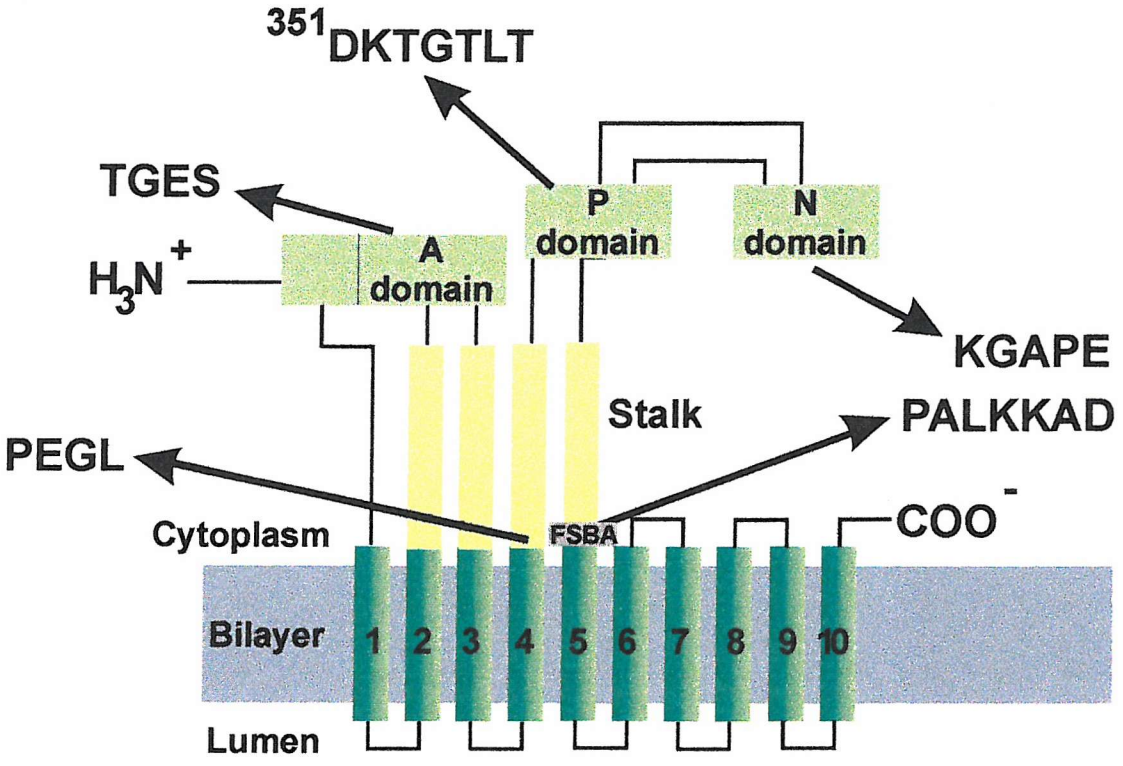

Figure 1.6. The conserved regions of P-type ATPases

The diagram shows the three cytoplasmic domains of SERCA: A (activation), P (phosphorylation) and N (nucleotide binding). They are connected to the ten transmembrane domains by four stalk sections. The locations and amino acid sequences of some conserved residues are indicated.

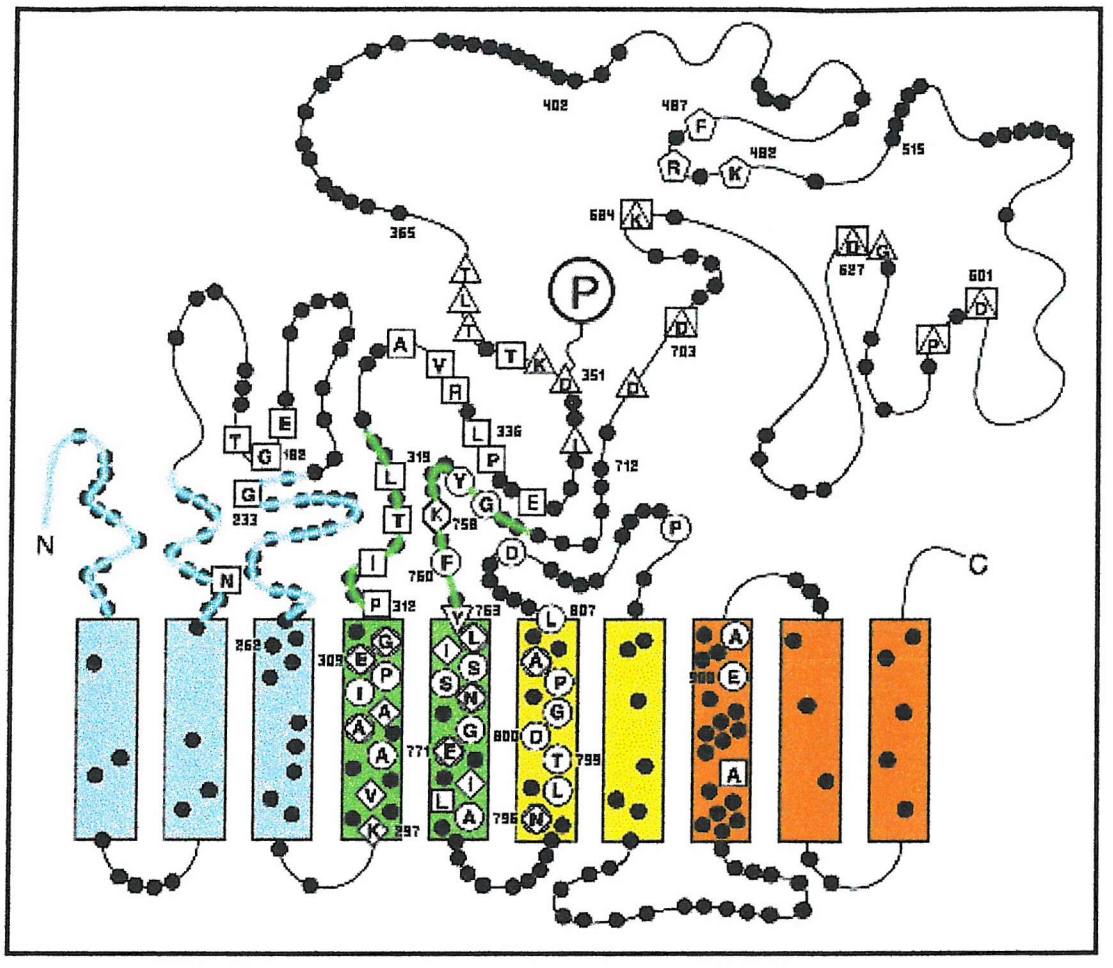

Figure 1.7. Model of the topology of the SR Ca^{2+}-ATPase.

Indicated are the numerous residues which have been studied by site directed mutagenesis. *Filled circles* indicate mutations with no or only a modest effect on Ca^{2+} transport. *Open circles* indicate Ca^{2+} affinity mutants. *Pentagons* indicate mutations that reduce ATP affinity. *Triangles pointing upwards* indicate mutants that are unable to phosphorylate with ATP as well as with P_i. *Open squares* indicate ADP sensitive mutants (whereby $E2PCa_2$ to E2P transition is blocked). *Diamonds* indicate ADP insensitive mutants (whereby E2P to $E2P_I$ is blocked). *The triangle pointing downwards* indicates the Y763G mutant that uncouples ATP hydrolysis from calcium transport. *The hexagon* indicates the K758I mutant that enhances dephosphorylation and blocks the E2 to E1 transition (Andersen and Vilsen, 1995).

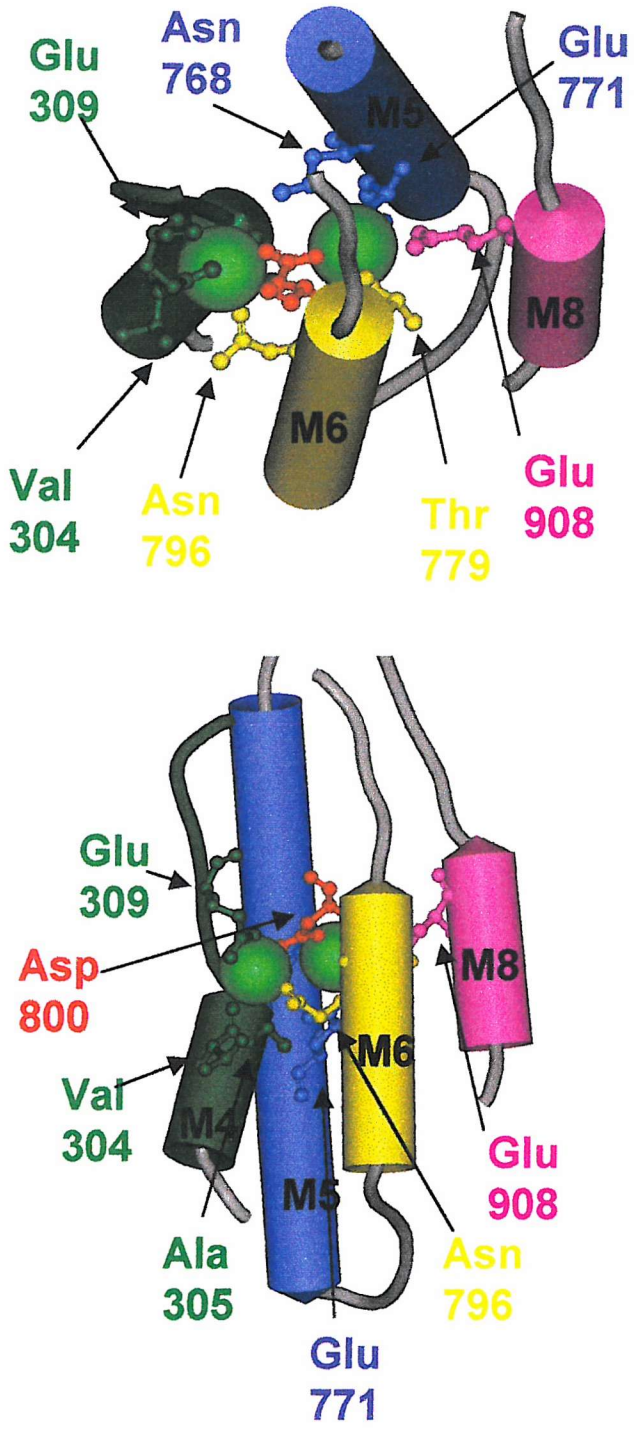

Figure 1.8. The two high affinity calcium binding sites on the calcium ATPase
Transmembrane helices M4 (green), M5 (blue), M6 (yellow) and M8 (pink) are shown. (A) shows a view from the cytoplasmic side down onto the plane of the membrane and (B) is a view from the side. The residues contributing towards the calcium binding sites are shown and are coloured according to the α-helix to which they belong. The two calcium ions at site I and II are represented by green spheres. Asp-800 (from M6) is coloured red; this residue contributes to binding site I and II.

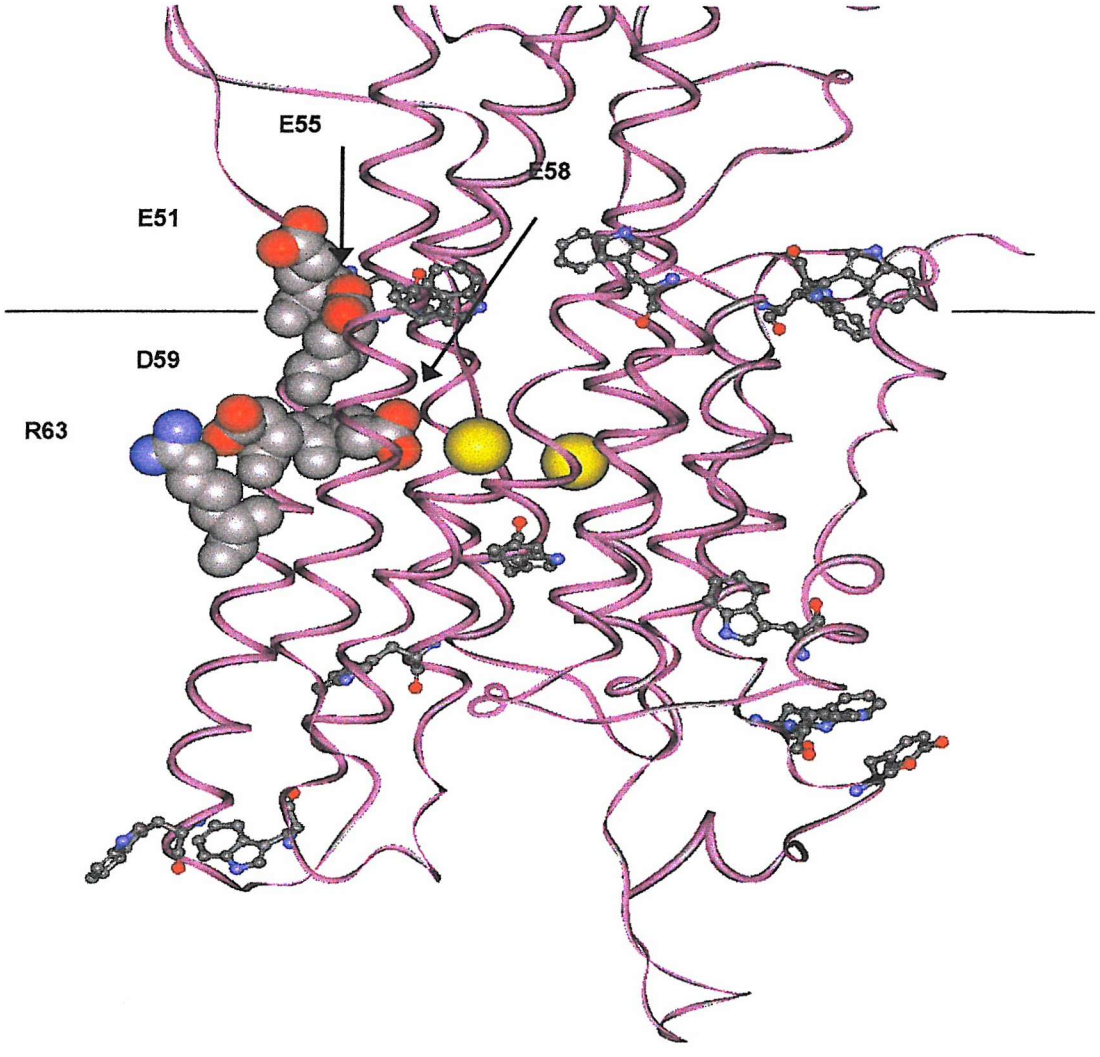

Figure 1.9. Residues in the transmembrane region M1 possibly contributing to a pathway for calcium access.

Trp residues are shown in ball-and-stick representation and the residues in M1 are shown in space-fill representation. The locations of Asp-59 and Arg-63 in the transmembrane α-helix pointing out into the lipid bilayer are shown. Also shown are the other acidic residues in M1, Glu-51, Glu-55 and Glu-58. The Trp residues are believed to anchor the ATPase in the membrane

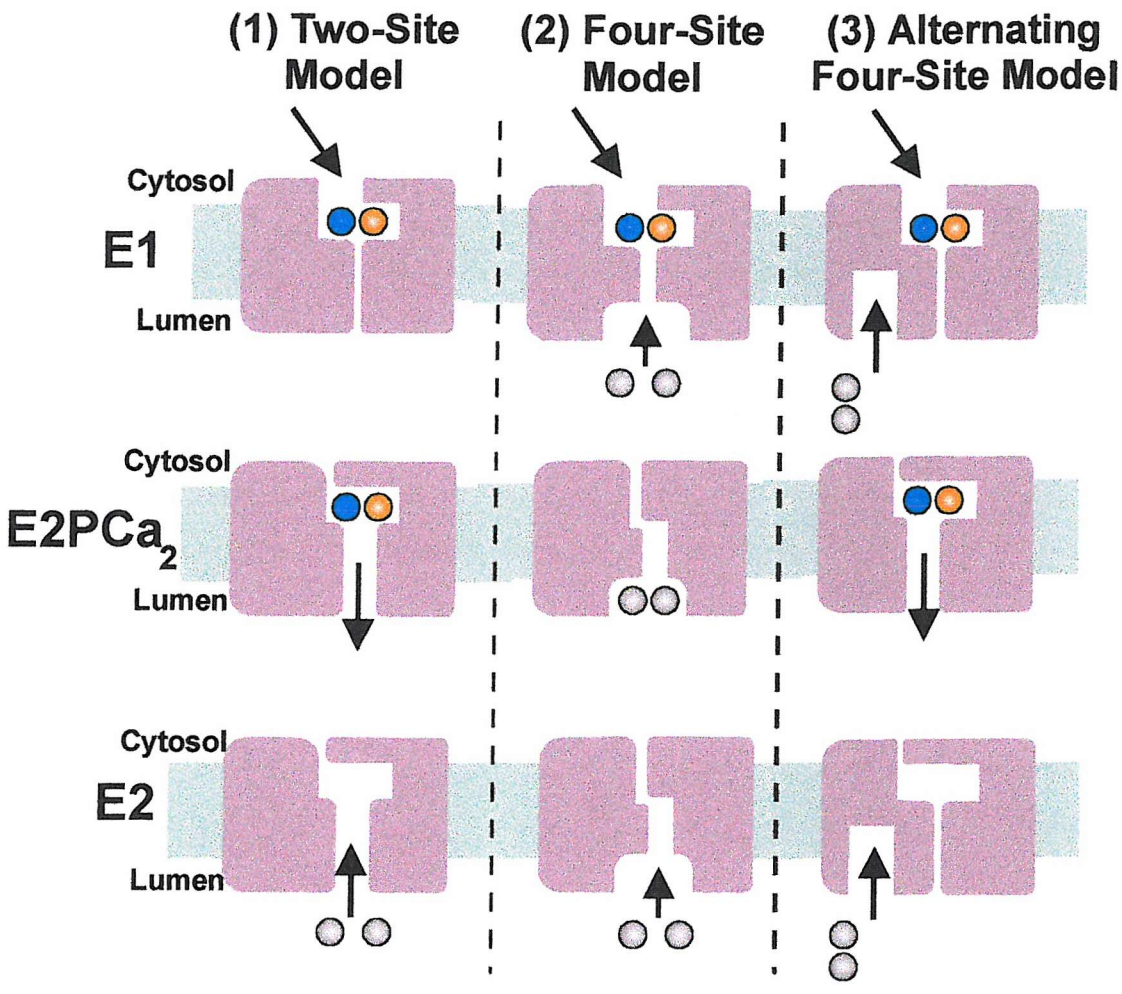

Figure 1.10. Three models for transport of calcium by the Ca^{2+}-ATPase

The two-site model proposes one pair of calcium binding sites which alternate between E1 (exposed to cytosol) and $E2PCa_2$ + E2 (exposed to lumen). The four-site model contains two pairs of binding sites. Calcium is released from a separate pair of sites (in E2) to that initially bound (in E1). The alternating four-site model proposes two pairs of sites, the cytosolic sites transport calcium and become exposed to the lumen upon phosphorylation, so that calcium ions are released from the sites to which they initially bind. The lumenal pair of sites are open in E1 and E2 but closed in $E2PCa_2$. The lumenal sites could serve a regulatory role.

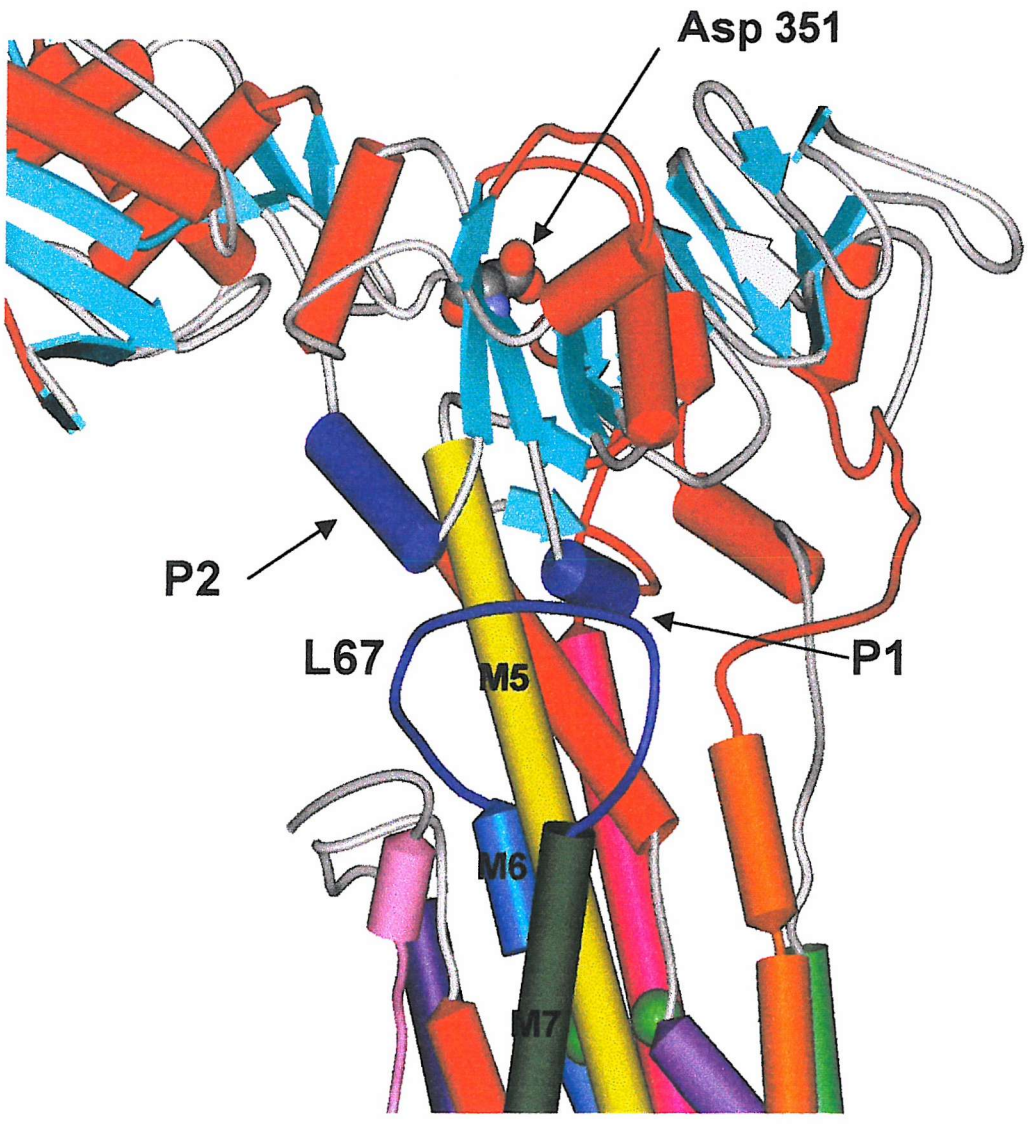

Figure 1.11. The link between the phosphorylation domain and the transmembrane α-helices.

Helices P1 and P2 in the phosphorylation domain are indicated in dark blue. These contact loop L67, also in dark blue. L67 connects transmembrane α-helices M6 (light blue) and M7 (dark green).

Type	Specificity
IA	K^+
IB	Heavy metals
IIA	Ca^{2+} (non calmodulin stimulated)
IIB	Ca^{2+} (calmodulin stimulated)
IIC	Na^+
IID	Na^+/K^+ H^+/K^+
IIIA	H^+
IIIB	Mg^{2+}
IV	Phospholipids
V	No assigned specificity

Table 1.1. Phylogenetic groups of the P type ATPases

The P-type ATPase family was analysed using conserved core sequences and then grouped according to substrate specificity (Axelsen and Palmgren, 1998).

See http://biobase.dk/~axe/Patbase.html

Chapter Two: General Materials and Methods

2.1. Materials and reagents

Agarose NA (Pharmacia)

Antibiotic/Antimycotic (Gibco-BRL)

A23187, free acid (Calibochem)

2-Aminoethoxydiphenylborate, 2-APB (Calbiochem)

Antibodies: goat anti-mouse IgG peroxidase conjugate (Sigma)

sheep anti-mouse IgG FITC conjugate (Sigma)

sheep anti-rabbit IgG FITC conjugate (Amersham)

Antipyrralazo III (Fluka)

ATP, disodium salt (Roche Molecular Biochemicals)

2,5-di (*tert*-butyl)-1,4-benzohydroquinone (BHQ) (Aldrich)

Bacto agar (DIFCO)

Bio-beads SM2, 20 – 50 mesh (Bio-Rad)

Butylated hydroxytoluene, BHT (Chemservice)

$C_{12}E_8$ (Calbiochem)

Calcium crimson AM ester and tetrapotassium salt (Molecular Probes)

Curcumin (ICN)

Dextrose (DIFCO)

Disc filters 0.025 μm VS (Millipore)

Disposable 0.2 cm electroporation cuvettes (Bio-Rad)

DNA ladder, 1 Kb (Gibco-BRL)

Dulbeccos' modified Eagles medium (DMEM) with glutamax^{TM} (Gibco-BRL)

DMEM/nutrient mix F/12 with glutamax^{TM} (Gibco-BRL)

ECL western blotting analysis system (Amersham)

Foetal calf or bovine serum (Gibco-BRL)

Fungizone ^{TM} (amphotericin B) (Gibco-BRL)

Gentamycin (Gibco-BRL)

Glass beads 425 – 600 microns, acid washed (Sigma)

Hybond – C^{TM} nitrocellulose (Amersham)

Hyperfilm MP (Amersham)

Lactate dehydrogenase (Park Scientific)

FuGENE - 6 ^{TM} transfection reagent (Roche Molecular Biochemicals)

Medium 199 modified Earles medium with L-glutamine (Gibco-BRL)

NADH (Park Scientific)

Nonylphenol (Fluka)

Protogel (National Diagnostics)

Qiaex II^{TM} gel extraction kit (Qiagen)

Rainbow markers (Amersham Life Sciences)

Restriction endonucleases and DNA Modifying Enzymes (New England Biolabs or Promega)

Sterile disposable pipettes, 3 ml (Alpha Laboratories)

Tissue culture flasks (Falcon)

Tissue culture dishes (Nunclon)

Trypsin – EDTA, 10x (Gibco-BRL)

Tryptose phosphate broth (Gibco-BRL)

Wizard ^{TM} DNA cleanup kit (Promega)

Wizard^{TM} miniprep DNA purification system (Promega)

Xestospongin C (Calbiochem)

Yeast synthetic drop out mix (Sigma)

Yeast nitrogen base without amino acids (DIFCO)

Yeast synthetic drop out supplement (Sigma)

Oligonucleotides were purchased from Oswell DNA Services and MWG Biotech.

The curcumin analogues were kindly supplied by Prof. W. Hänsel, Pharmazeutisches Institut, University of Kiel.

All other reagents were purchased from Sigma, BDH, Fischer scientific or Merck unless stated otherwise and were of analytical grade.

2.2. Methods

2.2.1. Preparation of rabbit sarcoplasmic reticulum (SR)

The SR Ca^{2+}-ATPase was prepared from rabbit fast twitch skeletal muscle, using a modification of the method described by Daiho *et al.* (Daiho *et al.*, 1993). A female New Zealand White rabbit was given a lethal dose of Sagatal anaesthetic (5 ml pentabarbitone, 60 mg/ml) and the blood was subsequently drained via the carotid artery. The remainder of the procedure was then carried out at 4 ^{0}C. Fast twitch skeletal muscle was initially removed from either side of the spine and from the hind legs of the carcass (500 g in total). This tissue was then chopped and blended (Waring blender, full speed) for 20 seconds, 4 times (at 5 second intervals), in 2 volumes of 0.1 M NaCl, 10 mM MOPS - Tris, pH 7.0. Centrifugation at 8300 g for 35 minutes produced a loose pellet which was filtered through muslin and further centrifuged at 12 000 g for 30 minutes to remove mitochondria. The resultant supernatant was centrifuged at 53 000 g for 40 minutes. The precipitate was resuspended in 40 volumes of 0.6 M KCl, 5mM Tris - Maleate, pH 6.5, and stirred for 40 minutes. The suspension was then centrifuged at 125 000 g for 45 minutes. The pellet obtained was resuspended in 0.1 M sucrose, 30 mM MOPS - Tris, pH 7.0 and centrifuged at 125 000 g for 45 minutes. The final pellet was resuspended in 1-2 ml of this same buffer. Aliquots of the SR vesicles were then snap frozen in liquid nitrogen and stored at –70 ^{0}C. The protein concentration was determined by the spectroscopic method described below.

2.2.2 Spectrophotometric measurement of protein concentration

The protein concentration of the SR vesicle suspensions was determined by the procedure of Hardwick and Green (Hardwicke & Green, 1974). The protein was diluted with 1 % SDS and the absorption spectrum of the sample was recorded from 340 - 260 nm. A_{280} nm was then used to calculate the protein content assuming that the optical density of a 1mg/ml solution of SR is 1.0.

2.2.3. Ca^{2+}-ATPase coupled enzyme assay

The activity of the SR Ca^{2+}-ATPase was measured using a coupled enzyme assay (Froud *et al.*, 1986a). A mixture of 100 mM KCl, 40 mM Hepes - KOH, pH 7.0 with 1.01 mM EGTA, 5.1 mM $MgSO_4$, 2.1 mM ATP, 0.53 mM PEP, 0.15 mM NADH, 7.5 I.U pyruvate kinase, 18 I.U lactate dehydrogenase was equilibrated at 25 ^{0}C. 5 μg ionophore A23187 and 10 μg SR were added and the reaction was initiated by the addition of $CaCl_2$ (to a final free concentration of 10 μM).

The oxidation of NADH (the extinction coefficient of which is 6,220 $M^{-1}cm^{-1}$ at 340 nm) was monitored by measuring the decrease in absorbance at 340 nm. This was related to ATPase activity using the equation:

$$\text{Activity (μmoles/min/mg)} = \frac{\text{Assay volume (ml) x Change in absorbance}}{6.22 \text{ x SR (mg)}}$$

2.2.4. Immunoblotting

Detection of proteins on nitrocellulose membrane was performed using an immunoblotting procedure. Unoccupied sites on the nitrocellulose were blocked by incubation in phosphate buffered saline, PBS (137 mM NaCl, 2.7 mM KCl, 8.1 mM Na_2HPO_4, 1.5 mM KH_2PO_4, pH 7.4) containing 0.05 % Tween-20, 5 % BSA, for 1 hour at room temperature, with gentle shaking.

The enhanced chemiluminescence (ECL) Western Blotting Analysis System (Amersham) was utilised for the immuno-blotting procedure. All the following incubations are performed with gentle shaking. The membranes were initially washed twice with PBS-Tween after the blocking. They were then incubated with the primary antibody for 1 hour, after which they were washed twice with PBS-Tween. The secondary antibody, conjugated to horseradish peroxidase (HRP) was then added and again incubated for one hour with two wash steps. The membrane was then washed in PBS, in the absence of Tween.

2.2.5. DNA preparation

Plasmid DNA was purified by the alkaline lysis procedure or by the Wizard ^{TM} (Promega) miniprep kit, using the protocol for the use with ABI automated sequencing.

2.2.6. Ligation of DNA

After digestion of the DNA, the cut fragments required were separated on a 1 % agarose gel, containing ethidium bromide. The DNA in the gel slice was then extracted using the Qiaex II^{TM} gel extraction kit (Qiagen) or by snap freezing the gel slice in liquid nitrogen. Once thawed the slice was centrifuged in a benchtop microcentrifuge for 5 minutes to elute the DNA. This was then cleaned using the Wizard ^{TM} Promega DNA cleanup kit. Fragments not requiring gel separation were cleaned up directly using the Promega kit. Ligations were performed using T4 ligase (Promega), at 16 ^{0}C overnight.

2.2.7. DNA agarose gel analysis

For analysis DNA samples were separated using 1 % agarose gels made with 40 mM Tris, 40 mM glacial acetic acid, 1 mM EDTA (TAE) buffer and 0.5 μg/ml ethidium bromide was added to the gel to permit visualisation. The DNA samples were mixed with 1 x agarose gel loading buffer (30 % glycerol in 1 x TAE with 3 mg/ml bromophenol blue) for loading into the gel. The samples were run alongside a 1 kb DNA ladder (Gibco BRL) using TAE as the electrophoresis buffer. The gel was run at a constant voltage between 100 - 120 volts until the samples had been separated as required. DNA bands were viewed using an ultraviolet transilluminator and photographed using Polaroid 667 instant pack film.

2.2.8. Transformation of DNA into bacteria

Transformation of *E.coli* was by heat shock (Nishimura *et al.*, 1990) or by the high efficiency electroporation method of Dower *et al.* (Dower *et al.*, 1988). For electroporation, sterile recycled 0.2 cm Biorad electroporation cuvettes (ethanol

washed or autoclaved) were used. Ligation reactions were dialysed for 20 minutes against 10 % glycerol before electroporation, using 0.025 μm VS disc filters (Millipore).

Chapter Three: Inhibitor Studies on SR Ca^{2+}-ATPase

3.1. Introduction - Inhibitors of Ca^{2+}ATPases

A whole host of compounds exist that are able to inhibit the functioning of the Ca^{2+}-ATPase. These have been and currently are used extensively to study the mechanism of the pump and its importance in calcium signalling and homeostasis (Thastrup *et al.*, 1990; Thastrup *et al.*, 1989; Llopis *et al.*, 1991).

3.1.1. Mechanism of inhibition

Inhibitors of the Ca^{2+}-ATPase are generally hydrophobic and contain at least one hydroxyl moiety, which is likely to interact with the protein by hydrogen bonding. These compounds are structurally diverse with different hydroxyl group spacing and therefore unlikely to bind to the same site. Their hydrophobicity creates difficulties in identifying the actual site of binding on the ATPase.

Inhibition could be non-specific, following from binding at the lipid-protein interface. The ATPase is embedded in the membrane and the lipid environment around the protein is important for function (Mintz & Guillain, 1997). The lipid supporting highest activity is dioleoyl-phosphatidyl choline, DOPC (Lee *et al.*, 1995; Starling *et al.*, 1995). Other phospholipids with different fatty acyl chains or different headgroups support lower activities (East & Lee, 1982; Froud *et al.*, 1986a; Dalton *et al.*, 1998). An inhibitor that binds at the lipid-protein interface would change the environment around the ATPase and so reduce the activity of the ATPase. Specific inhibition is also possible, with the inhibitor binding at a particular site on the ATPase. This binding would be expected to show greater structural specificity than for binding at the lipid-protein interface.

3.1.2. Sesquiterpene lactones

The most specific and powerful inhibitors are the sesquiterpene lactones (Figure 3.1). Thapsigargin (Tg) and thapsigargicin (TgC) are both isolated from the umbilleferous plant *Thapsia gargancia* (Christensen *et al.*, 1982). Thapsivillosin A (TvA) is isolated from *Thapsia villosa* (Rasmussen *et al.*, 1981) and trilobilide (Tb)

is isolated from *Laser trilobum* (Holub *et al.*, 1973). Tg is specific for SERCAs (Lytton *et al.*, 1991; Davidson & Varhol, 1995) and does not inhibit the plasma membrane Ca^{2+}-ATPase or the Na^{+}/K^{+}-ATPase (Davidson & Varhol, 1995). Photolabelling using a thapsigargin azido derivative (Hua & Inesi, 1997) and chimeras of P-type ATPases have been used to evaluate the role of specific regions of the Ca^{2+}-ATPase in inhibitor binding (Norregaard *et al.*, 1993; Sumbilla *et al.*, 1993; Ishii *et al.*, 1994). Using chimeras of the Ca^{2+}-ATPase and Na^{+}/K^{+}-ATPases the region conferring Tg sensitivity was located in the first third of the Ca^{2+}-ATPase sequence (Norregaard *et al.*, 1993). Subsequently, Nørregaard *et al.* exchanged residues 253 - 284 (S3-M3 segment), which reduced the affinity for Tg from the picomolar range (Davidson & Varhol, 1995) to as much as 2 μM (Norregaard *et al.*, 1994). The role of the S3 stalk region was then studied by mutating residues in the stalk region (254 – 259) and observing the concentration dependence of inhibition by Tg (Zhong & Inesi, 1998). Yu *et al.* found that Tg resistant cells had developed mutations at residue 256 and implicated this residue in the interaction between SERCA and Tg (Yu *et al.*, 1998). Indeed Ma *et al.* (1994) concluded that the single mutation of Phe-256 decreased Tg sensitivity (Ma *et al.*, 1999). The structure of the transmembrane segments of SERCA from the recent crystal structure (Toyoshima *et al.*, 2000) can be seen in Figure 3.2. Indicated are the residues 254 and 259, in the stalk sector above helix 3, between which Tg is thought to bind.

The affinity of the ATPase for Tg is very high and was calculated to be greater than 2 pM at a pH 7.0, 26 ^{0}C (Davidson & Varhol, 1995). Tg inhibits both the calcium transport function (Sagara & Inesi, 1991) and pump activity (Wictome *et al.*, 1992). The importance of the hydroxyl groups for the inhibitory effect of these compounds has been demonstrated using trilobilide. The C7 and C11 hydroxyl groups are necessary for the inhibition since deoxytrilobilide (Figure 3.1), a derivative where the two hydroxy groups are absent is unable to inhibit the ATPase (Wictome *et al.*, 1994).

Effects of inhibitors on the conformational state of the ATPase have been studied using a variety of fluorescence methods. The shift of the Ca^{2+}-ATPase from the E1-E2 equilibrium can be monitored by the use of fluorescent labels such as 4-nitrobenzo-2-oxa-1,3-diazole, NBD, (Wakabayashi & Shigekawa, 1990) or fluorescein isothiocyanate, FITC. NBD and FITC react with Cys-344 and Lys-515 respectively and the fluorescence of these probes is sensitive to the conformation of

the ATPase, E1 or E2. Binding of calcium shifts the equilibrium to the E1 conformation and vanadate shifts the equilibrium to the E2 conformation. Addition of Tg shifts the ATPase to the E2 state (Wictome *et al.*, 1992). Phosphorylation of the Ca^{2+}-ATPase by P_i in the presence of Tg is decreased even though the enzyme is in the E2 conformation (Sagara *et al.*, 1992b). Sagara *et al.* proposed that Tg only interacts with Ca^{2+}-ATPase that has no calcium bound (Sagara *et al.*, 1992a; Sagara *et al.*, 1992b). They showed that if the Ca^{2+}-ATPase was pre-incubated with EGTA and Tg, followed by addition of calcium and then ATP to initiate reaction, there was no phosphorylation of the enzyme. However, if the ATPase was pre-incubated with calcium, and then Tg and ATP were added then a single cycle of ATP hydrolysis was observed before inhibition by Tg. Hence they concluded that only in the absence of calcium was a catalytically inactive enzyme complex formed that could no longer function. However, Wictome *et al.* found that this could not be so (Wictome *et al.*, 1995). If Tg and calcium bound competitively to the ATPase then the apparent affinity of the ATPase for calcium would decrease with increasing Tg concentration. However it was found that beyond a 1:1 molar ratio of Tg to ATPase, Tg had no further effect on the apparent affinity for calcium. Thus a simple 'dead end' complex (ATPase.Tg) could not be formed. Rather it was suggested that Tg bound with equal affinity to the E1, $E1Ca_2$ and E2 conformations but that when bound to E2, the ATPase could then undergo a further conformational change to a modified E2 state, $E2^ATg$: $E2 + Tg \leftrightarrow E2Tg \leftrightarrow E2^ATg$. It is the fact that the $E2Tg \leftrightarrow E2^ATg$ change was favourable that results in a shift towards the E2 conformations on addition of Tg. This model explains the lack of phosphorylation by P_i in the presence of Tg, if $E2^ATg$ (unlike E2) could not be phosphorylated by P_i (Wictome *et al.*, 1995).

3.1.3. 2,5-di(*tert*-butyl)-1,4-benzohydroquinone (BHQ)

The di-hydroxybenzene, BHQ, (Figure 3.3) inhibits the SR Ca^{2+}-ATPase with an IC_{50} of 0.4 μM (Wictome *et al.*, 1992) and like Tg, BHQ both stabilises the E2 conformation of the enzyme and decreases phosphorylation of the Ca^{2+}-ATPase by P_i (Wictome *et al.*, 1992). Thus a similar mechanism with the formation of the modified $E2^AI$ state was suggested (Khan *et al.*, 1995). However despite similar mechanisms it was shown the effects of Tg and BHQ on the E2-E1 equilibrium were additive, so BHQ and Tg must bind to separate sites on the ATPase (Khan *et al.*,

1995). Acetyl BHQ (Figure 3.3), in which the -OH groups are modified, has a much lower potency than BHQ. This highlights the importance of the two hydroxyl moieties (Wictome *et al.*, 1994). Although the two –OH groups in the sesquiterpene lactones have also been shown to be important the separations between the hydroxyl groups in the structures of BHQ and Tg are different so that their binding sites on the ATPase are likely to be different (Khan *et al.*, 1995). Both BHQ and Tg have been shown to inhibit the Ca^{2+}-ATPase of ER and SR in a number of cell types (Thastrup *et al.*, 1990; Llopis *et al.*, 1991; Sagara & Inesi, 1991).

3.1.4. Curcumin

Curcumin (di-feruloylmethane; Figure 3.3) is the major active pigment of turmeric and mustard, and contributes largely to the distinctive colour and flavour of this widely used spice and colouring agent. Curcumin is a pharmacologically active compound used in the treatment of anti-inflammatory diseases (Huang *et al.*, 1988) and has many cellular effects. Among the effects, curcumin acts as an anti-oxidant and induces apoptosis in human leukocyte cells (Kuo *et al.*, 1996), inhibits epidermal growth factor receptor kinase (Kuo *et al.*, 1996) and suppresses the transcription factor NF-κB (Singh and Aggarwal, 1995). Studies have shown that curcumin inhibits the SR Ca^{2+}-ATPase with an IC_{50} of 4 μM (Lockyer, 1997) and does not appear to be competitive with ATP. Unlike the other Ca^{2+}-ATPase inhibitors addition of curcumin to QF18 cells does not result in an increase in intracellular calcium levels (Lockyer, 1997). Indeed, pre-treatment with curcumin actually blocks the effects of Tb and BHQ. Thus as well as inhibiting the Ca^{2+}-ATPase curcumin appears to be able to block the passive efflux of calcium from ER. Recently, the mitochondrial F_0/F_1-ATPase has been shown to be inhibited by curcumin with a much higher IC_{50} of 45 μM (Zheng & Ramirez, 2000).

Unfortunately, the spectroscopic properties of this compound make fluorescence studies difficult because the broad absorption spectra of curcumin (λ max at 420-430 nm) overlaps the fluorescence spectra of calcium indicators such as Indo-1, the fluorescence of which is measured at 405 and 485 nm.

3.1.5. Ellagic acid

Ellagic acid (Figure 3.3) is a plant polyphenol present in the skins of soft fruits in the form of tannins (ellagitannins) from which it is released by hydrolysis (Stoner & Mukhtar, 1995). This antioxidant also exhibits pharmacological activity and functions through a number of mechanisms. It is a potential chemopreventive agent (Stoner & Mukhtar, 1995) and reduces haemorrhaging both in humans and animals (Botti & Ratnoff, 1964). Murakami *et al.* (Murakami *et al.*, 1991) showed that ellagic acid inhibitied the gastric H^+/K^+-ATPase with an IC_{50} of 2.1 μM. The IC_{50} of ellagic acid for SERCA was shown to be approximately 5 times this at 10 μM, with no apparent competition with calcium or ATP (Lockyer, 1997) and it does not shift the E1-E2 equilibrium as do other inhibitors (Lockyer, 1997). Ellagic acid produced less than 15 % inhibition of activity of the mitochondrial F_0/F_1-ATPase, at a concentration of 70 μM (Zheng & Ramirez, 2000).

3.1.6. Nonylphenol

Sokolove *et al.* showed that the Ca^{2+}-ATPase was inhibited by bis-phenol and nonylphenol (Sokolove *et al.*, 1986). Nonylphenol (Figure 3.3), a phenolic antioxidant, has a large hydrophobic tail and only one hydroxyl group and is thus likely to insert into the lipid bilayer and could be a non specific inhibitor of the type described earlier. A decrease in both the equilibrium constant for phosphorylation by P_i and in the E2 to E1 transition implies interaction of nonylphenol with the E2 form of the enzyme (Michelangeli *et al.*, 1990). Nonylphenol has recently been shown to induce sertoli cell death in rat testis, by inhibition of SERCA (Hughes *et al.*, 2000).

3.1.7. Diethylstilbestrol (DES)

Diethylstilbestrol (DES) is an artificial estrogen (Figure 3.3) first synthesised in 1938 (Dodds *et al.*, 1938). It was initially employed as a therapeutic agent to treat gynaecological problems (Noller & Fish, 1974) and its potential as an agent in prostate cancer therapy has been evaluated (Lau *et al.*, 2000). Inappropriate exposure to high levels of estrogens may actually result in reproductive and developmental toxicity (Gray *et al.*, 1997; Daston *et al.*, 1997). DES was found to

inhibit proton translocation of an H^+-ATPase (McEnery & Pedersen, 1986) and subsequently the effect of DES and related compounds on Ca^{2+}-ATPase activity of SR were studied (Martinez-Azorin *et al.*, 1992). At low concentrations of DES, a small increase in activity was observed but 15 μM DES gave approximately 50 % inhibition of activity. Trans-stilbene (Figure 3.3) which does not contain the important hydroxyl moieties or the side chains present in DES, does not inhibit Ca^{2+}-ATPase activity (Martinez-Azorin *et al.*, 1992). This highlights the structural importance of Ca^{2+}-ATPase inhibitors.

3.2 Methods

3.2.1. Data analysis

Compounds that bind to an enzyme without covalently modifying it, but lead to a loss of enzyme activity may be classed as reversible inhibitors. These may be further classified as competitive, non-competitive, un-competitive or mixed inhibitors (Fersht, 1985). In the following examples K represents association constants and k represents rate constants.

Competitive inhibition

A competitive inhibitor I binds to the active site of an enzyme and prevents the substrate S from binding, and likewise substrate S can bind and prevent I binding. So, S and I are in competition. Thus, in the presence of inhibitor, E can bind either substrate S or inhibitor I:

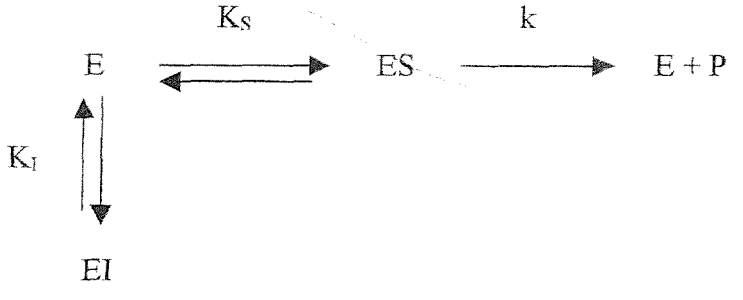

Non-competitive inhibition

If the substrate and the inhibitor can bind simultaneously to the enzyme the effects are different and can be described by the scheme:

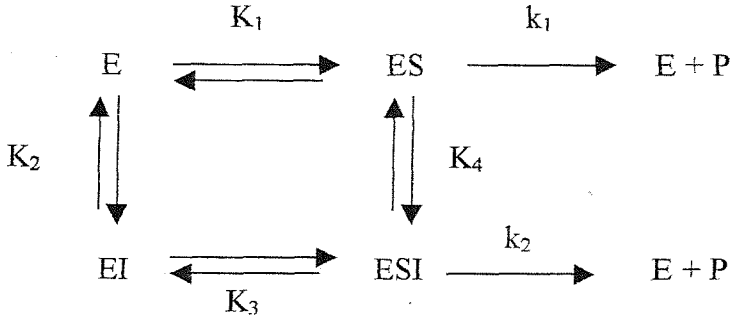

The simplest case where I and S can bind simultaneously is non-competitive inhibition. The binding of I has no effect on the binding of S (so that $K_1 = K_3$ and $K_2 = K_4$) and the inhibitor bound ESI form does not react, so that $k_2 = 0$, i.e. it forms a simple "dead end complex". The affinity for S is unaffected by binding of I but the maximum rate is reduced depending on the amount of enzyme in the ESI form. This depends simply on the concentration of I, and the association constant K_4. The rate is therefore reduced by a factor $(1+[I]K_4)$ The measured $k_{effective}$ is simply:

$$k_{effective} = k_1/(1+[I]K_4). \quad (1)$$

In some cases the rate constant k_2 may be *less* than k_1 but not equal to zero. In this case, as long as the rate of binding of inhibitor I is fast (the quasi-equilibrium assumption), an effective rate constant $k_{effective}$ can be defined as the sum of k_1 and k_2 weighted by the fraction of enzyme in the inhibitor-free (F) and inhibitor bound forms (F_I), respectively:

$$F = [E]/([E] + [EI]) = 1/(1 + [I]K_4) \quad (2)$$

$$F_I = [EI]/([E] + [EI]) = [I]K_4/(1 + [I]K_4) \quad (3)$$

$$k_{effective} = k_1 F + k_2 F_I$$

$$= k_1/(1+[I]K_4) + k_2[I]K_4/(1+[I]K_4) \quad (4)$$

Mixed inhibition occurs when the affinity for substrate S and/or the rate of reaction changes (i.e. K_1 no longer equals K_3 and k_2 is less than k_1). In un-competitive inhibition the inhibitor I binds to the enzyme substrate complex ES, but not to E (Fersht, 1985).

Effects of mixtures of inhibitors of the non-competitive type

One approach to determining whether sets of inhibitors bind to the same site on a protein or to different sites is to study the effects of pairs of inhibitors, to see whether or not the effects of the two inhibitors compete with each other. As described below, effects of many inhibitors on the steady state rate of ATP hydrolysis by the Ca^{2+}-ATPase fit well to simple non-competitive inhibition.

Two non-competitive inhibitors binding to the same site

The case where two inhibitors of the non-competitive type, I and J, bind to the same site on the protein can be described by the following scheme:

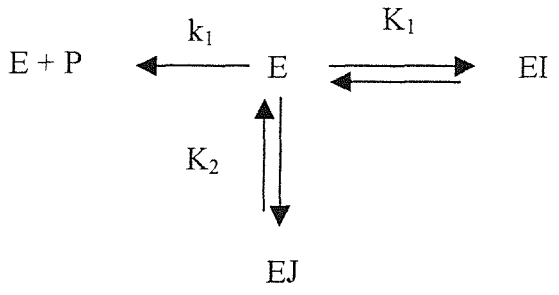

The association constants K_1 and K_2 are defined as follows:

$K_1 = [EI]/[E][I]$ (5)

$K_2 = [EJ]/[E][J]$ (6)

The fraction F of enzyme that is un-bound by inhibitor is given by:

$F = [E]/([E] + [EI] + [EJ])$ (7)

This is equal to:

$$F = \frac{1}{1 + K_1[I] + K_2[J]} \quad (8)$$

It is convenient to consider an experiment in which the concentration of one inhibitor (I) is varied in the presence of a constant concentration of the second inhibitor J. The fraction of the enzyme in the I-bound form EI, F_I , can be written as:

$$F_I = \frac{[EI]}{[E]+[EI]+[EJ]} = \frac{K_1[I]}{1+K_1[I]+K_2[J]} \quad (9)$$

This can be rearranged as follows:

$$F_I = \frac{K_1[I]/(1+K_2[J])}{(1+K_1[I]+K_2[J])/(1+K_2[J])} = \frac{[I]K_{eff}}{1+[I]K_{eff}} \quad (10)$$

where

$K_{eff}=K_1/(1 + K_2[J])$ (11)

Thus the presence of J decreases the effective affinity of the protein for I. This is equivalent to the effect of an inhibitor of the competitive type upon the affinity of a substrate for a protein.

An example where two inhibitors of the non-competitive type compete for binding to the same site is shown in Figure 3.4 graph 1, calculated from equation 8. Here it is assumed that the activity of the inhibitor bound enzyme is zero. The affinity K_1 for I has been set at $1x10^6$ M^{-1} and the affinity K_2 for J has been set at $1x10^7$ M^{-1}. In the absence of J (curve A), a plot of F, equivalent to fractional activity, against concentration of I shows a fractional activity of 0.5 at a concentration of 1 μM I as expected (50% binding when $[I]=1/K_1$). Figure 3.4 also shows a plot of F against concentration of I in the presence of 0.1 μM J, a concentration of J that will give half saturation of the inhibitor binding site with J in the absence of I (curve B). The fractional activity plot now starts at 0.5 and has dropped to half its initial value (fractional activity of 0.25) at 2.0 μM I. Thus the effective binding constant for I has halved in the presence of 0.1 μM J, as expected from equation (11). This shift in effective affinity can be shown more clearly in graph 1 by plotting activities in 0.1 μM J relative to the activity in 0.1 μM J alone, as shown by curve C.

Two inhibitors of the non-competitive type binding to separate sites

The case where two inhibitors of the non-competitive type, I and J, bind to the separate sites on the protein can be described by the following scheme:

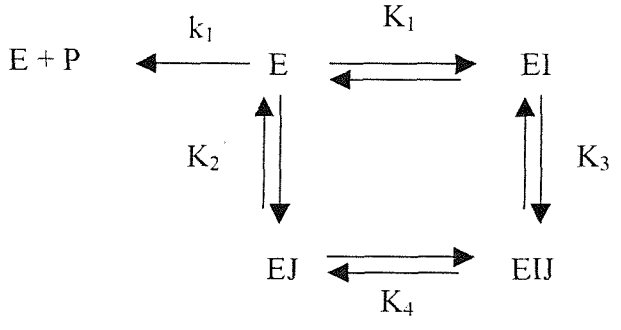

The association constants K_1-K_4 are defined as follows:

$K_1 = [EI]/[E][I]$ (12)

$K_2 = [EJ]/[E][J]$ (13)

$K_3 = [EIJ]/[EI][J]$ (14)

$K_4 = [EIJ]/[EJ][I]$ (15)

Only three of these four constants are independent since the law of microscopic irreversibility requires that

$K_1K_3=K_2K_4$ (16)

The fraction F of enzyme that is unbound by inhibitor is given by:

$F = [E]/([E] + [EI] + [EJ] + [EIJ])$ (17)

Substituting equations 12-15 into 17 gives:

$$F = \frac{1}{1+K_1[I]+K_2[J]+K_1K_3[I][J]} \quad (18)$$

If $K_1 = K_4$ (and $K_2 = K_3$) binding of inhibitor I will have no effect on binding of inhibitor J, and *vice versa.* That is I binds equally well whether or not J is already bound. However, if $K_4 > K_1$ (and $K_3 > K_2$) then binding is co-operative. Thus binding of I will *increase* the affinity for J and binding of J will *increase* the affinity for I. This could come about if binding of inhibitor results in a conformational change on the protein, leading to a conformation with increased affinity for inhibitor.

These possibilities are shown in Figure 3.4, graph 2. K_1 has been set at $1x10^6$ M^{-1} and K_2 at $1x10^7$ M^{-1} as previously. If $K_1 = K_4$ and $K_2 = K_3$ then the presence of J has no effect on the inhibition caused by I as shown in Figure 3.4, for a concentration of J of 0.1 μM (curve B); the concentration of I required to halve the initial activity is 1 μM, as in the absence of J. However, if $K_4 > K_1$ and $K_3>K_2$, the presence of J increases the apparent affinity for I. For example, as shown in graph 2 (curve C), if $K_4 = 10 \times K_1$ (so that $K_3 = 10 \times K_2$) the presence of 0.1 μM J decreases the concentration of I required to reduce the initial relative activity from 0.5 to 0.25 to 0.2 μM.

The effect of J on the apparent affinity of I can be calculated from equation 18. Equation 18 can be written as:

$$F = \frac{1}{1+K_1[I](1+K_3[J])+K_2[J]} \quad (19)$$

In the presence of J alone the fraction of enzyme free of inhibitor is

$$F_{J\,alone} = \frac{[E]}{[E]+[EJ]} = \frac{[E]}{[E]+K_2[E][J]}$$

$$F_{J\,alone} = \frac{1}{1+K_2[J]} \qquad (20)$$

The fractional activity in the presence of J, relative to that in the absence of J is given by the ratio $F/F_{J\,alone}$. The fractional activity is thus given by

$$Fractional\ activity = \frac{1+K_2[J]}{1+K_1[I](1+K_3[J])+K_2J} \qquad (21)$$

Rearranging gives

$$Fractional\ activity = \frac{1}{1+[I]K_1\left(\frac{1+K_3[J]}{1+K_2[J]}\right)} \qquad (22)$$

This is the normal equation for inhibition by I except that K_1 is replaced by:
$K_{deff} = K_1(1+K_3[J])/(1+K_2[J])$.

Thus if K_1, K_2 and K_3 are known, then the effective binding constant K_{deff} for I can be calculated as a function of the concentration of J.

Inhibitors that bind at multiple sites on the protein (the n site model)

In the above derivations it is assumed that each inhibitor binds to a single site on the protein. Inhibition of the Ca^{2+}-ATPase by nonylphenol does not fit to such a model as shown later; the dependence of inhibition on the concentration of nonylphenol is steeper than expected for an inhibitor binding to a single site. The simplest model to explain this pattern of inhibition is one in which the inhibitor binds to *n* identical sites on the protein, binding not affecting the affinity for the inhibitor. The fraction of enzyme without I bound is then given by

$$F = \frac{1}{(1+K_I[I])^n} \qquad (23)$$

where K_I is the affinity for I.

Inhibitors that cause stimulation at low concentrations (the two site model)

As will be described, some inhibitors cause a small increase in activity at low concentrations with inhibition appearing at higher concentrations. If the stimulation is not accounted for then this has significant effects on interpretation of the experimental data, and the interpreted K_I may be misleading. The point is made in Figure 3.5. In the absence of any initial stimulation, the affinity of the inhibitor $1/K_I$ corresponds to the concentration of inhibitor resulting in 50% of the initial activity. However, if stimulation occurs at low concentrations of the inhibitor, then the concentration of inhibitor giving 50% of the initial activity (point A in Figure 3.5) does not correspond to $1/K_I$. Rather, $1/K_I$ corresponds to the concentration of inhibitor at which the activity is 50% of the fully stimulated activity (i.e. the activity that would have been seen in the absence of any inhibition).

The simplest model to account for this stimulation is to assume that the inhibitor binds to a single site on the protein to cause stimulation.

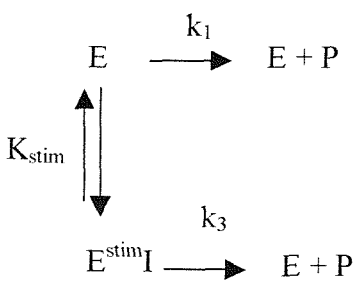

If the affinity for inhibitor at the stimulatory site is K_{stim} then the stimulated rate is given as a function of the concentration of I by:

$$k_{stim} = \frac{k_1}{1 + K_{stim}[I]} + \frac{k_3 K_{stim}}{1 + K_{stim}[I]} \qquad (24)$$

If binding at the stimulatory site is totally independent of binding at the inhibitory sites then the two can be treated separately, simply multiplying the stimulated rate calculated from equation 24 by the fraction of enzyme not bound to inhibitor, calculated from equation 18. This can be represented as in the following scheme:

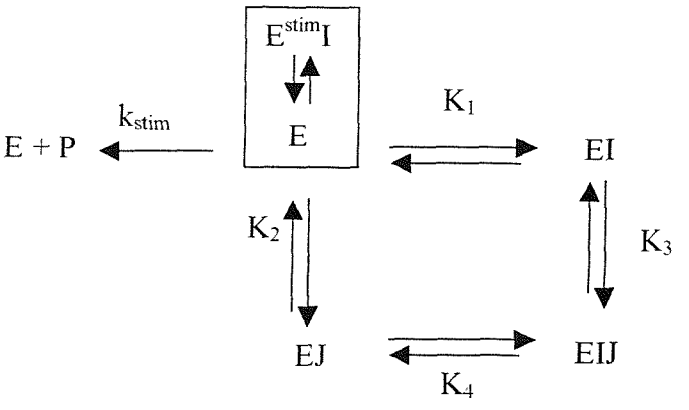

A complication of this analysis follows from the fact that stimulation occurs at low concentrations of inhibitor. The normal binding equations assume that the ligand is in large excess over the enzyme so that binding of ligand does not significantly deplete its concentration. In these cases, when the concentration of inhibitor is comparable to the concentration of protein it is necessary to use the full, quadratic form of the binding equation. The association constant K is written as

$$K = \frac{[EI]}{([E]^t - [EI])([I]^t - [EI])} \qquad (25)$$

where $[E]^t$ is the total concentration of enzyme and $[I]^t$ is the total concentration of inhibitor. This can be solved to give

$$[EI] = \frac{B - \sqrt{B^2 - 4C}}{2} \qquad (26)$$

where

$B = [E]^t + [I]^t + 1/K$

$C = [E]^t[I]^t$

The stimulated rate is then calculated as:

$k_{stim} = (([E]^t - [EI])k_1 + [EI]k_2)/[E]^t \qquad (27)$

and this equation is used instead of equation 24. Since inhibition occurs at much higher concentrations of inhibitor (where the concentration of bound inhibitor will be negligible compared to the total concentration), the simple form of the binding equation can be used to described inhibitor binding at the inhibition site, so that equation 18 can again be used to describe inhibition.

3.2.2. Data fitting

Experimental data were fitted to the above equations using the non-linear least squares fitting routine in Sigma Plot. The subroutines used are listed in Appendix 1.

3.2.3. Inhibition of the SR Ca^{2+}-ATPase Activity

In order to determine the binding constants of the Ca^{2+}-ATPase inhibitors, Ca^{2+}-ATPase activity assays were performed. A coupled enzyme assay was utilised (Section 2.3.3.), monitoring the oxidation of NADH spectrophotometrically, to measure ATPase activity. The inhibitors were dissolved in dimethyl sulfoxide (DMSO), with the final concentration of DMSO no more than 5 % v/v in the assay cuvette.

3.3. Results

3.3.1. Inhibition of SR Ca^{2+}ATPase activity by curcumin

Figure 3.6 shows the effect of curcumin on Ca^{2+}-ATPase activity. This graph shows the fractional activity of SR Ca^{2+}-ATPase in the presence of curcumin over a range of curcumin concentrations. The profile of curcumin effect shows an initial stimulation followed by the subsequent inhibition. This stimulation reaches 23% at 0.04 μM curcumin at which point the inhibition becomes prevalent. The activity is 50% of the initial activity at 6 μM curcumin, with maximum inhibition (~90 %) of activity at approximately 12 μM. The data fitted well to the two site model for stimulation and inhibition. The value of the rate constant giving the level of stimulated activity was well defined but, because stimulation occurred at very low concentrations of curcumin where most of the added curcumin will be bound, the dissociation constant describing binding to the stimulatory site (K_{dstim}) was not well defined. Any value for K_{dstim} less than ~ 0.1 μM gave an equally good fit, thus a high affinity of 0.01 μM was assumed for this site. Fitting the data then gave a dissociation constant for the inhibitory site (K_I) of 3.0 ± 0.5 μM, a stimulated fractional rate k_3 of 1.17 ± 0.03 and a residual fractional rate k_2 of zero (Table 3.1). The very different values for K_I and K_{dstim} suggest that the inhibitory and stimulation 'sites' are two distinct sites on the Ca^{2+}-ATPase. To check that these values were really different, attempts were made to fit the data forcing K_I and K_{dstim} to be equal (Figure 3.7). In this case vary poor fits to the data were obtained. The value for K_I is much lower than that for K_{dstim} indicating a higher affinity for the stimulatory site than the inhibitory site, described by the binding constant K_{dstim}.

3.3.2. Inhibition of Ca^{2+}-ATPase activity by curcumin analogues

The effects of curcumin analogues (Figure 3.8) were tested to determine the structural specificity of curcumin inhibition. Bisdesmethoxycurcumin is also an inhibitor of the Ca^{2+}-ATPase (Figure 3.6). In this case stimulation at low concentrations is less marked than for curcumin. 50 % inhibition of initial activity is achieved at 2.5 μM with approximately 90 % inhibition measured at 12 μM

(comparable to curcumin). The dissociation constant, K_I , of 1.23 ± 0.13 μM is slightly less than curcumin, with a residual fractional rate of 0 (Table 3.1).

The effect of compound 3 on Ca^{2+}-ATPase activity is shown in Figure 3.9. This compound lacks the –OH groups and gave a maximum of 40 % inhibition of Ca^{2+}-ATPase activity. Analysis of this compound using electrospray mass spectrometry (Figure 3.10) showed the sample was purely compound 3 (at a molecular weight of 364.2), with no curcumin contamination (at a molecular weight of 368.33).

Compounds 2 and 4 that do not contain –OH groups had no inhibitory effect up to 30 μM. Compound 5 has the same molecular weight as curcumin, the side groups on the ring structures are simply in exchanged positions. This compound causes a maximum of 20 % inhibition at 30 μM.

3.3.3. Inhibition of SR Ca^{2+}-ATPase activity by BHQ

Figure 3.11 shows the effect of BHQ on the fractional activity of the SR Ca^{2+}-ATPase. The range over which BHQ inhibits the ATPase is 0 – 2 μM, with approximately 20 % activity remaining at 2 μM BHQ. The concentration of BHQ required to give inhibition is 10 fold less than that of curcumin. The activity is 50 % of the initial activity at ~0.3 μM BHQ. The data does not exhibit stimulation at low concentrations of BHQ and were fitted to a single binding site model, with a dissociation constant for the inhibitory site, K_I of 0.19 ± 0.03 μM and a residual fractional rate of 0.14 ± 0.04 (Table 3.1).

3.3.4. Inhibition of SR Ca^{2+} -ATPase activity by PHQ

PHQ is a compound structurally similar to BHQ (Figure 3.12). Figure 3.13 shows the inhibitory effect of PHQ on the activity of SR Ca^{2+}-ATPase. PHQ inhibits activity over a 35 fold higher concentration range than BHQ, from 0 to 70 μM, with approximately 80 % inhibition of activity at this highest concentration. So, PHQ is less potent than BHQ with respect to its ability to inhibit Ca^{2+}-ATPase activity. 50 % inhibition of initial activity is produced at approximately 13 μM. This data were fitted to a single binding site model giving a dissociation constant K_I of 11.3 ± 0.5 μM and a residual fractional activity of 0.14 ± 0.03 (Table 3.1).

3.3.5. Inhibition of SR Ca^{2+}-ATPase activity by BHT

Butylatedhydroxy toluene (BHT) is another structurally similar compound to BHQ (Figure 3.12). Figure 3.14 shows the inhibitory effect of BHT on SR Ca^{2+}-ATPase activity. BHT inhibits over the concentration range 0 – 25 μM, approximately 10 fold higher than the concentrations of BHQ required for inhibition, with a maximum inhibition of about 80 %. 50 % inhibition of initial activity can be observed at 10 μM. This data shows stimulation of activity at low concentrations, unlike BHQ, with maximum stimulation at 0.8 μM. To account for the stimulation the data were fitted using the 'two site' model. If the dissociation for binding to the stimulatory site was fixed at 0.01 μM, as with curcumin, a poor fit was obtained (Figure 3.14). The best fit was obtained by fixing K_{dstim} at 1 μM. The data fitted to a dissociation constant for binding to the inhibitory site of 4.36 ± 0.1 μM, a stimulated fractional rate of 1.91 ± 0.3 and a residual fractional rate of 0 (Table 3.1).

3.3.6. Inhibition of SR Ca^{2+}-ATPase Activity by ellagic acid

Figure 3.15 shows the effect of ellagic acid on the fractional activity of the SR Ca^{2+}-ATPase. Ellagic acid inhibits activity over the concentration range 0 – 40 μM. The profile of this inhibition exhibits a stimulation of activity at low concentrations of ellagic acid followed by inhibition. Maximum stimulation of activity is reached at 0.6 μM, suggesting that binding to the stimulatory site is strong. 28 μM ellagic acid produces approximately 50 % inhibition of activity, with 40 μM producing about 70 % inhibition. The data were fitted to the 'two site' model, with an affinity of 0.01 μM assumed for the stimulatory site. A dissociation constant for binding to the inhibitory site of 25.5 ± 7.5 μM was obtained, with a stimulated fractional rate of 1.17 ± 0.02 and a residual fractional rate of 0 (Table 3.1). As observed with curcumin, the dissociation constant for binding to the stimulatory site is much lower than that for the inhibitory site indicating the presence of a higher affinity stimulatory site, with a lower affinity inhibitory site.

3.3.7. Inhibition of SR Ca^{2+}-ATPase activity by diethylstilbestrol (DES)

DES is another inhibitor of Ca^{2+}-ATPase activity. Figure 3.16 shows the inhibition of SR Ca^{2+}-ATPase activity in the presence of DES. DES inhibits activity from 0 – 25 μM, with approximately 75 % inhibition of activity produced at a concentration of 25 μM. The profile shows stimulation of activity, with a maximum at 1 μM, which is subsequently followed by inhibition. 50 % inhibition of initial activity is measured at approximately 10 μM. With the dissociation constant for the stimulatory site fixed at 0.01 μM the dissociation constant for the inhibitory site was 5.24 ± 1.19 μM, the stimulated fractional activity at 1.16 ± 0.07 and the residual fractional rate 0.09 (Table 3.1). Again the difference between the high affinity stimulatory site and the lower affinity inhibitory site can be noted from the predicted values.

3.3.8. Inhibition of SR Ca^{2+}-ATPase activity by nonylphenol

Figure 3.17 shows the effect of nonylphenol (NP) on the fractional activity of the SR Ca^{2+}-ATPase. NP affected activity over the concentration range from 0 – 25 μM. The profile of the effect of NP on Ca^{2+}-ATPase activity shows an initial stimulation followed by subsequent inhibition. At 1.6 μM NP the stimulation reaches a maximum of 37 % of original activity. The concentration of NP required for maximum stimulation is higher than the concentration required for stimulation by curcumin. This suggests that binding of NP to its stimulatory site is weaker. 50 % inhibition can be seen at 5 μM. Inhibition shows a steeper dependence on NP concentration than would be expected from binding at a single inhibitory site and the fit to a model with a single inhibitory site is poor (Figure 3.17, graph A). With the dissociation constant for the stimulatory site fixed at 1 μM, stimulation occurred at lower concentrations of NP than observed experimentally, and levels of inhibition were higher than observed experimentally. Fixing the value at 0.01 μM gave a worse fit. A free fit to the data was also very poor. Attempts were made to fit just the inhibitory part of the curve (10 – 25 μM). As shown in Figure 3.18 (A), the fit is poor. In particular, the experimental data shows a steeper inhibition curve than that predicted by the 'two site model'. This suggests that the inhibitor may in fact follow, not from binding to a single inhibitory site, but from binding to more than one

inhibitory site. As shown in Figure 3.18 (B), the inhibitory part of the curve can in fact be fitted well to such a model. This model for inhibition was then incorporated into the stimulatory/inhibitory model (Section 3.2.1.), giving the n site model, and the whole data set were fitted. Figure 3.17 shows the whole data set fitted using the 'n site model'. Equally good fits to the data were obtained for a range of values for the number n of inhibitory binding sites greater then 3. Since the important parameter for these experiments was not the value of n but the value for the inhibitory binding constant, the value of n was fixed at 3. This gave a value for the inhibitor dissociation constant of 11.1 ± 1.9 μM, the stimulated fractional activity of 2.51 ± 1.8 and a residual fractional rate of 0 (Table 3.1).

3.3.9. Inhibition of Ca^{2+}-ATPase activity by two inhibitors

Many compounds are able to inhibit Ca^{2+}-ATPase activity. It seems feasible that some of the binding sites must overlap. If two compounds, I and J, bound to the same inhibitory site on the Ca^{2+}-ATPase then they would compete for binding. Thus, the affinity for inhibitor I in the presence of inhibitor J would decrease i.e. the dissociation constant would increase.

3.3.10. Effects of mixtures of PHQ and BHQ

The effect of BHQ on the inhibitory profile of PHQ was investigated. Given their similar structures, inhibition of the ATPase by PHQ and BHQ would be expected to be competitive, and this is indeed what is observed (Figure 3.13). In the presence of BHQ, PHQ inhibits ATPase activity (Figure 3.13), however 70 μM PHQ inhibits activity by less than 50 % (a concentration that gives 80 % inhibition in the absence of BHQ). Fixing the residual fractional activity at 0.14, the effect of PHQ fits to a dissociation constant for the inhibitory site of 46.4 ± 5.0 μM (Table 3.1) compared to 11.3 μM in the absence of BHQ. The increase in the dissociation constant becomes clearer in the activity plots if the effect of PHQ is plotted starting from a fractional activity of 1. Thus BHQ decreases the affinity of PHQ for the ATPase: the compounds are competitive and bind to the same inhibitory site. With a dissociation constant of 0.19 μM for BHQ (Table 3.1) the affinity for PHQ in the presence of 0.4 μM BHQ (an effective K_d) can be calculated. Using equation 11 (for

two inhibitors of the non-competitive type competing for binding to the same site)the K_{deff} is 35.0 μM, in good agreement with the experimental value.

3.3.11. Effects of mixtures of BHQ and curcumin

Inhibition by curcumin in the presence of 0.4 μM BHQ fits to a simple single site inhibitory model, with no evidence for an initial stimulatory phase (Figure 3.6). Competition between BHQ and curcumin for binding to the inhibitory site would have been expected to result in a reduced affinity of curcumin for the inhibition site. In fact the affinity increases, i.e. inhibition by curcumin in the presence of BHQ is seen over a lower curcumin concentration than in the absence of BHQ. Indeed the dissociation constant for binding to the inhibitory site was 0.81 ± 0.06 μM compared to 3.0 μM in the absence of BHQ (Table 3.1). This suggests some allosteric effect on the Ca^{2+}-ATPase, with BHQ shifting the Ca^{2+}-ATPase into a conformational state with a higher affinity for curcumin.

A similar effect is seen in studies on the effect of curcumin on inhibition by BHQ, where the presence of curcumin leads to an increase in affinity for BHQ (Figure 3.11). The dissociation constants for the inhibitory site are 0.07 ± 0.01 μM with BHQ alone, and 0.17 μM in the presence of curcumin. (Table 3.1).

3.3.12. Effects of mixtures of BHT and BHQ

The effect of BHQ, on inhibition by BHT was measured (Figure 3.14). BHT is able to inhibit activity with ~ 50 % inhibition of initial activity at 5 μM (compared to 10 μM in the absence of BHQ). The data were fitted to the two site model for stimulation and inhibition. The dissociation constant for binding of BHT to the stimulatory site was fixed at 1 μM giving a dissociation constant for the inhibitory site was 1.62 ± 0.52 μM in the presence of BHQ compared to 4.36 μM in the absence of BHQ.

3.3.13. Effects of mixtures of ellagic acid with curcumin and BHQ

The effects of curcumin and BHQ on the inhibition of the ATPase by ellagic acid were investigated. In the presence of curcumin, ellagic acid inhibits ATPase

activity (Figure 3.15). A stimulation is observed at low concentrations of ellagic acid. 50 % inhibition of activity is measured at ~ 8 μM. The data were fitted using the two site model for stimulation and inhibition. Fixing the stimulatory site dissociation constant at 0.01 μM, the inhibitory site dissociation constant, K_I , fitted to 6.6 ± 2.7 μM compared to 25.5 μM in the absence of curcumin.

Likewise in the presence of BHQ (Figure 3.15) the data were fitted using the two site model for stimulation and inhibition giving values of K_I = 9.78 ± 2.6 μM. Again a stimulation of activity at low inhibitor concentrations was observed. In the presence of BHQ 50% inhibition of activity was measured at approximately 10 μM, (in the absence of BHQ this was 28 μM). This decrease in the dissociation constant implies that the compounds are binding to different inhibitory sites, and that the presence of BHQ actually increases the affinity of ellagic acid for the ATPase.

3.3.14. Effects of mixtures of DES with curcumin and BHQ

The effects of BHQ and curcumin upon the inhibitory profile of DES were also measured. In the presence of curcumin, DES still inhibits ATPase activity (Figure 3.16). 50 % inhibition of initial activity was observed at approximately 10 μM. A stimulation of activity at low concentrations of DES was not seen and therefore a single binding site model was used to fit the data. A dissociation constant for binding to the inhibitory site of 5.08 ± 1.26 μM in the presence of curcumin was obtained. In the absence of curcumin this value was 5.24 μM (Table 3.1).

In the presence of BHQ, a stimulation of activity was also not seen and the data were fitted to the two site model for stimulation and inhibition (Figure 3.16). A dissociation constant for the inhibitory site of 1.28 ± 0.2 μM was obtained. In the presence of BHQ, 50% inhibition of initial activity can be seen at 2 μM DES, in the absence of BHQ this was observed at 10 μM. These values, in the presence of both BHQ and curcumin, show that the dissociation constant for DES has decreased. This is consistent with an increase in affinity and binding of DES and curcumin, and DES and BHQ, to separate inhibitor sites on the Ca^{2+}-ATPase.

3.3.15. Effects of a mixture of nonylphenol and BHQ

To test whether BHQ and NP bind to the same site on the Ca^{2+}-ATPase the effect of a mixture of the two inhibitors was tested. Figure 3.17 shows the effect of BHQ on the profile of the effect of NP on the Ca^{2+}-ATPase. Stimulation of activity was seen, followed by an inhibitory effect. The 'n site model' was used to fit the data, with n sites fixed at 3. The dissociation constant for binding to the inhibitory site was 6.76 ± 1.55 μM, as compared to 11.1 μM in the absence of BHQ (Table 3.1).

3.4 Discussion

3.4.1. Stimulatory and inhibitory effects of Ca^{2+}-ATPase inhibitors

The effect of several inhibitors on the Ca^{2+}-ATPase was looked at using measurements of Ca^{2+}-ATPase activity. Some of the inhibitors of the ATPase, such as curcumin, stimulate activity at low concentrations, with inhibition prevalent at higher concentrations. Curcumin for example increases activity by a maximum of 17 % (Figure 3.6) and low concentrations of DES, ellagic acid and nonylphenol also increase activity with inhibition being observed as the concentrations increase (Figures 3.15-3.17). A variety of compounds have been shown to stimulate the ATPase, including diethylether (Bigelow & Thomas, 1987), short chain alcohols (Melgunov *et al.*, 1988), jasmone (Starling *et al.*, 1994) and the pyrtheroid deltamethrin (Jones & Lee, 1986). Since the inhibitors of the highest specificity and affinity, the sesquiterpene lactones, show no stimulatory phase with only inhibition it is likely that stimulation and inhibition follow from binding to different sites on the ATPase. Table 3.2 shows the K_I values obtained by fitting the data to the two site model. Also given are values of $K_{0.5}$ taken directly from the inhibition curves as the concentration giving 50 % inhibition of activity (without accounting for stimulation). The values of K_I and $K_{0.5}$ are very different and in each case the K_I is lower than the apparent $K_{0.5}$, as expected. Thus, it is important to account for stimulation in deriving the binding constant for inhibition.

There are two possibilities that could explain the stimulatory effect of the inhibitors on the Ca^{2+}-ATPase. The first is that the inhibitory and stimulatory sites on the Ca^{2+}-ATPase could be the same, with the inhibitor increasing the rate of one or more steps in the reaction cycle (resulting in stimulation) and decreasing the rate of other steps leading to inhibition. This seems unlikely since the apparent inhibitor binding constants are different for stimulation and inhibition (Table 3.1). As shown in Figure 3.7, the very poor fit to the data is obtained if the two binding constants are forced to be equal. Nevertheless, only apparent inhibitor binding constants are obtained from the kinetic analysis, and these could be different to the true binding constants (in the same way that K_m and K_d values for substrates can be different).

The second possibility is that the stimulatory and inhibitory sites are different sites. This raises the question of whether there are separate stimulatory and

inhibitory sites for all the inhibitors looked at or whether there is one stimulatory site to which all the inhibitors bind, and numerous inhibitory sites. Unfortunately, stimulation occurs at very low concentrations and the fitting procedure gave only an upper limit for K_{dstim}. It was not therefore possible to determine whether or not the inhibitors competed for binding to the stimulatory sites.

3.4.2. Structural importance of the inhibitors of Ca^{2+}-ATPase activity

There are a wide variety of inhibitors of the Ca^{2+}-ATPase. These are generally hydrophobic compounds but with very diverse structures. In the 1,4-dihydroxybenzenes (Figure 3.12) the hydrophobic groups at positions 2 and 5 are essential for activity (Khan *et al.*, 1995); with the amyl group being the optimal size for inhibitor potency. This implies that the groups at the 2 and 5 positions are likely to insert into the same kind of hydrophobic pocket on the ATPase of limited size. In contrast bisdesmethoxycurcumin inhibits ATPase activity with the same potency as curcumin (Figure 3.6), showing that the methoxy groups that flank the –OH groups in curcumin are not essential for activity. Removal of the –OH residues from curcumin analogues 2 and 4 (Figure 3.8) removes their inhibitory action. Moreover, switching the methoxy and the -OH groups, as in compound 5, also renders this compound inactive. Thus the presence of two –OH groups in the right position are essential for activity. Removal of both the –OH groups and the hydrophobic chains in DES produces trans-stilbene (Figure 3.3), which has no inhibitory effect on ATPase activity (Andersen *et al.*, 1982). Two compounds related in structure to DES are resveratrol and piceatannol (Figure 3.3), which only contain three or four –OH groups and not the ethyl groups that flank the central carbon-carbon double bond in DES. Both resveratrol and piceatannol inhibit the mitochondrial F_0/F_1-ATPase (Zheng & Ramirez, 2000), piceatannol having a higher affinity (IC_{50} = 8 μM) than resveratrol (IC_{50} = 19 μM). However resveratrol, a component of red wine and grapes, did not inhibit SERCA up to a concentration of 80 μM (unpublished data). It has also been shown that resveratrol has no effect on a Na^+/K^+-ATPase (Zheng & Ramirez, 2000).

The positions of the –OH groups is important for the inhibition of the Ca^{2+}-ATPase, yet the separations between these positions is different in the different inhibitors. The separation between the two hydroxy oxygen atoms in the 1,4-

dihydroxybenzenes is 5.5 Å (Patil *et al.*, 1984), compared to the separation of 17 Å between the two hydroxy oxygen atoms of curcumin (Mathieson, 1968). The conjugated system existing in curcumin makes this a flat rigid molecule thus this distance is likely to be the relevant one for the inhibitor bound at the inhibitory site. Trilobilide contains two hydroxy oxygen atoms that are separated by 3.64 Å (Kutschabsky *et al.*, 1986). In ellagic acid, hydroxy oxygen atoms on the same ring are separated by 2.65 Å, whilst those across the molecule are separated by distances of 8.33 and 9.65 Å (Mathieson, 1968).

3.4.3. Investigation of the binding sites of the Ca^{2+}-ATPase inhibitors

A common feature of the inhibitors is the presence of hydroxyl residues that are proposed to interact with the Ca^{2+}-ATPase, and the absence of any charged groups. The importance of these -OH groups has been demonstrated using the compounds deoxytrilobilide and acetyl BHQ (Wictome *et al.*, 1994). Previously, Tg and BHQ have been shown to bind to separate sites on the ATPase using fluorescence techniques (Khan *et al.*, 1995). Curcumin, with its characteristic yellow colour interferes with fluorescence measurements and therefore this type of study could not be used. So a kinetic method was employed. The effects of mixtures of inhibitors were looked at to determine whether the inhibitors were competitive, or bound to separate sites on the Ca^{2+}-ATPase (Section 2.3.9.). It would be expected that if two inhibitors were to bind to the same site, the presence of one inhibitor would decrease the affinity of the second inhibitor, i.e. it would be harder to bind to the ATPase. This procedure cannot however be used with the sesquiterpene lactones because of their high affinities.

Curcumin and BHQ are non-competitive inhibitors, in that they do not compete with ATP and therefore do not bind to the ATP binding site (Lockyer, 1997). The observation that ellagic acid is a potent inhibitor of numerous protein kinases might suggest that ellagic acid binds to the nucleotide binding site on the kinases, but this is probably not the case since inhibition of the protein kinases is not simply competitive with ATP (Yamasaki *et al.*, 1997). Similarly, inhibition of the ATPase by ellagic acid is not competitive with ATP (Lockyer, 1997). Table 3.1 shows the results for the mixtures of inhibitors. As would be expected from their similar structures BHQ and PHQ compete for binding, therefore interacting at the

same inhibitory site. In contrast the presence of BHQ actually increases the affinity of the ATPase for curcumin and *vice versa* (Figures 3.6 and 3.11; Table 3.3). So, the results clearly show that curcumin and BHQ must bind to separate sites on the ATPase. Furthermore, the binding of one must increase the affinity of the ATPase for the other. Knowing the K_d values for the two inhibitors separately, equation 22 can be used to calculate the effective dissociation constants for binding of the first inhibitor in the presence of another (K_{d3} and K_{d4}). Values for these dissociation constants are given in Table 3.3. The calculated dissociation constant for BHQ decreases by a factor of 5 on binding curcumin and the calculated dissociation constant for curcumin decreases by a factor of 3.5 on binding BHQ. The close agreement of these values (which should theoretically be equal) suggests that the method of analysis is correct.

Similar effects are observed with mixtures of BHT, ellagic acid, DES and nonylphenol; the presence of 0.4 μM BHQ increases their affinities for the ATPase by a factor of between 2 to 6 (Table 3.4). Ellagic acid also increases the affinity of the ATPase for curcumin by a factor of ~7 but the presence of 3 μM curcumin had no effect on the apparent affinity for diethylstilbestrol (Table 3.1 and Figure 3.16). This shows that curcumin and diethylstilbestrol must bind to separate sites on the ATPase with the affinity for curcumin being the same for diethylstilbestrol-bound and free ATPase (Table 3.4).

An increase in affinity for one inhibitor on binding a second inhibitor is consistent with the previous proposal (Wictome *et al.*, 1995) that inhibitors bind to the E1 and E2 conformations of the ATPase with equal affinity but that binding to E2 leads to a conformation change to a new state $E2^{A}I$:

$$E2 + I \leftrightarrow E2I \leftrightarrow E2^{A}I$$

In terms of this model $E2^{A}I$ would have a higher affinity for the second inhibitor than E2.

The inhibition by nonylphenol is different to the inhibition seen with other inhibitors, the concentration dependence suggesting that the inhibition results from binding to more than one site on the ATPase. Indeed, fitting the data to the two-site model (Figure 3.17) did not fit the data well. Nonylphenol differs from the other inhibitors structurally, containing only one –OH group, and therefore nonylphenol may interact non-specifically with the ATPase to cause inhibition. The membrane environment is important for the function of the ATPase (Lee *et al.*, 1995; Mintz &

Guillain, 1997; Lee, 1998) and disruption would decrease the rate of ATP hydrolysis. Thus at high concentrations NP may act as a detergent. By binding at the lipid protein interface surrounding the ATPase, with the -OH group located at the lipid-water interface, the environment around the ATPase would be changed, decreasing ATPase activity. It has been suggested that the effects of long – chain alcohols on ATPase activity follows from such an interaction (Froud *et al.*, 1986b).

The hydrophobicity of the inhibitors suggests that the inhibitors could bind in the transmembrane region of the Ca^{2+}-ATPase. The structure of the Ca^{2+}-ATPase shows four stalk regions close to the membrane surface, connected to four of the transmembrane α -helices (Jorgensen *et al.*, 1977). Stalk region S3, connected to the third transmembrane α -helix, between residues 254 and 259 has been shown to be important for binding thapsigargin (Figure 3.2) and another class of inhibitor, cyclopiazonic acid (Blostein *et al.*, 1993). However, binding sites for the two inhibitors do not completely overlap since mutation of Phe-256 reduces the affinity for thapsigargin but not for cyclopiazonic acid (Blostein *et al.*, 1993). It is possible therefore that this region of the ATPase contains multiple binding sites for inhibitors. Binding to some of these sites might be relatively non-specific. For example, whereas inhibition by the sesquiterpene lactones is highly specific for the SR/ER Ca^{2+}-ATPases, ellagic acid inhibits H^+/K^+-ATPase as well as Ca^{2+}-ATPase (Toyoshima *et al.*, 2000) and curcumin and diethylstilbestrol, but not ellagic acid, are also inhibitors of the mitochondrial F_OF_1-ATPase (Moller *et al.*, 1996).

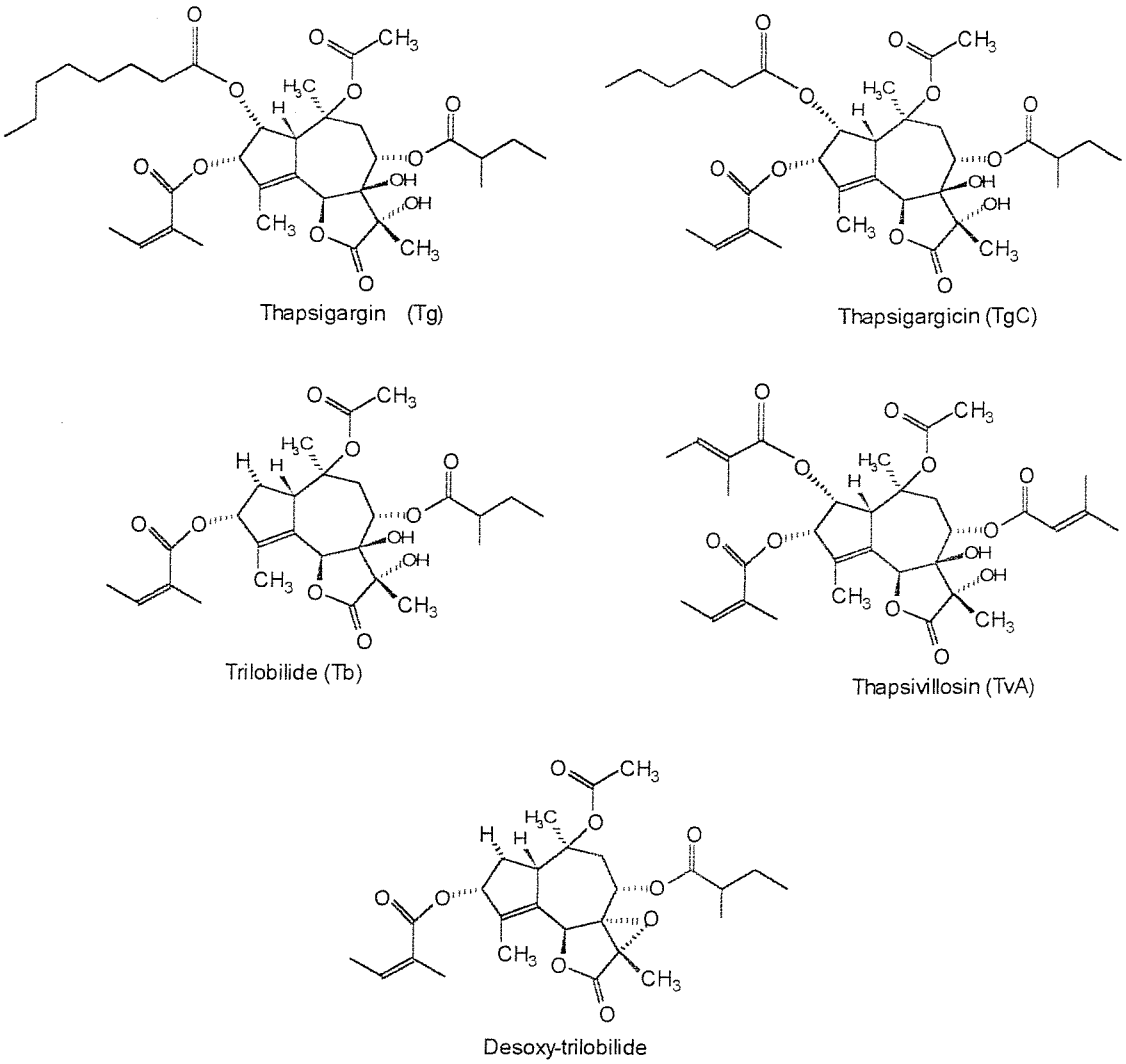

Figure 3.1. Structures of the sesquiterpene lactone inhibitors of the Ca^{2+}-ATPase and the derivative desoxy-trilobilide.

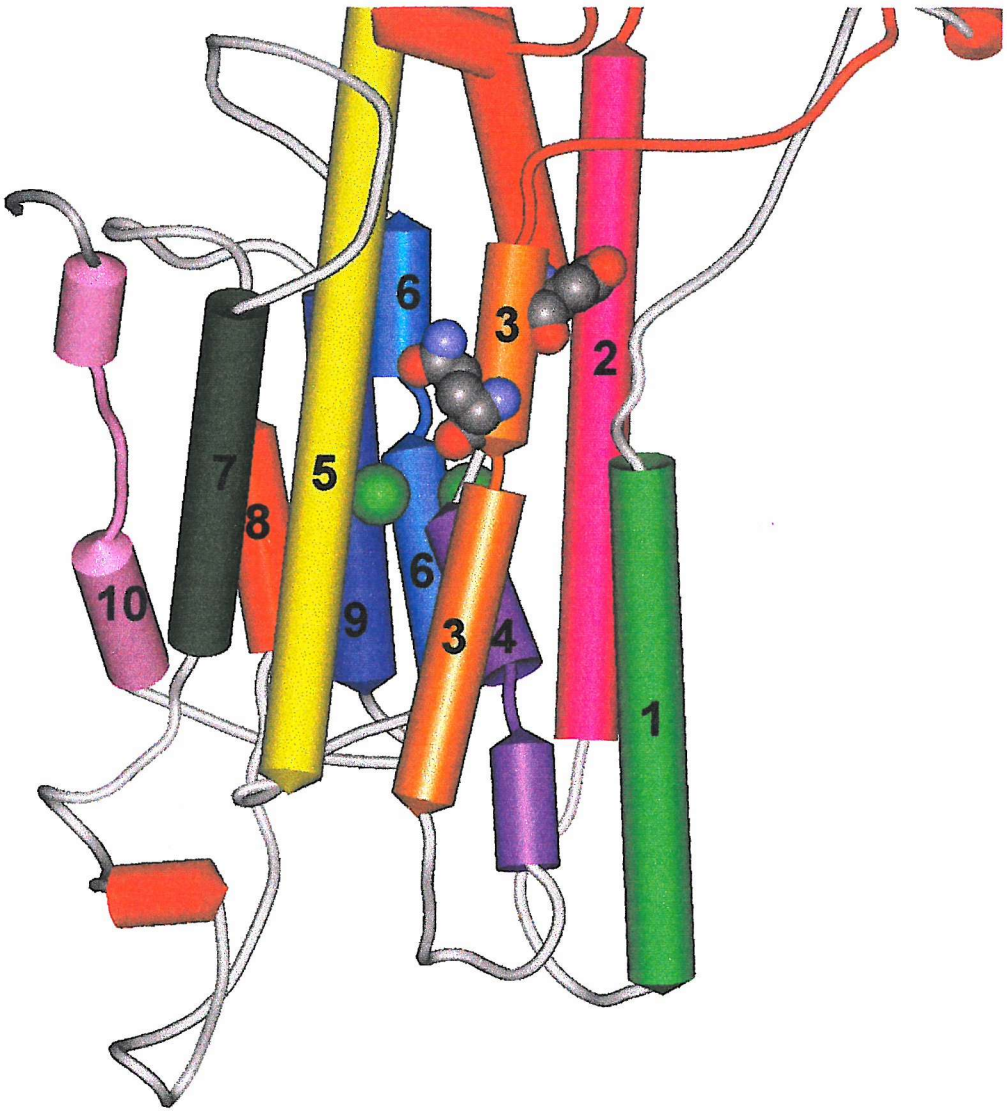

Figure 3.2. The binding site of thapsigargin in the SERCA1 structure

The diagram is taken from the 2.6 Å structure of SERCA 1 (Toyoshima *et al.*, 2000). The 10 trans-membrane α-helices are numbered. The green spheres represent the two calcium ions. Indicated are the residues Asp-254 and Gln-259 in the stalk sector above trans-membrane helix 3. These are the outermost residues in the portion where thapsigargin is thought to bind.

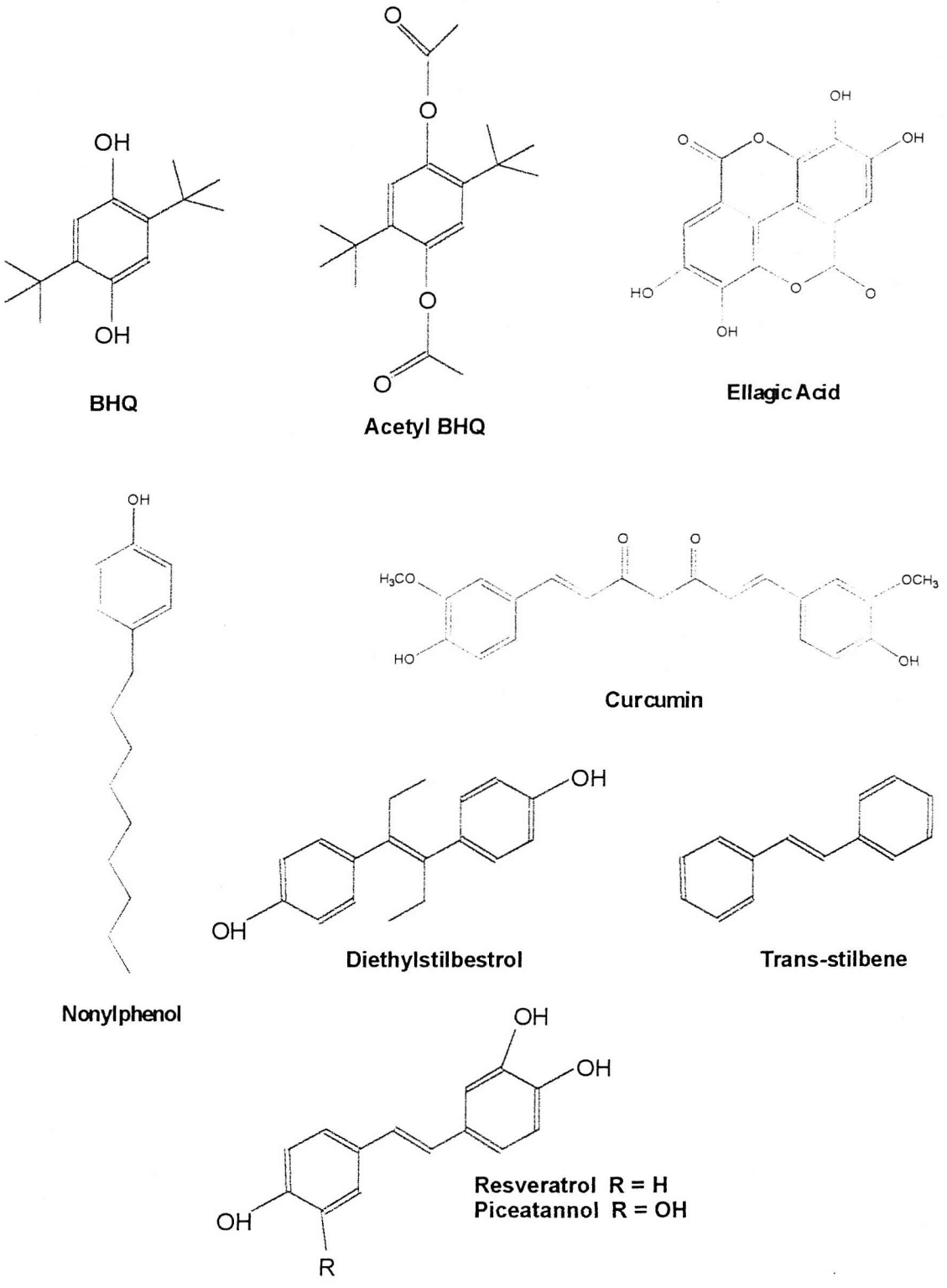

Figure 3.3. Structures of inhibitors of the Ca^{2+}ATPase and derivatives

BHQ, ellagic acid, nonylphenol, curcumin and diethylstilbestrol are all inhibitors of Ca^{2+}-ATPase activity. The derivatives are acetyl BHQ, trans-stilbene, resveratrol and piceatannol.

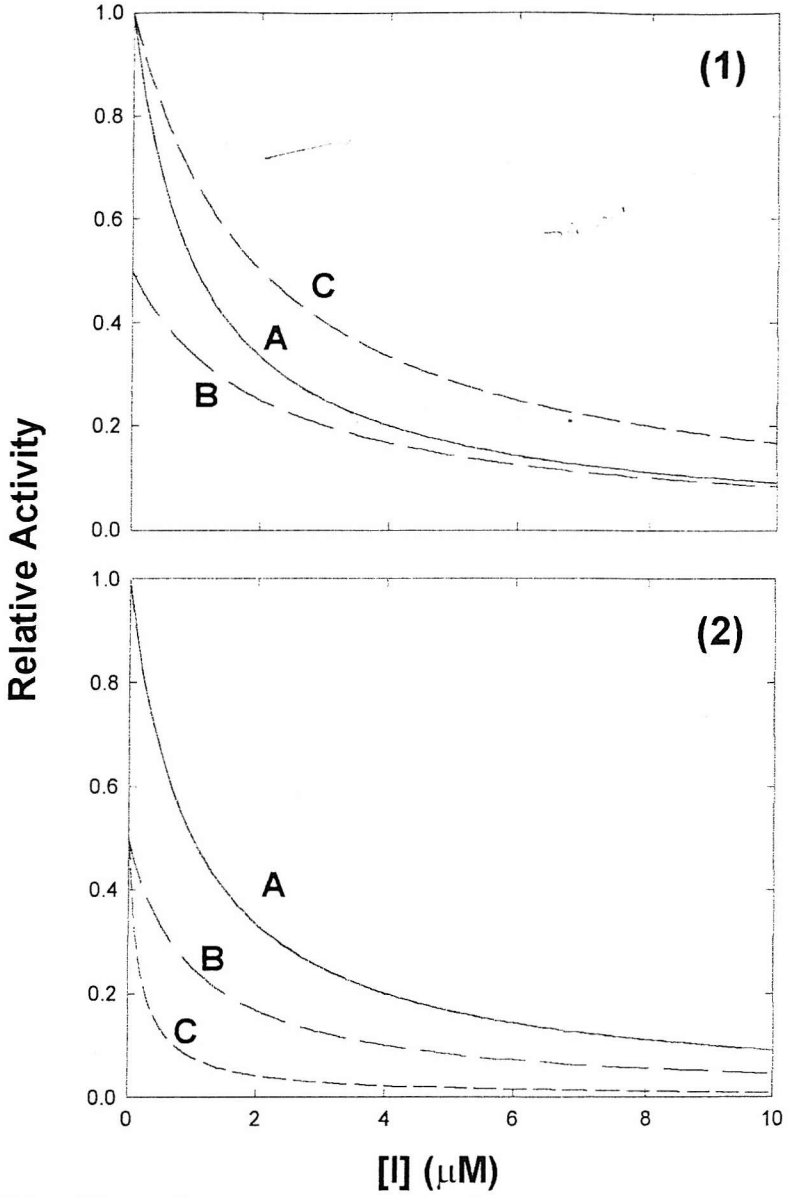

Figure 3.4. The effects of non-competitive inhibitors

Fractional activities were calculated as a function of the concentration if inhibitor I, assuming zero activity for inhibitor bound enzyme. Association constants K_1 for I of $1x10^6\ M^{-1}$ and K_2 for J of $1x10^7\ M^{-1}$ have been used. Graph (1) shows the effects of two-non competitive inhibitors binding to the same site on a protein: (A) shows fractional activity in the absence of J; (B) shows fractional activity in the presence of 0.1 μM J, calculated relative to the activity in the absence of inhibitor; (C) shows curve (B) but now expressed relative to the activity in 0.1 μM J alone. Graph (2) shows the effects of two-non competitive inhibitors binding to separate sites on a protein: (A) shows fractional activity in the absence of J; (B) shows fractional activity in the presence of 0.1 μM J, when $K_4 = K_1$ and $K_3 = K_2$; (C) shows fractional activity in the presence of 0.1 μM J, when $K_4 = 10 \times K_1$ and $K_3 = 10 \times K_2$.

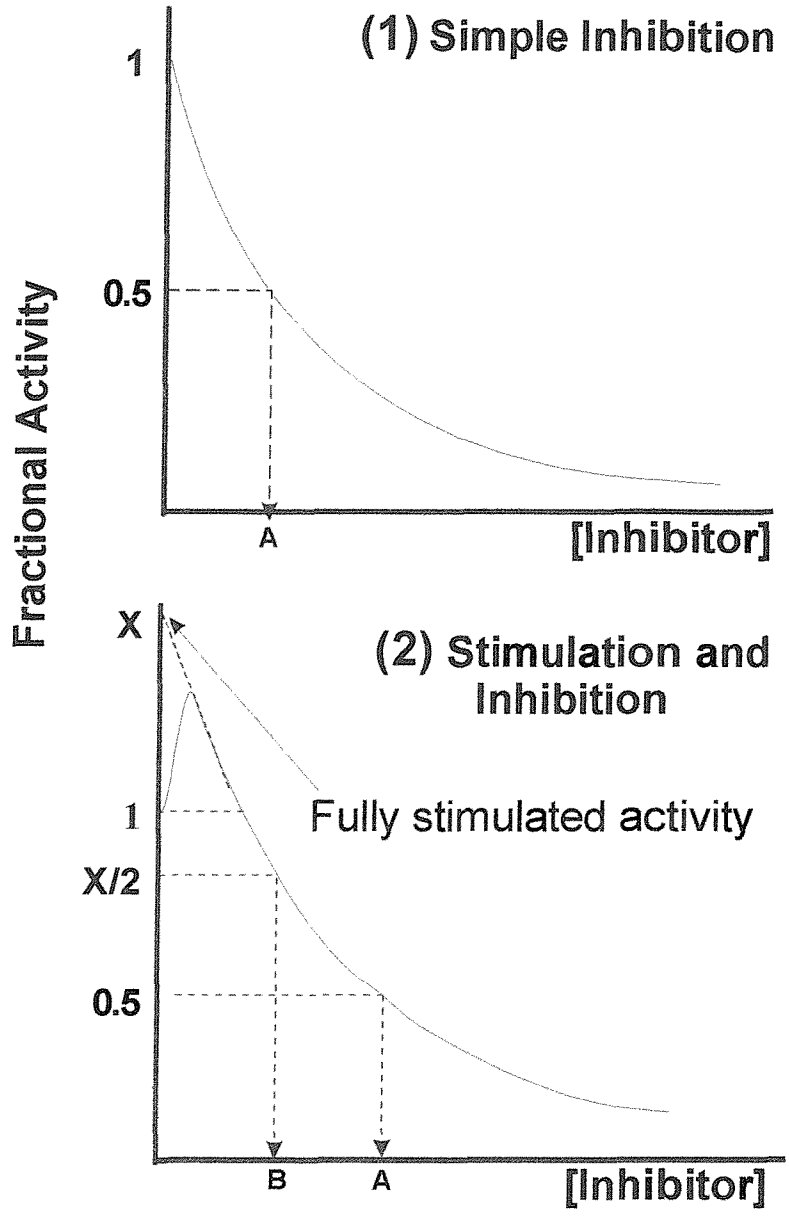

Figure 3.5. The effects of an inhibitor causing stimulation at low concentrations
Graph (1) shows simple inhibition where the concentration of inhibitor resulting in 50 % inhibition (point A) is equal to $1/K_I$. Graph (2) shows an inhibitor that causes stimulation at low concentrations and inhibition at higher concentrations. In this case, the concentration of inhibitor giving 50 % inhibition of initial activity (point A) does not equal $1/K_I$. Rather, the inhibition curve needs to be extrapolated back to give the fully stimulated activity (X) that would have been observed in the absence of any inhibition, as shown by the dotted line. The concentration giving 50 % of this fully stimulated activity (point B) is then equal to $1/K_I$.

Figure 3.6. The effect of curcumin on Ca^{2+}-ATPase activity.

Activities were measured in the presence of the given concentrations of curcumin at an ATP concentration of 2.1 mM, in the presence of a maximally stimulating concentration of Ca^{2+} (ca 10 μM). (A) The solid line shows a fit to the two site model for stimulation/inhibition, giving the values listed in Table 3.1. The insert shows the effects of bisdesmethoxycurcumin on Ca^{2+}-ATPase activity, measured under the same conditions as for curcumin. The solid lines show a fit to the one site model for inhibition, giving the values listed in Table 3.1. (B) Effects of curcumin on fractional activity in the presence of 0.4 μM BHQ. The solid line shows a fit to the one site model with the values given in Table 3.1.

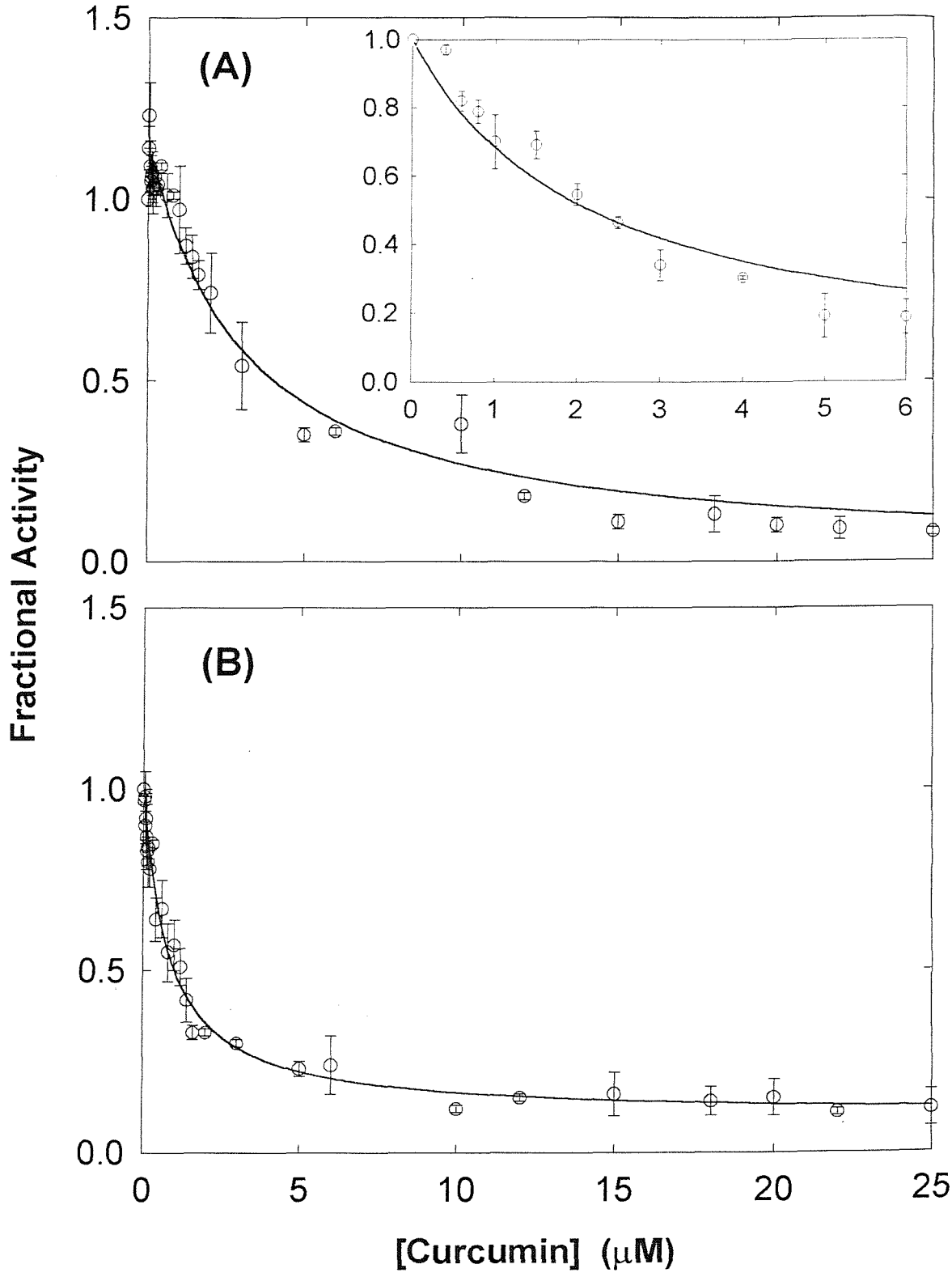
(A)
(B)
Fractional Activity
[Curcumin] (μM)
1.5
1.0
0.5
0.0
0
5
10
15
20
25
0.8
0.6
0.4
0.2
1
2
3
4
5
6

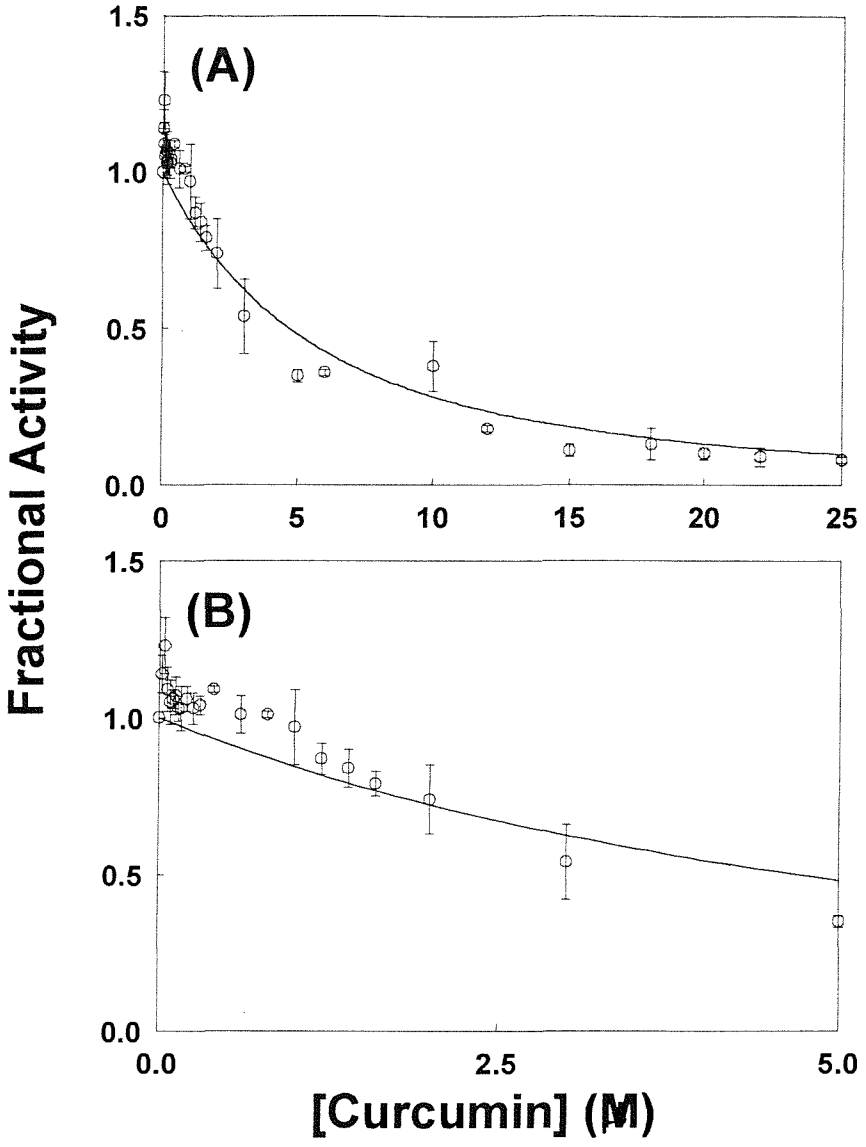

Figure 3.7. The effect of curcumin on Ca^{2+}-ATPase activity

The figures show the fractional activity versus curcumin concentration. The data were fitted using the two site model, with $K_{dstim} = K_I$. (A) shows the full data set; (B) shows the data up to 5 μM curcumin. Clearly the fit to the data are poor.

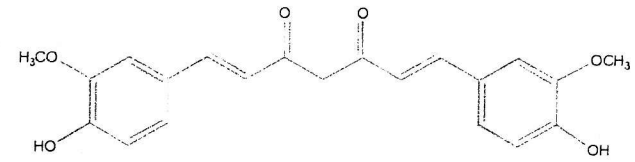

Curcumin

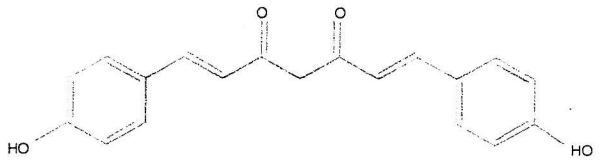

Compound 1:
Bisdesmethoxycurcumin

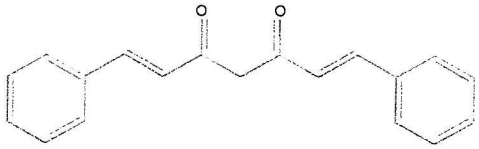

Compound 2:
1,7-diphenyl-5-hydroxy-
1,4,6-heptatrien-3-on

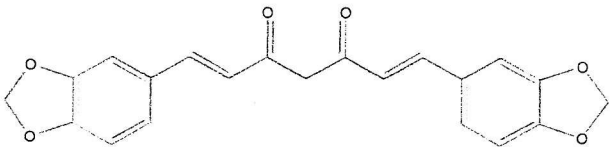

Compound 3:
1,7-dipiperonyl-5-hydroxy-
1,4,6-heptatrien-3-on

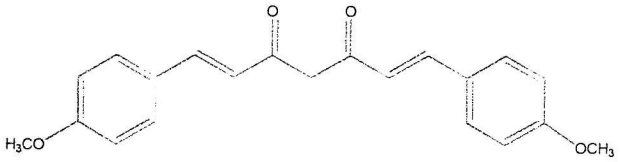

Compound 4:
5-hydroxy-1,7-bis(4-methoxyphenyl)-
1,4,6-heptatrien-3-on

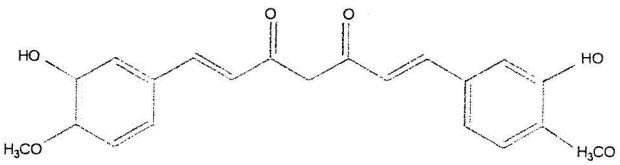

Compound 5:
5-hydroxy-1,7-bis(3-hydroxy-4-
methoxyphenyl)-1,4,6-heptatrien-3-on

Figure 3.8. The structure of curcumin and its analogues.

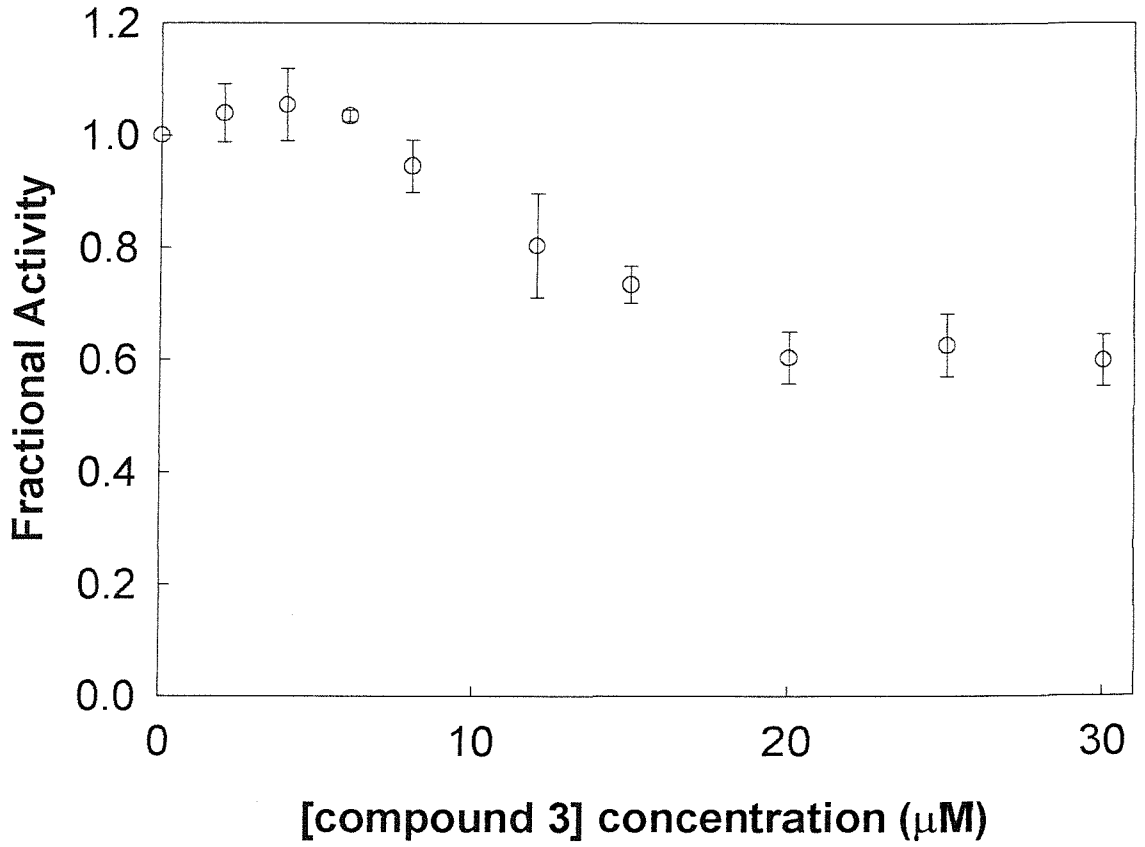

Figure 3.9. The effect of curcumin analogue 3 on Ca^{2+}-ATPase activity

The figure shows fractional activity versus concentration of curcumin analogue number 3. Activity was measured at 25 ^{0}C, pH 7.2, with 0.25 μg/ml SR vesicles, using the ATPase coupled enzyme assay.

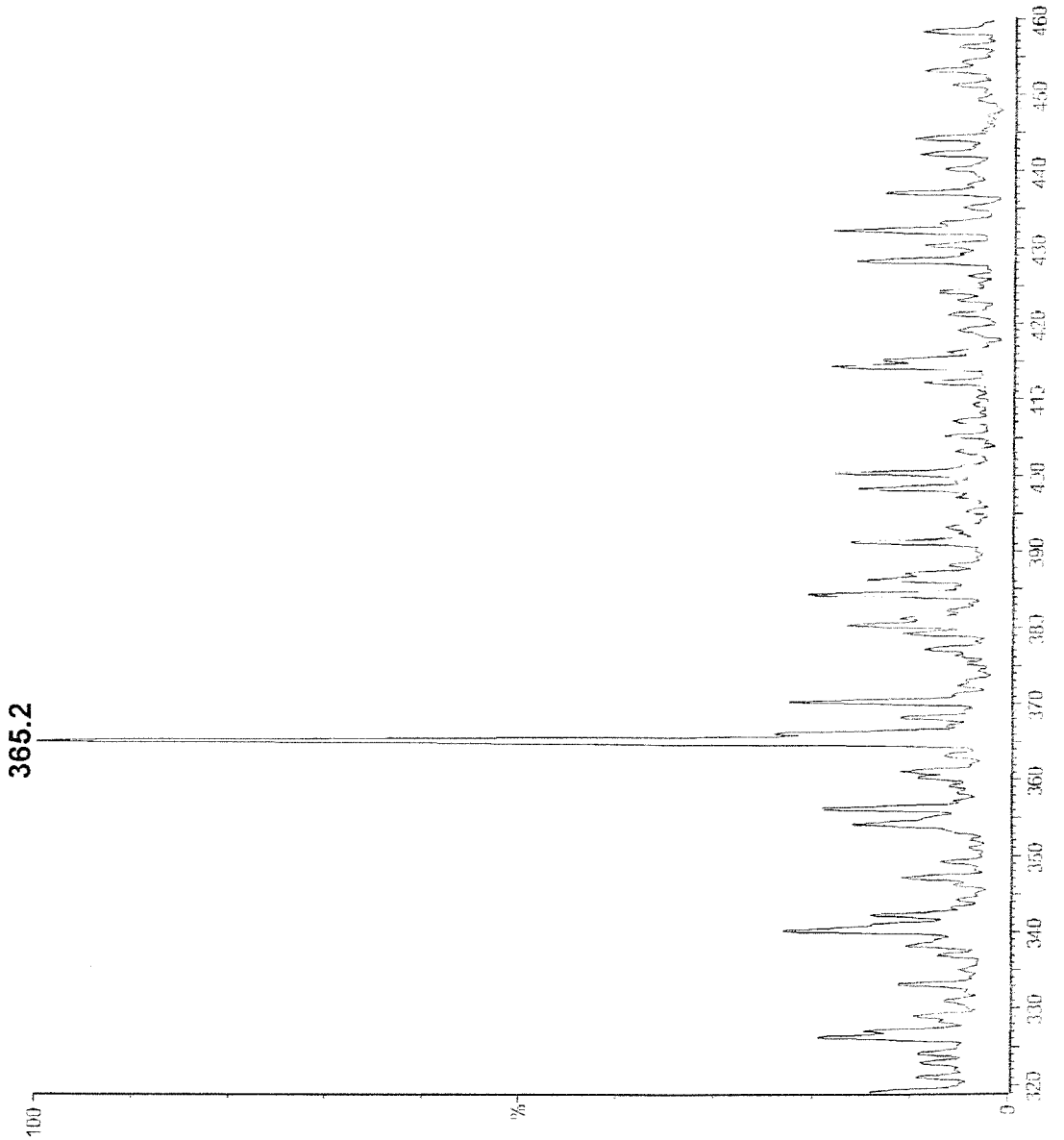

Figure 3.10. The mass spectrometry trace of curcumin analogue 3

The molecular weight of curcumin analogue 3 was determined using electrospray ionisation mass spectrometry. The major peak at 365.2 corresponds to curcumin analogue 3 (molecular weight 364.2) as the spectrum was recorded in the positive ionisation mode.

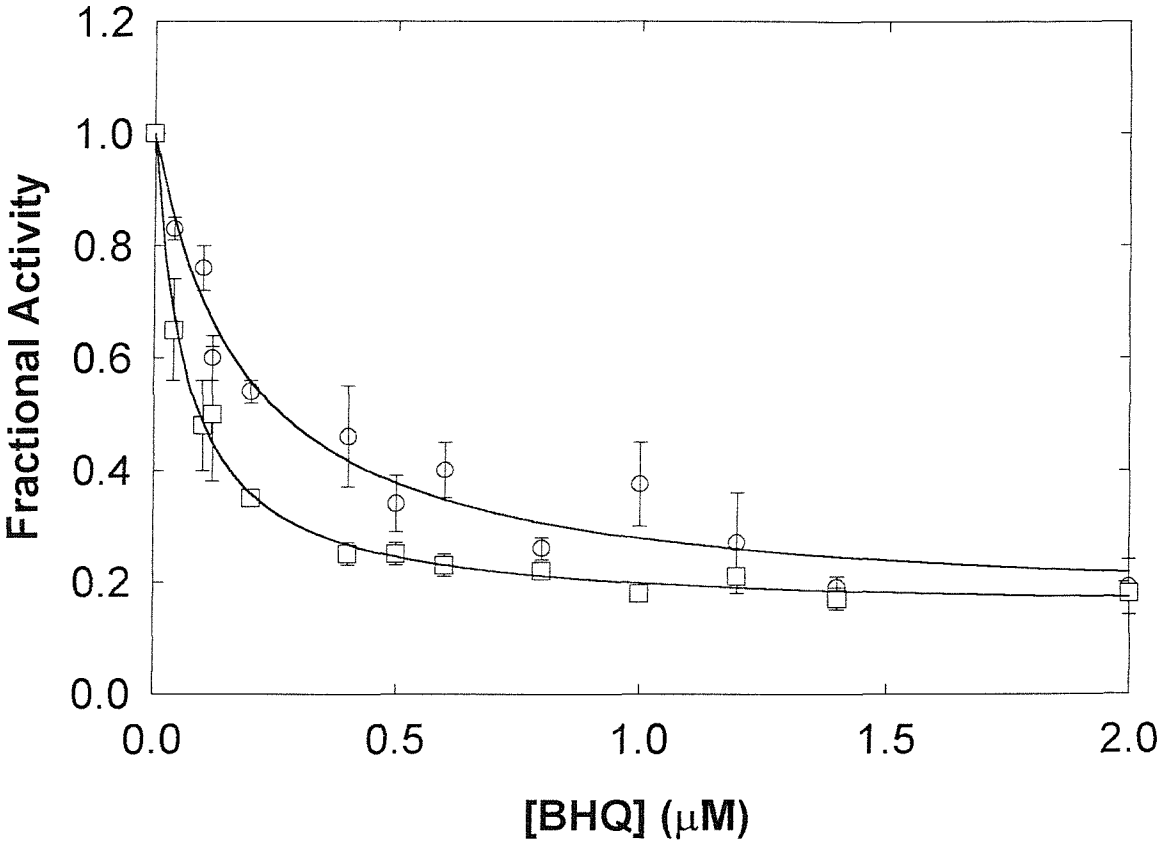

Figure 3.11. The effect of BHQ on the activity of the ATPase in the presence or absence of curcumin.

Activities were measured in the presence of the given concentrations of BHQ in the absence (o) or presence (□) of 6 μM curcumin. The lines show fits to single binding site models, with the parameters given in Table 3.1.

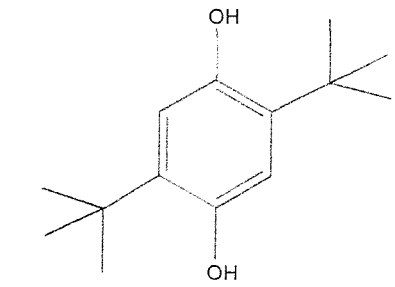

BHQ
2,5-di(*tert*-butyl)-1,4-benzohydroquinone

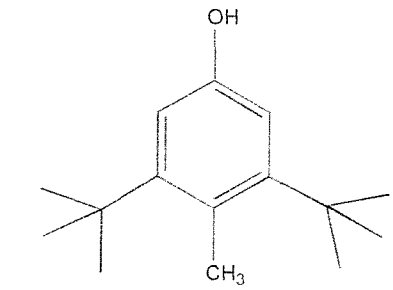

BHT
3,5-di(*tert*-butyl)-4-hydroxytoluene

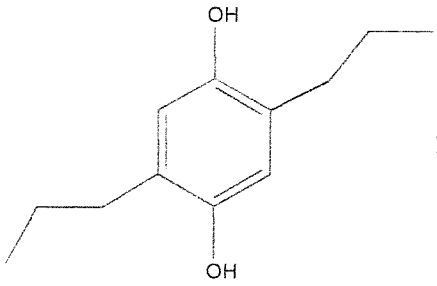

PHQ
2,5-di(propyl)-1,4-benzohydroquinone

Figure 3.12. Structures of BHQ, BHT and PHQ.

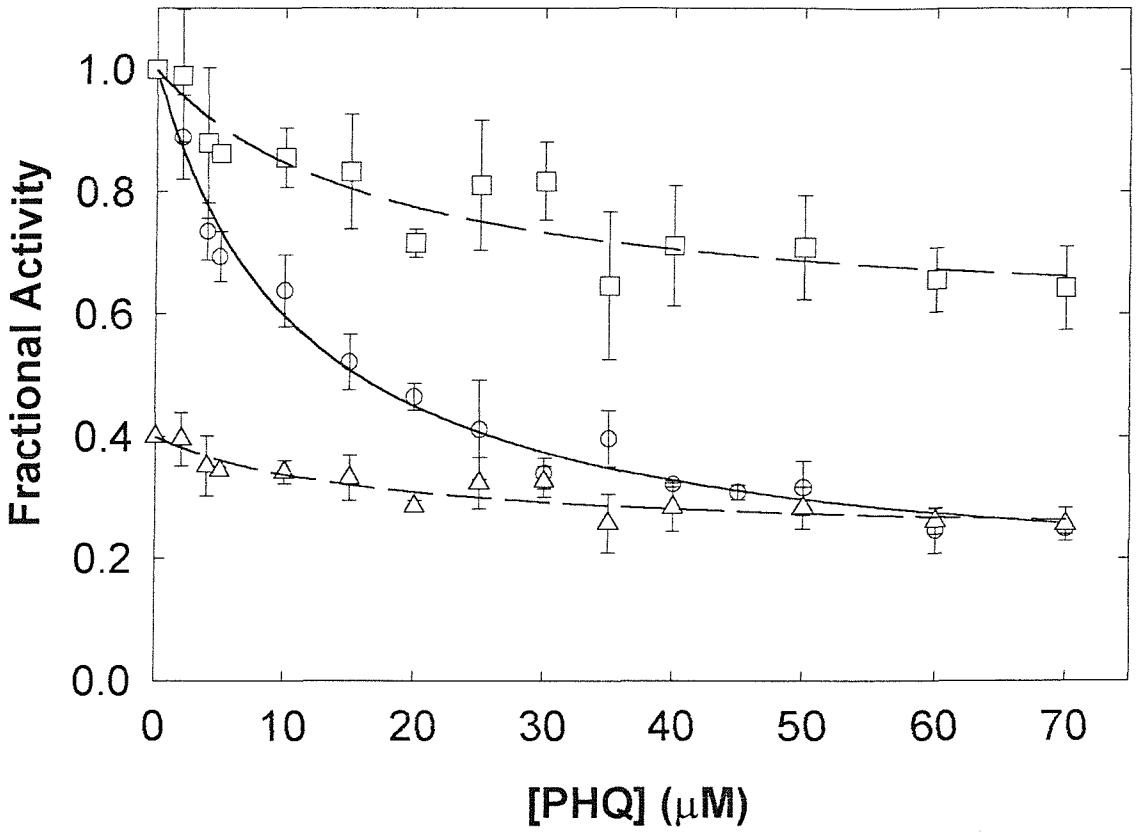

Figure 3.13. The effect of PHQ on Ca^{2+}-ATPase activity in the presence or absence of BHQ.

Activities were measured in the presence of the given concentrations of PHQ in the absence (o) or presence (Δ) of 0.4 μM BHQ. The data in the presence of 0.4 μM BHQ are also plotted starting from a fractional activity in the absence of BHQ of 1.0 (□). The lines show fits to a single binding site model, giving the K_d values and residual rates given in Table 3.1.

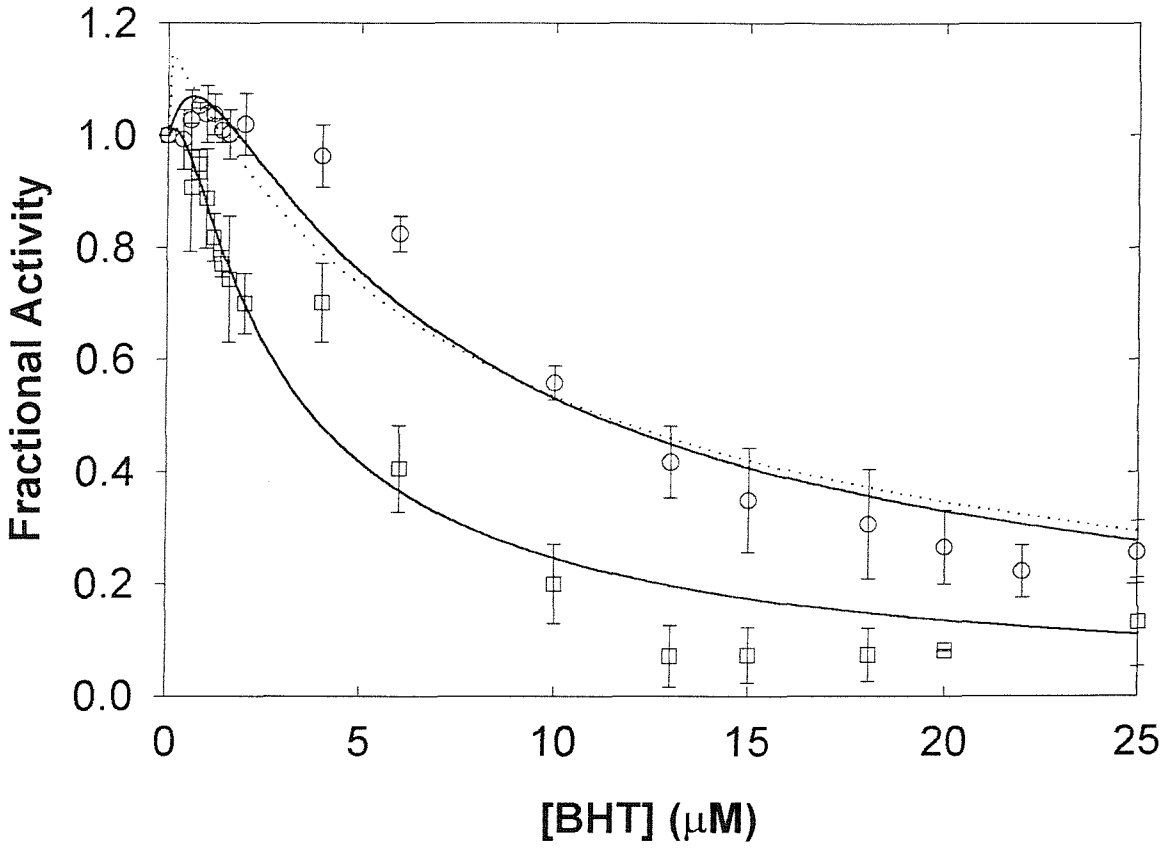

Figure 3.14. The effect of BHQ on the activity of the ATPase in the presence or absence of BHT.

Activities were measured in the presence of the given concentrations of BHT in the absence (o) or presence (□) of 0.4 μM BHQ. The data were fitted to the two site model. For BHT alone K_{dstim} was fixed at 0.01 μM (dotted line) or 1 μM (solid line). Parameters are listed in Table 3.1.

Figure 3.15. The effect of ellagic acid on the activity of the ATPase in the presence or absence of other inhibitors.

Activities were measured in the presence of the given concentrations of ellagic acid (A) in the absence (o) or presence (□) of 0.4 μM BHQ and (B) in the presence of 3 μM curcumin. The data were fitted to the two site model for stimulation/inhibition giving the parameters listed in Table 3.1.

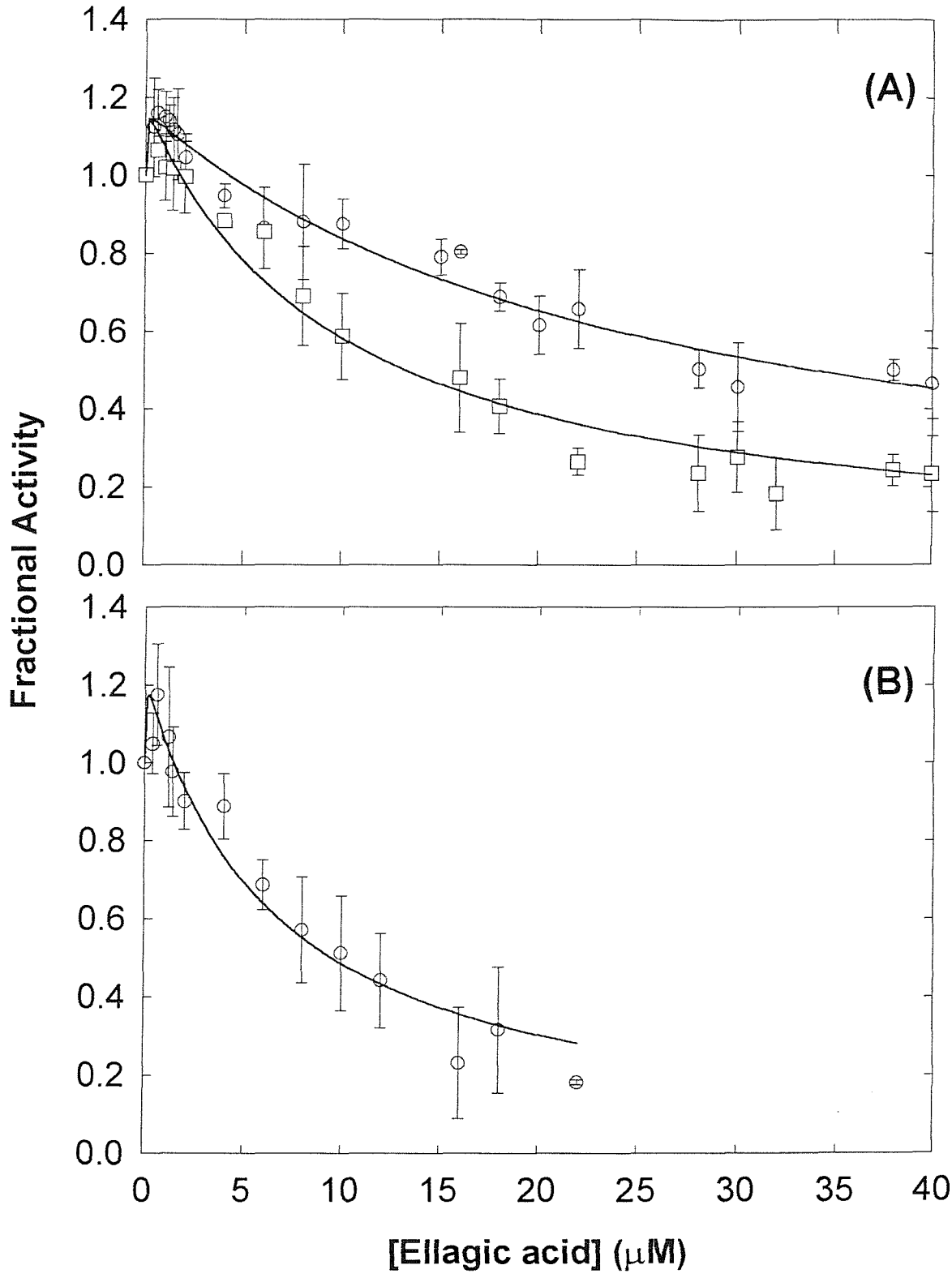
(A)
(B)
Fractional Activity
[Ellagic acid] (μM)
0.0
0.2
0.4
0.6
0.8
1.0
1.2
1.4
0
5
10
15
20
25
30
35
40

Figure 3.16. The effect of diethylstilbestrol on the activity of the ATPase in the presence or absence of other inhibitors.

Activities were measured in the presence of the given concentrations of diethylstilbestrol (A) in the absence (o) or presence (□) of 0.4 μM BHQ and (B) in the presence of 3 μM curcumin. The data for diethylstilbestrol alone was fitted to the two site model for stimulation/inhibition giving the parameters listed in Table 3.1. The data in the presence of BHQ or curcumin were fitted to a single site model giving the parameters again listed in Table 3.1.

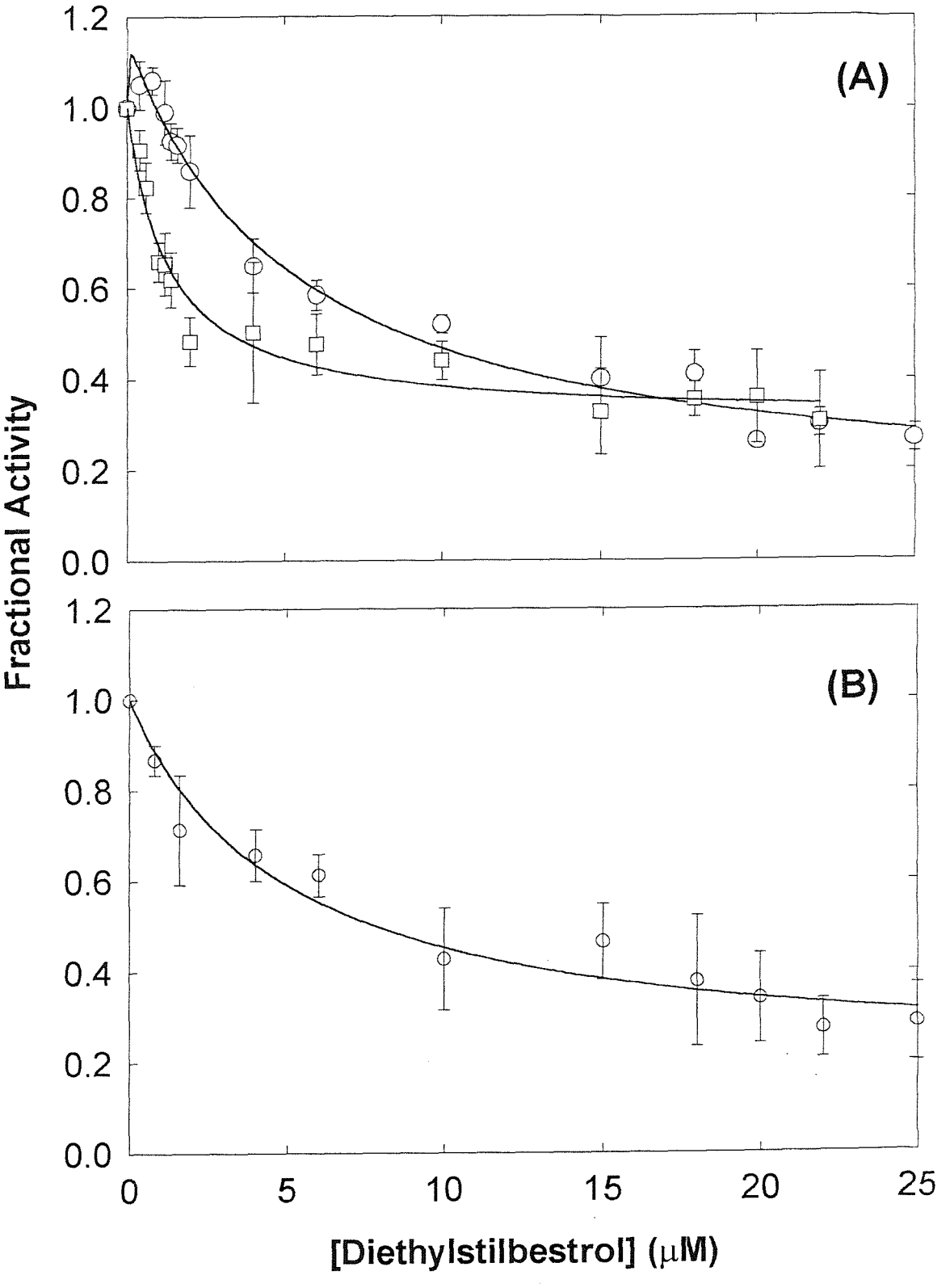
(A)
(B)
Fractional Activity
[Diethylstilbestrol] (μM)
1.2
1.0
0.8
0.6
0.4
0.2
0.0
0
5
10
15
20
25

Figure 3.17. The effect of nonylphenol on the activity of the ATPase in the presence or absence of BHQ.

Activities were measured in the presence of the given concentrations of nonylphenol in the absence (o) or presence (□) of 0.4 μM BHQ. (A) shows the data fitted to the two site model, with K_{dstim} fixed at 1 μM (solid line), 0.01 μM (dotted line) and with K_{dstim} allowed to vary (dashed line). (B) shows the data fitted to the stimulatory/multiple binding site model, with the number of inhibitor binding sites (*n*) fixed at 3, giving the parameters listed in Table 3.1.

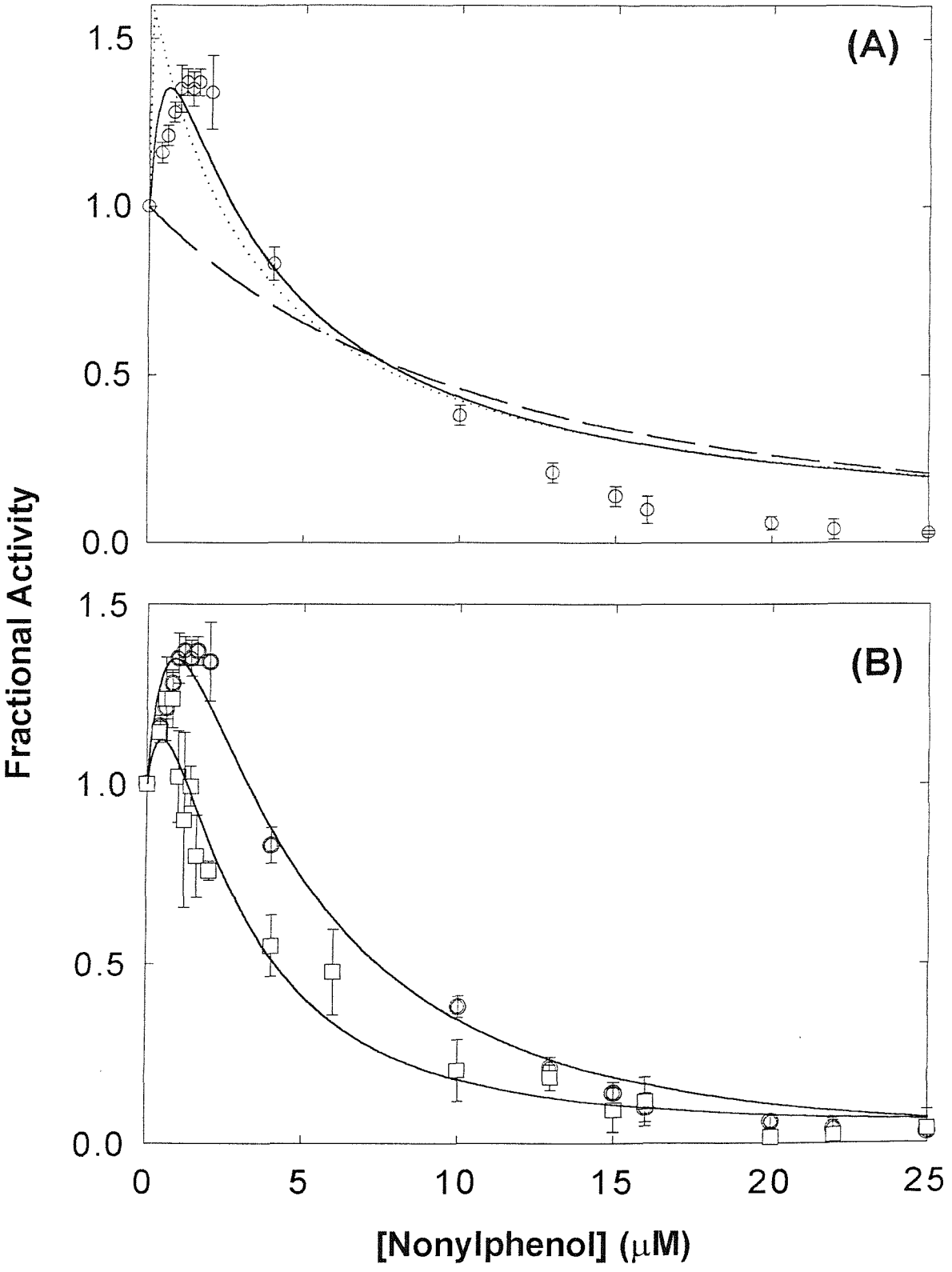
(A)
(B)
1.5
1.0
0.5
0.0
0
5
10
15
20
25
Fractional Activity
[Nonylphenol] (μM)

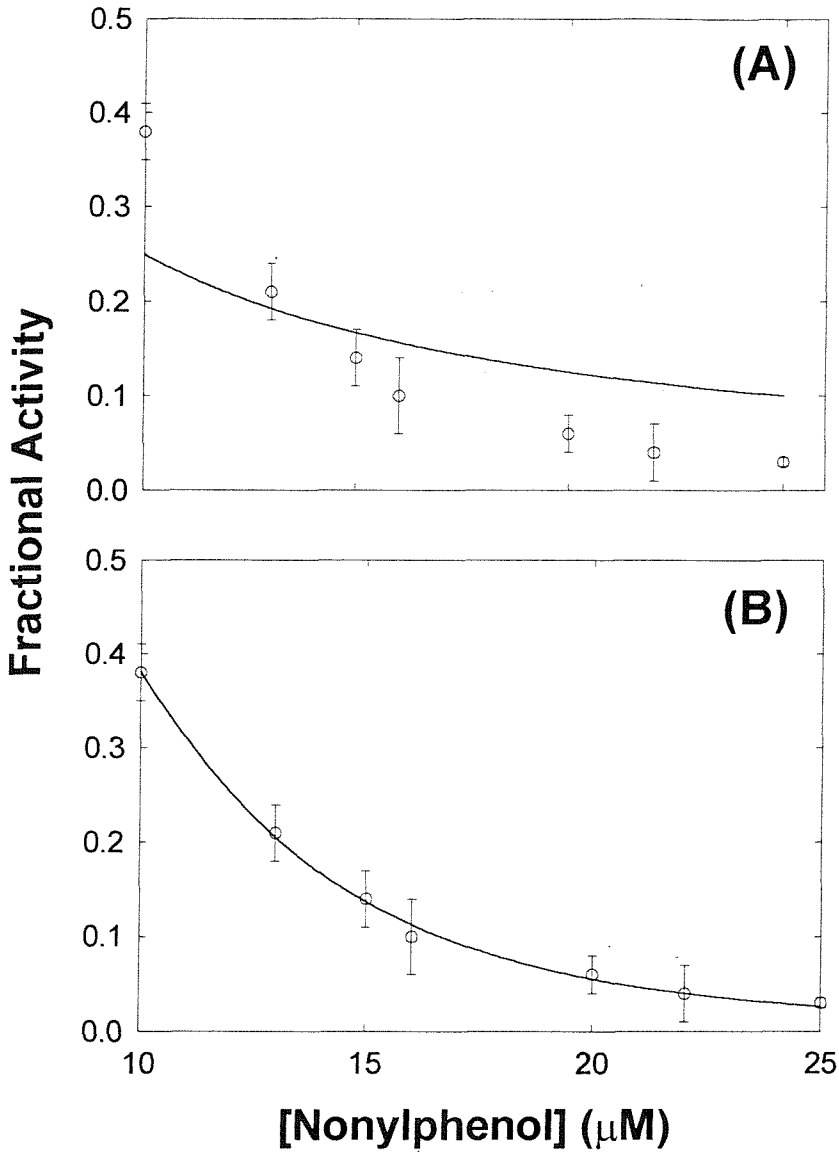

Figure 3.18. Nonylphenol data fitted using two different models for inhibition

Shown are the fractional activity data for Nonylphenol from 10 – 25 μM. (A) shows the curve fit using the two site model. (B) shows the curve fit using the n site model.

Table 3.1. Analysis of inhibitor binding to the Ca^{2+}-ATPase

Effects of inhibitors and pairs of inhibitors on ATPase activity were analysed according to the equations given in the methods. K_{dstim} is the dissociation constant for the stimulatory site, K_I is the dissociation constant for the inhibitory site, k_3 is the stimulated fractional rate and k_2 is the residual fractional rate.

Inhibitor	2nd inhibitor	K_{dstim} (μM)	K_I (μM)	k_3	k_2
PHQ	-	-	11.3 ± 0.5	-	0.14 ± 0.03
	0.4 μM BHQ	-	46.4 ± 5.0	-	0.14 (fixed)
BHQ	-	-	0.19 ± 0.03	-	0.14 ± 0.04
	6 μM curcumin	-	0.07 ± 0.01	-	0.15 ± 0.01
Curcumin	-	0.01 (fixed)	3.0 ± 0.5	1.17±0.03	0
	0.4 μM BHQ	-	0.81 ± 0.06	-	0.1 ± 0.02
Bisdes methoxy curcumin	-	-	1.23 ± 0.13	-	0
Ellagic acid	-	0.01 (fixed)	25.5 ± 7.5	1.17 ± 0.02	0
	0.4 μM BHQ	0.01 (fixed)	9.78 ± 2.6	1.17 ± 0.05	0
	3 μM curcumin	0.01 (fixed)	6.6 ± 2.7	1.22 ± 0.07	0
DES	-	0.01 (fixed)	5.24 ± 1.19	1.16 ± 0.07	0.09
	0.4 μM BHQ	-	1.28 ± 0.2	-	0.31± 0.03
	3 μM curcumin	-	5.08 ± 1.26	-	0.18 ± 0.06
BHT	-	1 (fixed)	4.36 ± 0.1	1.91 ± 0.3	0
	0.4 μM BHQ	1 (fixed)	1.62 ± 0.52	1.84 ± 0.91	0
Nonylphenol	-	1 (fixed)	11.1 ± 1.9	2.51 ± 1.8	0
	0.4 μM BHQ	1 (fixed)	6.76 ± 1.55	2.18 ± 3.0	0

Inhibitor	K_d (μM)	~$K_{0.5}$ (μM)
Curcumin	3.0	4.0
Ellagic Acid	25.5	35
DES	5.24	10
Nonylphenol	11.1	10
BHT	4.36	13

Table 3.2. Fitted binding constants for inhibitors of the Ca^{2+}-ATPase

The K_d values were analysed using the models described in the methods. $K_{0.5}$ values were taken from the inhibition curves, as the apparent concentration of inhibitor giving 50 % inhibition of Ca^{2+}-ATPase activity.

Inhibitor	K_d (μM) Inhibitor alone	K_d (μM) in the presence of second inhibitor	Fractional Increase in affinity
BHQ	0.19	0.038	5
Curcumin	3.0	0.85	3.5

$$K_{deff} = K_1(1+K_3[J])/(1+K_2[J]) \qquad \text{(Section 3.2.1.)}$$

Table 3.3. Cooperative effects in the binding of BHQ and curcumin

Data were analysed in terms of equation 22 using scheme 1 (below) for binding of two inhibitors, of the non-competitive type, to separate binding sites.

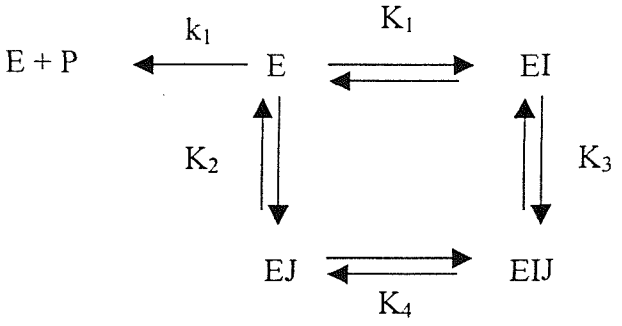

Scheme 1

Second Inhibitor	K_d (μM) for BHQ	Fractional increase in affinity for BHQ	K_d (μM) for curcumin	Fractional increase in affinity for curcumin
Ellagic acid	0.056	3	0.44	7
DES	0.034	6	2.85	Nil
Nonylphenol	0.097	2	-	-
BHT	0.054	4	-	-

Table 3.4. Dissociation constants for BHQ and curcumin in the presence of a second inhibitor

Data were analysed in terms of equation 22 using scheme 1 (refer to previous page) for binding of two inhibitors, of the non-competitive type, to separate binding sites.

Chapter Four: Effect of Ca^{2+}-ATPase Inhibitors on Uptake and Release of Calcium

4.1 Introduction

4.1.1. Leak and slippage

The Ca^{2+}-ATPase couples the hydrolysis of ATP to the active transport of ions across the membrane into the lumen of the SR. During the first cycle of the ATPase before the lumenal concentration of calcium has increased to a high level (Inesi *et al.*, 1978) two calcium ions are transported into the lumen for each molecule of ATP hydrolysed. This is 'full coupling' of the pump and may also occur in the presence of oxalate, which precipitates the internal calcium, thus maintaining low levels of calcium in the lumen of the SR. However, when the lumenal calcium concentration rises, reaching mM, the accumulation of calcium into the vesicle becomes less than 2:1 with respect to ATP hydrolysed (Inesi & de Meis, 1989; McWhirter *et al.*, 1987b). This suggests the presence of a calcium leak pathway.

Two types of calcium leak are proposed to exist, namely passive leak and slippage. Passive leak of calcium down its concentration gradient could involve the Ca^{2+}-ATPase or another protein present in the SR. Slippage however occurs when the phosphorylated, calcium-bound ATPase, releases calcium to the cytosol rather than to the lumen of the SR (Scheme 4.1).

Inesi and de Meis (1989) demonstrated the presence of a passive leak pathway in SR vesicles using calcium-loaded vesicles lacking the ryanodine receptor (Inesi & de Meis, 1989). They measured the rate of calcium release and showed that it is inhibited by μM concentrations of cytosolic calcium, unlike release through the ryanodine sensitive calcium channel that is stimulated by μM concentrations of calcium. This suggested the presence of a passive leak pathway through the Ca^{2+}-ATPase. Passive leak has also been observed in vesicles reconstituted from purified Ca^{2+}-ATPase, supporting the suggestion of leak through the ATPase (Inesi *et al.*, 1983; Gould *et al.*, 1987b; Gould *et al.*, 1987a).

Evidence for a slippage pathway also exists (Inesi & de Meis, 1989; Nayar *et al.*, 1982). Calcium uptake by SR vesicles upon addition of ATP is followed by spontaneous release of some of the accumulated calcium. This release is still

observed in the presence of ATP and external calcium, which inhibit the simple passive leak pathway (McWhirter *et al.*, 1987b). The effect is not due to the back reaction (de Meis, 1981) since it is also observed when calcium uptake is driven by acetyl phosphate instead of ATP in which calcium efflux is linked to the conversion of ADP to ATP (McWhirter *et al.*, 1987b). In reconstituted systems the rate of slippage is dependant on the phospholipid composition of the membrane and anionic phospholipids have been shown to decrease the rate of slippage on the Ca^{2+}-ATPase (Dalton *et al.*, 1998), with high rates of slippage observed in phosphatidylcholine bilayers.

Passive leak and slippage give rise to very different time dependencies for accumulation of calcium (Dalton, 1998). For passive leak, the accumulation of calcium initially increases linearly with time (see Figure 4.10 (C)). When the rate of transport into the vesicles equals the rate of leak out, the maximal level of accumulation is achieved. This level decreases with increasing the rate of leak. In contrast, accumulation of calcium in the presence of slippage increases non-linearly with time (see Figure 4.10 (D)). The maximal level of calcium accumulation also decreases with increasing slippage.

4.1.2. Studies of intracellular calcium homeostasis

A range of extracellular stimuli communicate with target cells via an interaction with cell surface receptors which stimulate second messengers such as DAG and IP_3, with subsequent downstream effects. DAG activates protein kinase C (PKC) and IP_3 causes the release of calcium from intracellular stores, through the IP_3 receptor (IP_3R). To define the importance and elucidate the roles of proteins in these signalling pathways specific pharmacological tools, i.e. inhibitors/modulators of protein function have been used. The use of these compounds has been invaluable, in particular for studying the mechanism of store operated calcium (SOC) entry (Section 1.1.4) and calcium homeostasis.

4.1.3. Modulation of Ca^{2+}-ATPase function

Thapsigargin (Tg) is the most widely used inhibitor of SERCA (Treiman *et al.*, 2001). Once identified as a specific inhibitor of SERCA (Lytton *et al.*, 1991;

Davidson & Varhol, 1995) Tg became a standard tool in studies that required empty intracellular stores and for studying the effects of store depletion, and subsequent calcium entry. Tg actually depletes stores indirectly, preventing calcium being pumped into the stores, counterbalancing the leak of calcium out. Hence, an increase in cytosolic calcium levels is seen in cells. Thus, calcium release by Tg depends upon the presence of Ca^{2+}-ATPase molecules sensitive to Tg and the presence of a passive leak pathway. BHQ also inhibits the SR Ca^{2+}-ATPase (Wictome *et al.*, 1992) and like Tg stabilises the E2 conformation of the enzyme and decreases phosphorylation of the Ca^{2+}-ATPase by P_i (Wictome *et al.*, 1992).

The effects of Tg on cells in culture have been widely monitored. Hakii *et al.* (1986) showed that Tg promoted carcinogenesis in mouse skin (Hakii *et al.*, 1986) and since then Tg has been studied in a vast array of cells including: basophilic leukaemia cells (Horikoshi *et al.*, 1994), DDT_1 MF-2 smooth muscle cells (Ghosh *et al.*, 1991), neuronal cells (Paschen *et al.*, 1996) and human hepatoma cells (Kaneko & Tsukamoto, 1994). Both Tg and BHQ are inhibitors of Ca^{2+}-ATPase activity (see Chapter 3). Upon addition to cells in culture they both cause sustained growth arrest. A direct correlation between the state of store filling (by the ATPase) and the ability of the cells to maintain protein and DNA synthesis and full cycle progression has been suggested (Ghosh *et al.*, 1991). The cells progress through S-phase but stop in a quiescent G_0 like phase. Tg blocks protein synthesis (Ghosh *et al.*, 1991), with rapid effects on mRNA translation, protein processing and gene expression (Wong *et al.*, 1993). Although Tg stopped cell division and the calcium pool was depleted for a week, the cells still appeared healthy, whereas cells treated with a calcium ionophore died within 24 hours (Ghosh *et al.*, 1991). Removal of BHQ reinstates store calcium levels in these cells and the cycle progresses (Short *et al.*, 1993). Tg binds so strongly its effects are effectively irreversible. Thus, for recovery of the Tg treated cells, 20 % serum is required and this has been linked to the synthesis of new functional pump proteins (Short *et al.*, 1993; Waldron *et al.*, 1995). The association of Tg with programmed cell death has recently become recognised (Jiang *et al.*, 1994; Furuya *et al.*, 1994) and this might explain the decrease in the fraction of mice with skin tumours following the initial rise after Tg treatment (Hakii *et al.*, 1986). Indeed Tg induced apoptosis is thought firstly to be associated with the activation of the protease caspase-3, which mediates apoptosis (Qi *et al.*, 1997) and secondly to be subject to inhibition by Bcl-2 (an anti-apoptotic oncogene) that inhibits apoptosis (Qi

et al., 1997). Furthermore, Tg increases expression of proto-oncogenes (Schonthal *et al.*, 1991) and the caspase inhibitor p35 can prevent Tg induced apoptosis (Qi *et al.*, 1997).

4.1.4. Calcium release mediated by IP_3R and RyR

The IP_3 second messenger mediated pathway is used by many cell types to release calcium from internal stores (Section 1.1.2), but the RyR predominates in muscle cells. In order to characterise these receptors and to study their physiological role in calcium signalling selective modulators of channel activity are required. Originally caffeine was thought to stimulate only the RyR and was used to demonstrate activation of this calcium release pathway (Endo, 1985). Likewise heparin was thought to solely inhibit the IP_3R. However both of these compounds are known to have multiple effects (Ehrlich *et al.*, 1994). Heparin, which targets the IP_3 binding site, has low affinity and selectivity, and is also membrane impermeable (Ghosh *et al.*, 1988). As well as inhibiting the coupling between the plasma membrane receptor and G proteins (Dasso & Taylor, 1991), studies have indicated that heparin inhibits IP_3 synthesis (Berridge, 1993) and stimulates the RyR in the same range that inhibits the IP_3R (Bezprozvanny *et al.*, 1993). All these effects have complicated the interpretation of experiments designed to elucidate the role of the IP_3R and RyR. Moreover, caffeine (Parker & Ivorra, 1991) and cADP ribose (Missiaen *et al.*, 1998) also inhibit the IP_3R and activate the RyR (Galione, 1992). Membrane impermeable antibodies for the IP_3R are available that modulate activity (Nakade *et al.*, 1991; Sullivan *et al.*, 1995) but these require specialised microinjection techniques for access into intact cells or actual disruption of the plasma membrane. Chen *et al.* (1993) also reported an antibody for the ryanodine receptor that inhibited calcium induced activation of this receptor (Chen *et al.*, 1993). In 1997, Maruyama *et al.* identified a membrane-penetrable modulator of the IP_3R that had no effect on calcium influx (Maruyama *et al.*, 1997a): 2-aminoethoxydiphenyl borate (2-APB). 2-APB has been a useful tool to modulate the kinetics of intracellular calcium signals (Maruyama *et al.*, 1997b; van Rossum *et al.*, 2000; Wu *et al.*, 2000). Ma *et al.* (2000) used 2-APB to show that the IP_3R is required for the activation of SOC channels (Ma *et al.*, 2000). Naturally occurring xestospongins are also specific potent blockers of the IP_3R (Gafni *et al.*, 1997)

without interacting with the IP_3 binding site. De Smet *et al.* (1999) suggested that Xestospongin C (XeC) also inhibits the endoplasmic reticulum Ca^{2+}-ATPase (De Smet *et al.*, 1999) but this was based on indirect evidence that the calcium content of stores was ~60 % lower than normal in the presence of 100 μM XeC. They ascribe this to a non-specific interaction of XeC with the membrane, affecting ATPase activity. Gafni *et al.* (1997) showed that the presence of XeC resulted in a decrease in calcium release in PC12 cells following addition of Tg and attributed this to inhibition of the IP_3R or RyR, which contribute to basal leak (Gafni *et al.*, 1997). However, De Smet *et al.* (1999) suggested that the decrease in calcium release was related to depletion of stores owing to inhibition of the calcium pumps (De Smet *et al.*, 1999). Gafni *et al.* (1997) reported an IC_{50} for XeC of 358 nM and found that a concentration of 5 μM adequately inhibits all IP_3R transport in cerebellar microsomes, whilst 20 μM blocks the bradykinin response in PC-12 cells (Gafni *et al.*, 1997). Thus the 100 μM concentration of used by De Smet *et al.* (De Smet *et al.*, 1999) is a particularly high concentration and this could lead to non-specific effects on Ca^{2+}-ATPase activity through disruption of the membrane. Examples of non-specific inhibitors of the Ca^{2+}-ATPase have been described in Chapter 3. Rosado and Sage (2000) used 20 μM XeC to inhibit the IP_3R and found this inhibited SOC entry and inferred that a conformational coupling exists between the plasma membrane and the IP_3R. Ruthenium red (Smith *et al.*, 1988; Jianjie, 1993) and ryanodine (Fleischer *et al.*, 1985; Smith *et al.*, 1988) are specific inhibitors of the RyR, neither having an effect on the IP_3R. Ruthenium red inhibits the reversal of the SR Ca^{2+}-ATPase by P_i and competes with calcium for the high affinity calcium binding sites (Alves & de Meis, 1986). However, in the presence of calcium concentrations above 5 μM, up to 200 μM ruthenium red had no effect on ATPase activity and uptake (Alves & de Meis, 1986; Kargacin *et al.*, 1998). Low concentrations (<10 μM) of ryanodine activate the RyR with higher concentrations having an inhibitory effect.

4.1.5. Measurement of calcium

Calcium levels in cells may be monitored by the use of calcium-binding fluorescent indicators (Thomas & Delaville, 1991). The cell permeant acetoxymethyl (AM) esters can be applied to cells in culture (Figure 4.1). The ester

makes the indicator membrane permeant. Non-specific esterases remove the ester to give the $-COO^-$ form which complexes calcium (Figure 4.1) and binding of calcium leads to a conformation change and a change in spectral properties. For some dyes the absorbance maxima are different for the calcium free and the calcium bound forms; these can be used in ratiometric measurements. For others the absorbance and emission maxima are the same, but the fluorescence intensity is different for the calcium free and the calcium bound forms. In this case measurements of changes in fluorescence intensity gives calcium concentration. The more recent dyes have greater fluorescence intensity and therefore smaller amounts may be used. This in turn decreases the calcium buffering effect making the dyes better suited to measure small physiological changes in calcium levels, as seen in the cytoplasm of stimulated cells. The ratiometric dyes, such as Fura-2 and Indo-1 (Molecular Probes) permit accurate quantification of these calcium levels. However, the spectral properties of curcumin make measurements with any type of fluorescent indicator difficult. Previously, Indo-1 was used in conjunction with curcumin (Lockyer, 1997) but interaction with the dye complicated the analysis. The problem is the large absorption peak of curcumin at ~420-430, which coincides with spectral properties of many of the useful calcium indicators. Calcium crimson (Molecular Probes) is a longer wavelength indicator that reports in the infrared range (Figure 4.2), where the spectral properties of curcumin are minimal.

Metallochromic indicators, such as Antipyrylazo III and Arsenazo III, are also useful in the measurement of ion fluxes in biological systems (Thomas, 1991). Fluorescent dyes are sensitive to calcium in the micromolar and sub-micromolar range. In studies of calcium uptake by SR vesicles there is a need to measure changes in the external calcium concentration in the 100 μM range. Thus dyes are needed that are sensitive to this range of calcium concentrations. Antipyrylazo III and Arsenazo III (Figure 4.1) are sensitive in this range. These dyes undergo a change in the absorbance spectra best detected by dual-wavelength spectrometry. The dye on the outside of the vesicles undergoes a change in absorbance when the concentration of free calcium changes.

4.2. Methods

4.2.1. Quail fibroblast cell culture

Quail fibroblasts (QT-6 cells) were maintained in Medium 199 Modified Earles Medium (Gibco BRL) supplemented with 10 % Tryptose Phosphate Broth, 5 % foetal bovine serum, 1 % DMSO, 1% Antibiotic/Mycotic (Penicllin and streptomycin), in a 5 % CO_2, 37 ^{0}C incubator.

4.2.2. Loading of cells with calcium crimson

Cells were grown to confluence in thin glass bottomed wells to enable visualisation using the confocal microscope. Calcium crimson (Molecular Probes) was solubilised before loading into the cells. 50 µl DMSO was added to 50 µg of dye and sonicated in a bath for 30 seconds. 5 µl cremophor was added to solubilise the dye and the sample sonicated for another 30 seconds. After addition of 500 µl DMEM/F-12 media (without phenol red) the dye was sonicated again for 30 seconds. The calcium crimson was made up to a final concentration of 10 µM in DMEM/F-12. The dye suspension was loaded onto the cells and incubated at 37 ^{0}C, 5 % CO_2, for one hour. Prior to use the media was removed from the cells and replaced with DMEM/F-12. The cells were visualised using the confocal microscope.

4.2.3. The Bio-Rad MRC-600 laser confocal imaging system

As mentioned above, numerous calcium sensitive dyes are commercially available and have been used to study calcium homeostasis in cells. The use of such a dye in conjunction with the confocal scanning microscope enables measurement of accurate internal cellular calcium levels ($[Ca]_i$). Confocal scanning microscopy permits visualisation of a sample in a single plane of focus. The illumination and detection by the microscope are confined to the same spot and only what is in focus is detected. The regions that are out of focus appear black and do not contribute to the image. The laser light source, in this case a krypton/argon laser, gives a high resolution and sensitivity. The final 3D video images produced of the sample are

created electronically by means of collection, filtering, enhancing and assembly by the computer (details in the systems user guide for the Bio-Rad MRC-600 laser confocal imaging system).

Data were processed using the Confocal Assistant Software and the Scion Image analysis program.

4.2.4. Calcium uptake

Calcium uptake by SR or reconstituted SR vesicles was measured spectrophotometrically using metallochromic indicators. 80 μM of Antipyrylazo III or 50 μM Arsenazo III were equilibrated at 25 ^{0}C in 10 mM PIPES, 100 mM K_2SO_4, pH 7.1, 5 mM $MgSO_4$, with 0.24 or 0.48 mg SR or 0.065 mg reconstituted SR in 3 ml. 0.25 μM FCCP was added to the reconstituted SR (in order to equilibrate protons across the membrane) before the next step. Three aliquots of 120 nmoles $CaCl_2$ were then added (to a final calcium concentration of 120 μM), followed by 0.8 mM ATP, pH 7.1, to initiate the uptake of calcium into the vesicles. The change in absorbance of the dye due to calcium uptake was measured using the Aminco DW2000 dual wavelength spectrophotometer, using the wavelength pair 720-790 for Antipyrylazo III and 675-685 for Arsenazo III. The amount of calcium accumulated was quantified by relating the change in absorbance of the dye when 120 nmoles calcium was added to the change measured after ATP addition. In some experiments a regeneration system of 1.5 mM phosphoenol pyruvate and 7.5 IU of pyruvate kinase was added to the cuvette and allowed to equilibrate before addition of calcium. In some experiments accumulation of calcium was driven by 1.6 mM acetyl phosphate at pH 7.1.

Simulations of calcium accumulation were performed by Prof. A.G.Lee, using the programme FACSIMILE (UKEA).

4.2.5. Reconstitution of SR into sealed lipid vesicles

Biobeads were prepared by soaking in methanol, stirring in a beaker for 15 minutes. Using a Buchner funnel, the methanol was removed and the beads washed in fresh methanol. The Biobeads were then placed in a glass column, with buffer A (10 mM PIPES-HCl, pH 7.1, 100 mM K_2SO_4). The Biobeads were washed with

buffer until approximately 500 ml buffer A had passed through the column. The beads were stored in the same buffer at 4 ^{0}C.

16 mg of phospholipid (90 % dioleoylphosphatidylcholine, DOPC/10 % dioleoylphosphatidic acid, DOPA) were dried down on the walls of a glass vial, in a vacuum dessicator. The DOPC/DOPA mixture was resuspended in 1 ml of buffer A and heated at 37 ^{0}C to remove the lipid from the walls of the vial. The suspension was then sonicated to clarity in a bath sonicator. The resultant liposomes were diluted 1:4 to a final concentration of 4 mg lipid/ml buffer A. Octyl-glucoside (OG) was added to a final concentration of 40 mM to solubilise the liposomes. SR was solubilised in buffer B (10 mM PIPES, pH 7.1, 100 mM K_2SO_4, 6 mg/ml $C_{12}E_8$, 0.1 mM $CaCl_2$) at a final concentration of 2 mg/ml, at room temperature. The solubilised lipid and SR were then mixed gently and within two minutes, 80 mg Biobeads per ml of lipid/protein suspension was added. The mixture was swirled gently, sealed under nitrogen and incubated for one hour at room temperature. The addition of Biobeads was repeated three times. Five minutes after the last addition the proteoliposome suspension was removed and placed on ice until use. To check the viability of the reconstituted SR, the ATPase activity was measured using the method described in Section 2.3.3. The reconstitution results in vesicles in which the ATPase molecules are randomly distributed between the two faces of the membrane since addition of $C_{12}E_8$ which allows ATP to reach the 'wrong way round' ATPases, leads to a doubling of ATPase activity (Dalton, 1998). This increase indicates that the Ca^{2+}-ATPase has reconstituted into the vesicles.

4.2.6. Dot blot analysis

Protein was serially diluted to the desired concentration. 1 µl of each diluent was then blotted onto dry nitrocellulose paper. The dots were air dried and immunoblotting was performed as described in Section 2.2.4.

4.2.7. Preparation of light and heavy SR

Light and heavy SR was prepared by the method of Saito *et al.* (Saito *et al.*, 1984). The procedure for preparation of SR (Section 2.2.1) was followed for collection and homogenisation of the tissue, with the exception of the buffer used.

The muscle was homogenised in 0.3 M sucrose, 5 mM imidazole, pH 7.4. The homogenate was centrifuged for 10 minutes, at 8300 g. The supernatant was saved and the pellets were rehomogenised and centrifuged as before. The supernatants were pooled, filtered through muslin and then centrifuged for 90 minutes, at 100 000 g. The pellet was then resuspended in a minimal volume of the homogenisation buffer. Discontinuous sucrose gradients were prepared by using 7 ml of each gradient, layering the 45 % first with 38 %, 32 % and 27 % sucrose on top. These were buffered with the homogenisation medium. The homogenate was loaded evenly onto the gradients, which were then centrifuged overnight at 95 000 g. The fractions of light and heavy SR were and diluted in the homogenisation buffer and then centrifuged at 125 000 g for 2 hours. The pellets were resuspended in the homogenisation buffer and aliquots were snap frozen in liquid nitrogen and stored at – 70 ^{0}C. The protein concentration was determined as in Section 2.2.2.

4.3. Results

4.3.1. The effect of Ca^{2+}-ATPase inhibitors on calcium levels in QT-6 cells

In cells pre-loaded with calcium indicator dyes, a rise in cytosolic calcium levels are observed when Ca^{2+}-ATPase inhibitors are added. This increase in cytosolic calcium levels is due to release of calcium predominantly from stores, however some may be the result of calcium influx across the plasma membrane (Berridge, 1995) as Tg and BHQ both initiate store operated calcium entry due to the depletion of stores (Section 4.13). Inhibition of the Ca^{2+}-ATPase prevents replenishment of the stores and in conjunction with calcium leak, results in increased cytosolic calcium levels. Thus, inhibitors such as Tg and BHQ are able to indirectly increase intracellular levels. $[Ca^{2+}]_c$ were monitored using calcium crimson.

Figure 4.3 shows the effect of trilobilide (Tb), a sesquiterpene lactone inhibitor of the Ca^{2+}-ATPase (Wictome *et al.*, 1994), on QT-6 cells pre-loaded with calcium crimson. Addition of 10 μM Tb leads to a large increase in $[Ca^{2+}]_c$ as seen by an increase in calcium crimson fluorescence (Set (1)). Addition of 25 μM BHQ produces the same effect (Figure 4.3, Set (2)). In contrast, as shown in Set (3) addition of 25 μM curcumin, another Ca^{2+}-ATPase inhibitor, results in a reduction in fluorescence suggesting either a decrease in the rate of leak of calcium from internal stores or that the dye is quenched by curcumin. To show that the fluorescence intensity of calcium crimson is still sensitive to calcium in the presence of curcumin, a fluorescence titration was performed (Figure 4.4). Calcium crimson shows a normal fluorescence titration curve in the presence of curcumin, with no shift in the curve, showing curcumin does not alter the affinity of the dye for calcium. At all concentrations of curcumin, there is ~28 % reduction in fluorescence intensity, attributable to the absorbance of exciting light by curcumin. The small decrease in fluorescence intensity caused by curcumin can be corrected for in the confocal pictures using the Scion image software, increasing the measured intensity values by 28 %. To demonstrate that an increase in cytoplasmic calcium would be detectable by calcium crimson in the presence of curcumin the calcium ionophore, A23187, was used to raise intracellular calcium levels. Figure 4.5 shows the effect of 50 μM of the calcium ionophore A23187, on QT-6 cells, in the absence or presence of curcumin. As shown a clear increase in $[Ca^{2+}]_c$ is observed in the presence of 25 μM

curcumin showing that cytosolic calcium changes can be measured in the presence of curcumin.

It can be shown that the increase in intracellular calcium seen on addition Tb is due to release from internal stores rather than due to calcium entering through the plasma membrane by inclusion of $MnSO_4$ in the media. Mn^{2+} ions quench the fluorescence of calcium sensitive dyes (Tsien *et al.*, 1982; Hallam & Rink, 1985) and the presence of 1 mM $MnSO_4$ in the external media leads to a gradual decrease in the fluorescence of the unstimulated QT-6 cells (Figure 4.6). Subsequent addition of 10 μM Tb results in the characteristic increase in cytosolic calcium levels (Figure 4.6). If calcium was entering through the plasma membrane a decrease in fluorescence would have been observed due to the presence of Mn^{2+} ions. This confirms that calcium release is from internal stores.

Not only does curcumin decrease the resting level of calcium in cells, it can actually block the increase in calcium normally seen on addition of Ca^{2+}-ATPase inhibitors. This is shown in Figure 4.7. Set (1) shows that curcumin blocks the increase in calcium normally seen on addition of Tb and set (2) shows that it also blocks the increase in calcium normally seen on addition of BHQ. It has been suggested that the calcium release observed following addition of Ca^{2+}-ATPase inhibitors is via IP_3R (Gafni *et al.*, 1997). To confirm this under the conditions used here, the effects of XeC were studied. It was not possible to use 2-APB, another inhibitor of IP_3R, since it has fluorescent properties at the wavelengths used for calcium crimson. 2-APB and XeC are both inhibitors of IP_3 induced calcium release from cerebellar microsomes (Maruyama *et al.*, 1997a; Delong & Blasie, 1993). QT-6 cells, loaded with calcium crimson, were pre-incubated with 10 μM XeC for 10 minutes. The effect of 10 μM Tb was then monitored (Figure 4.3, Set (4)). As can be seen, XeC blocks the increase in $[Ca^{2+}]_c$ by Tb. Gafni *et al.* (1997) reported a similar result with XeC and Tg (Gafni *et al.*, 1997). This indicates that the release of calcium on blocking the Ca^{2+}-ATPase with Tb is mediated through IP_3 sensitive calcium channels. The similar effect of XeC and curcumin (Figure 4.3, Set (3)) suggests that curcumin also blocks the IP_3 sensitive calcium channel in ER.

The effect of curcumin on calcium release in QT-6 cells appears to be less structurally specific than the effect on the ATPase (see Chapter 3). Thus, 25 μM of analogue 3 which lacks the –OH and methoxy groups (Figure 4.12) has a very small effect on ATPase activity is as effective as curcumin in blocking Tb induced increase

in cytosolic calcium (Figure 4.8, Set (2)). 25 μM bisdesmethoxycurcumin, which has the same inhibitory effect on the Ca^{2+}-ATPase as curcumin produces a similar effect in the QT-6 cells (Figure 4.8, Set (1)). Curcumin analogue 5 caused the same effect on QT-6 cells as analogue 3, in the absence and presence of Tb (data not shown). The different structural effects on Ca^{2+}-ATPase activity and on release of calcium from ER in response to addition of Tb would be consistent with the proposal that release of calcium from ER does not involve binding of curcumin to the Ca^{2+}-ATPase.

4.3.2. Calcium accumulation by SR

Cells in culture provide a useful system to study the effect of Ca^{2+}-ATPase inhibitors, but are a complex system. A simpler system to further study the effects of these inhibitors is that of sarcoplasmic reticulum (SR) vesicles in which approximately 75 % of the protein is the Ca^{2+}-ATPase (McWhirter *et al.*, 1987b). Calcium accumulation by SR vesicles was measured spectrophotometrically with the use of the calcium indicative dyes, Antipyrylazo III and Arsenazo III. Unfortunately, the final level of calcium accumulation into the SR vesicles varies significantly between different SR preparations (McWhirter *et al.*, 1987b) as will be seen in the results described below.

4.3.3. The effect of Ca^{2+}-ATPase inhibitors on calcium uptake by SR

Figure 4.9 shows accumulation of calcium by SR vesicles on addition of ATP. Accumulation of calcium reaches a maximum of approximately 150 nmoles calcium/mg protein after 200 seconds for this preparation. Addition of 2 or 4 μM BHQ reduces the rate of calcium accumulation into the SR vesicles with little effect on the final level of calcium accumulation. This is consistent with inhibition of Ca^{2+}-ATPase activity.

Figure 4.10 shows the effect of curcumin on calcium accumulation. Addition of 6, 10 and 15 μM curcumin lead to an increase in the rate of calcium accumulation (Figure 4.10 (A)). Thus, in contrast to the effect seen with BHQ, low concentrations of curcumin increase the rate of calcium accumulation, without affecting the level of uptake. Figure 4.10 (B) shows effects of lower concentrations of curcumin on

another preparation of SR showing lower levels of accumulation of calcium. We know from Chapter 3 that the K_d for binding of curcumin to the inhibitory site is 3 μM and the lowest measurable change in the rate of uptake is measured at 0.5 μM curcumin. The effect of curcumin was characterised by plotting the level of calcium accumulated after a fixed period of time as a function of curcumin concentration. Results after 21 seconds are plotted in Figure 4.11, with very similar results being obtained for other time periods. The data fit to a simple Michaelis-Menten scheme with a maximum stimulated level of accumulation 77 % greater than the unstimulated level, with a concentration of curcumin causing the half maximal effect being 1.03 ± 0.25 μM (Figure 4.11). Figure 4.11 also shows the effect of curcumin on ATPase activity taken from Chapter 3.

In Chapter 3 the effect of mixtures of inhibitors on ATPase activity were tested. The effects of mixtures of BHQ and curcumin on calcium uptake by SR vesicles were also tested. Figure 4.9 shows calcium uptake by SR vesicles in the presence of 2 μM BHQ and 15 μM curcumin. The data shows a decrease in the level of calcium uptake. This shows that in the presence of both curcumin and BHQ the observed effect is simple inhibition of calcium uptake.

The effects of curcumin on calcium uptake are structurally specific, as shown by experiments with curcumin analogues (Figure 4.12). Bisdesmethoxycurcumin, which inhibits Ca^{2+}-ATPase activity with a similar potency to curcumin, also increases the rate of calcium accumulation into SR vesicles. Compound 3, which marginally inhibits ATPase activity, has no effect on the rate of calcium uptake. Compound 5, has no effect on ATPase activity and also has no effect on calcium accumulation. An interesting comparison can be made with effects of the curcumin analogues on calcium release in QT-6 cells following addition of Tb. Here compound 3 and 5 have no effect on calcium accumulation in SR, whereas in the QT-6 cells compound 3 and 5 have the same effect as curcumin and bisdesmethoxycurcumin.

4.3.4. The effect of ruthenium red on calcium uptake by SR

The effect of curcumin on the rate of calcium accumulation could, in principal, follow from an effect on a leak pathway from SR. By decreasing the rate of leak, an increase in the rate of accumulation might be observed. Leak could be

through the Ca^{2+}-ATPase or through another protein present in the SR membrane. Dot blot analysis (Figure 4.13) was performed to determine the protein components present in SR, compared to a pure ATPase preparation. Membranes were probed with antibodies RRZAS, C1F9 and Y1F4, against the ryanodine receptor, calsequestrin and the ATPase respectively. As expected, Y1F4 gave a positive result for both the preparations. C1F9 was slightly positive at 1 μg and 0.1 μg of ATPase, with much larger quantities of calsequestrin present in SR vesicles. RRZAS gave a negative result for ATPase and a positive result for SR, indicating the absence of ryanodine channel in the ATPase preparation. Thus, the ryanodine receptor was present in the SR preparation and could, in principle, account for a proportion of the leak pathway, which may be affected by curcumin. This is unlikely since calcium release by RyR is blocked by external calcium and the experiments reported here were performed in the presence of 120 μM external calcium. It was confirmed that the RyR was not important for the results observed with curcumin by using ruthenium red as a specific inhibitor of the RyR (Jianjie, 1993). Figure 4.14 (A) shows calcium uptake by SR vesicles in the presence of 200 μM ruthenium red and as shown ruthenium red has no significant effect. In the presence of ruthenium red, curcumin again results in an increase in the rate of uptake of calcium. This shows that the curcumin effect is independent of the RyR. This was further verified by fractionation of SR into light (LSR) and heavy SR (HSR), the LSR fraction being devoid of the RyR (Figure 4.15), whereas the heavy fraction contained RyR. In the presence of 100 μM ruthenium red, calcium uptake into the LSR fraction was slightly decreased (Figure 4.14 (B)), with no effect on the rate of uptake. The effect of 10 μM curcumin was still observed in either the absence or presence of ruthenium red. The HSR fraction shows very low levels of calcium accumulation because it is a "leaky" preparation, which contains a high proportion of calcium release channel (Figure 4.14 (C)). In the presence of 100 μM ruthenium red a small but significant increase in the rate of calcium uptake is observed. This indicates that ruthenium red is blocking a leak pathway, which is not observed in the LSR fraction and thus indicates blocking of the RyR. Curcumin again causes an increase in the rate of calcium uptake.

Figure 4.16 shows the effect of 2 μM BHQ on calcium uptake by LSR vesicles. As shown, addition of BHQ results in a reduction in the rate of

accumulation of calcium, with no significant effect on the final level of calcium accumulation.

4.3.5. The effect of calcium channel blockers on calcium uptake by SR

2-APB and XeC are both inhibitors of IP_3 induced calcium release (Maruyama *et al.*, 1997a; Gafni *et al.*, 1997). The presence of IP_3 channels in SR has not been demonstrated to date but these inhibitors were used to confirm that the effects of curcumin were not due to inhibition of IP_3 channels. Maruyama *et al.* (1997) showed high concentrations of 2-APB induced calcium release from cerebellar microsomes, possibly due to partial inhibition of Ca^{2+}-ATPase activity (Maruyama *et al.*, 1997a). Effects of 2-APB on ATPase activity of SR vesicles in the presence of A23187 were determined using the coupled enzyme assay (Section 2.2.3). At 50 μM no effect on activity was measured but at 100 μM, 11.3 % inhibition of activity was observed. Effects of 2-APB on calcium accumulation by SR vesicles could not be determined using Antipyrylazo III since addition of 2-APB to a solution of Antipyrylazo III resulted in a large decrease in absorbance. However, 2-APB had no effect on the absorbance of Arsenazo III and this could therefore be used to measure calcium accumulation. Figure 4.17 (A) shows calcium uptake by SR using Arsenazo III. As can be observed, addition of 50 μM 2-APB had no effect on calcium accumulation by SR vesicles consistent with the suggestion of the absence of IP_3 sensitive calcium channels in SR. Addition of 15 μM curcumin increased the rate of uptake, comparable with the effect observed using Antipyrylazo III. Addition of 15 μM curcumin in the presence of 50 μM 2-APB still resulted in an increase in the rate of calcium accumulation. XeC also had no effect on calcium accumulation by the SR vesicles (Figure 4.17 (B)) and in the presence of XeC, the effect of curcumin is still measured.

4.3.6. Reconstitution of the Ca^{2+}-ATPase

Effects of curcumin were also tested on calcium accumulation by vesicles reconstituted from SR and excess lipid. In previous studies it was shown that high levels of accumulation of calcium could be seen on reconstitution with 90 % DOPC/5 % DOPA. Calcium accumulation into these vesicles was measured using

the same method as described previously (Figure 4.18). The uptake by these vesicles is much higher than that obtained with SR with an average maximum uptake of approximately 1200 nmoles calcium/mg protein. The uptake is also slower as compared to SR and takes approximately 800-1000 seconds to reach 1200 nmoles calcium. Figure 4.18 shows the effect 2 μM BHQ and 15 μM curcumin. The effects of both of these compounds are purely inhibitory, with a decrease in the rate and level of calcium accumulation. These effects can be attributed to the much greater volume of the reconstituted vesicles per mg of ATPase as compared to SR vesicles (Levy *et al.*, 1990; Levy *et al.*, 1992). The exact interpretation of this result is uncertain, but the balance between leak and uptake will be different in the reconstituted vesicles and in SR.

4.3.7. Use of acetyl phosphate and a regeneration system with SR

ATP phosphorylates the Ca^{2+}-ATPase, with the production of ADP, and increasing amounts of ADP favour the back reaction of the Ca^{2+}-ATPase (McWhirter *et al.*, 1987b). This can have significant effects on the accumulation process and complicates the process. Acetyl phosphate (AcP) may be used in the experiment instead of ATP (de Meis, 1981). Upon phosphorylation of the pump by AcP there is no ADP production, although AcP is less efficient and a greater concentration is required to produce the same uptake as observed using ATP. Figure 4.19 (A) shows calcium accumulation by SR using 1.6 mM AcP. The graph shows the uptake compared to that using 0.8 mM ATP. The uptakes are comparable, with the same level of calcium accumulated into the vesicles. Addition of 2 μM BHQ in the presence of AcP results in a decrease in the rate of calcium accumulation, consistent with inhibition of the Ca^{2+}-ATPase. Although effects are much smaller than with ATP (Figure 4.10), the addition of curcumin up to 6 μM results in a small increase in the rate of accumulation of calcium when uptake is driven by AcP (Figure 4.19 (B)). At higher concentrations of curcumin (15 μM) a decrease in the rate of accumulation of calcium is seen.

A build up of ADP can also be prevented by adding a regeneration system, composed of PEP and pyruvate kinase, to regenerate ATP. Figure 4.19 (C) shows calcium uptake in the presence of this regeneration system. In the presence of a regenerating system, calcium accumulation continues to increase almost linearly with

time after the initial burst of uptake, reaching a level of 140 nmoles/mg after 300 seconds, compared to 100 nmoles/mg protein in the absence of the regenerating system (Figure 4.9). Figure 4.19 (C) shows that the presence of 15 μM curcumin increase the rate of calcium uptake, with no effect upon the overall level of accumulation. 2 μM BHQ decreases the rate of calcium accumulation slightly.

4.3.8. The effect of P_i , and oxalate as precipitating agents in SR vesicles

Calcium leak from SR vesicles occurs when the concentration of calcium within the vesicle builds up to a high level. Precipitating the calcium inside the vesicle can reduce leak by reducing the concentration gradient across the membrane. The membrane of the SR contains a transporter for phosphate (Stefanova *et al.*, 1991; Hasselbach & Weber, 1974). Addition of inorganic phosphate, P_i, will result in formation of the $Ca_3 (PO_4)_2$ complex (Figure 4.20) that precipitates within the vesicle (Weber *et al.*, 1964). This keeps the internal free calcium concentration low, decreasing the rate of calcium leak out of the vesicles resulting in higher levels of calcium accumulation (Hasselbach & Weber, 1974; Stefanova *et al.*, 1991). Figure 4.21 (A) shows calcium accumulation by SR vesicles in the presence of P_i, in which the calcium accumulation is greatly increased, and increases almost linearly with time. Addition of 2 μM BHQ decreases the rate of accumulation, consistent with inhibition of Ca^{2+}-ATPase activity. Upon addition of 15 μM curcumin the rate of calcium accumulation increases. This shows that with the leak pathway abolished curcumin still has an effect. The experiment was also performed in the presence of 2 mM oxalate (Weber, 1966; Hasselbach, 1964). As can be seen in Figure 4.21 (B) 2 μM BHQ again decreases the rate of calcium accumulation and the presence of 15 μM curcumin again increases the rate of accumulation.

4.4. Discussion

The sesquiterpene lactone, Tg, has been used widely as a tool to deplete intracellular calcium stores (refer to Section 4.1.3). When the Ca^{2+}-ATPase is inhibited in unstimulated cells, calcium is able to leak out of the ER and cytosolic calcium levels increase (Thastrup *et al.*, 1990; Treiman *et al.*, 2001). Addition of other Ca^{2+}-ATPase inhibitors such as the sesquiterpene lactone Tb, and the bisphenol BHQ, also produce the characteristic increase in cytosolic calcium levels (Figure 4.3), due inhibition of the reloading mechanism, the Ca^{2+}-ATPase. The fact that the calcium is released from intracellular stores and is not a result of calcium entry through the plasma membrane was shown by studying the effect of Tb in the presence of Mn^{2+} ions in the external media. Since the addition of Tb still results in an increase in fluorescence, the calcium ions must come from internal stores (Figure 4.6).

Gafni *et al.* (1997) demonstrated that XeC is a membrane permeable blocker of the IP_3R and additionally reduces the ER calcium leak that is usually observed after addition of Tg (Gafni *et al.*, 1997). These results agree with the observations presented here (Figure 4.3) that XeC prevents an increase in cytosolic calcium levels upon addition of Tb in QT-6 cells. This suggests that the pathway for calcium leak from the ER occurs via the IP_3 sensitive calcium channel (Gafni *et al.*, 1997), since leak is blocked by XeC. To conclusively demonstrate that curcumin is an inhibitor of the IP_3R direct inhibitor studies could be performed using cerebellar microsomes, which contain a high level of the IP_3R (Sayers *et al.*, 1993). The effects of curcumin on the calcium release from these microsomes would indicate whether this compound directly inhibits the IP_3R.

It may quite reasonably be assumed that all inhibitors of the Ca^{2+}-ATPase would be expected to deplete intracellular stores by inhibiting the ATPase. However, the addition of curcumin gave a very different result. The cytosolic calcium levels in cells actually decreased on addition of curcumin (Figure 4.3) and moreover curcumin blocked the effect of Tb and BHQ (Figure 4.7). Lockyer (Lockyer, 1997) demonstrated this using the fluorescent dye Indo-1, but interaction of curcumin with the dye made the interpretation of the results difficult. The results presented here using calcium crimson show the same result. The experiments imply that curcumin is also an inhibitor of the IP_3 sensitive calcium channel in ER.

Whereas structural specificity is important for inhibition of the Ca^{2+}-ATPase activity (Chapter 3) the effect on the IP_3 sensitive calcium channel is different (Figure 4.7). Curcumin analogue 3 (Figure 3.9) and analogue 5 that do not inhibit ATPase activity have the same effect as bisdesmethoxycurcumin and curcumin on QT-6 cells, both of which inhibit ATPase activity significantly in the low micromolar range (Figure 3.6). Thus it would appear that the structural specificity is more important to produce inhibition of Ca^{2+}-ATPase activity in the SR than that required for inhibition of the IP_3R in the ER.

BHQ, as expected, as a typical inhibitor of Ca^{2+}-ATPase activity decreased the level of calcium uptake by SR vesicles (Figure 4.9). Curcumin however gave an unexpected result, actually increasing the rate of calcium accumulation by SR vesicles (Figure 4.10). This can be explained by either an increase in the uptake rate of calcium into the vesicle by the Ca^{2+}-ATPase or by a decrease in the leak rate. Leak could be a result of movement of calcium through a channel present in the membrane or could be through the Ca^{2+}-ATPase. It has been shown that SR vesicles do not contain IP_3 sensitive calcium channels since addition of IP_3 to SR vesicles does not result in a release of calcium (Meissner, 1994; Scherer & Ferguson, 1985; Mikos & Snow, 1987). 2-APB and XeC had no effect on the level of calcium accumulation by SR (Figure 4.17), confirming the absence of the IP_3R. The terminal cisternae of the SR contain the ryanodine calcium release channel (RyR) and this has been shown to be present in the SR preparation, but is absent from the light SR vesicle preparation (Figure 4.15). Ruthenium red is a selective blocker of the RyR (Jianjie, 1993) and it has been shown using this compound that the effect of curcumin is independent of any effect on the RyR (Figure 4.14). Ruthenium red marginally increases the rate of calcium accumulation in the HSR fraction (Figure 4.14), which contains a high proportion of the RyR, making HSR preparations very leaky to calcium. The fact that this effect is not seen in the SR preparation shows that the contribution of RyR to the calcium leak pathway is minimal. Moreover, cytosolic calcium levels over 1 μM inhibit calcium release through the RyR (Meissner *et al.*, 1986) and since the concentration of calcium at the start of these experiments was 120 μM the contribution of the RyR towards leak must be small in SR.

To show that the back reaction was not important in explaining the effect of curcumin, uptake in the presence of AcP and in the presence of an ATP regeneration

could involve the Ca^{2+}-ATPase (Inesi *et al.*, 1983; Gould *et al.*, 1987b; Gould *et al.*, 1987a; Inesi *et al.*, 1983; de Meis, 1991) or another protein present in the SR. Slippage however occurs when the phosphorylated, calcium-bound ATPase, releases calcium to the cytosol rather than to the lumen of the SR (Scheme 4.1). Passive leak occurs when calcium is pumped into the vesicle and the lumenal concentration rises to mM levels (Figure 4.20 (A)). The presence of P_i and oxalate can prevent the build up of high lumenal concentrations of free calcium by complexing the calcium inside the SR vesicle (Figure 4.20 (B)). As Figure 4.21 shows, curcumin has a large stimulatory effect on calcium accumulation in the presence of both P_i and oxalate. This shows that curcumin cannot be affecting the passive leak of calcium. An alternative effect is therefore on the rate of slippage, a process whereby calcium is released into the cytosol rather than the lumen of the SR. Evidence for such a pathway exists since uptake of calcium by SR vesicles is followed by spontaneous release of some accumulated calcium, even in the presence of ATP and external calcium, conditions under which simple passive leak is inhibited (Inesi & de Meis, 1989; Yu & Inesi, 1995; McWhirter *et al.*, 1987b).

Accumulation of calcium by SR vesicles was simulated using the simplified form of the reaction scheme for the ATPase used previously (Dalton *et al.*, 1999). The internal volume of the SR vesicles was taken as 5 μl per mg protein (Duggan & Martonosi, 1970; McWhirter *et al.*, 1987a). Furthermore, it was assumed that 75 % of the protein present in the SR was Ca^{2+}-ATPase (McWhirter *et al.*, 1987b) and that 30 % was capable of phosphorylation by ATP, in agreement with experimental data (Dalton *et al.*, 1999). In the presence of passive leak calcium accumulation increases almost linearly with time (Figure 4.10 (C)). At a point where the rate of transport of calcium into the lumen of the vesicle equals the rate of calcium leak out the maximal level of calcium accumulation is achieved. Conversely, in the presence of slippage (Figure 4.10 (D)) accumulation of calcium does not increase linearly with time, effects of slippage being seen at very short times; the level of calcium accumulation decreases with increasing slippage. As can be seen by comparison of the simulations to the effect measured in the presence of curcumin, the effects of curcumin are similar to those expected when the rate of slippage is decreased, as opposed to an effect on the passive leak pathway. Calcium accumulation into SR vesicles can be simulated in terms of a low rate of passive leak, which determines the maximum amount of calcium that can be accumulated and a slippage rate of about 65 s^{-1}

similar to those expected when the rate of slippage is decreased, as opposed to an effect on the passive leak pathway. Calcium accumulation into SR vesicles can be simulated in terms of a low rate of passive leak, which determines the maximum amount of calcium that can be accumulated and a slippage rate of about 65 s^{-1} (Figure 4.10 (D)). This is the same as the slippage rate determined in reconstituted vesicles of a lipid composition comparable to that of the native membrane; dioleoylphosphatidylcholine with 10 % anionic phospholipid (Dalton *et al.*, 1999). The effect of curcumin can be simulated assuming a decrease in the rate of slippage with for example, the effect of 2 μM curcumin corresponding to a decrease in the rate of slippage to 35 s^{-1} (Figure 4.10 (D)). Thus to conclude, curcumin decreases the rate of slippage on the Ca^{2+}-ATPase in SR, in essence increasing the efficiency of calcium uptake, at micromolar concentrations, despite being a potent inhibitor of ATPase activity.

Low concentrations of curcumin stimulate Ca^{2+}-ATPase activity, with inhibition becoming dominant at higher concentrations (Figure 4.11). The apparent dissociation constants for the stimulatory and inhibitory sites (refer to Chapter 3) were approximately 0.01 μM and 3 μM respectively. The effects of curcumin on the rate of calcium accumulation fit to an apparent dissociation constant of 1 μM (Figure 4.10). These apparent dissociation constants for the inhibition of ATPase activity and for stimulation of calcium accumulation are similar. Thus it follows that the effects could follow from binding of curcumin to one site on the ATPase. Curcumin may for example decrease the rate of de-phosphorylation of $E2PCa_2$ both by the normal transport pathway and by the slippage pathway (Scheme 4.1). The one binding site theory is supported by the effects of the curcumin analogues. Bisdesmethoxycurcumin has similar effects to curcumin on both ATPase activity and accumulation of calcium (Table 4.1). Analogues 3 and 5, lacking the hydroxyl moiety at position 4 on the two rings, fail to inhibit the ATPase activity (Chapter 3) and have no effect on calcium accumulation (Table 4.1).

The high resolution crystal structure of SERCA (Toyoshima *et al.*, 2000) has enabled the localisation of specific residues within the structure of the pump, providing clues as to how slippage may occur. The high affinity calcium binding sites are located between transmembrane helices M4, M5, M6 and M8 (Figure 1.8). The hydrophobic residues Phe-760, Tyr-763 and Leu-764 are located above one of the calcium binding sites, on the cytoplasmic side of the membrane. Mutation of Phe

760 and Leu 764 reduced calcium affinity, but mutation of Tyr-763 (to Gly) gave rise unexpectedly to a mutant whereby calcium transport was uncoupled from ATP hydrolysis (Andersen, 1995b; Rice & MacLennan, 1996), as did mutation of Lys-758 (Andersen, 1995a). Thus, these two residues could be important in reducing the rate of dissociation of calcium from the phosphorylated ATPase to the cytoplasmic side of the membrane. If curcumin binds in this region it could also decrease the rate of this slippage. The residues in the stalk region above transmembrane helix M3, between 254 and 259, are known to be important for binding thapsigargin (Blostein *et al.*, 1993).

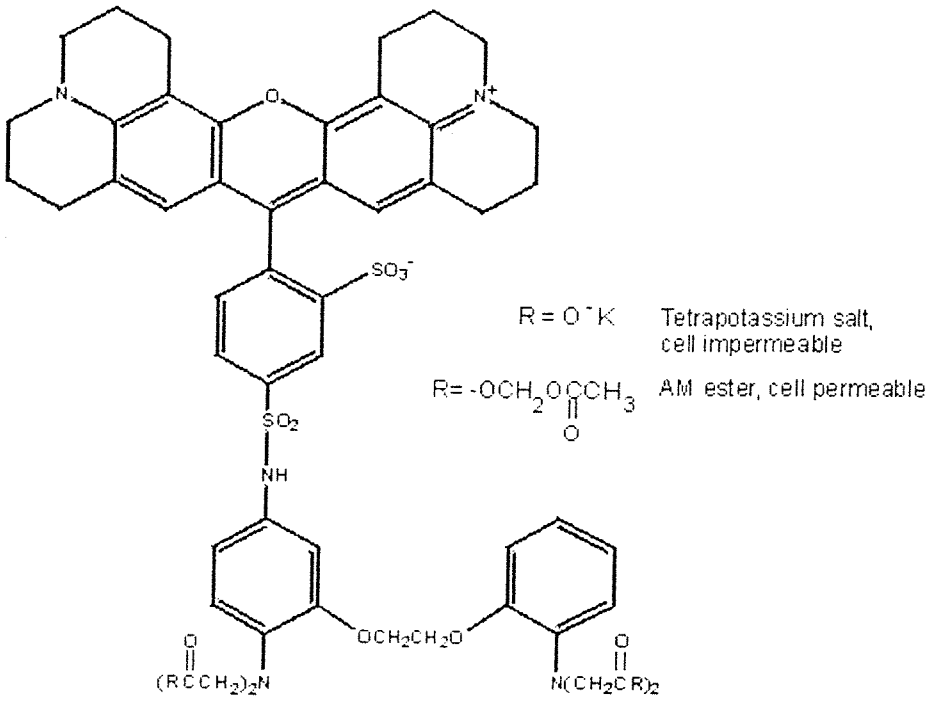

Calcium crimson

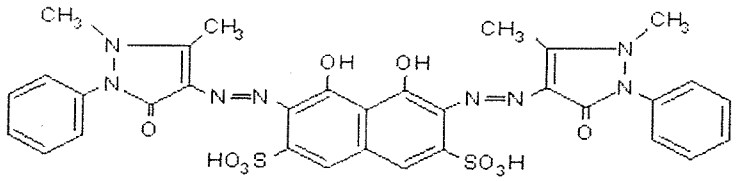

Antipyrylazo III

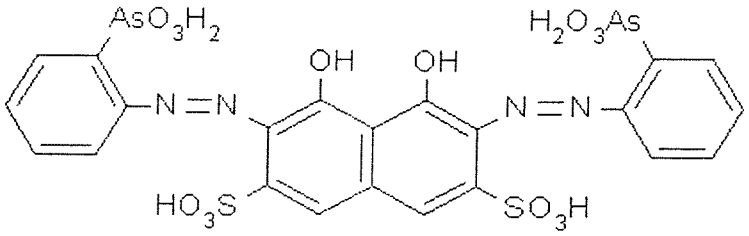

Arsenazo III

Figure 4.1. Structures of calcium crimson, Antipyrylazo III and Arsenazo III

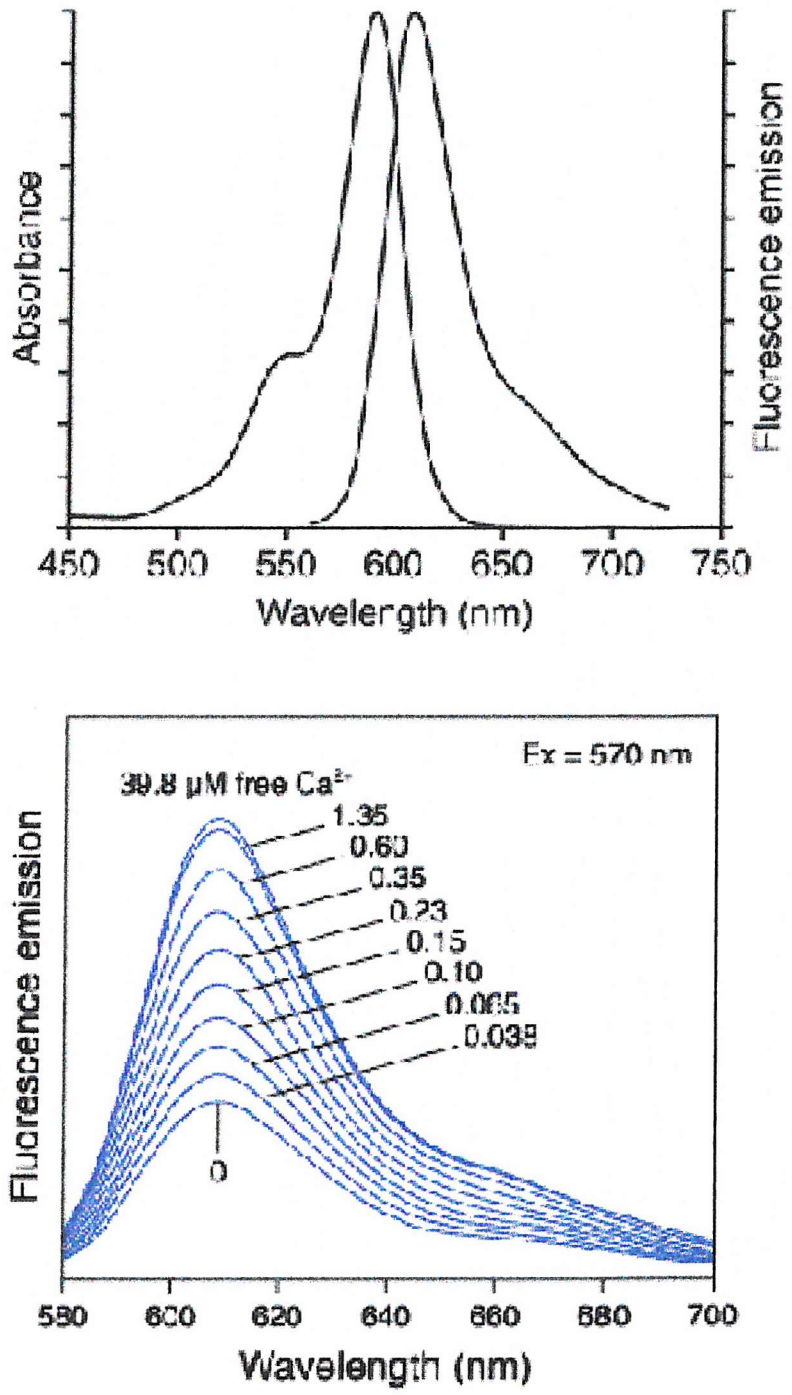

Figure 4.2. Spectra of calcium crimson fluorescence

With an excitation maximum at 590nm, calcium crimson is the longest wavelength calcium indicator supplied by Molecular Probes. (A) shows the excitation and emission maximum of calcium crimson at 590 and 615 nm respectively. (B) shows the increase in fluorescence emission intensity upon binding to calcium. This data are at www.probes.com.

Figure 4.3. The effect of Ca^{2+}-ATPase inhibitors on calcium release in QT-6 cells

To monitor calcium levels, QT-6 cells were loaded with 10 μM calcium crimson AM ester in DMEM/F-12 media, in a 5 % CO_2 incubator, at 37 ^{0}C for 1hour and then washed in the same media without dye. Changes in the fluorescence of calcium crimson upon addition of the inhibitors were measured using the Bio-Rad MRC 600 Confocal imaging system. The excitation wavelength was set at 568 nm and fluorescence emission collected above 585 nm. The images collected were rendered in false colour, with blue indicating low levels of calcium, with red and pink indicating higher cytosolic calcium levels. The time course of inhibitor response was measured and pictures collected at (A) t = 0, (B) = 0.5 min and (C) 2.5 min after inhibitor addition. Set (1) shows the effect of 10 μM trilobilide, set (2) shows the effect of 25 μM BHQ, set (3) shows the effect of 25 μM curcumin and set (4) shows the effect of 10 μM trilobilide on cells pre-incubated with 10 μM xestospongin C (XeC) for 10 min.

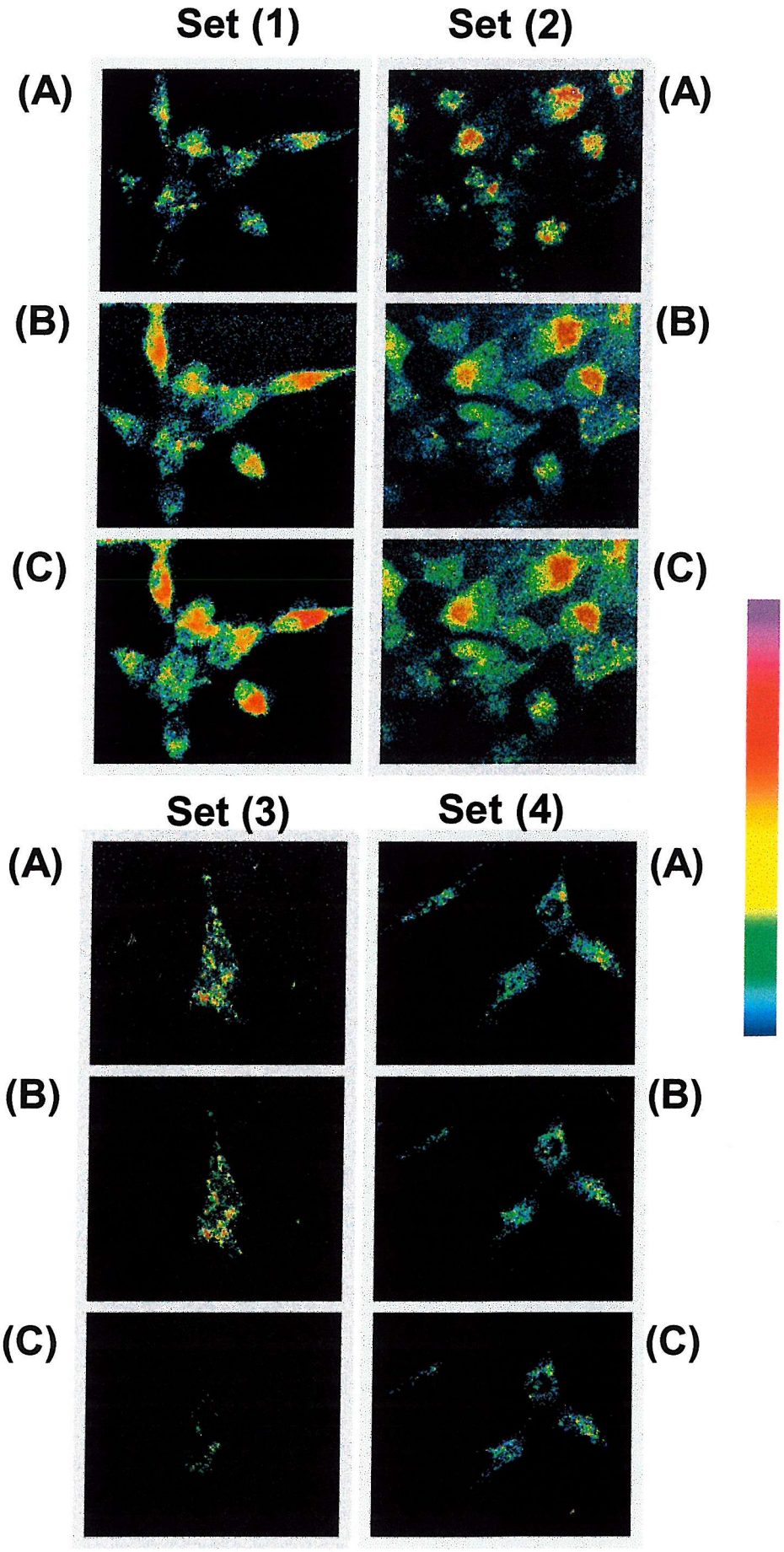
Set (1)
Set (2)
(A)
(B)
(C)
Set (3)
Set (4)

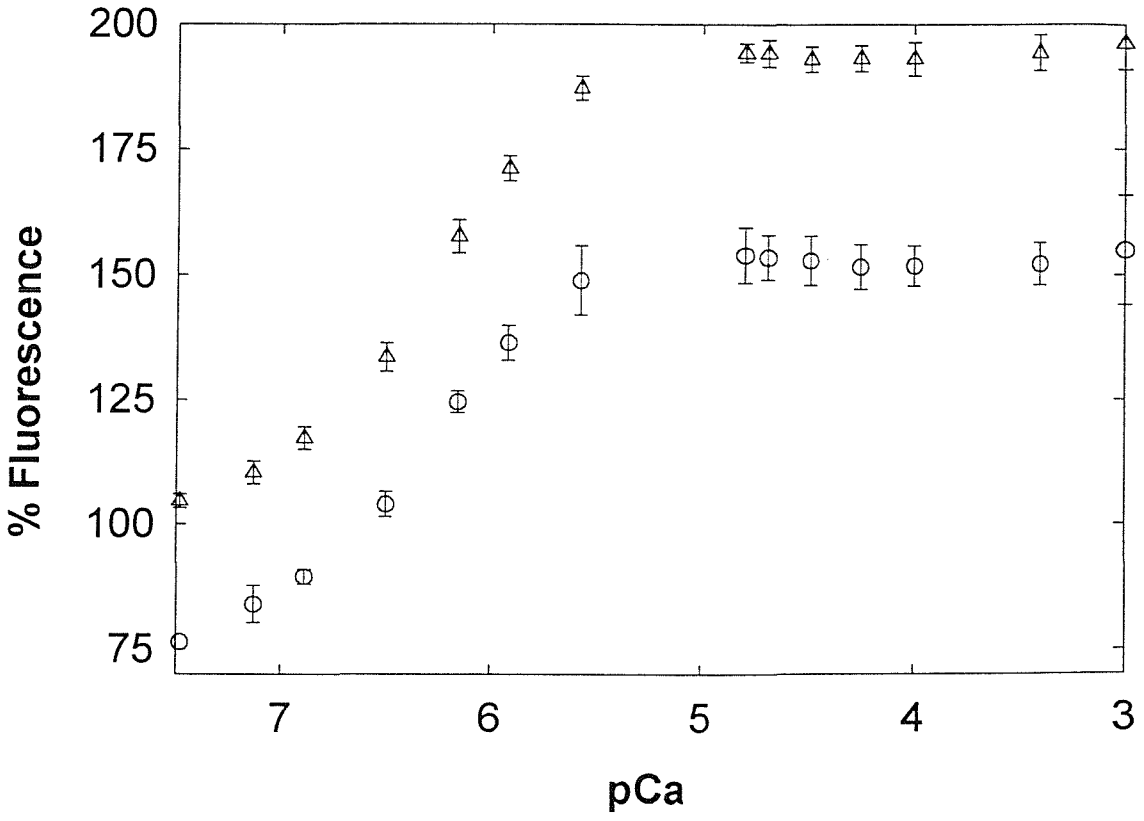

Figure 4.4. Effect of calcium concentration on the fluorescence of calcium crimson

The fluorescence intensity at the emission maximum was plotted. Excitation was set at 578 nm and the emission intensity was measured at 612 nm. (Δ) indicate the percentage fluorescence of calcium crimson in the absence of curcumin; (o) indicate the percentage fluorescence of calcium crimson in the presence of 25 μM curcumin. The midpoint of the curve gives a pCa value of ~6 and remains the same in the presence of curcumin.

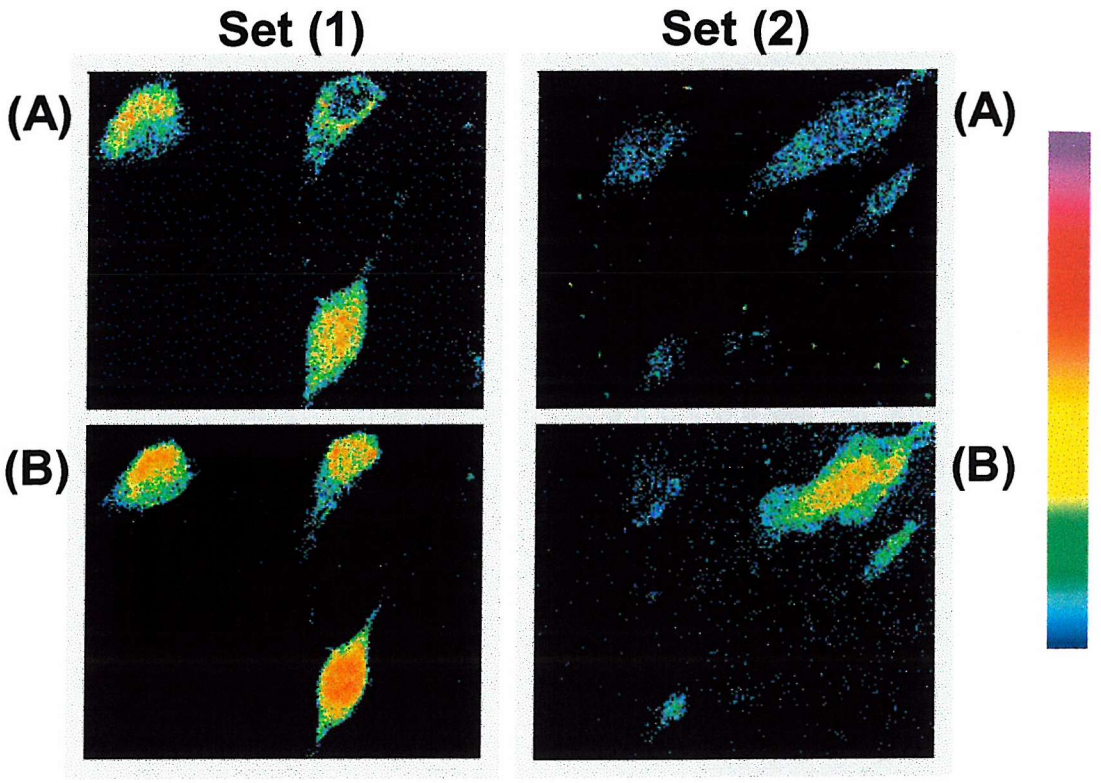

Figure 4.5. Ionophore increases cytosolic calcium levels

QT-6 cells were loaded with calcium crimson and pictures collected as previously described. Set (1) shows QT-6 cells at (A) t = 0 and (B) 2.5 min after addition of 50 μM of the ionophore A23187. Set (B) shows the response to A23187 after incubation with 25 μM curcumin for 2.5 min.

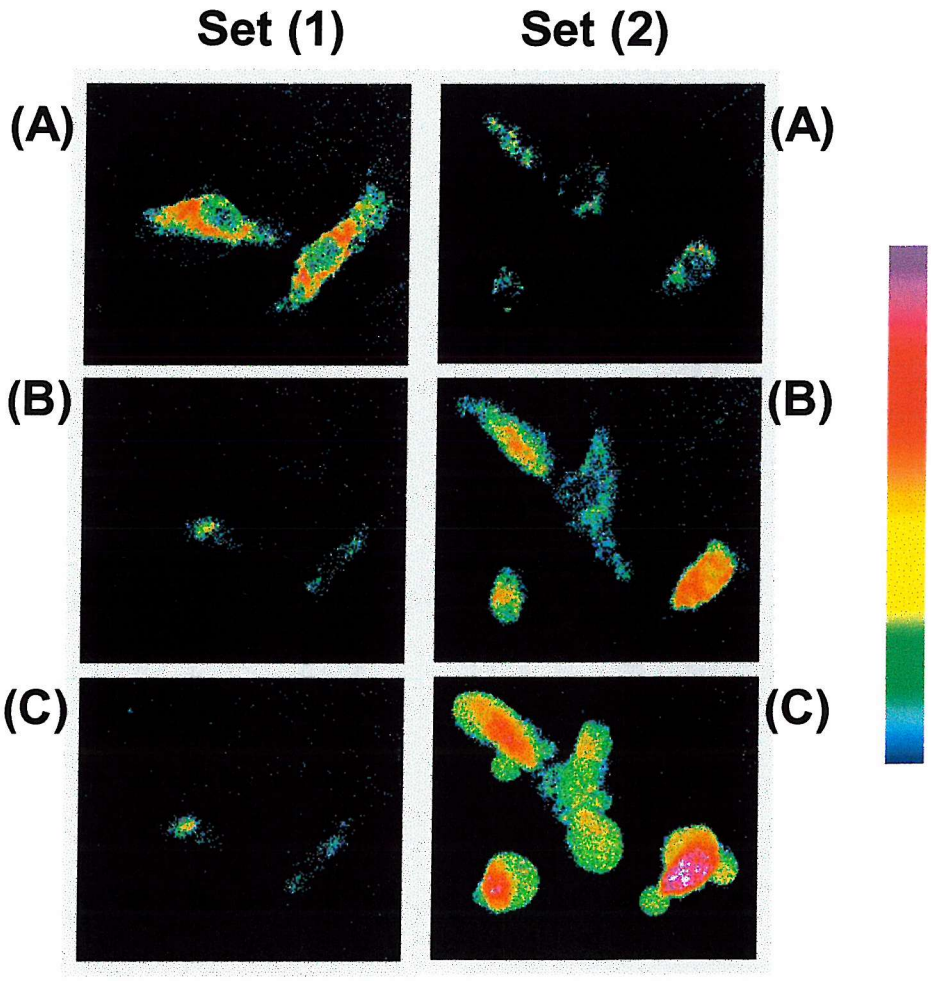

Figure 4.6. Mn^{2+} ions quench calcium crimson fluorescence

QT-6 cells were loaded with calcium crimson and pictures collected as previously described. Pictures were collected at (A) t = 0, (B) = 0.5 min and (C) 2.5 min. Set (1) shows the effect of addition of 1 mM $MnSO_4$ and set (2) shows the effect of 10 μM trilobilide on cells pre-treated with $MnSO_4$ for 2.5 min.

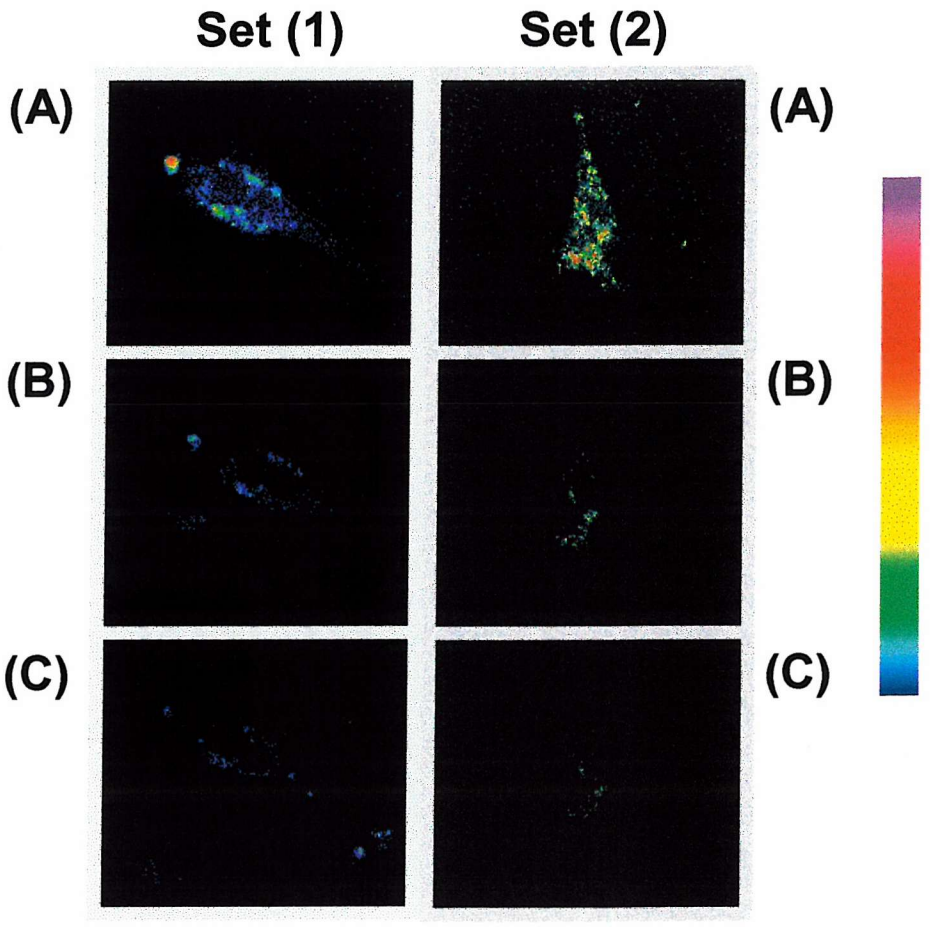

Figure 4.7. Curcumin blocks calcium release by trilobilide and BHQ

QT-6 cells were loaded with calcium crimson and pictures collected as previously described. The effects of 25 μM curcumin on calcium release by a second Ca^{2+}-ATPase inhibitor were measured, either 10 μM trilobilide (set (1)) or 25 μM BHQ (set (2)). Pictures were collected at (A) t = 0, (B) 2.5 min after curcumin addition, followed by the addition of the second inhibitor and collection 2.5 min later ((C) t = 5 min).

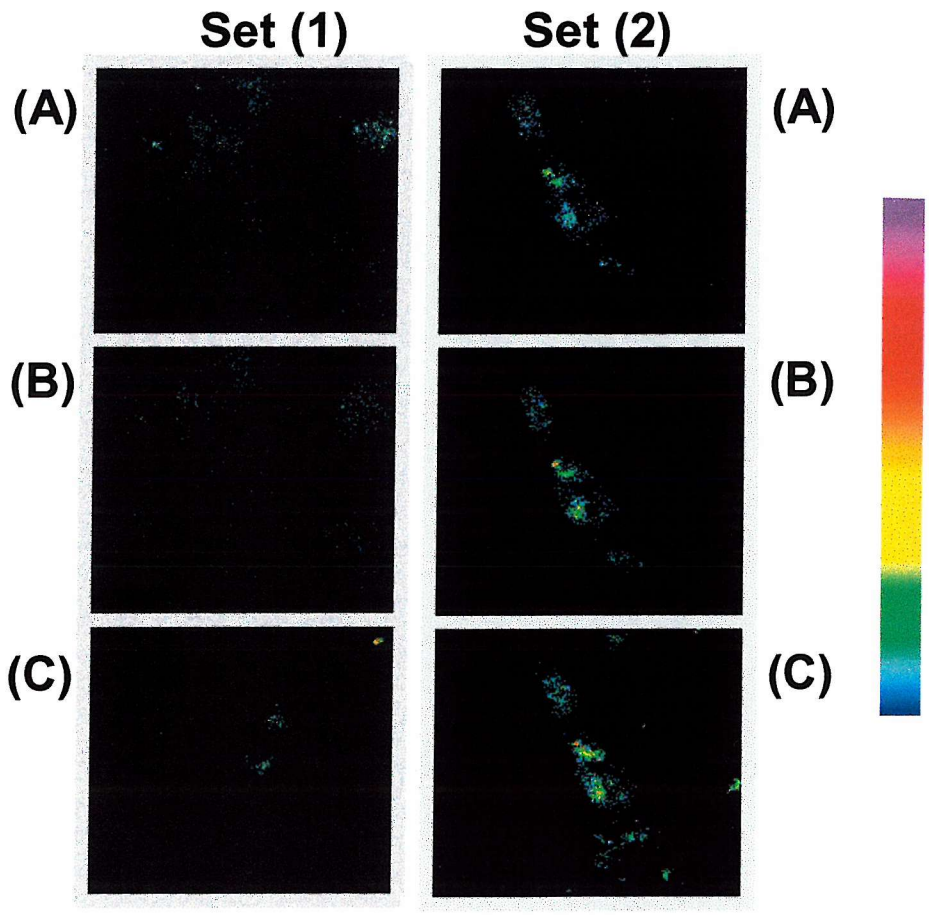

Figure 4.8. The effect of curcumin analogues on calcium release in QT-6 cells

QT-6 cells were loaded with calcium crimson and pictures collected as previously described. The effects of 25 μM bisdesmethoxycurcumin (set (1)) and analogue 3 (set (2)) and their effect on calcium release by trilobilide were measured. Pictures were collected at (A) t = 0, (B) 2.5 min after the addition of the curcumin analogue, followed by the addition of the trilobilide and collection 2.5 min later ((C) t = 5 min).

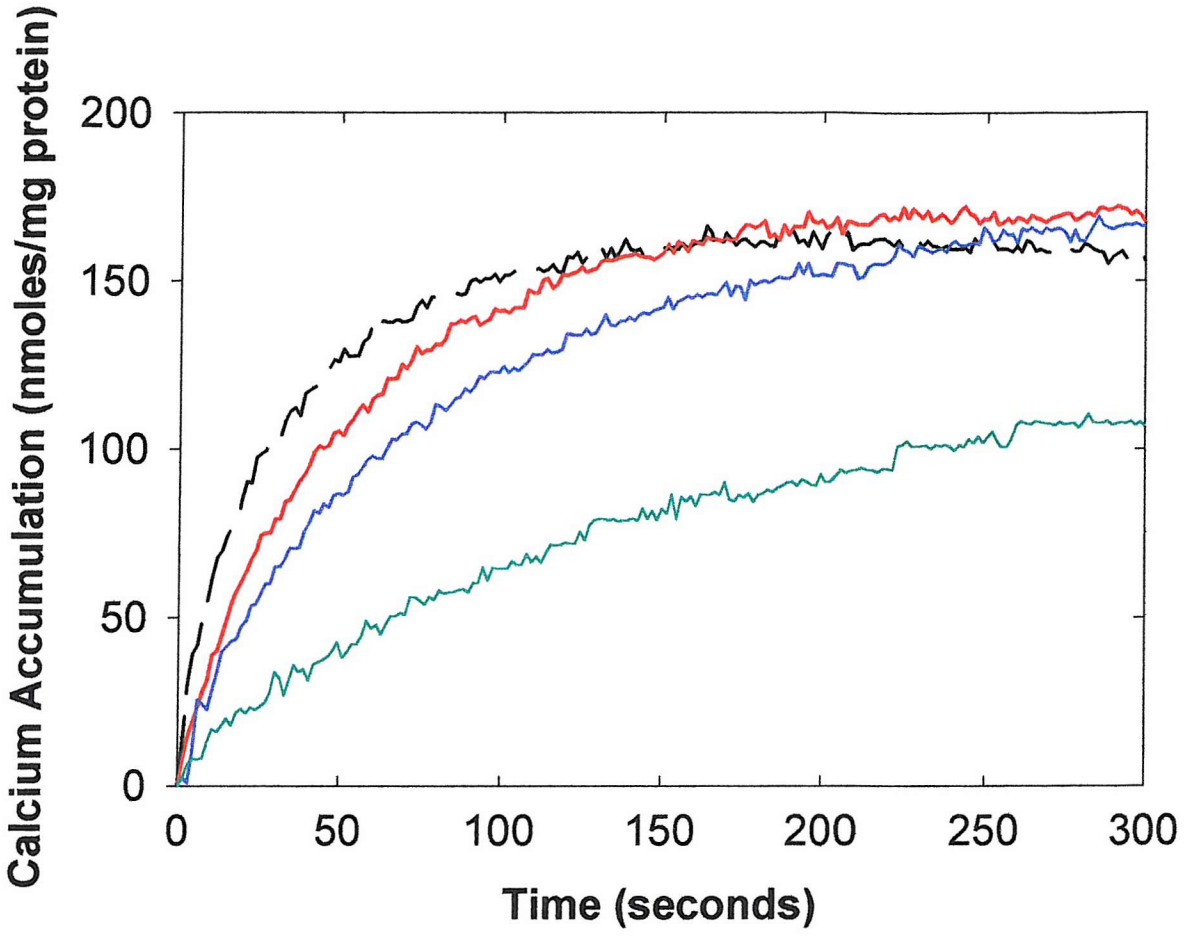

Figure 4.9. The effect of BHQ and curcumin on Ca^{2+} accumulation

The figure shows calcium uptake by SR vesicles in the absence or presence of 2μM BHQ and 15 μM curcumin. Uptake was measured at 25 ^{0}C, pH 7.1 0.08 mg protein/ml was used and the uptake was started by addition of 0.8 mM ATP. Shown are the uptakes for: (_ _ _) SR; (___) SR in the presence of 2 μM BHQ; (___) SR in the presence of 4 μM BHQ; (___) SR in the presence of 2 μM BHQ + 15 μM curcumin.

Figure 4.10. The effect of curcumin on Ca^{2+} accumulation

The figures show calcium uptake by SR vesicles in the absence or presence of curcumin. 0.08 mg protein/ml was used. (A): Shown are the uptakes for: (_ _ _) SR; (___) SR in the presence of 6 μM curcumin; (___) SR in the presence of 10 μM curcumin; (___) SR in the presence of 15 μM curcumin. (B): Shown are the uptakes for: (_ _ _) SR; (___) SR in the presence of 0.5 μM curcumin; (___) SR in the presence of 1 μM curcumin; (___) SR in the presence of 2 μM curcumin; (___) SR in the presence of 6 μM curcumin. (C) and (D) show results of simulations of accumulation of calcium. In (C) the rate of slippage was fixed at zero and rates of passive leak (s^{-1}) were a: 1×10^{-5}, b: 1.5×10^{-5} and c: 2×10^{-5}. In (D) the rate of passive leak ($Ca_I \rightarrow Ca_o$) was fixed at $2 \times 10^{-6} s^{-1}$ with values for the rate of slippage steps (s^{-1}) of a: 65, b:55, c:40 and d:35.

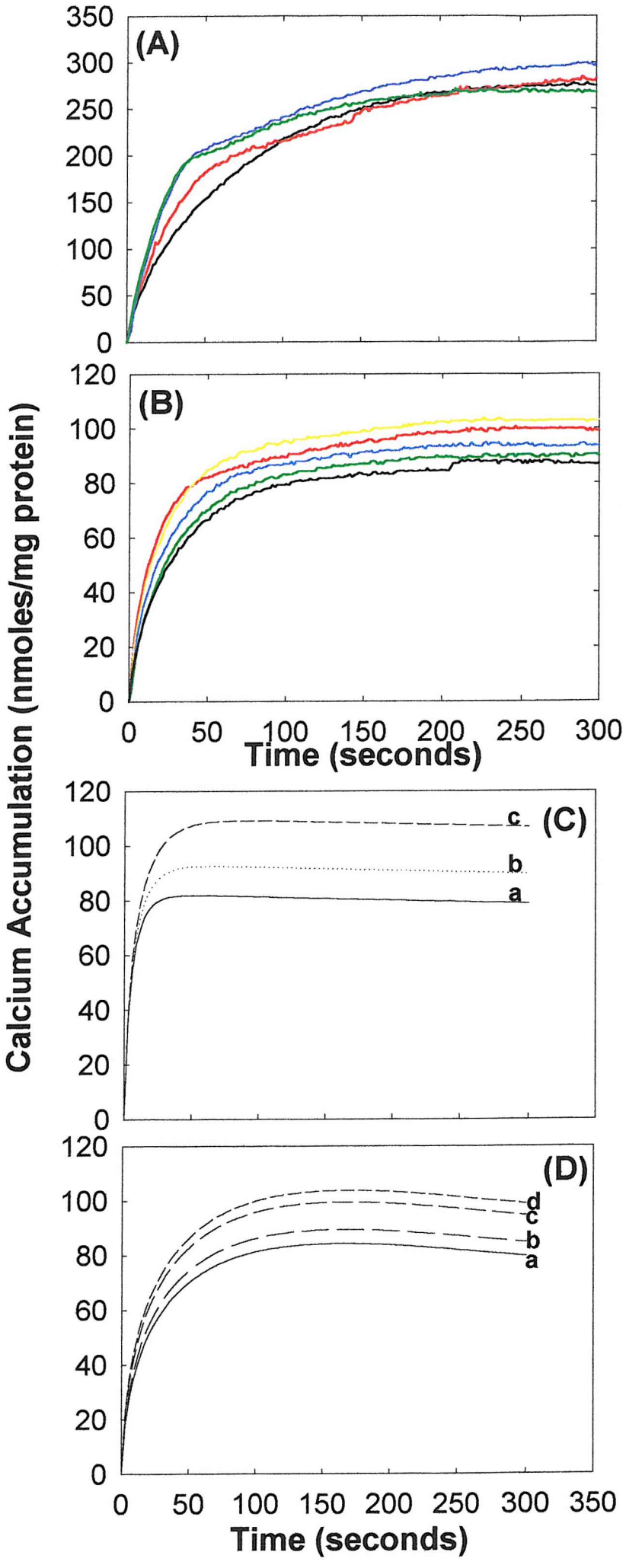
(A)
(B)
(C)
(D)
Calcium Accumulation (nmoles/mg protein)
Time (seconds)
Time (seconds)
a
b
c
d

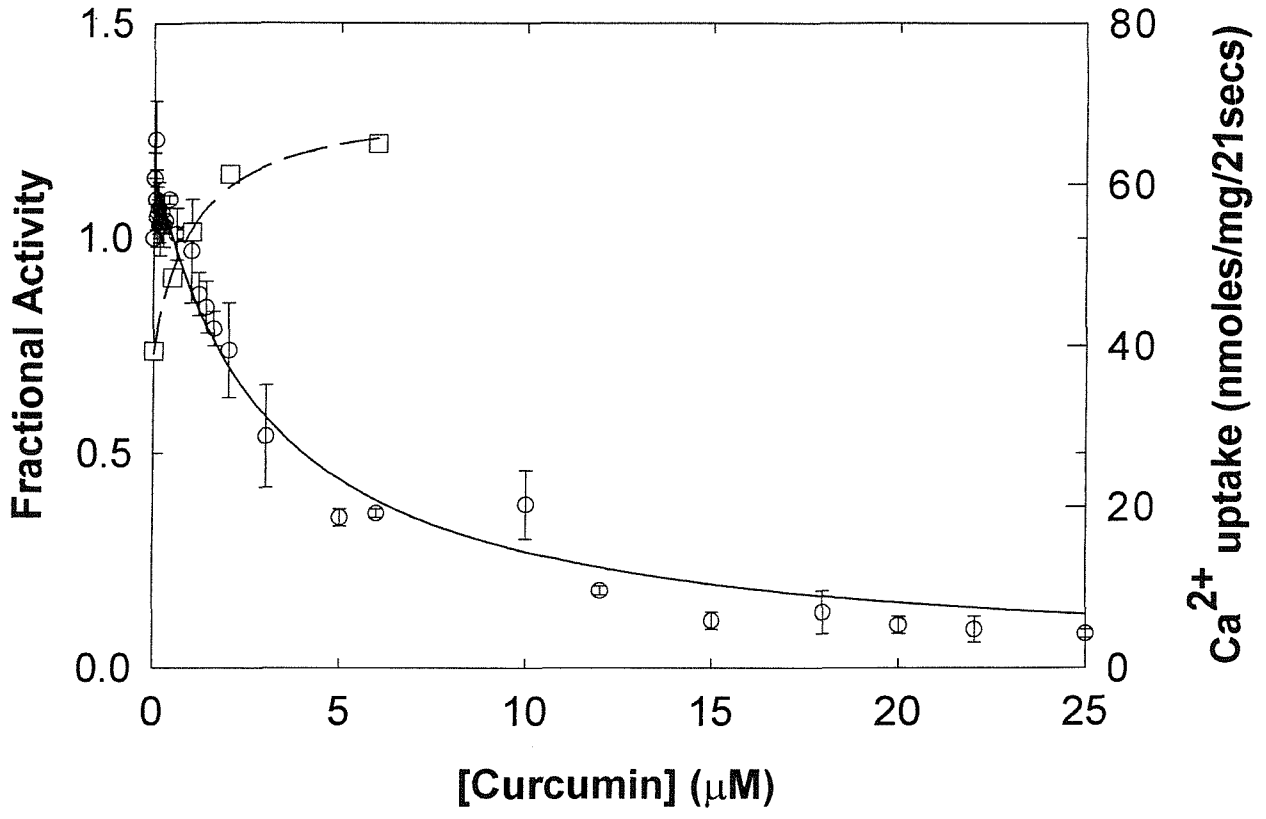

Figure 4.11. Comparison of effects of curcumin on the accumulation of calcium and the rate of hydrolysis of ATP

Rates of hydrolysis of ATP were determined for SR vesicles in the presence of 5 μg of the calcium ionophore A23187, as a function of curcumin concentration and expressed as a fraction of the value in the absence of curcumin. The solid line shows a fit to a two site model (Appendix 1). Levels of accumulation of calcium (nmoles/mg protein) were determined after 21 seconds as a function of curcumin concentration. The broken line shows a fit to a simple Michaelis-Menten scheme for stimulation of accumulation with a maximal increase in the level of accumulation of 30.1 ± 6.4 nmoles calcium/mg protein/21 seconds, with a concentration of curcumin giving 50 % maximal effect at 1.03 ± 0.25 μM.

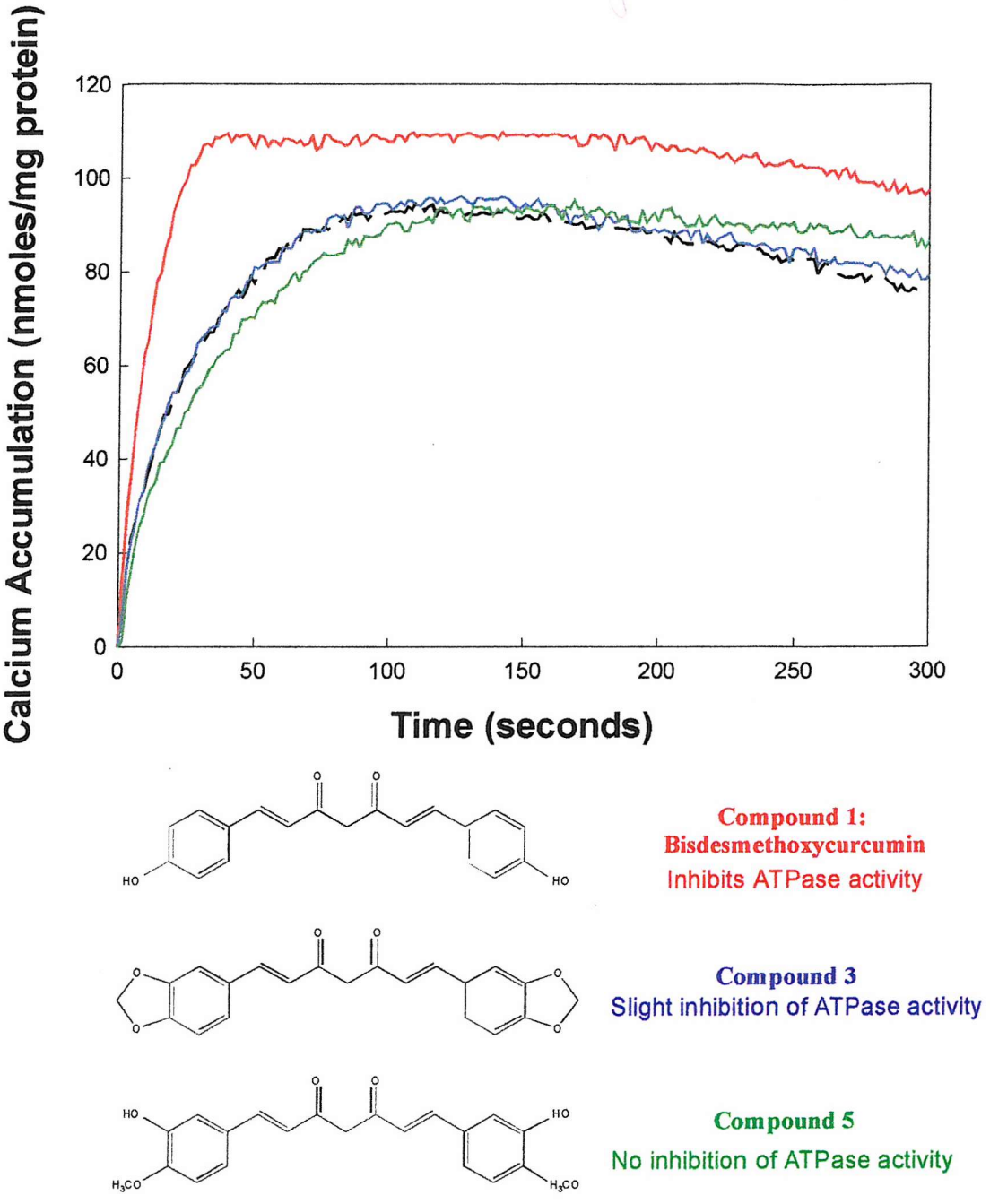

Figure 4.12. The effect of curcumin analogues on Ca^{2+} Uptake

The figure shows calcium uptake by SR vesicles in the absence or presence of curcumin analogues. 0.08 mg protein/ml was used. Shown are the uptakes for: (_ _ _) SR; (___) SR in the presence of 6 μM analogue number 5; (___) SR in the presence of 6 μM analogue number 3; (___) SR in the presence of 6 μM bisdesmethoxycurcumin.

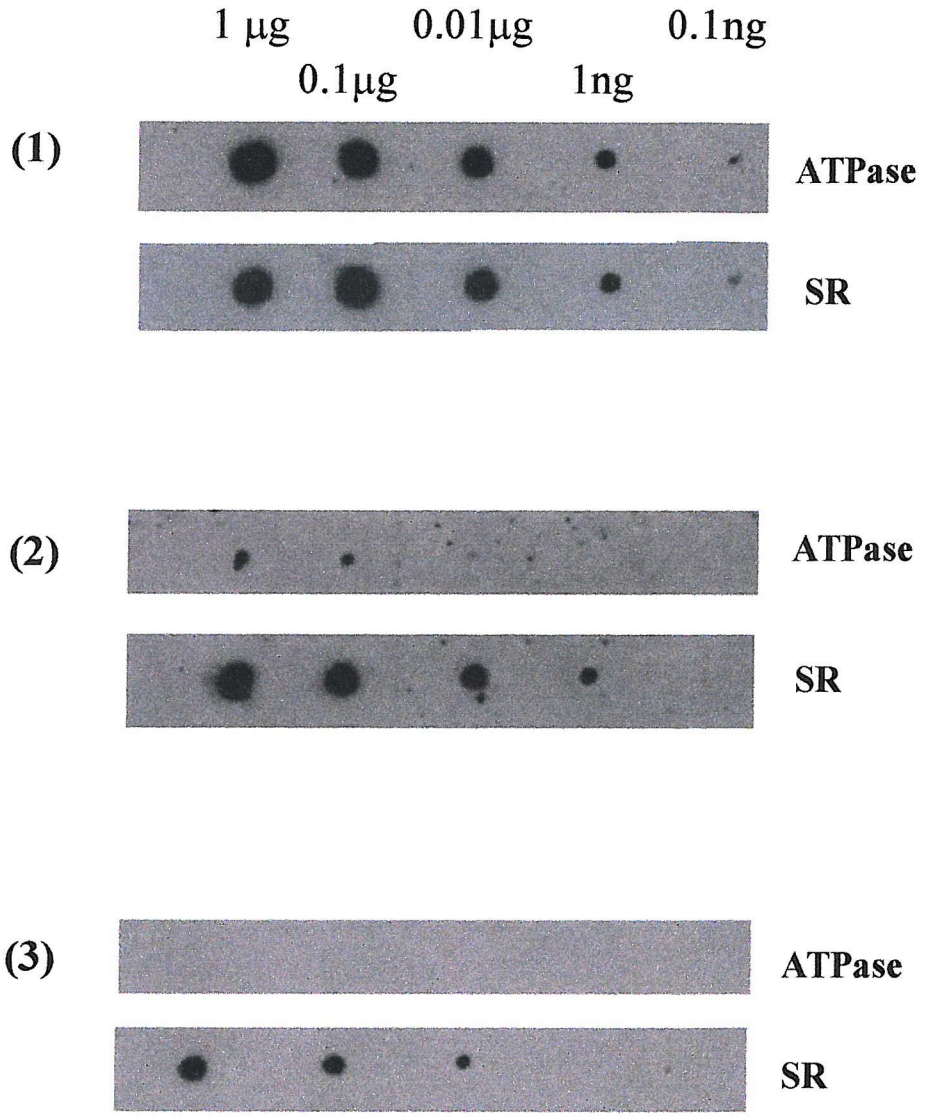

Figure 4.13. Analysis of proteins present in SR

The figure shows dot blots of ATPase and SR. Set (1) were probed with the primary antibody Y1F4, against SERCA; Set (2) were probed with the antibody C1F9, against calsequestrin; Set (3) were probed with the antibody RRZAS, against the ryanodnine receptor. The primary antibody was diluted 1:10. The secondary antibody was HRP conjugated (Sigma; diluted 1:80000). An enhanced chemiluminescence kit (Amersham) was used for detection.

Figure 4.14. The effect of curcumin and ruthenium red on Ca^{2+} accumulation

Figure (A) shows calcium uptake by SR vesicles in the absence or presence of curcumin and ruthenium red. 0.08 mg protein/ml was used. Shown are the uptakes for: (_ _ _) SR; (___) SR in the presence of 200 μM ruthenium red; (___) SR in the presence of 200 μM ruthenium red and 10 μM curcumin. Figure (B) shows calcium uptake by light SR (LSR) vesicles in the absence or presence of curcumin and ruthenium red. Shown are the uptakes for: (_ _ _) LSR; (___) LSR in the presence of 15 μM curcumin; (___) LSR in the presence of 100 μM ruthenium red; (___) LSR in the presence of 15 μM curcumin + 100 μM ruthenium red. Figure (C) shows calcium uptake by heavy SR (HSR) vesicles in the absence or presence of curcumin and ruthenium red. Shown are the uptakes for: (_ _ _) HSR; (___) HSR in the presence of 15 μM curcumin; (___) HSR in the presence of 100 μM ruthenium red; (___) HSR in the presence of 15 μM curcumin + 100 μM ruthenium red.

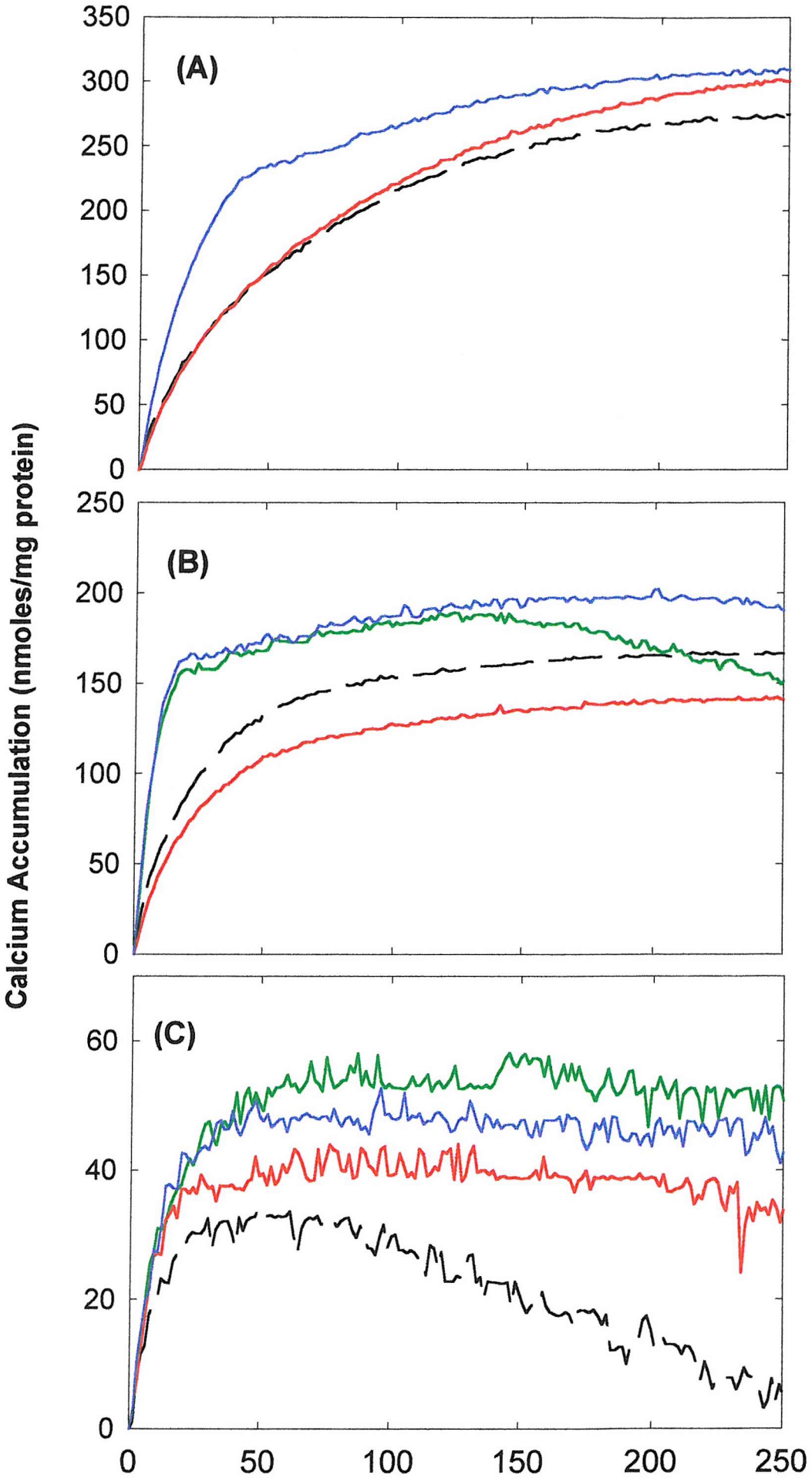
(A)
(B)
(C)
Calcium Accumulation (nmoles/mg protein)
350
300
250
200
150
100
50
0
250
200
150
100
50
0
60
40
20
0
0
50
100
150
200
250

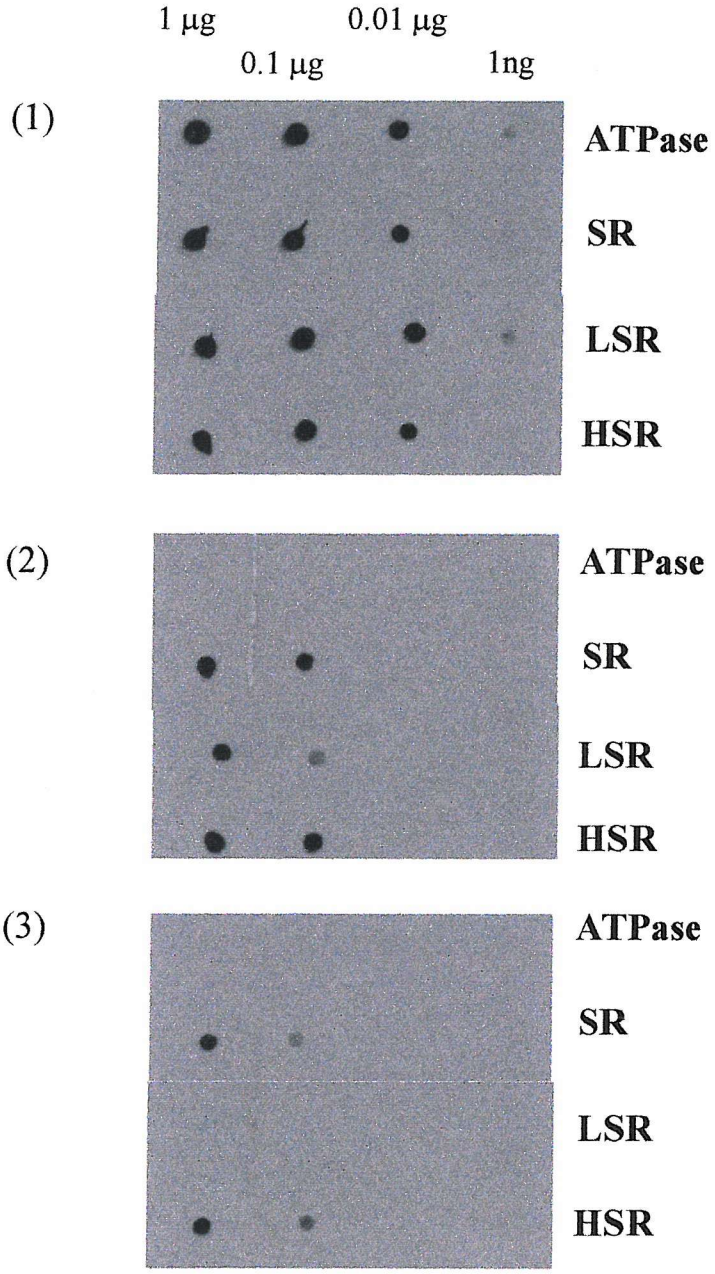

Figure 4.15. Qualitative analysis of LSR

The figure shows dot blots of ATPase, SR, LSR and HSR. Set (1) were probed with the primary antibody Y1F4; Set (2) were probed with the antibody C1F9; Set (3) were probed with the antibody RRZAS. The primary antibody was diluted 1:10. The secondary antibody was HRP conjugated (Sigma; diluted 1:80000). An enhanced chemiluminescence kit (Amersham) was used for detection.

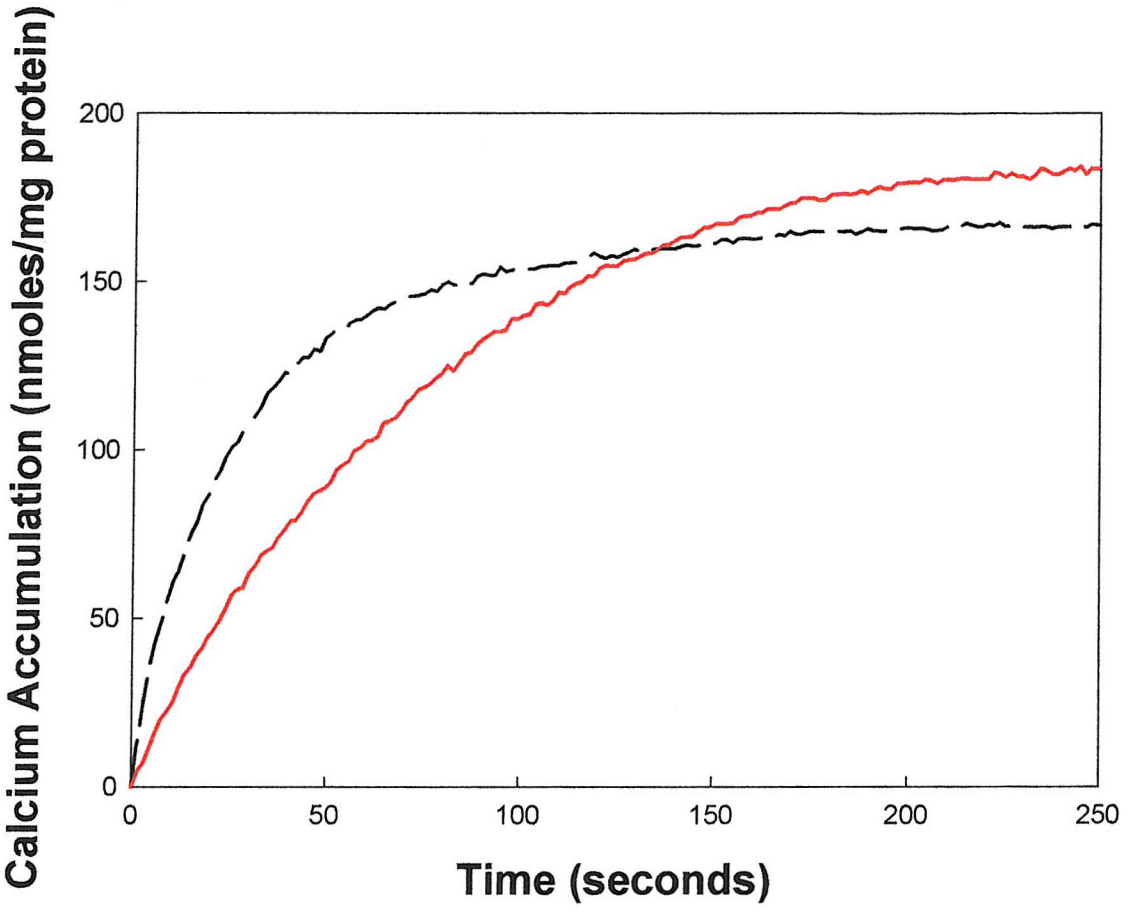

Figure 4.16. The effect of BHQ on Ca^{2+} accumulation by LSR

The figure shows calcium uptake by light SR (LSR) vesicles in the absence or presence of BHQ. 0.08 mg LSR protein/ml was used. Shown are the uptakes for: (_ _ _) LSR; (___) LSR in the presence of 2 μM BHQ.

Figure 4.17. The effect of IP_3 receptor blockers on Ca^{2+} accumulation

The figures show calcium uptake by SR vesicles in the absence or presence of curcumin with 2-APB and xestospongin C (XeC). 0.16 mg protein/ml was used for the uptake with 2-APB, 0.08 mg protein/ml was used with XeC. In (A) Arsenazo III was used to measure uptake. Uptakes are shown for: (_ _ _) SR; (___) SR in the presence of 15 μM curcumin; (___) SR in the presence of 50 μM 2-APB; (___) SR in the presence of 15 μM curcumin and 50 μM 2-APB. In (B) Antipyrylazo III was used to measure uptake. Uptakes are shown for: (_ _ _) SR; (___) SR in the presence of 15 μM curcumin; (___) SR in the presence of 10 μM XeC; (___) SR in the presence of 15 μM curcumin and 20 μM XeC.

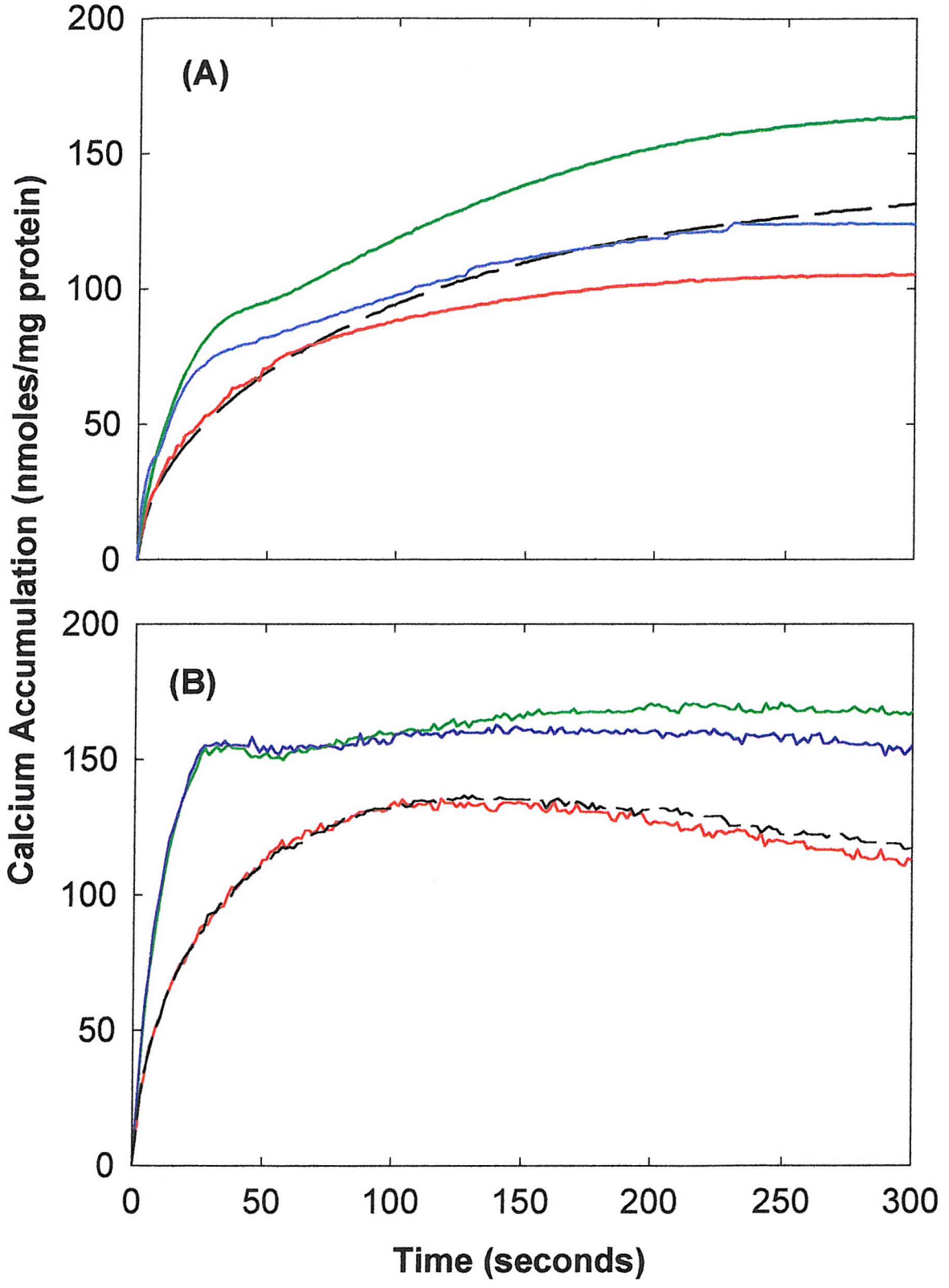
(A)
(B)
Calcium Accumulation (nmoles/mg protein)
Time (seconds)
0
50
100
150
200
250
300

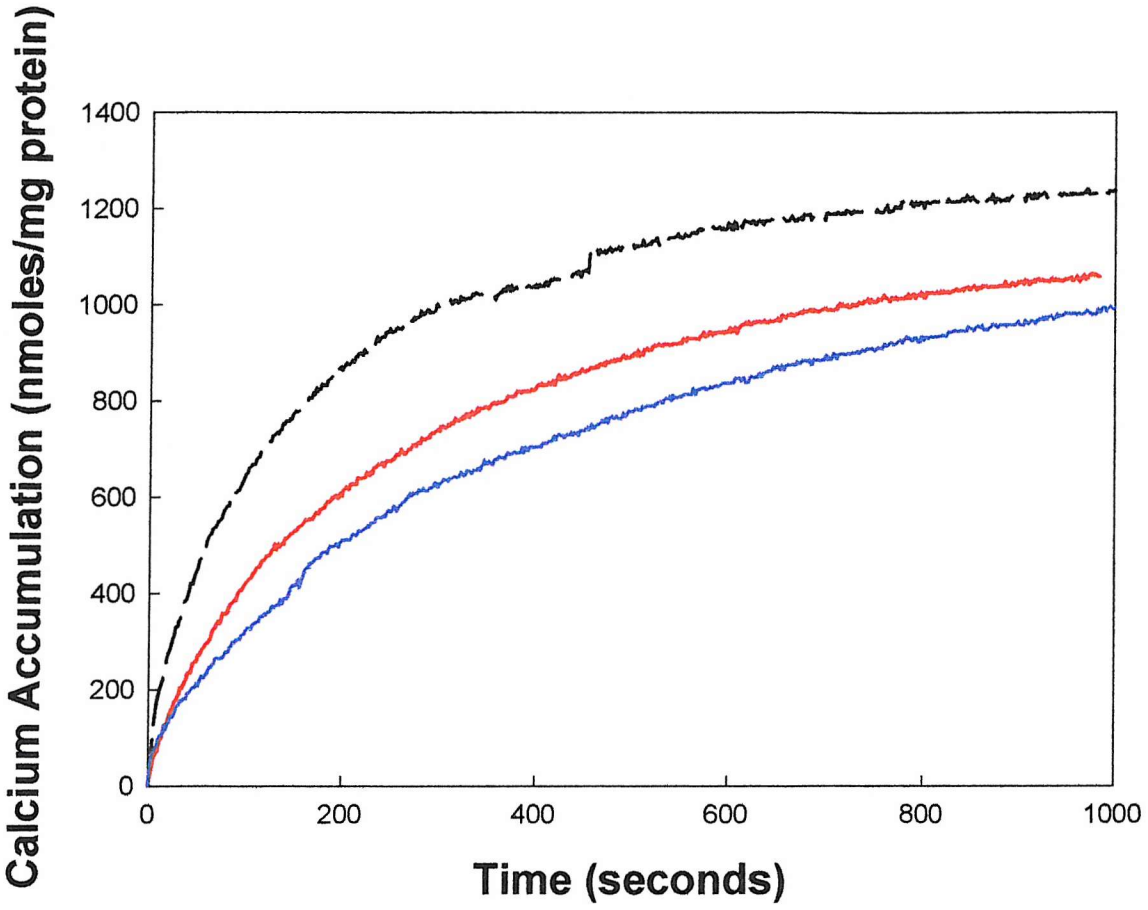

Figure 4.18. The effect of BHQ and curcumin on Ca^{2+} accumulation by reconstituted SR

The figure shows calcium uptake by reconstituted SR (rSR) vesicles in the absence or presence of curcumin and BHQ. 0.065 mg protein was used in the assay. Shown are the uptakes for: (_ _ _) rSR; (___) rSR in the presence of 15 μM curcumin; (___) rSR in the presence of 2 μM BHQ.

Figure 4.19. Accumulation of calcium in the presence of acetyl phosphate or a regenerating system

The figures show calcium uptake by SR vesicles in the absence or presence of BHQ and curcumin. Uptake was started by addition of 0.8 mM ATP or 1.6 mM acetyl phosphate (AcP). (A): Shown are the uptakes for: (_ _ _) SR using AcP; (___) SR using ATP; (___) SR in the presence of 2 μM BHQ using AcP. (B): Using AcP, shown are the uptakes for: (_ _ _) SR; (___) SR in the presence of 1 μM curcumin; (___) SR in the presence of 6 μM curcumin; (___) SR in the presence 15 μM curcumin. (C) Using a regeneration system (1.5 mM PEP and 7.5 IU pyruvate kinase), shown are the uptakes for: (_ _ _) SR; (___) SR in the presence of 2 μM BHQ; (___) SR in the presence 15 μM curcumin

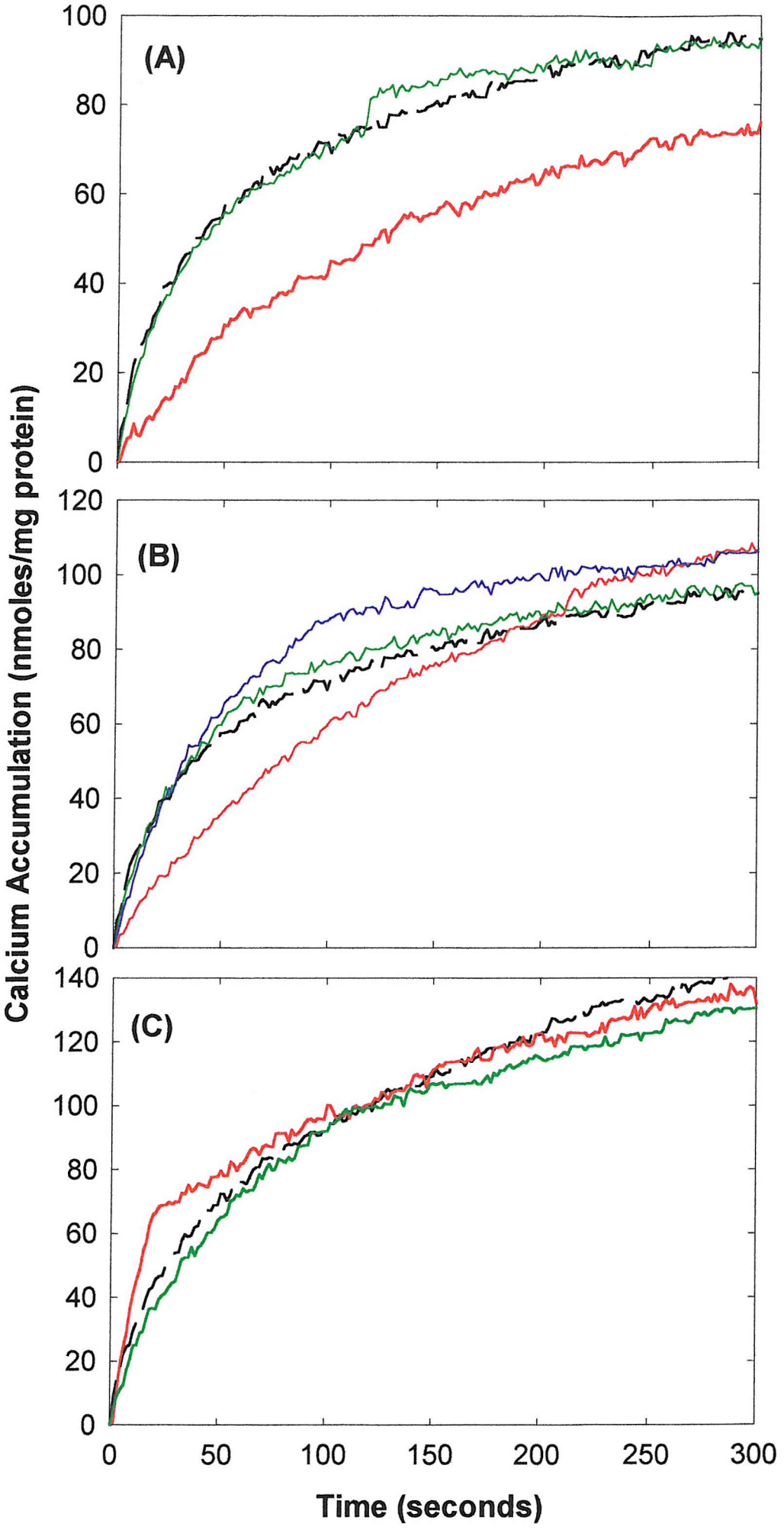
(A)
(B)
(C)
Calcium Accumulation (nmoles/mg protein)
Time (seconds)
0
20
40
60
80
100
120
140
0
50
100
150
200
250
300

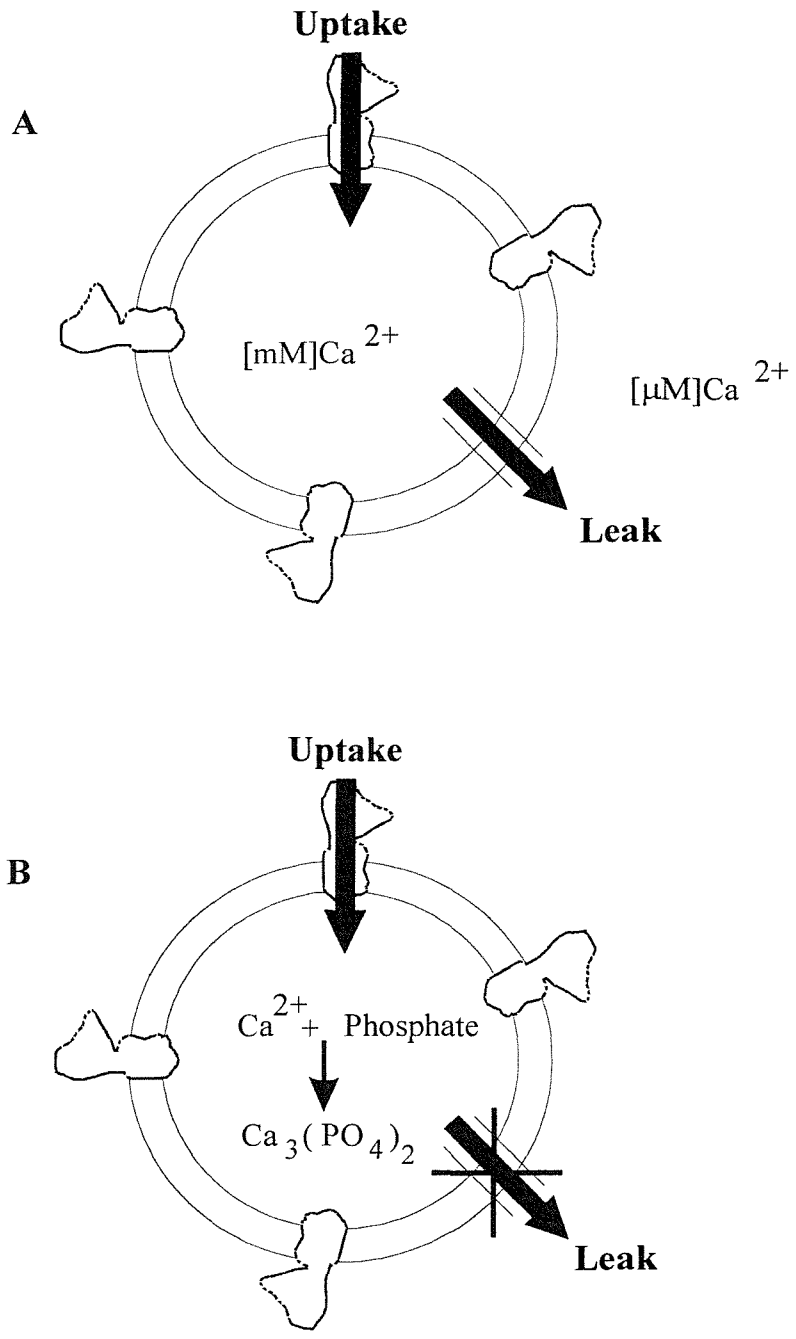

Figure 4.20. Schematic representation of SR Vesicles

(A) shows uptake and leak of calcium from a vesicle. The accumulated calcium inside the vesicles reaches millimolar. (B) shows uptake and leak in the presence of phosphate. Phosphate enters through a phosphate channel and complexes with the calcium on the inside of the vesicle keeping the concentration of free calcium within the vesicles low, so reducing the rate of leak.

Figure 4.21. The effect of P_i and oxalate on Ca^{2+} accumulation

The figures show calcium uptake by SR vesicles in the absence or presence of BHQ and curcumin, with P_i or oxalate present. 0.16 mg protein/ml was used for uptake with 5 mM P_I and 0.08 mg protein/ml was used for the uptake with 2 mM oxalate. (A): Shown are the uptakes for: (_ _ _) SR in the presence of P_i; (___) SR in the presence of P_i + 15 μM curcumin; (___) SR in the presence of P_i + 2 μM BHQ. (B): Shown are the uptakes for: (_ _ _) SR in the presence of 2 mM oxalate; (___) SR in the presence of 2 mM oxalate + 15 μM curcumin; (___) SR in the presence of 2 mM oxalate + 2 μM BHQ.

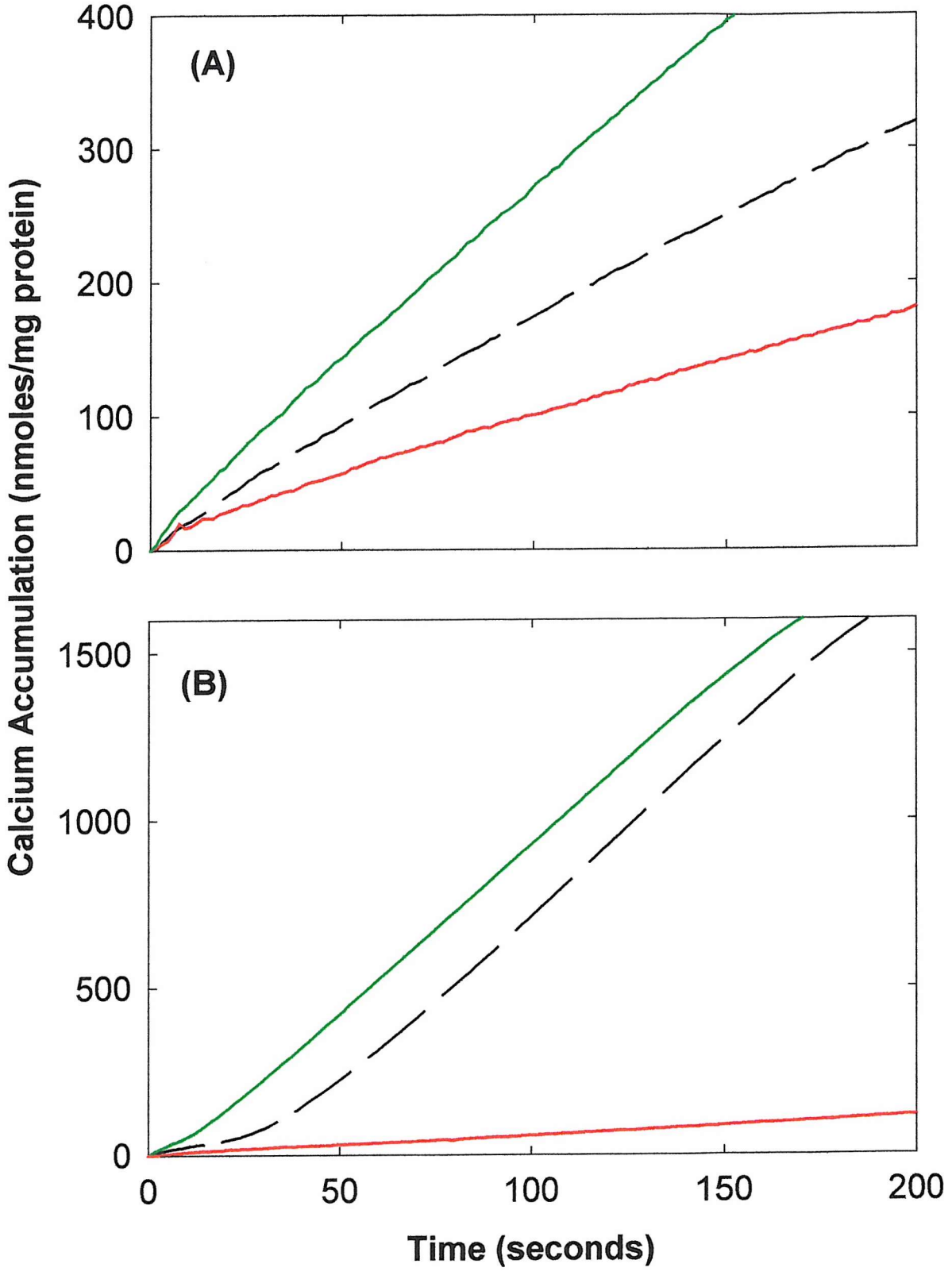
(A)
(B)
400
300
200
100
0
1500
1000
500
0
0
50
100
150
200
Calcium Accumulation (nmoles/mg protein)
Time (seconds)

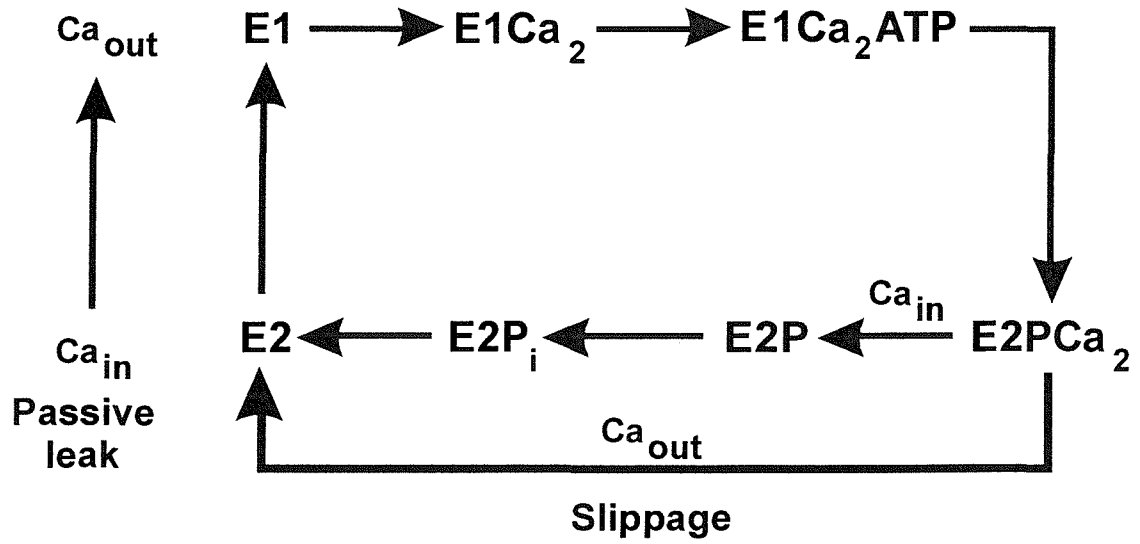

Scheme 4.1. The E1-E2 reaction scheme of the Ca^{2+}-ATPase

Two Ca^{2+} ions bind sequentially to the two high affinity sites in the E1 conformation of the enzyme. ATP binds and subsequent phosphorylation occurs, with a conformation change to E2. The two Ca^{2+} ions are released from the now low affinity sites and the enzyme is dephosphorylated giving E2. The Ca^{2+}-ATPase then returns to the E1 conformation. Passive leak occurs when the concentration of calcium inside the vesicle rises. Slippage occurs when the phosphorylated ATPase releases calcium to the cytosol, not to the lumen (uncoupling of the ATPase).

Inhibitor	Calcium Accumulation	% ATPase Activity
-	53	100
Curcumin analogue 3 (6 μM)	46	100
Curcumin analogue 5 (6 μM)	54	100
Bisdesmethoxycurcumin (6 μM)	95	18
Curcumin (6μM)	109	36
Ruthenium red (200 μM)	50	-

Table 4.1. Effects of compounds on calcium accumulation and on ATPase activity

The table shows the level of accumulation of calcium (nmoles/mg protein) after 21 seconds in the absence of curcumin or in the presence of curcumin, its analogues or ruthenium red. Also shown is the % of initial ATPase activity in the presence of curcumin and its analogues.

Chapter Five: Expression of Ca^{2+} -ATPases in Cos-7 cells

5.1. Introduction

5.1.1. Chimeric ATPase constructs

Chimeric molecules are widely used to facilitate identification of critical domains in proteins (Luckie *et al.*, 1992). The areas involved in targeting, binding ions, inhibitors and regulatory proteins may be identified using recombinant DNA approaches. Within the P-type ATPase field constructs of SERCA and the Na^+/K^+-ATPase have been used to identify the critical domains for ATPase function (Luckie *et al.*, 1992) and to elucidate the binding site of thapsigargin (Norregaard *et al.*, 1993; Sumbilla *et al.*, 1993; Ishii *et al.*, 1994). Chimeric SERCA/PMCA pumps were also created to investigate the structural determinants responsible for specific cellular location (Foletti *et al.*, 1995). Chimeras of the Na^+/K^+-ATPase and the H^+/K^+-ATPase were used to study trafficking and functional properties (Blostein *et al.*, 1993; Dunbar *et al.*, 2000) as well as the catalytic subunits responsible for cation specificity and drug binding (Koenderink *et al.*, 2000).

5.1.2. The role of the N terminus

The P-type ATPases form a large family of membrane proteins. They all couple hydrolysis of ATP to the translocation of cations across membranes (Section 1.2). Even though the primary sequences are quite different over the whole family, with less than 15 % homology in some cases (Axelsen & Palmgren, 1998), regions of high homology are present (Figure 1.6). The conserved elements are involved in the functions that are common to all P-type ATPases: ion and nucleotide binding and the coupling of ATP hydrolysis to ion transport (Luckie *et al.*, 1992; Moller *et al.*, 1996). The N and C terminal sequences are the most divergent domains within this family (Lutsenko & Kaplan, 1995; Palmgren & Axelsen, 1998) and therefore may have evolved particular functions specific to each ATPase.

The type II A and B groups of P-type pumps (Axelsen & Palmgren, 1998) consist of the Ca^{2+}-ATPases: the type II B calcium pumps are stimulated by calmodulin whereas the type II A pumps are not (Table 1.1). The mammalian

plasma membrane Ca^{2+}-ATPase (PMCA) is classified as a type II B pump. The C terminus of PMCA is the target for calmodulin binding, phosphorylation and calpain cleavage and serves as an auto-inhibitory site (Carafoli, 1994; Carafoli *et al.*, 1996; Penniston & Enyedi, 1998). However, in plants calmodulin has been found to bind to a putative N terminal auto-inhibitory domain of a vacuolar Ca^{2+}-ATPase, Bca1, from cauliflower (Palmgren & Askerlund, 1997). SERCA, a type II A pump, is not regulated by calmodulin. The N terminus of SERCA forms part of the A (actuator) domain (Toyoshima *et al.*, 2000) that is believed to participate in coupling ATP hydrolysis to ion transport. Yamasaki *et al.* (1997) found that modification of His-5 with diethylpyrocarbonate (DEPC) inhibited EP formation from P_i (Yamasaki *et al.*, 1997). They suggested that this residue, along with the rest of the N terminus may contribute to the catalytic site, but this is difficult to see since in the X-ray structure the N terminus is remote from the phosphorylation and nucleotide binding domain (Toyoshima *et al.*, 2000). However, given that there is evidence that movement of the A domain may play a role in organising events linked to the P and N domains, modification of His-5 could possibly interfere with these changes.

It is possible that a regulatory role of the N terminus may exist. In SERCA2, the V_{max} for calcium transport was found to increase when the Ca^{2+}-ATPase was phosphorylated by a calcium/calmodulin dependent protein kinase II (Xu *et al.*, 1993; Xu & Narayanan, 1999), at residue Ser-38 (Toyofuku *et al.*, 1994). Reddy *et al.* (1995) and Odermatt *et al.* (1996) did not observe this increase. The experimental difficulty is proving selective and direct phosphorylation of the enzyme without achieving phosphorylation of phospholamban (PLN), which causes an increase in calcium affinity (Odermatt *et al.*, 1996). Xu and Narayanan (1999) prevented phosphorylation of PLN with a specific antibody and used ruthenium red to prevent RyR phosphorylation. In these experiments they still demonstrated a significant increase in the V_{max} of calcium sequestration (Xu & Narayanan, 1999). It is noteworthy however that Ser-38 is not present in the SERCA1 or SERCA3 sequence and therefore these isoforms could not be regulated by such a mechanism (Dode *et al.*, 1996). Ser and Thr residues in the N terminal domain of a Na^+/K^+-ATPase are also the target of PKC phosphorylation (Beguin *et al.*, 1994). The heavy metal transporting ATPases, group IB (Axelsen & Palmgren, 1998), contain an extended N terminal domain (Lutsenko & Kaplan, 1995). This could have a role in the selectivity of ions or less directly serve as a store whereby occupancy of the binding

sites is coupled to ATPase activity (Lutsenko & Kaplan, 1995). Thus, the exact roles of the N terminus vary however it is possible that along with the C termini these regions have a structural importance within the P-type ATPase family (Adamo *et al.*, 2000).

The presence of a sequence that may regulate the expression or assist with the folding and membrane insertion of the P-type ATPases has been investigated. Skerjanc *et al.* (1993) deleted most of the residues from Glu-2 to His-32 and observed a decrease in Cos-1 expression of SERCA and inactivation of ATPase activity (Skerjanc *et al.*, 1993a). Daiho *et al.* (1999) subsequently deleted or substituted amino acids in the NH_2 terminal region of SERCA1a and expressed the products in Cos-1 cells (Daiho *et al.*, 1999). They found single deletions (residues 3 to 6) or multiple deletions (residues 3 to 9) reduced expression levels, with a small decrease in the rate of calcium transport, and suggested the NH_2 domain played a functional role in ER mediated quality control ensuring a correctly folded, stable protein was produced. Removal of the amino and carboxy termini destroyed Ca^{2+}-ATPase function (Skerjanc *et al.*, 1993a) and deletion of residues 34-116 (the first transmembrane loop) prevented stable membrane integration however, removal of the NH_2 terminal sequence alone did not affect protein incorporation into the membrane (Skerjanc *et al.*, 1993a).

In order to identify the functions of the N and C termini in the yeast plasma membrane H^+-ATPase deletions were made (Portillo *et al.*, 1989). It was found that most of the N domain is required for functional insertion of the enzyme into the plasma membrane. Adamo *et al.* (2000) deleted residues in the N terminal segment of PMCA and suggested that the N terminus was not essential for synthesis or catalytic function, but was critical for expression of a correctly folded functional Ca^{2+}-ATPase (Adamo *et al.*, 2000). Whereas deletions in the N terminal region of yeast plasma membrane H^+-ATPase (Portillo *et al.*, 1989) and SERCA (Skerjanc *et al.*, 1993a; Daiho *et al.*, 1999) caused rapid degradation of the protein, drastically reducing expression levels, this was not the case with PMCA. Thus, PMCA may be less tightly regulated by the systems that degrade misfolded proteins. Additionally, the N terminus appears to protect against degradation as proteolysis experiments that expose parts of the enzyme previously protected give rise to a protein that is more sensitive to degradation (Adamo *et al.*, 2000).

If the N terminus has a modulatory role in determining levels of expression (due to involvement with membrane insertion and degradation) then it is feasible that this domain of a poorly expressed protein may be exchanged for a sequence from that of a highly expressed pump. Indeed, expression of SERCA in yeast was improved by construction of N terminal chimeras between SERCA and the plasma membrane yeast H^+-ATPase (Reis *et al.*, 1999). Addition of the first 88 residues of the H^+-ATPase to the SERCA sequence improved expression levels three fold, as compared to the unmodified SERCA. The N terminal cytoplasmic segment of this yeast H^+-ATPase is also involved in targeting to the plasma membrane (Portillo *et al.*, 1989). Indeed a shift from the heavy ER fraction to the light ER (possible en route to the plasma membrane) was observed with this chimera (Reis *et al.*, 1999). A replacement chimera in which the N terminal end of SERCA was replaced with that of the H^+-ATPase did not stably express in the yeast system. It would therefore seem that the N terminal portion of SERCA plays a role in enzyme assembly and ER retention (Reis *et al.*, 1999). Indeed, Foletti *et al.* (1995) concluded that the NH_2 terminal region extending to the first transmembrane loop must have some function in ER retention (Foletti *et al.*, 1995).

5.1.3. Heterologous expression systems

Heterologous expression of proteins is now possible in a range of systems. The specific method employed for over-expression depends upon the requirements of the protein of interest. In the case of a membrane protein such as the Ca^{2+}-ATPase there are numerous requirements. Firstly, a properly folded protein must be produced. Secondly, the Ca^{2+}-ATPase requires specific phospholipids for maximal activity and assembly (Lee *et al.*, 1995). The expression process ideally needs to be rapid and the detection of the heterologous pump simple. Eukaryotic systems have been used to express mutated P-type SERCAs (Andersen & Vilsen, 1995) in order to provide information on the functional roles of domains and individual residues. High levels of expression are required to produce enough protein for biochemical analysis in addition to a low background endogenous Ca^{2+}-ATPase activity (Maruyama *et al.*, 1989a). The heterologous protein must also possess the same characteristics as its endogenously expressed counterpart.

In 1988, Maruyama and MacLennan first achieved overexpression of the neonatal and adult isoforms of rabbit SERCA1 in Cos-1 cells for site directed mutagenesis studies (Maruyama & MacLennan, 1988). Later, Hussain *et al.* (1992) stably transfected Chinese hamster lung cells with chicken SERCA1a to try to increase expression levels (Hussain *et al.*, 1992). Although successful, the speed of production and the amount of protein generated was not an improvement on the Cos-1 system and the expression levels decreased by approximately 50 % after continuous culture for 6 months. SF9 cells were then infected with a baculovirus vector containing the SERCA1a rabbit fast twitch cDNA (Skerjanc *et al.*, 1993b), that yielded up to 3 mg per litre of SERCA with high activity. However, although this system has some advantages, it still lacks the speed and convenience of the mammalian system. More recently, Strock *et al.* (1998) improved expression levels of their mutant constructs in Cos-1 cells using recombinant adenovirus vectors, yielding enough protein for calcium binding studies (Strock *et al.*, 1998). They demonstrated 97-100 % transfection efficiency using green fluorescent protein (GFP). With the entire population of Cos-1 cells infected larger quantities of their recombinant ATPase were produced. Interaction of the SV-40 promoter with T antigen helps plasmid amplification in Cos cells (Gluzman, 1981). However, when using the adenovirus vector a different promoter is used and thus protein expression is entirely dependent on the strength of this promoter (Zhang *et al.*, 2000). The adenovirus method is still time-consuming and the practical implications of viral technology must be met.

5.14. The Cos-7 expression system

The Cos-7 mammalian expression system fulfils the requirements for production of SERCA in a heterologous manner. The Cos cells were developed from a CV-1 line of simian cells (Gluzman, 1981). These cells were obtained by transformation with an origin defective mutant SV-40. Cos-7 cells constitutively express functional SV-40 large T-antigen and the SV-40 permissive factors required for plasmid replication to a high copy number. The pcDNA3.1+ plasmid carries viral origin of replication to drive replication but lacks the coding region of the viral genome. After transfection, expression is transient with no viral particles produced. The transfection efficiency of SERCA is 5-10 % in Cos-1 cells and these cells die

70-90 hours post-transfection (Maruyama *et al.*, 1989a). Antibody detection methods are rapid, the expression of the endogenous Ca^{2+}-ATPase is low and the activity of SERCA is high (Maruyama *et al.*, 1989a). Vectors have been designed for high level stable and transient expression in mammalian cells. pcDNA3.1+ (Invitrogen) is such a plasmid (Figure 5.1), containing the SV-40 origin of replication and suitable cloning sites that are compatible with SERCA1b and HVSERCA DNA.

5.15. Transfection of vector DNA

A range of methods have been used for transfection of foreign DNA into cells. These include calcium phosphate co-precipitation (Graham & van der Erb, 1973), high molecular weight polycations (Farber *et al.*, 1975), electroporation (Andreason & Evans, 1988; Shigekawa & Dower, 1988), viral vectors (Shigekawa & Dower, 1988) and cationic liposome mediated transfection (Felgner *et al.*, 1987). The mechanism of lipofection delivery of DNA into cells is not well understood but is thought to occur through a process of endocytosis of the lipid / DNA complex rather than by plasma membrane fusion (Xhou & Huang, 1994). Fugene^{TM} 6 (Roche Molecular Biochemicals) is one of the many transfection reagents available (Simberg *et al.*, 2000). It is a modified liposome protocol, using a blend of lipids and other compounds to maximise transfection efficiency. Fugene^{TM} 6 can be used to transfect a wide variety of cell types with minimal cytotoxicity.

5.2. Methods

A list of all the primers used in this Chapter, with their sequences, can be found in Appendix 2.

5.2.1. Cloning of SERCA1b into pcDNA3.1+

SERCA1b was cloned into pc3.1+ (Invitrogen) using the construct containing the Ca^{2+}-ATPase, ppA8 (Adams *et al.*, 1998; Black, 1999). This involved sub-cloning into pcINeo (Promega) and final ligation into pc3.1+ NheI/Not1.

5.2.2. Construction of a SERCA/HVSERCA chimera

Lockyer *et al.* (1997) cloned an insect Ca^{2+}-ATPase from the tobacco budworm *Heliothis virescens* (Lockyer *et al.*, 1998). Expression levels in the mammalian Cos-7 system were low. If a signal sequence for membrane insertion and expression exists in the first portion of SERCA then it was postulated that by replacing this part of the HVSERCA sequence with the N terminus of SERCA, the levels of expression in Cos-7 cells may be increased, producing sufficient enzyme for functional studies.

Firstly, inclusion of the first three trans-membrane domains of SERCA may have an effect on the expression levels and secondly by replacing these domains an epitope may be included to permit detection of the expressed Ca^{2+}-ATPase with a SERCA specific antibody.

Figure 5.2 shows the PCR strategy for construction of the SERCA/HVSERCA chimera. A SERCA1b DNA fragment was produced from the 5' end of SERCA1b (in pcDNA3.1+) including the start codon ((A) Figure 5.2). The primers used were S1bNhe1s and S1bKpnHVa. The former primer introduced a NheI site at the 5' end before the start codon. Using the latter primer an overlap of HVSERCA sequence and a KpnI site was introduced at the 3' end. A HVSERCA fragment was generated using the PCR edited HVSERCA cDNA construct in pcDNA3.1+ (Figure 5.1) as a template (Lockyer, 1997). The primers HVKpnS1bs and HVXhoa were used to produce a HVSERCA fragment. The forward primer HVKpnS1bs introduced a SERCA1b overlap and Kpn I site at the 5' end ((B) Figure 5.2). At the 3' end using the other (reverse) primer a XhoI site was introduced. The

sequence overlaps were designed as a template for the second round of PCR (Figure 5.2, stage (C)). The second round of PCR used the two fragments generated above and the end primers S1bNhe1s and HVXhoa (used above). The final PCR product was subsequently cloned into the polylinker of pcDNA3.1+ using the restriction sites Nhe1/Xho1 (Figure 5.3) that had been generated in the PCR process. Figure 5.4 illustrates the chimera generated.

5.2.3. Construction of SERCA-GFP

The green fluorescent protein (GFP) from the *Aequorea* jellyfish is widely used as a marker reflecting levels of gene expression and localisation (Tsien, 1998). Clontech developed a variant called enhanced GFP (eGFP) that is more efficiently expressed and has greater fluorescence intensity and this has been used in these experiments. The gene for GFP can be attached to the end of a specific protein of interest and upon translation the GFP is made and can be visualised directly using fluorescent microscopy. Additionally, an antibody epitope in a small linker sequence between the two proteins can be introduced.

For cloning purposes restriction sites were introduced into a SERCA-GFP template. The construct used as a template for this procedure was ppA50 (Adamo *et al.*, 2000). This consists of the construct ppA8 (described above) with a c-myc epitope and the GFP gene fused on the 3' end. Oligonucleotide directed mutagenesis was used to introduce a DNA sequence encoding the human c-myc epitope downstream and in frame with the SERCA1b gene. Subsequently the gene encoding GFP was engineered into this construct at the 3' end.

Figure 5.5 shows the strategy for the construction of SERCA-GFP. The construct of pcDNA3.1+ SERCA1b was used. Initially a 2.1 kb SERCA1b fragment was generated from the 5' end of SERCA1b including the start codon ((A) Figure 5.5) and ending at the Afl II site within the SERCA1b sequence. The primers S1bNhe1s and S1bAflIIa were used to introduce the NheI and Afl II sites. This product was ligated into the polylinker of pcDNA3.1+ using these two restriction sites ((C) Figure 5.5). A DNA fragment of the last 1 kb of SERCA and GFP was then produced from the ppA50 construct described above ((B) Figure 5.5). The primers S1bAflIIs and GFPXho1a were used to produce this 1.5 kb fragment, introducing an Afl II and Xho I site at the 5' and 3' ends respectively. This was then

cloned onto the end of the pc3.1+2.1kb SERCA1b construct using the AflII and XhoI restriction sites ((D) Figure 5.5).

5.2.4. Construction of HVSERCA-GFP

At present, there is no antibody for the insect Ca^{2+}-ATPase that is of use for detecting expression of HVSERCA. Linking GFP onto the protein would directly reveal the heterologous expression levels of this protein.

Initially, HVSERCA was sub-cloned into pNEB193 (New England Biolabs) to give the required restriction sites for the cloning procedure (Figure 5.6). Figure 5.7 shows the strategy for construction of HVSERCA-GFP. A 1.5 kb PCR fragment of the 3' end of HVSERCA was generated using the primers HV1650s and HVXhoPmeNSa ((A) Figure 5.7). In the latter primer the stop codon was removed and the Xho1 and Pme1 restriction sites were introduced to allow for the addition of the GFP gene. A PCR product of the c-myc epitope and the GFP gene was produced using ppA50 (pcDNA1.1 SERCA-GFP) as a template ((B) Figure 5.7). The primers GFPXhos and GFPClaPmea were used to introduce the restriction sites Xho1, Cla1 and Pme1 for future cloning purposes. The 1.5 kb 3' end of HVSERCA was cut out of pNEB193 and replaced with the 1.5 kb PCR product described above ((C) Figure 5.7). This removed the stop codon from the HVSERCA sequence so that translation continued after the HVSERCA sequence, to translate GFP. This construct and the GFP PCR product were digested using Xho1 and Pme1 and ligated together ((D) Figure 5.7). This produced the final pNEB193 HVSERCA-GFP construct. This was then sub-cloned into pcDNA3.1+ (Bam HI/Pme I) for expression purposes.

5.2.5. Cos-7 cell culture

Cos-7 cells were maintained in Dulbecco's Eagles medium (DMEM; Gibco BRL with Glutamax^{TM}) supplemented with 10% foetal bovine serum, 50 μg/ml gentamycin, 2.5 μg/ml amphotericin B (Fungizone ^{TM}), in a 5 % CO_2, 37 ^{0}C incubator.

5.2.6. Transfection of Cos-7 cells

Cos-7 cells were transfected using FuGENE^{TM} 6 (Boeringer Mannheim) transfection reagent, using the manufacturers guidelines. For transfection of 6 x 13 mm diameter coverslips, 2.5 µl FuGENE 6 was added to 83 µl of serum free DMEM in a sterile microcentrifuge tube and incubated at room temperature for 5 minutes. The diluted FuGENE 6 was than added dropwise to a tube containing 1.65 µg DNA. This was left at room temperature for 15 minutes after which time the media was aspirated off the coverslips and the DNA FuGENE mix was added to the cells. Two volumes of DMEM^{3+} was added to the cells and the coverslips were incubated at 37 ^{0}C, for 48 hours.

5.2.7. Fixation of Cos-7 cells

Coverslips with Cos-7 cells grown on the surface were washed 3 times with ice cold PBS. The individual coverslips were then removed from the well plates and immersed in cold 70 % acetone/30 % methanol, for 10 minutes at room temperature in a glass petri dish. The coverslips were then air dried for 10 minutes and then stored in a sealed 24 -well plate, at -20 ^{0}C.

5.2.8. Immunofluorescent staining

Primary antibody was diluted with PBS-Triton X-100 (0.1 %), to the desired concentration. Coverslips were covered with PBS-Triton for 15 minutes at room temperature. This was removed and 100 µl of diluted antibody was added to the coverslips. The 24 -well plate was then put in a humid environment, in a sealed container, at 37 ^{0}C for 1 hour. The individual coverslips were rinsed in PBS-Triton, and then washed twice for 15 minutes at room temperature, with gentle agitation. 100 µl of second antibody FITC conjugate, diluted in PBS-Triton, was then added to each coverslip. The well plate was again incubated in a humid environment, at 37 ^{0}C for 1 hour. The coverslips were rinsed and washed twice as previously. Coverslips were mounted on glass slides using 60 % glycerol in PBS, 2.5 % DABCO (an anti-quench agent) and stored for 2 - 3 days, in the dark, at 4 ^{0}C. The immunofluorescent staining of the cells was visualised using a Leitz fluorescence microscope or a

modified Biorad MRC-600 confocal imaging system equipped with a krypton/argon laser.

5.3. Results

5.3.1. Over-expression of Ca^{2+}-ATPases in Cos-7 cells

The pattern of over-expression was visualised using immunofluorescent staining of fixed cells, 48 hours post-transfection. The monoclonal Y1F4 antibody (Colyer *et al.*, 1989) and a secondary sheep anti-mouse FITC labelled antibody (Amersham) were used. Untransfected Cos-7 cells were initially treated with the primary (1:10 dilution) and secondary antibody (1:200 dilution). These cells exhibited undetectable levels of FITC fluorescence (data not presented) showing there was not any non-specific binding of Y1F4. The Cos-7 cells were transfected with the cDNA of SERCA1b in pcDNA3.1+ at approximately 50 % confluency. Figure 5.8 (A) shows SERCA1b over-expression in these cells, detected using the same concentrations of antibody as above. Expression of SERCA1b can be seen in the endoplasmic reticulum of these cells. The staining shows a typical reticular "lace like" peri-nuclear pattern, with the reticular network extending to the plasma membrane. Cos-7 cells were also transfected with HVSERCA cDNA in pcDNA3.1+ (Figure 5.8 (B)). These cells were probed with the HV-2 polyclonal antibody (Lockyer, 1997) and a sheep anti rabbit FITC conjugated antibody (1:200 dilution (Amersham). Lockyer (1997) used a 1:10 dilution of HV-2 to achieve suitable detection in a single Cos-7 cell (Lockyer, 1997), however this concentration yielded high non-specific binding of the antibody to the cells (data not shown), thus a concentration of 1:100 was used. The secondary antibody was diluted as above. As can be seen in Figure 5.8 (B) the edges of the cells are fluorescent, as are the nuclei of the cells. This shows considerable non-specific binding of the HV-2 antibody. Indeed, probing of control untransfected cells under the same conditions showed the same pattern of fluorescence (data not shown). Therefore the HV-2 antibody is binding non-specifically to proteins on the cell. Diluting the antibody reduced the amount of non-specific binding, but it still proved difficult to determine the actual amount of HVSERCA expression.

5.3.2. Generation of a SERCA and HVSERCA chimera

As the expression of HVSERCA is low in Cos-7 cells a chimera was generated between SERCA and HVSERCA to see if this would increase the expression of the insect pump. Additionally, introduction of an epitope for a SERCA antibody would facilitate indirect detection of expressed protein.

The strategy for construction of the SERCA/HVSERCA chimera is described in Section 5.2.2. Figure 5.9 (gel (1)) shows the two chimeric DNA PCR products that were generated with overlapping sequences. The 0.67 kb band (B) represents the SERCA1b fragment. This is the 5' sequence of SERCA1b including the start codon and contains a portion of HVSERCA sequence at the 3' end as a template for the next PCR step. The 2.5 kb band (A) indicates the HVSERCA fragment. This is from the 3' end of the HVSERCA sequence, including the stop codon. This also contains a portion of SERCA1b sequence (at the 5' end) as a template for the next PCR step. Figure 5.9 (gel (2)) shows the final DNA PCR product. This was generated from the two fragments described above and is 3.17 kb in size (band(C)). The chimera was cloned into pcDNA3.1+. Restriction analysis of the ligated product using Nhe I/Xho I gave two products as expected. Gel (3) shows the digest products. Band (D) is at 3 kb and represents the final chimera construct and band (E) at 5.4 kb is the plasmid pcDNA3.1+. This construct was fully sequenced (Oswel, Figure 5.10) using the primers S1b115a, S1b450s, HV3190s, HV2200A, HV1235s, HV 3292a, HV1995s and a standard T7 primer (Appendix 2). The entire PCR construct contained two errors as compared to the published sequences for SERCA1b (Brandl *et al.*, 1986) and HVSERCA (Lockyer *et al.*, 1998). Firstly, base number 580 from the SERCA1b sequence was changed from a T to a C. As this was situated at the wobble position, the actual residue coded by the three bases was not altered. Secondly, base number 1296 in the chimera (1424 in the HVSERCA sequence) was changed from C to A, changing the triplet codon from TCC (Ser) to TAC (Tyr). This amino acid is not in a conserved region and therefore only expression and functional studies would show whether this mutation would have an effect on the function of the protein. Other than this the sequence is correct with the start (ATG) and stop (TAA) codons, the correct restriction sites and the entire sequence is in frame.

5.3.3. Expression of the SERCA/HVSERCA chimera in Cos-7 cells

The chimera was transfected into Cos-7 cells, as previously, when the cells were approximately 50 % confluent. The morphological pattern of expression was then detected using a SERCA specific polyclonal antibody, antipeptide antibody 191, ApAb 191: the epitope for which are the amino acid residues 191 to 205 of SERCA (Mata *et al.*, 1992), and the sheep anti rabbit FITC antibody. Untransfected Cos-7 cells were initially probed with 1:50 primary antibody and 1:200 secondary antibody (Figure 5.11 (A)). As can be seen, there is considerable non-specific binding of ApAb 191. The dilution was increased to 1:100 (Figure 5.11 (B)). This reduced the background fluorescence, practically abolishing non-specific binding, permitting subsequent detection of expressed protein. Cells transfected with SERCA were used as a positive control for detection of expression levels. Figure 5.12 (A) shows SERCA expression detected with the ApAb 191 and the FITC conjugate. The pattern of expression is comparable to that detected with the Y1F4 antibody (Figure 5.8) with the staining pattern consistent of a typical ER localised protein. Figure 5.12 (B) shows SERCA/HVSERCA chimera expression. The same antibody dilutions were used as above. The reticular staining pattern is the same as that of SERCA (Figure 5.8) and the level of expression is also comparable. Thus the SERCA/HVSERCA chimera appears to express well as compared to the low expression levels of HVSERCA.

5.3.4. Generation of SERCA-GFP

Linking GFP to a protein of interest permits direct visualisation of heterologous proteins in live cells abolishing the need for indirect immunological methods.

GFP was linked to SERCA using a PCR strategy that is described in Section 3.2.3. Figure 5.13 shows the two DNA PCR products made for generation of SERCA-GFP. Band (A) at 2.1 kb on gel (1) indicates the SERCA1b fragment, from the 5' end of the sequence, including the start codon. Band (B) at 1.5 kb on gel (2) represents the last of the SERCA sequence (not included in the other fragment) with the c-myc epitope and GFP gene attached. Figure 5.14 shows the final DNA product pc3.1+ SERCA-GFP that has been diagnostically digested Afl II/Xho I, cutting out

the 1.5 kb SERCA fragment (band (B)) from the vector with the 2.1 kb fragment (a total of 7.5 kb, band (A)). The final pc3.1+ SERCA-GFP product is 9 kb in size. Cos-7 cells were transfected with the DNA as previously described. 48 hours post-transfection the coverslips were mounted onto glass slides and visualised using fluorescence microscopy. Figure 5.15 shows the expression of the SERCA-GFP construct. The fluorescence observed is a direct indication of expression levels because the GFP is linked to the expressed protein. The reticular pattern of expression can be seen, a peri-nuclear network, continuing through to the cell periphery. This shows successful linkage of GFP to SERCA, as a tool for direct detection of expression levels. The pattern of expression of this construct is the same as SERCA1b detected with antibodies (Figure 5.8 and 5.12).

5.3.5. Generation of HVSERCA-GFP

The detection of HVSERCA expression was not possible because of the background levels of HV-2 antibody binding and thus high secondary antibody FITC fluorescence. If expression levels were also very low then detection of the HVSERCA protein would be impossible. Therefore GFP was linked to HVSERCA using a PCR based method. The strategy for construction of HVSERCA-GFP is described in Section 5.2.4. Figure 5.16 shows the two PCR products made for generation of the construct. On gel (1) the 1.5 kb band (A) represents the PCR product of HVSERCA from the 3' end of the sequence. This does not contain the stop codon and has the Xho I and Pme I restriction sites introduced. On gel (2) the 0.7 kb band (B) represents the c-myc and GFP gene fragment. Figure 5.17 (gel (1)) shows the diagnostic digest of the pNEBHVSERCA ligation product. This was cut AflII/PmeI, cutting out the 1.5 kb PCR product (the 3' end of HVSERCA with the stop codon removed and restriction sites introduced). Figure 5.17 (gel (2)) shows the digest of the final HVSERCA-GFP construct in pNEB193. This was diagnostically digested using Xho I/Pme I. As can be seen on gel (2) this successfully cut out the 0.7 kb GFP fragment (band (D)) from the 6 kb pNEB HVSERCA construct (band (C)). The HVSERCA-GFP construct was transfected into Cos-7 cells as described previously. No reticular fluorescence (as would be expected) was observed. The HVSERCA appears to have essentially no expression in Cos-7 cells. The diagnostic digest of the PCR product showed the presence of the correct size of product. The

end of the HVSERCA product was sequenced (Oswel) to ensure that the stop codon had been removed and the restriction sites introduced. Figure 5.18 shows the electropherogram trace of the sequence. This starts from base 3150 in the HVSERCA sequence. (A) indicates CTC, the site where the stop codon was showing successful removal of this sequence. As can also be seen the sequences for the Xho I and the Pme I restriction sites are present. However the construct was not fully sequenced and possible errors could be present.

5.4. Discussion

Expression of proteins is possible in a variety of systems and indeed expression of P-type ATPases has been possible in a range of cells. The Cos system has been successfully employed for expression of mammalian (Maruyama & MacLennan, 1988; Maruyama *et al.*, 1989a), avian (Campbell *et al.*, 1991) and amphibian SERCAs (Vilsen & Andersen, 1992) although a yeast secretory pathway ATPase could not be expressed (Shull *et al.*, 1992).

This study has investigated the expression of Ca^{2+}-ATPases and chimeric constructs in Cos-7 cells. SERCA1b expresses well in these cells, as detected by immunofluorescent procedures (Figures 5.8 and 5.12). The SERCA-GFP construct exhibited comparable levels of expression to that of its unlabelled counterpart (Figure 5.15). Additionally the localisation of expression was the same, within the peri-nuclear reticular network, extending to the cell periphery.

The expression of the putative Ca^{2+}-ATPase from *Heliothis virescens* has not been demonstrated. Unfortunately the polyclonal antibody HV-2 raised against a sequence in the cytoplasmic domain of HVSERCA (Lockyer, 1997) was found not to be highly specific and therefore could not be used to detect expression. A chimera between SERCA and HVSERCA, with the N terminus of SERCA, the rest being from the HVSERCA sequence, was successfully constructed. Expression of this chimera in Cos-7 cells was detected using immunofluorescence (Figure 5.12). By introducing the N terminus of SERCA, the epitope for the antipeptide antibody 191 (Mata *et al.*, 1992) was also introduced which enabled detection of the expression levels of the chimera. The reticular pattern of over-expression of SERCA1b and the chimera are similar (Figure 5.12) and it would appear that the chimera expresses as well as SERCA1b in Cos-7 cells. This result implies that the N terminus of SERCA1b increases expression of HVSERCA. The exact role of the N terminus in the type IA Ca^{2+}-ATPases is unknown but a possible role in regulation (Toyofuku *et al.*, 1994), expression or folding and membrane insertion is postulated (Skerjanc *et al.*, 1993a; Daiho *et al.*, 1999).

The signals that are required for targeting of the Ca^{2+}-ATPases are unknown at present. Additionally, whether proteins are permanently resident in the ER or whether they are able to leave and are subsequently retrieved is unknown. However unpublished results using SERCA/PMCA chimeras would indicate the latter was true (personal communication with Newton,T. and East, J.M.). SERCA is retained in the

ER, yet PMCA is expressed at the plasma membrane of cells. Sub-cellular targeting of proteins such as the P-type pumps has been studied using chimeric constructs. Foletti *et al.* (1995) used SERCA/PMCA constructs and found that a chimera consisting of the first 85 residues of SERCA (encompassing the first transmembrane helix) with the remaining sequence derived from PMCA was retained in the ER (Foletti *et al.*, 1995). Luckie *et al.* (1991) constructed a chimera between Ca^{2+} and Na^{+}/K^{+} ATPases (Luckie *et al.*, 1991). Inclusion of the last third of the Na^{+}/K^{+} at the C terminus in the SERCA sequence targeted the construct to the plasma membrane. The opposite construct, with only the last third of the SERCA sequence produced a protein that was localised in the ER. This suggests that the ER targeting/retention signal is located at the C terminus. More recently Black (1999) constructed pairs of constructs between the Ca^{2+} and Na^{+}/K^{+} ATPase and suggested that the first 212 residues were important in mediating ER retention (Black, 1999). Guerini *et al.* (1998) stated that the first 28 residues were important for ER retention but the lack of functional studies for these proteins makes this result unclear (Guerini *et al.*, 1998) since retention could be due to misfolding and not due to a signal that may be absent or present.

Known ER retrieval/retention signals such as KDEL (Munro & Pelham, 1987), K(X)KXX (Jackson *et al.*, 1990), and KK (Jackson *et al.*, 1993), are not found in the SERCA sequence. However, it is possible that the important signal sequences actually reside within the transmembrane region. The placement of a single charged residue in the transmembrane region of a protein destined for the cell surface was found to be enough to retain it in the ER where it was degraded (Bonifacino *et al.*, 1991). Additionally a 23 amino acid sequence for targeting and retention of the a chain of T cell antigen receptor (TCRα) within the ER was described by Bonifacino *et al.* in 1990 (Bonifacino *et al.*, 1990). Comparison of the first transmembrane α-helix of TCRα with sequences from SERCAs shows the presence of a conserved sequence (Magyar & Varadi, 1990). This pentapeptide motif R/KILLL in the transmembrane α- helix M1 of SERCA (ideally placed for protein-protein interactions) is not found in the sequence of PMCA (Magyar & Varadi, 1990), thus suggesting that it might function as an internal signal sequence. However, mutation of the RILLL sequence, changing the Arg to Leu did not alter the targeting of SERCA (Black, 1999). This sequence is also present in the cDNA sequence of HVSERCA as KILLL (as in the *Drosophila* sequence).

Construction of the chimera between SERCA and HVSERCA appeared to increase expression levels in Cos-7 cells. Misfolding of the insect Ca^{2+}-ATPase after synthesis could have resulted in ER retention and rapid degradation of the protein. The replacement of the N terminal sequence of HVSERCA in the chimera may have facilitated correct processing and successful expression of this calcium pump. It is possible that by making the chimera a sequence in SERCA that has a regulatory role in expression could have been introduced, which directly raised the expression levels. It is interesting to note that the locations of SERCA and of the chimera are similar, which agrees with the observation of the target sequence being located in the first 212 residues of SERCA (Black, 1999) as this sequence is present in this construct.

This study reiterates the importance of the N terminus of the Ca^{2+}-ATPase and its possible function in regulation of expression. Functional studies would show whether the SERCA/HVSERCA chimera has Ca^{2+}-ATPase activity and transports calcium. It would be interesting to dissect the N terminal sequences further using molecular cloning techniques to introduce smaller changes and deduce which sequences may have a role in N terminal regulation. The HVSERCA-GFP construct was created, but expression was not observed. It would therefore appear that HVSERCA does not express in Cos-7 cells, but the chimera does. The GFP construct was not fully sequenced, although removal of the stop codon was demonstrated (Figure 5.18). Thus, the absence of expression could be purely because the pump does not express in Cos-7 cells or a functional problem with the GFP construct.

The insect Sf9 cell baculovirus system has been increasingly used for expression purposes as they exhibit high levels of expression. The H^+/K^+ ATPase (Klaassen *et al.*, 1993), Na^+/K^+ ATPase (Koster *et al.*, 1996), SERCA (Maruyama *et al.*, 1989a) and putative cation channels of *Drosophila* (Hu & Schilling, 1995) have all been expressed in Sf9 cells. Expression of a Ca^{2+}-ATPase from *Arabidopsis thalania* (Liang *et al.*, 1997) and of SERCA (Centeno *et al.*, 1994; Degand *et al.*, 1999) have also been demonstrated in yeast (Centeno *et al.*, 1994). The use of yeast would be simpler as regards the methodology and thus would seem a suitable method for yielding high quantities of heterologous Ca^{2+}-ATPase for both functional and inhibitor studies (Chapter 6).

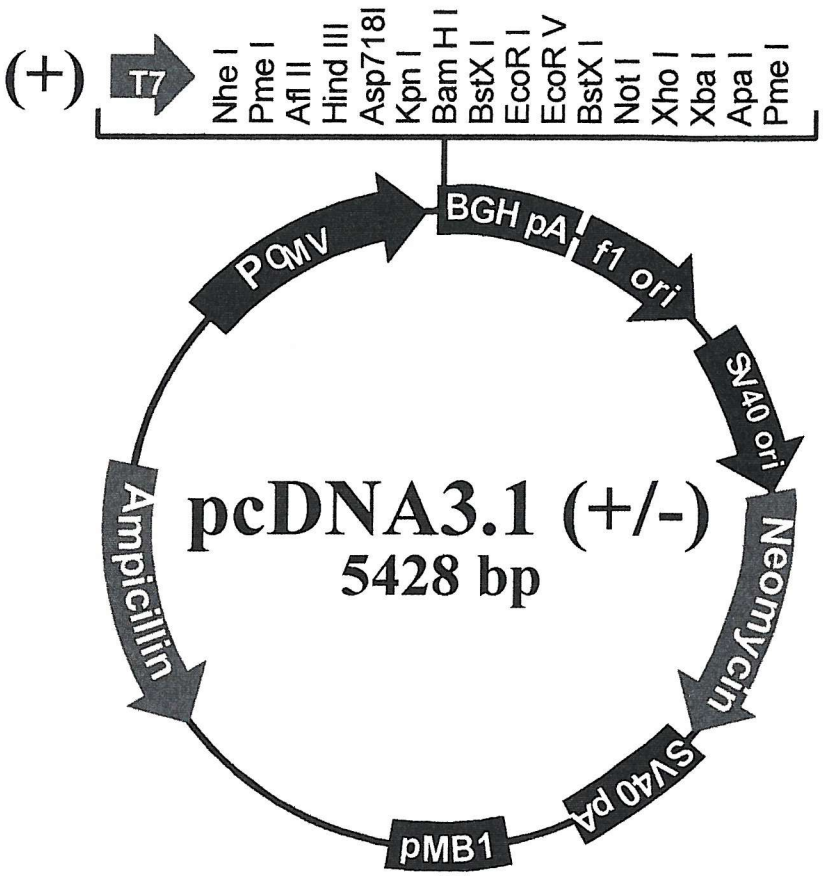

Figure 5.1. Map of pcDNA3.1+ (Invitrogen)

The multiple cloning site is shown, following on from the T7 promoter. The vector contains the ampicillin resistance gene and the SV40 promoter and origin for replication on Cos – 7 cells. This map can be located at www.Invitrogen.com.

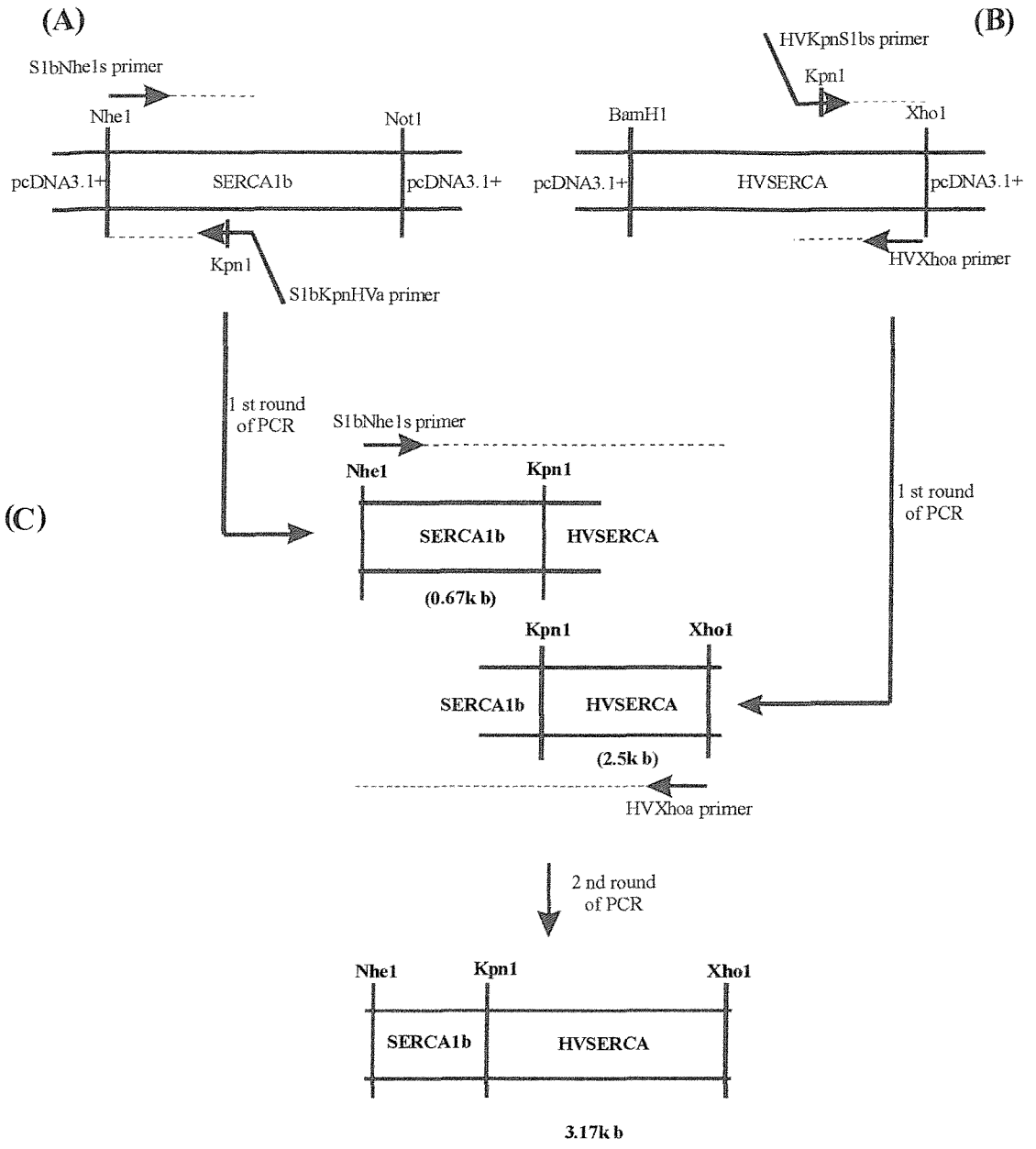

Figure 5.2. Schematic diagram showing the PCR and cloning strategy for construction of the SERCA/HVSERCA chimera.

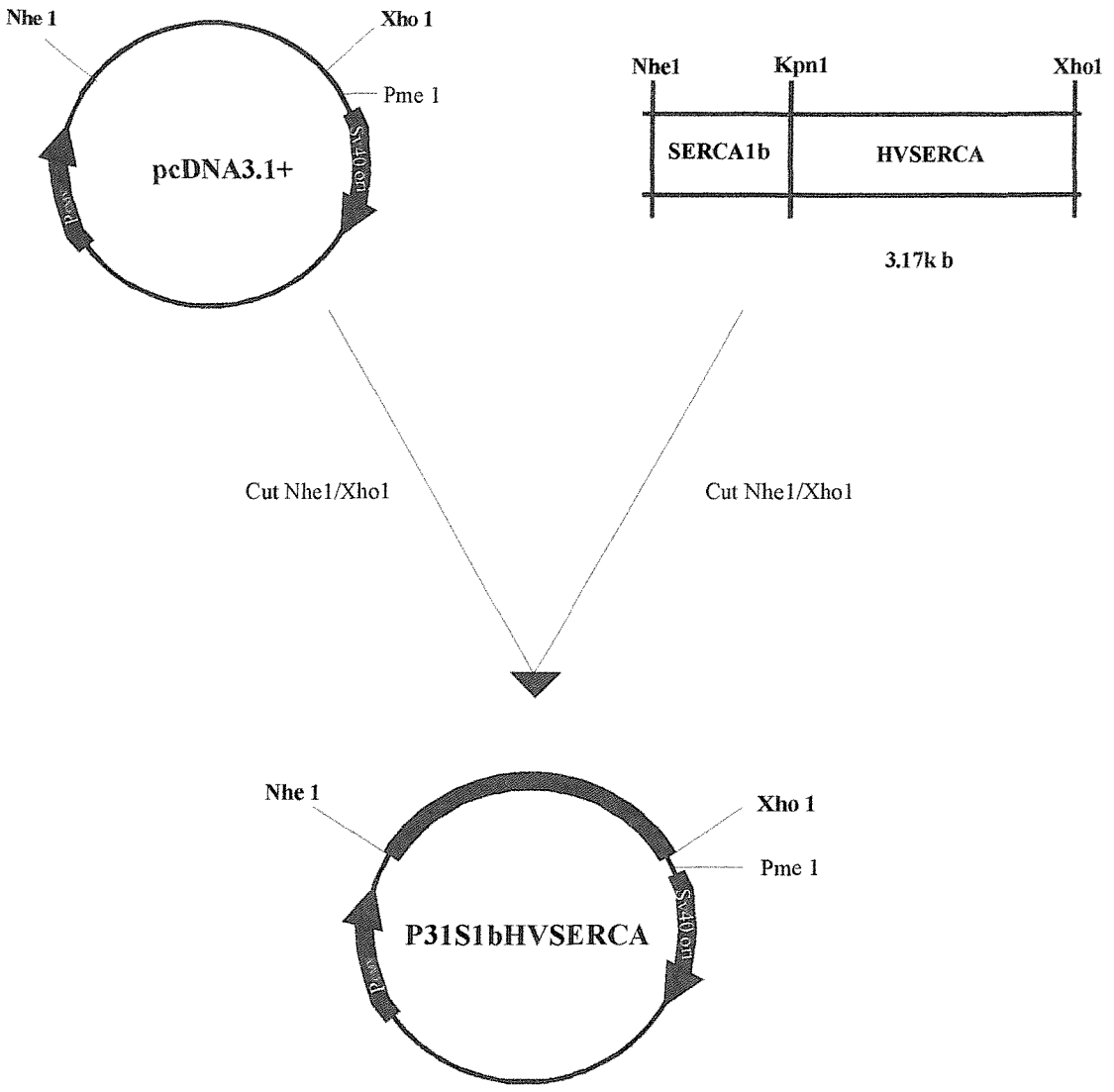

Figure 5.3. Generation of the pcDNA3.1+ chimera construct

Both pcDNA3.1+ and the chimera PCR product were digested using Nhe I/Xho I and then ligated, producing the final construct.

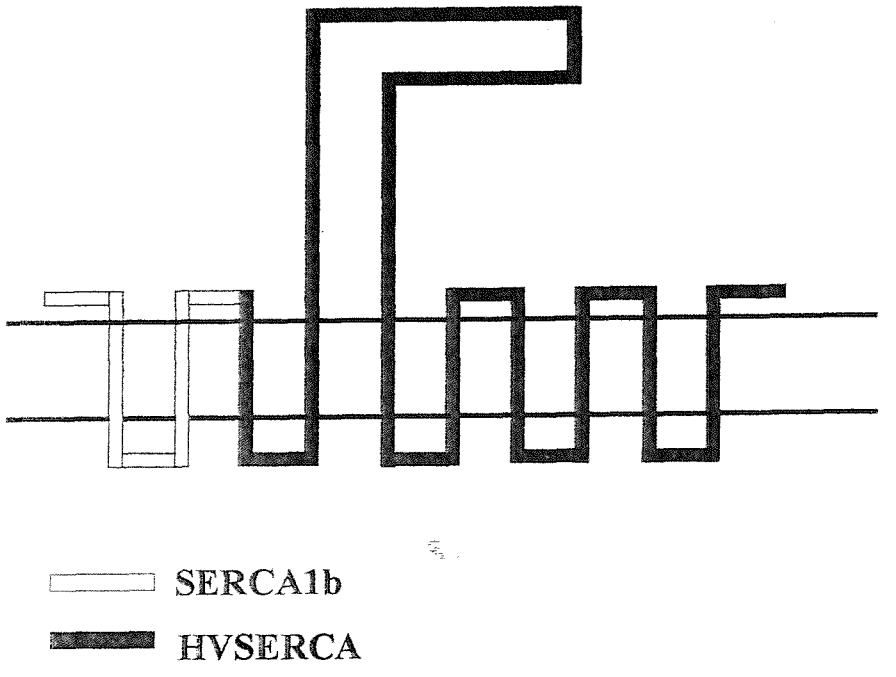

Figure 5.4. The diagram illustrates the chimera generated between SERCA and HVSERCA.

The first two transmembrane regions of the chimera are from SERCA1b and the rest of the sequence is from HVSERCA.

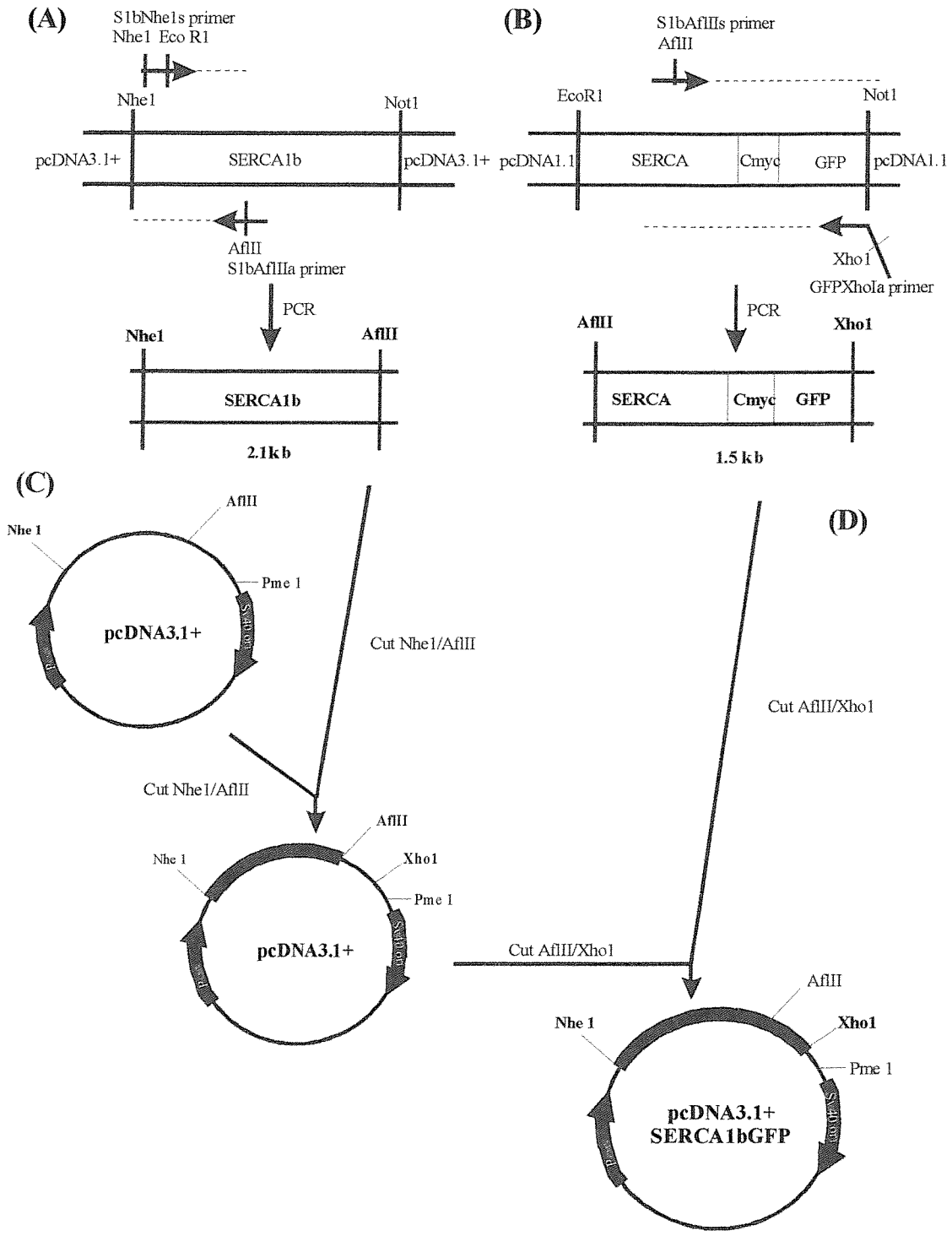

Figure 5.5. Schematic diagram showing the PCR and cloning strategy for construction of the SERCA-GFP construct.

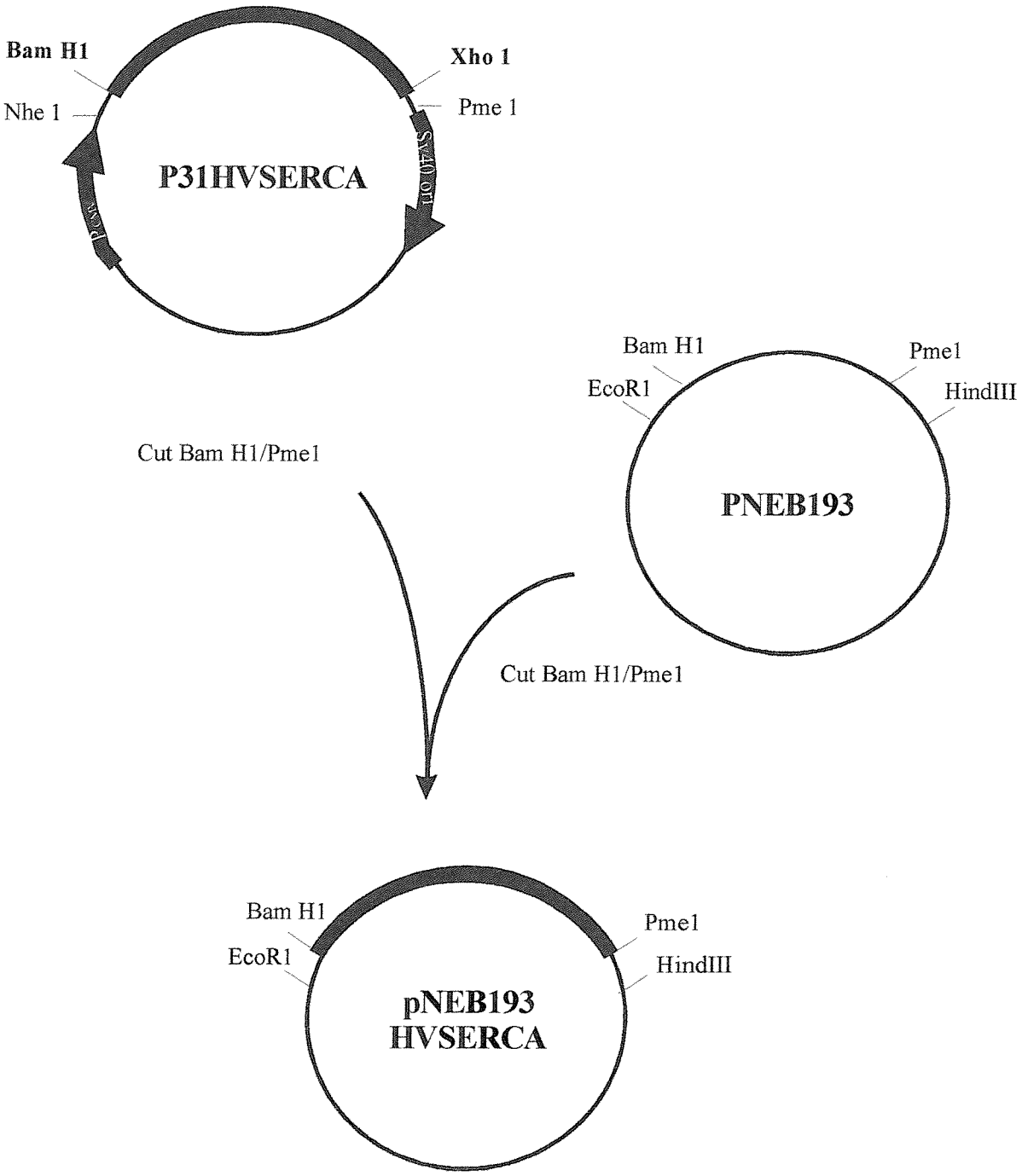

Figure 5.6. Schematic diagram showing the cloning strategy of the HVSERCA into pNEB193.

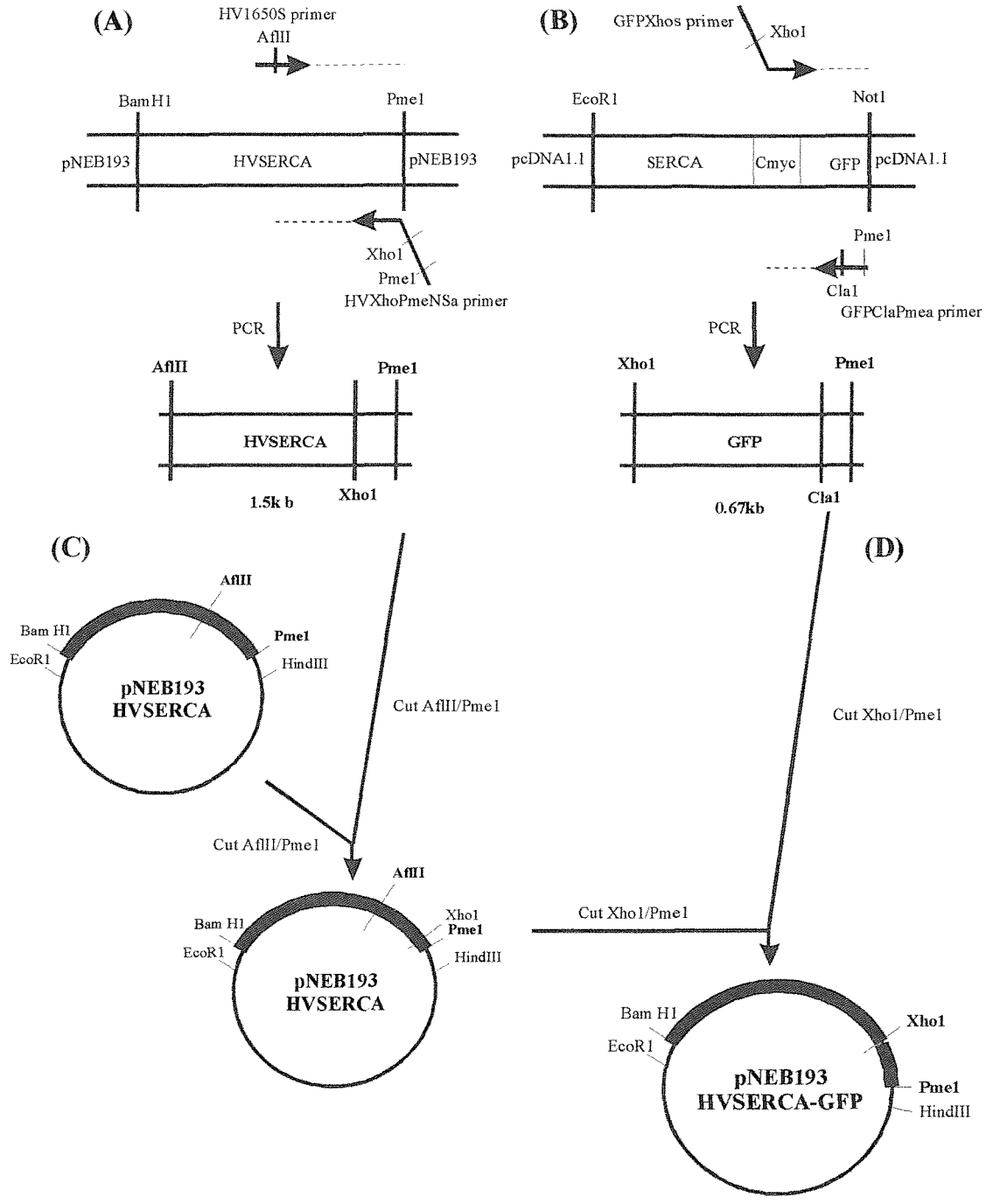

Figure 5.7. Schematic diagram showing the PCR and cloning strategy for construction of the HVSERCA-GFP construct

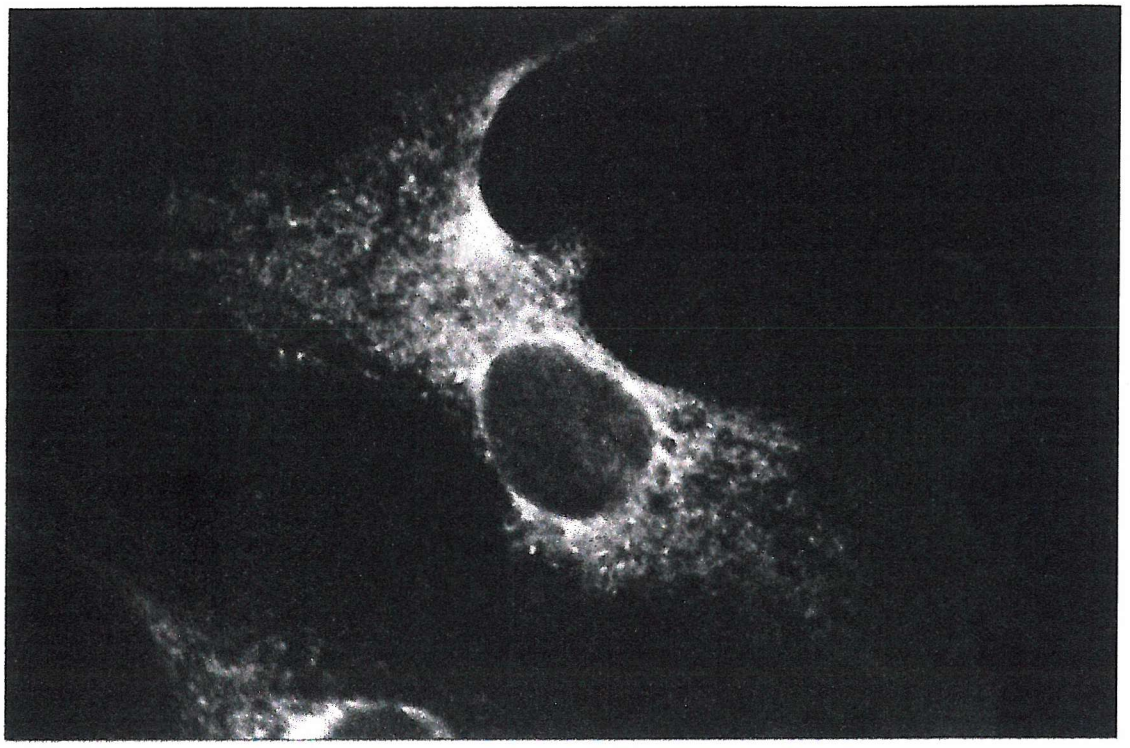

Figure 5.8. Expression of Ca^{2+}-ATPases in Cos-7 cells

Shown is a Cos-7 cell transiently expressing SERCA 1b: primary antibody was Y1F4 (diluted 1:10) and secondary antibody, a sheep-anti mouse FITC conjugate (diluted 1:200).

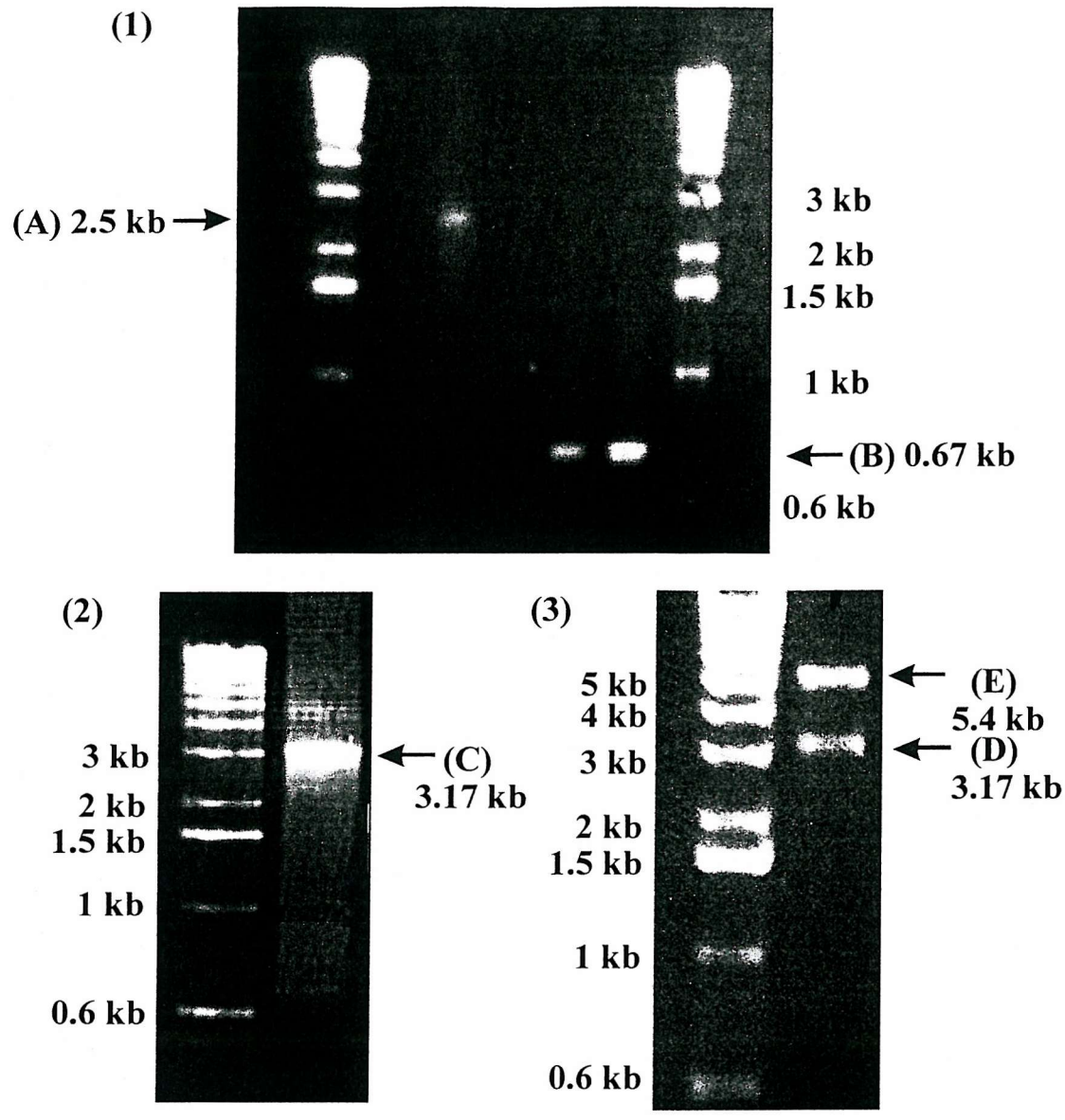

Figure 5.9. Diagnostic agarose gels of the SERCA/HVSERCA chimera products

Gel (1) shows the PCR products generated for construction of the SERCA1b, HVSERCA chimera. Band (A) is the 0.67 kb SERCA DNA fragment with the HVSERCA overlap at the 3' end. Band (B) is the 2.5 kb HVSERCA DNA fragment with the 5' SERCA overlap. Band (C) on gel (2) shows the chimera DNA at 3.17 kb generated from the two PCR products. Gel (3) shows the products from the digest of pcDNA3.1+ containing the chimera (digested Nhe I/Xho I, to remove the insert).

Figure 5.10. cDNA sequence of the SERCA/HVSERCA chimera

The primers used for the sequencing are listed in appendix 2 and section 5.3.2. Shown are the restriction sites Nhe1 and EcoR1 at the 5' end, with Xho1 at the 3' end. The Kpn1 restriction site is where the two sequences were joined. The start codon ATG and the stop TAA are underlined. The errors in the sequence are at base 580, which should be a T and at base 1295, which should be a C (both are underlined).

```
GCTAGCGAAT TCGAGCTCCC  GGGATCCATG GAAGCTGCTC ACTCTAAGTC TACTGAAGAA 60
 Nhe1  EcoR1                    Start
TGTCTGGCTT ACTTCGGTGT  TTCTGAAACT ACTGGTCTGA CTCCAGACCA AGTTAAGCGA 120

CATCTAGAGA AATACGGCCA  CAATGAGCTT CCTGCTGAGG AAGGGAAATC CCTGTGGGAG 180

CTGGTGATAG AGCAGTTTGA  AGACCTCCTG GTGCGGATTC TTCTGCTGGC CGCCTGCATC 240

TCCTTTGTGC TGGCCTGGTT  TGAAGAAGGG GAAGAGACCA TCACTGCCTT CGTTGAGCCC 300

TTTGTCATCC TCCTGATCCT  CATTGCCAAT GCCATCGTGG GAGTTTGGCA GGAGCGGAAC 360

GCTGAGAACG CCATAGAGGC  GCTGAAGGAA TATGAGCCCG AGATGGGGAA GGTGTACCGG 420

GCTGACCGCA AGTCAGTGCA  AAGGATCAAG GCTCGGGACA TCGGTCCCCG GGGACATCGT 480

GGAGGTGGCG GTTGGGGACA  AAGTCCCTGC AGACATCCGC ATCCTGTCTA TCAAGTCCAC 540

CACCCTCCGC GTGGACCAGT  CCATCCTGAC AGGCGAGTCC GTGTCCGTCA TCAAGCACAC 600

GGAGCCAGTC CCTGACCCGC  GGGCTGTCAA CCAGGACAAG AAGAACATGC TTTTCTCGGG 660

TACCAATGTC GCCGCCGGCA  AGGCCCGTGG TATTGTCATC GGAACTGGTC TCAACACTGC 720
Kpn1
CATTGGTAAA ATCCGTACTG  AAATGTCCGA GACTGAGGAG ATCAAGACAC CTCTGCAGCA 780

AAAACTGGAC GAATTCGGTG  AGCAGTTGTC TAAGGTCATC TCAGTTATTT GCGTTGCCGT 840

ATGGGCCATC AACATCGGAC  ACTTCAACGA CCCCGCCCAC GGTGGAAGCT GGATCAAGGG 900

TGCCGTCTAC TACTTCAAAA  TCGCTGTCGC CCTGGCCGTC GCTGCCATCC CCGAAGGTCT 960

CCCCGCTGTC ATCACCACTT  GTCTCGCTCT CGGTACCAGG CGTATGGCTA AGAAGAACGC 1020

TATCGTGAGG TCGCTGCCCT  CTGTAGAGAC CCTCGGTTGC ACTTCTGTCA TCTGCTCCGA 1080

CAAGACCGGT ACTCTGACCA  CCAACCAGAT GTCTGTTTCC CGTATGTTCA TCTTTGAGAA 1140

GATCGAAGGT GGCGACAGCA  GCTTCCTTGA ATTTGAAATT ACTGGTTCCA CCTACGAGCC 1200

TATTGGTGAT GTCTACCTGA  AGGGACAGAA GATCAAGGCT GCTGAATTCG ATGCTCTGCA 1260

CGAACTTGGT ACCATTTGCG  TTATGTGCAA TGACTACGCT ATTGATTTCA ACGAATTCAA 1320

ACAGGCGTTC GAAAAGGTCG  GTGAAGCCAC TGAAACGGCT CTTATCGTAC TCGCTGAGAA 1380

AATGAACCCC TTCAACGTTC  CCAAGACTGG ACTTGACCGT CGCTCCTGCG CTATCGTTGT 1440

CCGCCAAGAG ATTGAAACCA  AATGGAAGAA AGAGTTCACT CTTGAGTTCT CCCGTGACAG 1500
```

GAAATCCATG TCCACCTACT GCACACCCCT TAAGCCTTCC CGTCTTGGCA ATGGACCCAA 1560

ACTGTTCGTC AAGGGTGCAC CTGAAGGTGT GCTTGAACGT TGCACGCACG CTCGTGTCGG 1620

AACTGCCAAA GTACCTTTGA ACTCGACCCT CAAGAACCGC ATCCTGGACC TCACCCGCCA 1680

ATACGGTACC GGTCGTGACA CCCTTCGTTG CTTGGCCCTC GCTACCGCTG ACAGCCCACT 1740

CAAACCTGAC GAAATGGACC TCGGAGACTC GACCAAGTTC TACACCTATG AAGTCAACCT 1800

TACATTCGTC GGTGTCGTCG GCATGTTGGA CCCTCCCCGT AAAGAAGTAT TCGACTCTAT 1860

CGTCCGTTGC CGCGCTGCTG GTATCCGTGT AATTGTCATC ACTGGTGACA ACAAGGCCAC 1920

CGCTGAAGCT ATCTGCAGGC GTATTGGCGT GTTCACTGAA GAAGAAGACA CCACCGGCAA 1980

ATCGTTCTCT GGTCGCGAGT TCGACGACCT GCCCGTGTCG GAACAGCGCG CCGCTTGCGC 2040

TAAGGCTCGC CTGTTCTCCC GCGTGGAACC CGCCCACAAG TCCAAGATTG TTGAGTTCCT 2100

GCAAAGCATG AACGAGATCT CTGCTATGAC TGGTGACGGT GTAAATGACG CCCCCGCTCT 2160

GAAGAAGGCC GAAATCGGTA TTGCTATGGG CTCTGGTACC GCTGTCGCTA AGTCTGCCGC 2220

CGAGATGGTG TTGGCTGATG ACAACTTCTC ATCCATTGTC GCCGCTGTTG AGGAAGGTCG 2280

TGCCATCTAC AACAACATGA AGCAGTTCAT CCGTTACCTG ATCTCCTCCA ACATTGGTGA 2340

AGTCGTGTCC ATCTTCTTGA CTGCCGCTCT GGGTCTCCCC GAAGCTCTGA TCCCCGTCCA 2400

ACTGTTGTGG GTCAACTTGG TCACTGACGG TCTGCCCGCC ACCGCCCTCG GCTTCAACCC 2460

CCCTGATCTC GACATCATGG ACAAGCCCCC CCGTAAGGCT GATGAGGGTC TCATCTCTGG 2520

ATGGCTGTTC TTCAGGTACA TGGCTATCGG TGGTTACGTC GGTGCCGCTA CCGTCGGAGC 2580

CGCGTCGTGG TGGTTCATGT ACTCTCCTTT CGGACCCCAG ATGTCTTACT GGCAGCTCAC 2640

CCACCACTTA CAGTGCCTCA GCGGAGGTGA TGAATTCAAG GGCATCGACT GCAAGATCTT 2700

CACTGACCCT CACCCTATGA CAATGGCCCT GTCCGTATTA GTAACAATTG AAATGTTGAA 2760

CGCCATGAAC AGTTTGTCTG AGAACCAGTC GCTGGTGACC ATGCCGCCCT GGTCCAACAT 2820

GTGGCTCGTC GGCTCCATGG CCCTCTCCTT CACTCTCCAC TTCGTCATCC TCTACGTTGA 2880

GGTCCTGTCG GCCGTGTTCC AAGTGACGCC GCTGTCCATC GACGAGTGGG TGACGGTGAT 2940

GAAGTTCTCG ATACCCGTGG TGTTGCTGGA CGAGGTGCTG AAGTTCGTCG CGCGCAAGAT 3000

CTCGGACGCC CAGCCGACGT GGAAGCTGTA ACGCCGGACG CCGTCGCAGC GCCACTGCAC 3060

Stop

GCACATATTC CATGAACACT CATTGTTTGT TGTGATCCCG CAGTGAAACT ACACATTTAA 3120

TGTAACTACG ACACGGTTGT GATATCTGCA TAAGACCTAG TAAGTTCGGA CGGCACCCCC 3180

GCTCGAG

XhoI

(A)

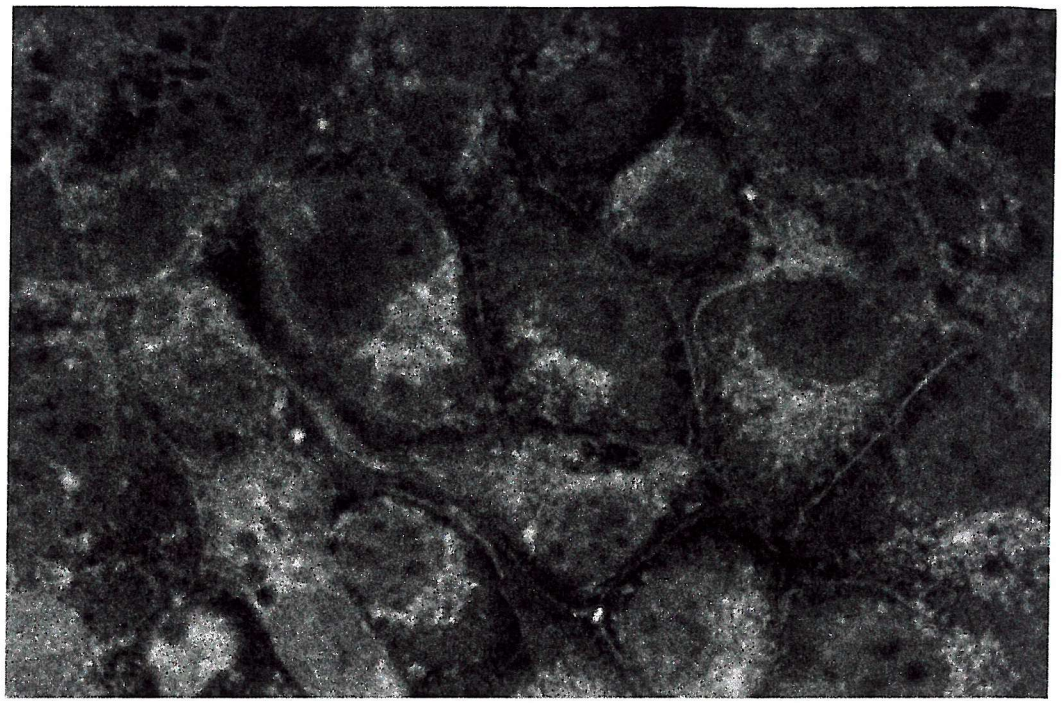

(B)

Figure 5.11. Untransfected Cos-7 cells probed with antibodies

Shown are: (A) Untransfected Cos-7 cells: primary antibody was antipeptide antibody 191 (diluted 1:50) and secondary antibody, a sheep anti rabbit FITC conjugate (diluted 1:200). (B) Untransfected Cos-7 cells: primary antibody as above (diluted 1:100), secondary antibody as above.

(A)

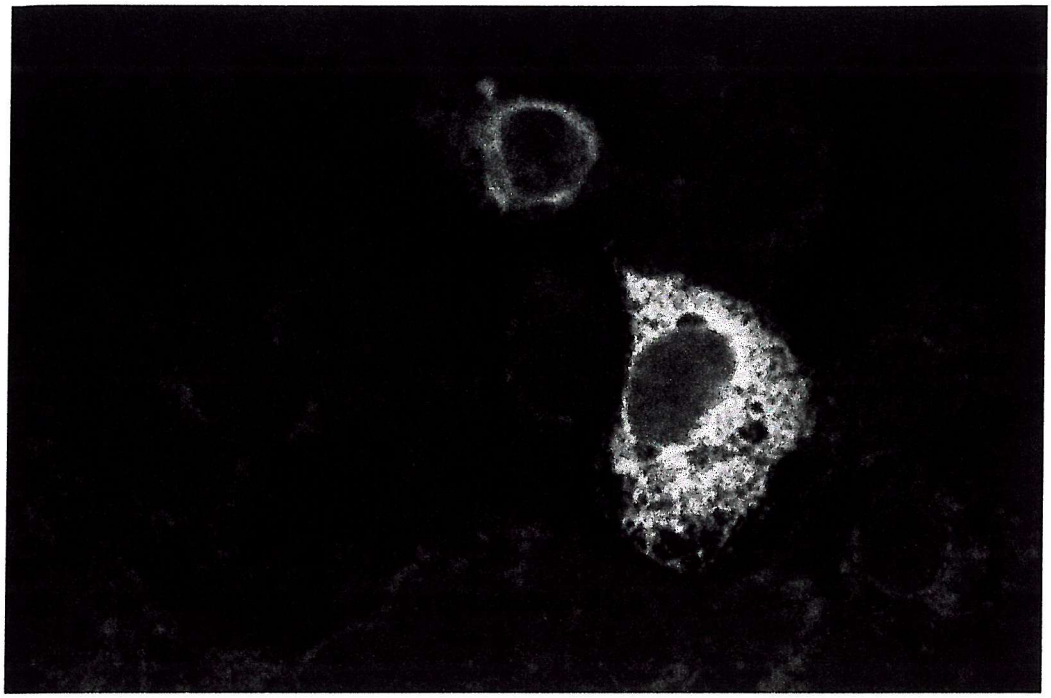

(B)

Figure 5.12. Expression of Ca^{2+}-ATPases in Cos-7 cells

Shown are: (A) Cos-7 cells transiently expressing SERCA 1b: primary antibody was antipeptide antibody (diluted 1:100) and secondary antibody, a sheep anti rabbit FITC conjugate (diluted 1:200). (B) Cos-7 cells transiently expressing SERCA/HVSERCA chimera: primary and secondary antibody as above.

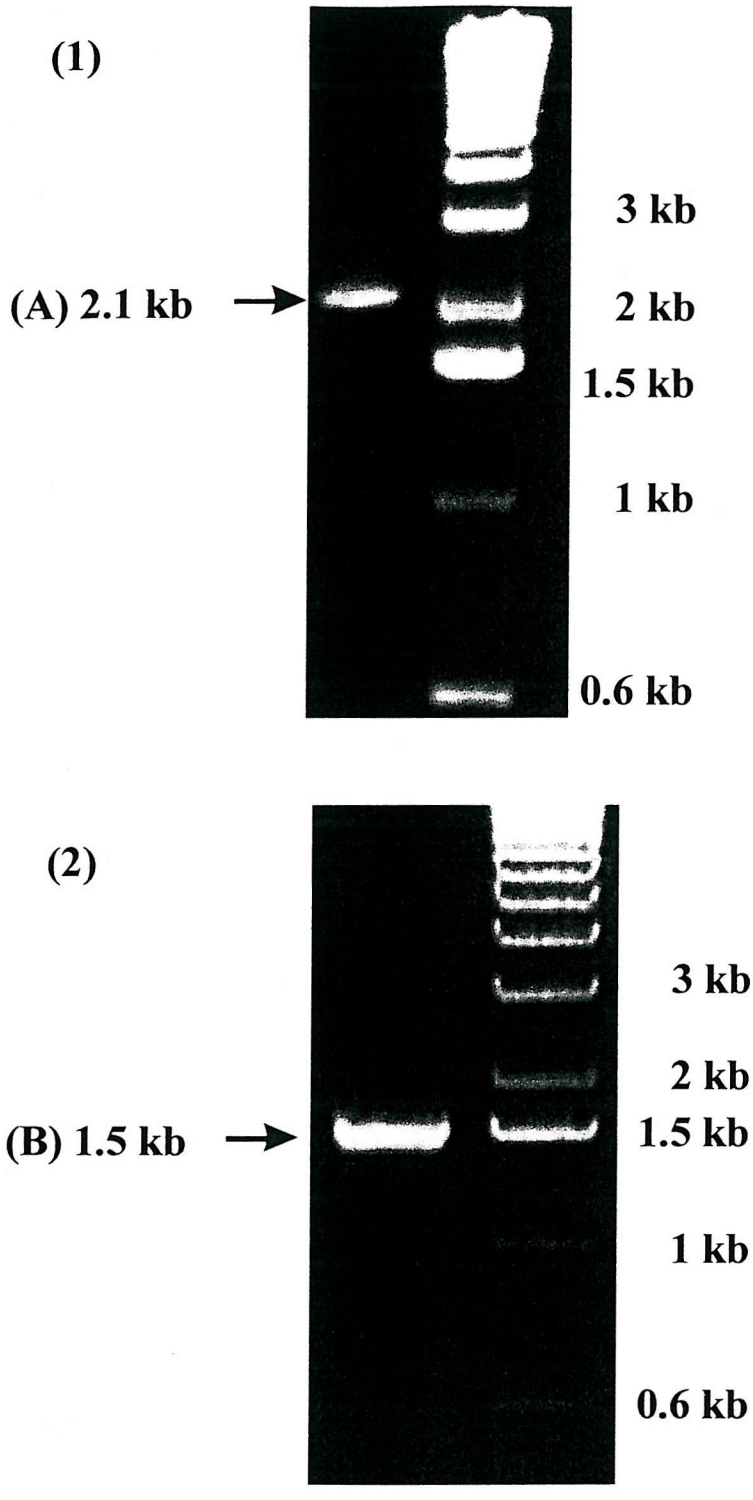

Figure 5.13. Diagnostic agarose gels of the SERCA1b PCR constructs

Band (A) on gel (1) shows the DNA PCR product of SERCA1b. This is a 2.1 kb fragment of SERCA sequence from the 5' end. Band (B) on gel (2) shows the SERCA-GFP PCR product at 1.5 kb.

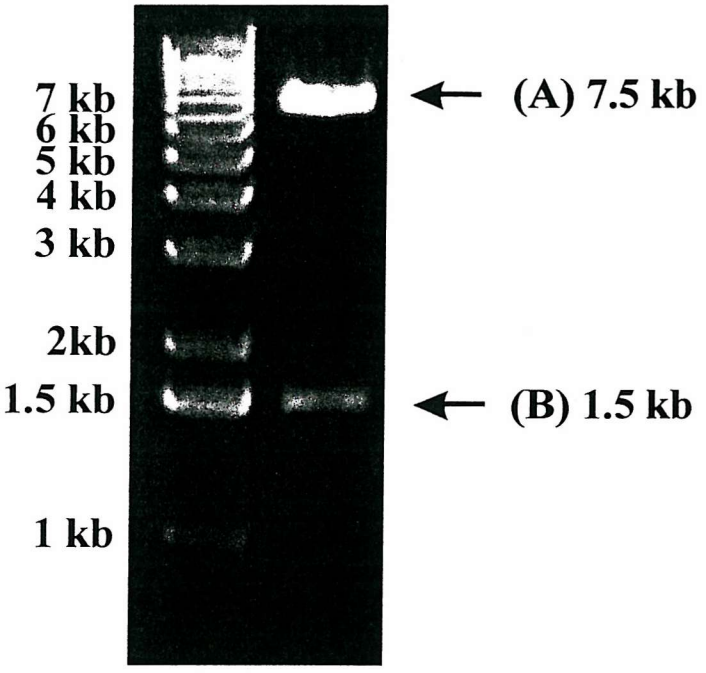

Figure 5.14. Diagnostic agarose gels of the pcDNA3.1+ SERCA1b construct digest

This shows the digested pcDNA3.1+ SERCA-GFP final product. The DNA was digested using Afl II/Xho I. Band (A) shows the 7.5 kb fragment of pcDNA3.1+ with the 2.1 kb SERCA fragment and band (B) shows the 1.5 kb SERCA-GFP fragment.

Figure 5.15. Expression of SERCA-GFP in Cos-7 cells

Shown is a Cos-7 cell transiently expressing the SERCA-GFP construct. The reticular network of expression can be seen directly when visualised using fluorescence microscopy.

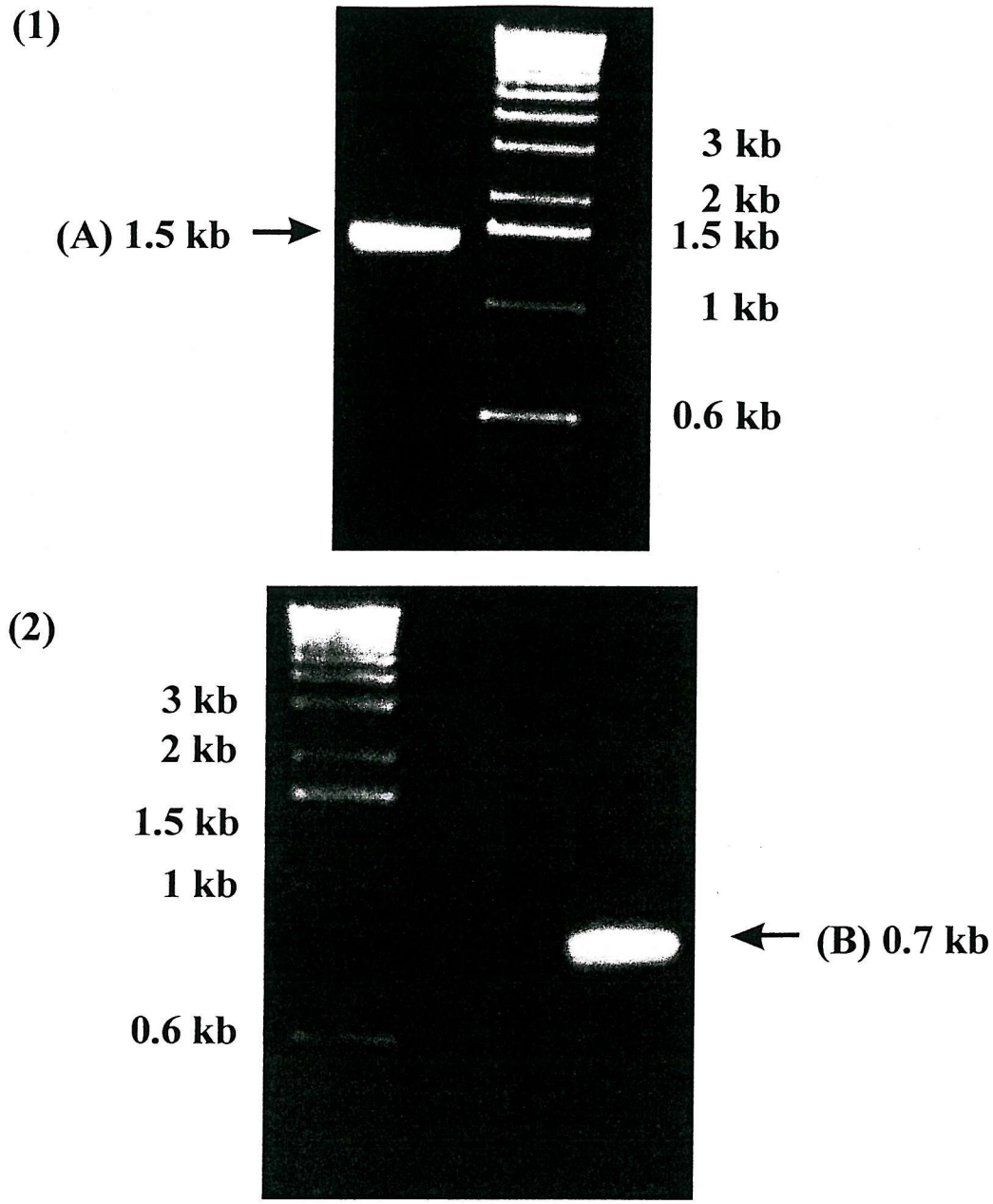

Figure 5.16. Diagnostic agarose gels of the HVSERCA PCR product

Band (A) on gel (1) shows the DNA PCR product of HVSERCA at 1.5 kb (contains no stop codon and the sites XhoI and PmeI have been introduced). Band (B) on gel (2) shows the DNA PCR product of GFP at 0.7 kb.

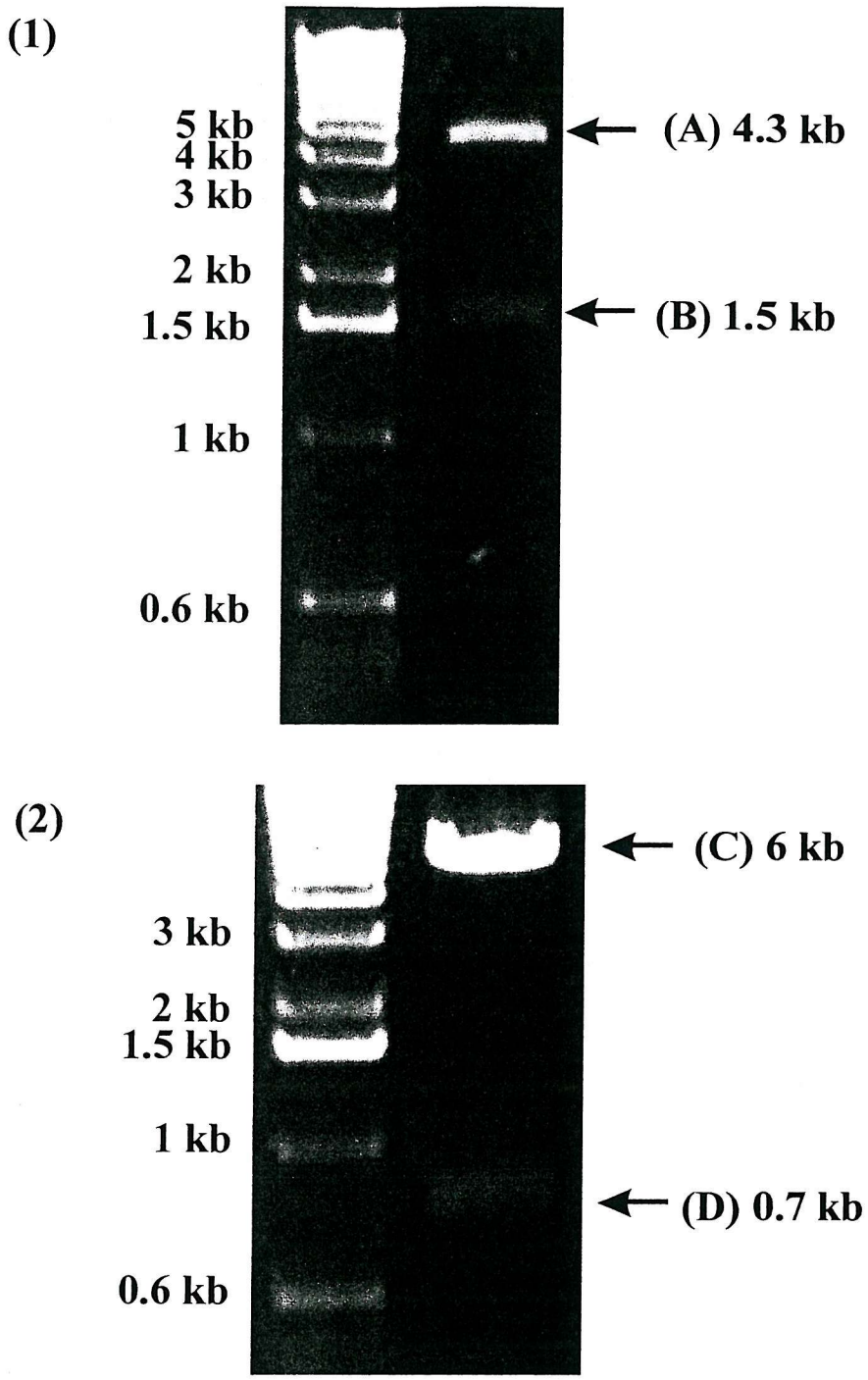

Figure 5.17. Diagnostic agarose gels of pNEBHVSERCA construct digests

Bands A and B on gel (1) are the digest products (cut AflII/PmeI) of the pNEBHVSERCA product, which does not have a stop codon and has the XhoI/PmeI sites introduced. Bands C and D on gel (2) are the digest products of the final pNEBHVSERCA GFP construct (cut XhoI/PmeI).

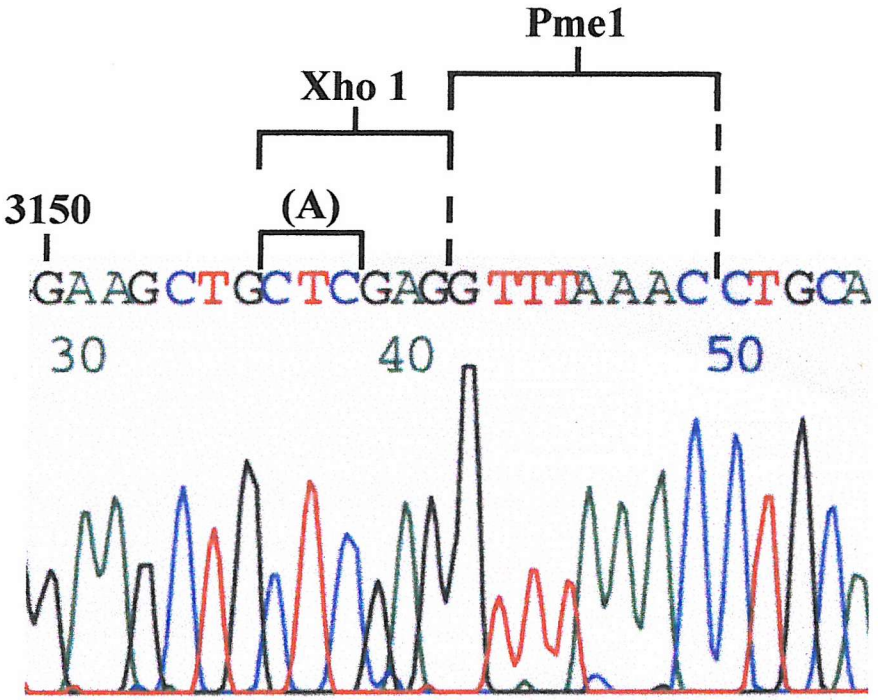

Figure 5.18. Sequence of the end of the HVSERCA 1.5 kb PCR product in pNEB193

DNA was sequenced by Oswel. The sequence is shown form residue 3150 in the HVSERCA sequence. (A) indicates the triplet codon CTC that replaced the TAA stop codon of the HVSERCA sequence. The Xho1 and Pme1 sites are labelled.

Chapter Six: Expression of Ca^{2+}-ATPases in Yeast

6.1. Introduction – Yeast as an expression system

Yeasts are unicellular organisms whose genetics and biochemistry are now well understood. They are being used to an increasing extent for the characterisation, isolation and cloning of genes, and are widely used for the expression of heterologous proteins. E. coli, which has been used for many years for expression, has limitations when trying to express genes from higher organisms. *S. cerevisiae* has been used as an alternative expression system because it is non-pathogenic and grows rapidly. Mutant isolation and transformation are simple (Romanos *et al.*, 1992).

6.1.1. The cell cycle

As a eukaryote, *S. cerevisiae* possesses the cellular features of higher eukaryotes, whilst its growth pattern is superficially similar to that of *E. coli* (Kreutzfeldt & Witt, 1991). *S. cerevisiae* is approximately 4 μm in diameter and is an oblately spheroid single celled organism which replicates by budding (as opposed to replication by fission seen with other yeast). The life cycle alternates between the stable haploid and diploid budding stages. Proliferation and transitions are the two components of this cycle. During proliferation, a haploid daughter cell is produced from a haploid mother cell mitotically, by the emergence of a bud. At this stage the cell is either mating type a or α. A process called transitions then occurs which involves mating and subsequent sporulation, involving three distinct cell types a, α and a,α. Mating (cellular and nuclear fusion) between a and α gives rise to a diploid a/α cell. Mating factors are secreted by cells and cause the opposite mating types to arrest in their cycle. α cells secrete α factor (a thirteen amino acid peptide) and a cells secrete a factor (of twelve amino acids). Mating then progresses into the mitotic growth and development stage, which occurs in a good nutritional environment. The a/α cell undergoes meiosis, producing four haploid a or α spores. Lack of nutrients in the media can halt the proliferative stage (as can the presence of another mating type). In the laboratory *S. cerevisiae* can be restricted to a single

mating type a or α that just buds mitotically. This is achieved by mutation of the HO (homothallism) gene that prevents diploid cell formation. This is useful in the laboratory because cell growth is limited to the simple haploid growth phase (Herskowitz, 1988).

6.1.2. The cell structure

The yeast cell consists of a rigid outer cell wall overlying the plasma membrane (Schreuder *et al.*, 1996), which are separated by the periplasmic space (Figure 6.1). The cell wall consists of two layers; the inner layer of β 1-6 and β 1-3 glucans complexed with chitin, which provides the strength, and the outer layer of mannoproteins, which are covalently linked to the underlying glucan layer, providing rigidity. This wall maintains structure and is freely permeable to solutes <600 Da. The plasma membrane underlies the cell wall. The plasma membrane contains membrane proteins involved in anchoring the cytoskeleton, in synthesis of outer membrane components, in transport of solutes and in signal transduction (Kreutzfeldt & Witt, 1991). The *S. cerevisiae* cell contains the sub - cellular components that would be expected to exist in a typical eukaryotic cell. These include the nucleus, endoplasmic reticulum, Golgi and mitochondria. Yeast cells also contain a vacuole that is involved in the storage of metabolites, proteases and hydrolases. The vacuole does not represent a clearly separated organelle but is part of a membrane system that could include the endoplasmic reticulum and Golgi (Kreutzfeldt & Witt, 1991). The Golgi in *S. cerevisiae* is actually scattered through the cytoplasm (Rossanese *et al.*, 1999).

6.1.3. Calcium homeostasis

The role of calcium in *S. cerevisiae* is analogous to its role in other eukaryotes; as a component in the transduction of external signals to elicit cellular responses (Figure 6.2). *S. cerevisiae* maintains calcium at sub micromolar (50 – 200 nM) levels in the cytosol (Halachmi & Eilam, 1993) by the use of calcium pumps and antiporters (Cunningham & Fink, 1994a). Calcium plays an important role as a second messenger and transient changes in cellular levels regulate a variety of functions. Calcium fluctuations can directly elicit responses in the cell by modifying

the functions of calcium binding proteins and their targets. Numerous proteins that exist in mammalian cells, which are directly or indirectly regulated by calcium, exist in yeast. These include: calmodulin (Davis *et al.*, 1986), calmodulin dependent kinases (Ohya *et al.*, 1991), a serine – protease, kex 2 (Mizuno *et al.*, 1989), glycogen phosphorylase (François & Hers, 1988), phospholipase C (Yoko-o *et al.*, 1993), protein kinase C (Levin *et al.*, 1990) and the calmodulin dependent phosphatase, calcineurin (Cyert *et al.*, 1991).

Calcium is important in a number of regulatory cascades in yeast. It is required for the mating process, for cell cycle progression (Iida *et al.*, 1990), for events such as bud emergence and mitosis and also for aspects of DNA replication. Hence the maintenance of low internal calcium concentration is essential for cell survival.

The inositol phospholipids (PtdIns) are involved in signalling pathways in many eukaryotic cells (Berridge, 1993; Clapham, 1995). Upon activation of G protein linked receptors, phospholipase Cβ (PLCβ) is activated (Berridge, 1993). In turn this hydrolyses the lipid precursor phosphatidylinositol 4,5-bisphosphate ($PtdIns(4,5)P_2$) to give DAG and IP_3. IP_3 binds to the IP_3 receptor and induces calcium release from the ER. PLCγ is activated by tyrosine kinase linked receptors (Berridge, 1993) and then has the same function as PLCβ. In yeast however, PtdIns metabolism is exceptional. Yeast contain PLCδ (Yoko-o *et al.*, 1993; Flick & Thorner, 1993) and a PKC (Levin *et al.*, 1990) and other enzymes involved in inositol signalling (Stolz *et al.*, 1998; Ives *et al.*, 2000; Odom *et al.*, 2000). However, the yeast genome contains no sequence corresponding to an IP_3 receptor, necessary for calcium mobilisation. Moreover the production of IP_3 has not been observed in yeast. IP_6 is produced and is involved in nuclear mRNA export (Ives *et al.*, 2000) but there appears to be no classical calcium signalling pathway present.

An important group of proteins involved in maintaining ion levels in cells, including calcium, are the P-type ATPases, characterised by the formation of a phosphorylated enzyme intermediate. Sixteen open reading frames encoding for P-type ATPases have been identified in the *S. cerevisiae* genome sequence (Catty *et al.*, 1997). By analysis of conserved core sequence P-type ATPases have been grouped into five major classes (Table 1.1) according to their substrate specificity (Axelsen & Palmgren, 1998). P-type ATPases are present in *S. cerevisiae*, belonging to all five of these groups. Two belong to group V; a poorly characterised group of

pumps with no assigned substrate specificity (Axelsen & Palmgren, 1998). Two distinct Ca^{2+}-ATPase pumps have been identified that belong to group II (Axelsen & Palmgren, 1998). Pmc1p (in the vacuole) belongs to IIB and Pmr1p (in Golgi / Golgi like organelles) to group IIA. In addition to the Ca^{2+}-ATPases, a Ca^{2+}/H^{+} antiporter has been described in yeast (Okorokov & Lehle, 1998), which is located in the vacuole.

6.1.4. The plasma membrane

The plasma membrane of yeast cells contains a non-specific mechanosensitive ion channel (Gustin *et al.*, 1988). Cations and anions can pass readily through this channel to relieve osmotic stress on the cell. Two other proteins have been identified that are important in calcium movement, Mid1 and Cch1. Mid1 is known to mediate calcium influx through the membrane in response to α mating pheromone (Iida *et al.*, 1994). Cch1 is also involved in calcium influx and in the late stage of the mating process (Fischer *et al.*, 1997). These two proteins may form the components of a calcium channel in the plasma membrane (Paidhurst & Garrett, 1997).

Pma1p, a yeast plasma membrane H^{+}-ATPase, belongs to the same class of P-type ATPases as mammalian Na^{+}/K^{+} and Ca^{2+}-ATPases (Serrano *et al.*, 1986). This pump extrudes protons from the cell, creating an electrochemical gradient that is the driving force for nutrient import. Withee *et al.* (Withee *et al.*, 1998) studied this H^{+}-ATPase in yeast mutants to determine the effect of the pump on ion tolerance. They found that the H^{+}-ATPase is required for effective calcium accumulation into intracellular compartments. Yeast without the pump failed to grow at high calcium concentration and there was a decrease in intracellular calcium levels. Two explanations were proposed for these observations: The first was that the H^{+}-ATPase helps to maintain the pH in cells and pH is important for vacuolar calcium accumulation. Therefore if no pump is present then cellular calcium loading will be compromised. The second possible explanation was that deletion in the H^{+}-ATPase gene decreased the uptake of a factor that is necessary for calcium sequestration. Either way this pump is essential for ion tolerance.

6.1.5. The vacuole

The vacuole is the predominant calcium store in *S. cerevisiae* and contains greater than 90% of the total cellular levels of calcium (Dunn *et al.*, 1994). This is referred to as the non-exchangeable Ca^{2+} pool since the calcium is complexed to vacuolar polyphosphate. The vacuole is thought to play a major role in maintaining calcium tolerance in the presence of environmental levels of Ca^{2+} ranging from <1 μM to 100 mM (Cunningham & Fink, 1994a). Two transporters facilitate calcium uptake into the vacuole: the $Ca^{2+}/2H^{+}$ antiporter encoded by *vcx1* (Cunningham & Fink, 1996), and the Ca^{2+}ATPase encoded by *pmc1* (Cunningham & Fink, 1994b). The role of Vcx1p is to import calcium into the yeast vacuole (Pozos *et al.*, 1996). Biochemical experiments indicate that calcium is actively transported into the vacuole via this antiporter (Cunningham & Fink, 1996; Dunn *et al.*, 1994) using the proton gradient formed by the vacuolar H^{+}-ATPase, Vma (Dunn *et al.*, 1994). The antiporter is a high capacity, low affinity calcium transporter that can rapidly sequester a sudden pulse of calcium (Miseta *et al.*, 1999b). Yeast without the H^{+}-ATPase (to drive the antiporter) have increased cytosolic calcium levels and cannot grow in high calcium conditions (Ohya *et al.*, 1986).

Pmc1p is the other calcium transporter present in the vacuole (Cunningham & Fink, 1994b). This has 41% homology (through 81% of the sequence; Pmc1p lacks the C terminus with the calmodulin binding domain) with the plasma membrane Ca^{2+}-ATPase of mammalian cells (PMCA) and has all the conserved features of a P-type pump (Figure 1.6). The major distinction however is that yeast use Pmc1p for calcium appropriation into the vacuole whereas mammalian cells use PMCA for calcium efflux through the plasma membrane. Pmc1p has been shown to be a major component of calcium homeostasis in yeast cells (Cunningham & Fink, 1994b; Pozos *et al.*, 1996) by analysis of mutations in *pmc1*, *pmr1* (Golgi ATPase), *vcx1* (H^{+}/Ca^{2} antiporter) and *cnb1* (a calcineurin mutation). The pump is necessary for tolerance to high external calcium concentrations (Cunningham & Fink, 1994b) and for efficient calcium movement into the vacuole. Miseta *et al.* (Miseta *et al.*, 1999b) proposed that Vcx1p and Pmc1p had complementary roles in Ca^{2+} homeostasis. Whilst Vcx1p rapidly sequesters calcium and attenuates activation of calcium signalling pathways, Pmc1p plays a minimal role. When calcium concentrations in the cytosol rise, the calmodulin / calcineurin pathway is activated, Vcx1p is down

regulated and the calcium mediated induction pathways are induced. This increases Pmc1p function. However, the separate physiological roles of the two calcium transporters in the vacuole are uncertain. When vacuolar biogenesis is compromised in the yeast cell, the Golgi apparatus plays a significant role in maintaining calcium homeostasis (Miseta *et al.*, 1999a).

6.1.6. The Golgi

The *pmr1* gene encodes a putative Ca^{2+}-ATPase (Pmr1p) that is thought to be localised to the Golgi or components of the secretory pathway (Antebi & Fink, 1992). Pmr1p is more closely related to the SERCA family of ATPases than is Pmc1p (Rudolph *et al.*, 1989; Serrano, 1991) and is proposed to directly transport calcium into the Golgi to support a variety of secretory functions (Rudolph *et al.*, 1989). Hence some yeast mutations in this protein lead to secretory defects (Okorokov *et al.*, 1993). Antebi and Fink (Antebi & Fink, 1992) reported that Pmr1p was localised to a novel Golgi like organelle and that it was not located in the vacuole, endoplasmic reticulum or plasma membrane. Sorin *et al.* (Sorin *et al.*, 1997) characterised Pmr1p biochemically using mutagenesis and calcium transport assays and located it to the Golgi in the yeast cell. Okorokov and Lehle (Okorokov & Lehle, 1998) also demonstrated that Pmr1p is a Ca^{2+}-ATPase, substantiating the findings of Sorin *et al.* (Sorin *et al.*, 1997). Cell fractionation and immunological studies have shown this ATPase is located in the Golgi / Golgi like membranes, by co-migration with sub-cellular markers. The occurrence of additional Ca^{2+}-ATPases located in the intracellular and in the Golgi / Golgi like membranes was demonstrated (Okorokov & Lehle, 1998). They found that yeast mutated in *pmr1* still exhibited 50 % ATPase activity in the membranes (suggesting the presence of another ATPase); the identity of the pump(s) is presently unknown. Although Pmr1 is predominantly localised in the Golgi it has also been found as a thapsigargin-insensitive component in calcium uptake in the ER (Strayle *et al.*, 1999). The location of Ca^{2+}-ATPases predominantly in the Golgi and not ER in yeast cells is in contrast with mammalian cells where the ER has long been known as the major calcium store. No distinct calcium pump has yet been identified in the ER of yeast cells. Recently however, in mammalian cells the Golgi has been identified as an IP_3 sensitive store, with a possible role in calcium signalling (Pinton *et al.*, 1998).

6.1.7. Calcineurin

A protein that is involved in calcium homeostasis and interacts with the calcium transporters is calcineurin. This calcium/calmodulin stimulated protein phosphatase is required for Na^+, Li^+, Mn^{2+} and OH^- tolerance and for calcium dependent signalling in many cell types (Withee *et al.*, 1998). It is highly conserved among yeast and mammals (Kuno *et al.*, 1991; Liu *et al.*, 1991) and has many regulatory functions. Calcineurin plays a role in neutrophil migration (Lawson & Maxfield, 1995). It has been shown in mammalian cells to shorten NMDA (N-methyl-D-aspartate) channel openings (Lieberman & Mody, 1994) and to be involved in regulation of calcium flux through IP_3 receptors (Cameron *et al.*, 1995). Thus, calcineurin has an important role in regulating ion homeostasis in numerous cell types and is likely to regulate multiple targets in yeast. Yeast cells differ from mammalian cells because instead of direct binding of calcium/calmodulin, calcium transporters are mainly regulated by calcineurin. Binding calcium and calmodulin (Yazawa *et al.*, 1999) activates calcineurin, which in turn inhibits the vacuolar calcium antiporter and also Pmr1p in the Golgi (Cunningham & Fink, 1994b). This decreases sequestration of calcium ions into these compartments and thus calcineurin acts to amplify the calcium signal through regulation of calcium sequestration into compartments. As well as inhibition of pump activity one mechanism by which calcineurin modulates yeast ion tolerance is by regulating the abundance of transporters Pmr2p (Na^+-ATPase), Pmr1p and Pmc1p through the transcription factor Tcn1p/Crz1p (Matheos *et al.*, 1997; Stathopoulos & Cyert, 1997) increasing tolerance to Ca^{2+}, Mn^{2+} and Na^+. Calcineurin is likely to regulate the function of the H^+/Ca^{2+} transporter Vcx1 by unidentified post-translational mechanisms (Cunningham & Fink, 1996).

The role of calcineurin in response to mating pheromone (which is analogous to the T-cell activation pathway) is distinct from its role of regulating calcium levels. The protein or proteins directly dephosphorylated by calcineurin *in vivo* to bring about cellular effects are yet to be identified. Together Vcx1p, Pmc1p and Pmr1p help to control cytosolic calcium concentrations in high calcium conditions and therefore modulate calcineurin function. This feedback control mechanism is important to promote efficient calcium signalling in yeast cells exposed to a wide

range of environmental conditions (Cunningham & Fink, 1996). The vacuolar H^+-ATPase co-operates with calcineurin to regulate free calcium (Tanida *et al.*, 1995).

Csg2p/Cls2p is a protein localised in the ER membrane in yeast cells (Tanida *et al.*, 1996). This protein is proposed to release calcium from the lumen of the ER, co-operating with calcineurin. Tanida *et al.* (Tanida *et al.*, 1996) proposed that the function of Cls2p is to release calcium because mutants in *cls2* cannot grow in high calcium due to the high accumulation of calcium in the ER. Csg2p/Cls2p has a putative calcium-binding site (Beeler *et al.*, 1994) but is not a homologue of a Ca^{2-}-ATPase, a calcium channel or an IP_3 receptor. It has been suggested that calcineurin, by inhibiting Pmr1p and the antiporter, acts to amplify the calcium signal, repressing calcium flux into a non-vacuolar compartment (Cunningham & Fink, 1994b), and that Cls2p/Csg2p releases calcium out into the cytoplasm which helps to increase the calcium signal (Tanida *et al.*, 1996).

The nature of the interaction between Pma1 and calcineurin is unclear. Yeast with mutations in *Pma1* fail to grow in the presence of high calcium and have decreased intracellular calcium levels, see Section 6.1.4 (Withee *et al.*, 1998). Yeast unable to express calcineurin showed the opposite effect; they are able to tolerate high calcium levels and have increased intracellular calcium levels (Withee *et al.*, 1998). It was proposed that calcineurin may therefore negatively regulate Pma1p. However, isolated calcineurin had no effect on membrane fractions enriched with Pma1p, and no increase in Pma1p activity was observed in calcineurin deficient yeast (Withee *et al.*, 1998).

Although knowledge of ion homeostasis in yeast is increasing, a general lack of understanding exists as regarding proteins that modulate transporter activity and of the co-operation between the different components of ion homeostasis. A complex network of interactions involving a plethora of proteins is established to maintain ion levels under different conditions of ion stress and pH in yeast cells. With the full genome of the yeast available, knowledge is increasing in the area of ion homeostasis and cell signalling in these fungi.

6.1.8. Mutated yeast strains

Pmc1p and Pmr1p function together in calcium transport and tolerance, transporting calcium from the cytosol into internal compartments (Figure 6.3 (A)).

Elevated cytosolic calcium levels result in activation of calcineurin by calmodulin and so sufficient Ca^{2+}-ATPase activity is essential to keep cytosolic calcium levels low for yeast growth and cellular ion homeostasis. Strains deleted in *pmc1*, encoding the vacuolar ATPase, are viable but exhibit decreased calcium tolerance. They are unable to grow in the presence of high calcium, which may be ascribed to a reduction in cytosolic calcium sequestration into the vacuole (20% of the levels compared to wild type) (Cunningham & Fink, 1994b). The residual calcium movement into stores in the absence of Pmc1p can be attributed to the vacuolar antiporter, Vcx1p, and Pmr1p in the Golgi. Calcineurin, which is activated by calcium/calmodulin under conditions of high calcium, is growth inhibitory to this mutant; by inhibiting the vacuolar H^+/Ca^{2+} antiporter this mutant cannot tolerate high levels of calcium (Cunningham & Fink, 1996). Inactivation of calcineurin (*cnb1* mutation) relieves this non-viability; growth is restored by the mutation and the double mutant (*pmc1 cnb1*) sequesters calcium at 90% of wild type levels. Hence inhibition of calcineurin function increases calcium accumulation in stores. As well as inactivation by mutation, calcineurin can also be inhibited by the use of cyclosporin/FK506 (Liu *et al.*, 1991).

Pmr1p in the Golgi is not fundamental for cell viability. However strains deleted in *pmr1* show defects in protein processing which can be overcome by high external calcium concentrations. Therefore, Pmr1p would appear to maintain sufficient calcium in the Golgi for the calcium dependent enzymes to work (Antebi & Fink, 1992).

Yeast with mutations in either *pmr1* or *pmc1* are viable but the *pmc1 pmr1* double mutation is lethal to the yeast cell (Cunningham & Fink, 1994a); the yeast is non-viable even at low calcium concentrations. This is due to the elevation of cytosolic calcium levels and activation of calcineurin. Disruption of the gene encoding the B subunit of calcineurin was necessary to relieve the inhibition of the vacuolar H^+/Ca^{2+} antiporter and restore growth in low calcium conditions. Therefore the function of Pmc1p and Pmr1p must in part be to prevent calcineurin activation through the maintenance of low cytosolic calcium levels.

Deletion of the *vcx1* gene does not significantly alter it sensitivity to calcium, unlike deletion of *pmc1*, which as mentioned above, increases the sensitivity to high calcium levels. With the deletion of both genes calcium tolerance decreases even further (Pozos *et al.*, 1996). This suggests that the roles of these two transporters

overlap but that their regulation is fundamentally different, because their responses to calcium stress are different.

6.1.9. Expression vectors

Yeast shuttle vectors are constructs of sequences derived from *E. coli* and from *S. cerevisiae* plasmids (Romanos *et al.*, 1992). The sequence from *E.coli* permits manipulation in *E. coli* and includes a bacterial origin of replication and a selectable marker such as ampicillin resistance. In most yeast a small circular DNA plasmid with the length of about 2 μm is present (the so called 2 micron plasmid), the biology of which has been studied in great detail. Properties of this DNA ensure it is stably maintained in populations, replicated and amplified (Futcher, 1988). Portions of this plasmid have therefore been incorporated into shuttle vectors permitting high level foreign protein production. The expression of heterologous proteins in yeast requires a yeast specific promoter (Goodey *et al.*, 1986) that is usually from a highly expressed gene such as alcohol dehydrogenase (Hitzeman *et al.*, 1981) or galactokinase (Stepien *et al.*, 1983). Efficient termination of transcription of heterologous cDNA is achieved by using terminator regions of yeast genes, e.g. a cyc terminator (Zaret & Sherman, 1982). The promoter and terminator will aid in the efficient transcription of a foreign gene. The yeast portion of the vector also contains a selectable marker such as Ura3 or Leu2 gene (for uracil or leucine selection). The vector pRS426 (Figure 6.4) is a multicopy yeast episomal plasmid (Mumberg *et al.*, 1994) that replicates in the yeast nucleus using the sequence derived from the 2 μm circular yeast plasmid. Selection pressure must be maintained during growth of the yeast by use of amino acid selection. Under non-selective growth conditions plasmids can be lost through mitotic segregation.

6.1.10. Expression of SERCA in yeast

Yeast are now widely employed to express heterologous proteins. Expression of Ca^{2+}-ATPases in *S. cerevisiae* has been successful for the *Schitosoma mansoni* Ca^{2+}-ATPase, SMA2 (Talla *et al.*, 1998), an *Arabadopsis thalania* Ca^{2+}-ATPase (Liang *et al.*, 1997) and for SERCA1a (Centeno *et al.*, 1994; Degand *et al.*, 1999). Yeast that have been altered with respect to their ability to grow in the presence and

absence of calcium are useful for Ca^{2+}-ATPase expression (Figure 6.3(B)). Expression of a heterologous pump can restore the ability of yeast to grow under certain conditions and this will depend on the mutation made. The SR Ca^{2+}-ATPase can complement yeast which do not contain Pmc1p or Pmr1p, and sequester calcium enough to sustain growth. This provides a simple way to monitor expression of the required protein since in the absence of expression there will be no growth. Liang *et al.* (Liang *et al.*, 1997) used the yeast K616 and the vector pRS426Gal1 (Figure 6.4) to express ECA1, an ER Ca^{2+}-ATPase from *Arabodopsis thalania*. They achieved expression demonstrated by complementation, immunostaining and functional studies. Centeno *et al.* (Centeno *et al.*, 1994) described a procedure for potentially producing milligram amounts of rabbit SERCA using the vector pYeDP118-10 (Figure 6.5). Talla *et al.* (Talla *et al.*, 1998) used the same yeast strain K616 but employed the vector p315 to obtain expression of SMA2.

6.2. Methods

6.2.1. Yeast growth

The yeast strain K616 (*MATα pmr1::HIS3 pmc1::TRP1 cnb1::LEU2*) was used (Cunningham & Fink, 1994b; Liang *et al.*, 1997). Yeast were grown in YPD (1 % Bacto-Yeast extract, 2 % Bacto peptone, 2 % dextrose or galactose), pH 6.2 or under selection conditions with SC (synthetic complete media; Gibco-BRL) with 2 % dextrose or galactose, Sigma synthetic drop out media (without histidine, leucine, tryptophan and uracil) 1.4 g/litre, pH 6.2. Leucine (30 mg/litre), histidine and tryptophan (20 mg/litre) were added to the media and uracil omitted, which was used for selection purposes (giving SC-Ura media). High calcium conditions were achieved by addition of $CaCl_2$ to a final concentration of 10 mM, and low calcium by addition of EGTA (final concentration, 10 mM).

6.2.2. Transformation of yeast cells

Yeast were transformed using the Frommer's method (Dohmen, 1991).

Preparation of competent yeast

A 5 ml pre-culture of yeast were grown overnight in YPD at 30 ^{0}C with shaking. This culture was used to inoculate 100 ml YPD. The cells were grown at 30 ^{0}C with shaking until an OD_{600} of 0.6 – 1.0 was acquired. The cells were subsequently pelleted at 3000 rpm and resuspended in 20 ml ice cold buffer 1 (1 M sorbitol, 10 mM bicine, pH 8.35, 3 % ethylene glycol). The cells were repelleted and resuspended in 2ml buffer 1. 200 µl aliquots of cells were stored at – 70 ^{0}C until use.

Transformation of DNA into Yeast

For the transformation 1µg of plasmid DNA and 50 µg of Herring sperm DNA (Sigma) were added to the top of the frozen competent cell aliquot. The cells were then defrosted at 37 ^{0}C for 5 minutes, during which time they were intermittently vortexed to mix. Once thawed, 1ml buffer 2 (40 % polyethylene

glycol (PEG) 1000, 200 mM Bicine, pH 8.35) was added and mixed by gentle inversion. The sample was incubated at 35 ^{0}C for 1 hour. The cells were centrifuged at 5000 rpm for 5 minutes and the pellet resuspended in 800 µl buffer 3 (150 mM NaCl, 10 mM bicine, pH 8.35). Finally the cells were centrifuged and resuspended in 300 µl buffer 3. The transformed cells were plated onto SC-Ura, 10mM $CaCl_2$. After 3 - 5 days growth the plates were washed with sterile distilled water and aliquots spread onto SC-Ura, 10 mM EGTA plates.

6.2.3. Preparation of yeast microsomes

Yeast microsomes were prepared using a modification of the method of Liang *et al.* (Liang *et al.*, 1997). 20 ml yeast cultures (YPD + $CaCl_2$ + 2 % dextrose for untransformed K616, and SC-Ura + 10mM EGTA + 2 % raffinose for transformed yeast) were grown to an OD_{600} of 1.8 – 2. The cells were then diluted 10 fold into YPD or SC-Ura+10 mM EGTA + 2 % galactose and grown to OD_{600} 1 – 1.8. The cells were pelleted at 3000 rpm, washed with 10 ml sterile distilled water and pelleted again. The yeast were resuspended in 10 ml glass beads buffer (10 % sucrose, 25 mM Hepes/KOH, pH 7.5, 3 mM EGTA, 2 mM DTT) and repelleted. The cells were then resuspended in an equal volume of glass beads buffer + 1 mM PMSF, 1 µg/ml pepstatin, leupeptin and aprotinin, and 0.5 mg/ml BSA. An equal volume of glass beads (425 – 600 micron, acid washed) were added and the cells vortexed for 2 minutes. The sample was centrifuged at 3000 rpm, the lysate removed and the procedure repeated with another volume of buffer. The supernatants were pooled and then spun at 55000 rpm for 1 hour to pellet the membranes. The pellet was resuspended in 100 mM KCl, 40 mM Hepes, pH 7.2, 2 mM DTT and 1 mM PMSF. 50 µl aliquots were snap frozen and stored at – 70^{0}C.

6.2.4. SDS-polyacrylamide gel electrophoresis (SDS-PAGE)

SDS page was performed according to the resolution required and the range of proteins (Laemmli, 1970). For separation of microsomes from yeast, a 7.5 % gel was used.

6.2.5. Western blotting

The method of Towbin *et al.* (Towbin *et al.*, 1979) was applied for the electro-transfer of proteins from SDS polyacrylamide gels to nitrocellulose (0.45 μm membrane). Initially gels were equilibrated for 10 minutes in the transfer buffer (0.192 M glycine, 0.025 M Tris, 20 % methanol). They were then placed on the wet nitrocellulose membrane and sandwiched between filter paper and nylon scouring pads. The gel sandwich was then placed in the transfer apparatus, with the transfer buffer, with the gel towards the cathode, for transfer of proteins onto the nitrocellulose towards the anode. Transfer was at 1.5 volts for 1.5-2 hours after which the gel was discarded and the nitrocellulose membrane air dried. Immunoblotting was performed as described in Section 2.2.4.

6.2.6. Bicinchoninic acid (BCA) protein assay

To measure protein content of yeast microsomes the sensitive BCA assay procedure was used (Smith *et al.*, 1985). Protein standards and samples were diluted 20 parts with the BCA assay reagent (one part 4 % $CuSO_4$ to 50 parts BCA) and incubated at 37 ^{0}C for 30 minutes. The absorbance was measured using a Dynatech MR 5000 plate reader (at 562nm) and protein concentrations calculated with reference to the relevant standard curve.

6.2.7. Cloning of Ca^{2+}-ATPase genes into pRS426Gal1

SERCA1b was sub-cloned into the yeast expression vector by Jon Pittman. The restriction sites EcoR1 and Xho1 were utilised for this purpose. HVSERCA was sub-cloned into the yeast vector by digesting the pcDNA3.1+ HVSERCA construct (Lockyer, 1997) BamH1/Xho 1, with subsequent ligation into pRS426 using these restriction sites.

6.2.8. Cloning of Ca^{2+} -ATPase genes into Y18

Marc le Maire (Centeno *et al.*, 1994) kindly supplied the yeast vector pYeDP1/8-10 (Y18) and the construct containing SERCA1a (Figure 6.5).

The Y18 construct did not contain any compatible restriction sites for insertion of SERCA-GFP or HVSERCA cDNA. A strategy for insertion of SERCA-GFP was designed (Figure 6.6). Firstly a 1kb fragment of SERCA was amplified by PCR using the primers Y18ENs and Y18Psa (Figure 6.6 (A)). This introduced the Eco RI and Nhe I restriction sites at the 5' end, with Pme I and Sac I at the 3' end. Next (Figure 6.6 (B)), Y18 and the PCR product were digested Eco RI/Sac I and ligated. The SERCA-GFP construct (Section 5.2.3.) and the Y18 construct created above were then digested Nhe I/Pme I and ligated together (Figure 6.6 (C)).

A strategy was also designed for introduction of the HVSERCA cDNA (Figure 6.6). Details of the primers are in appendix 2. Initially HVSERCA was amplified using PCR to introduce the Nhe I and Pme I restriction sites at the 5' and 3' end respectively (using the primers HVNheBams and HVXhoPmea, Figure 6.6 (D)). This product and the Y18 1kb SERCA construct above were subsequently digested using Nhe I and Pme I and ligated.

6.3. Results

6.3.1. Expression of Ca^{2+}-ATPases in the yeast K616

The strain K616 was used for expression of SERCA1b and the insect Ca^{2+}-ATPase HVSERCA. This yeast strain harbours mutations in the genes coding for the two yeast Ca^{2+}-ATPases, Pmc1p and Pmr1p (Cunningham & Fink, 1994b). These mutations make the yeast non-viable in media containing low levels of calcium. An additional mutation in Ura3 ensures that this yeast cannot grow in media that do not contain the nucleotide uracil. Thus, K616 will only grow in high calcium conditions (media supplemented with 10mM $CaCl_2$). Liquid media were used for the growth analysis of the yeast. After transformation, the yeast were plated out onto selection plates (without uracil, with either high or low calcium). Growth on plates can be misleading because cells are able to grow on cells that have died on the plate, gaining essential nutrients for growth, without being selected for. In liquid media, with the cells in suspension, the selection conditions are more stringent and therefore the growth observed is a better representation of the growth conditions.

6.3.2. Production of the p426 HVSERCA construct

To insert the cDNA for the insect Ca^{2+}-ATPase, HVSERCA, into the yeast plasmid p426 both the vector and the insert were digested with Bam HI/Xho I. After ligation, the construct was digested using these enzymes. Figure 6.7 shows this restriction analysis. The 3.1kb band (B), represents the HVSERCA cDNA and the higher 6.4 kb band (A), the vector p426.

6.3.3. Growth of K616 and K616 expressing Ca^{2+}-ATPases

Initial selection of transformed yeast was performed by selecting on SC-Ura plates supplemented with 10 mM $CaCl_2$, for the first selection and 10 mM EGTA for the second selection. Figure 6.8 shows three yeast plates. K616 is unable to grow on plates lacking uracil. K616 transformed with the p426 vector alone grows well in high calcium conditions but to a less well in low calcium. K616 p426 SERCA1b (K616S1b) and K616 p426 HVSERCA (K616HV) increase the yeast growth in low

calcium conditions, due to expression of the Ca^{2+}-ATPase genes. Liquid media was the next selection process, both in high and low calcium. The growth profile of K616 can be seen in Figure 6.9. In synthetic complete (SC) media + uracil, K616 can grow in the presence of 10 mM $CaCl_2$. In the presence of calcium the yeast shows a normal growth pattern, with a lag phase followed by a log phase proceeding to a plateau at an optical density measured at 600nm (OD_{600}) of approximately 2.0, where no further growth is observed. As can be seen in Figure 6.9, when 10 mM EGTA is added to the media (low calcium conditions), the yeast is unable to grow; the OD_{600} does not change over the 50 hour growth period of the yeast in high calcium. K616 was transformed with the DNA for SERCA and for HVSERCA. This DNA was contained in the shuttle vector pRS426 Gal1. This confers the ability to grow in the absence of uracil. As shown in Figure 6.9, yeast containing the shuttle vector with SERCA1b can grow at high calcium and can also grow at low calcium concentrations. Similarly, as shown on Figure 6.9, yeast containing the shuttle vector with HVSERCA can grow at both high and low calcium concentrations. The growth in SC-Ura+10 mM $CaCl_2$ media is permitted because, as mentioned, the yeast now contain the shuttle vector pRS426 which contains Ura3 and allows growth when uracil is not present in the media. In SC-Ura+10 mM EGTA, K616SERCA1b and K616HVSERCA are able to grow. The expression of the SERCA1b and HVSERCA Ca^{2+}-ATPase pumps in K616 complement the yeast growth. The yeast could not grow without the heterologous ATPases because K616 could not sequester calcium into intracellular stores. Expression of the heterologous pumps compensates for the two yeast pumps that are not expressed and is enough to make the yeast viable at low calcium concentrations.

6.3.4. SDS gel of yeast microsomes

Figure 6.10 shows an ECL blot of yeast microsomes run on a 7.5% SDS gel. After blocking the unoccupied sites with BSA, the nitrocellulose was probed with the anti SERCA antibody Y1F4 (1:10 dilution) and subsequently a goat anti mouse HRP conjugated antibody (Sigma, 1:80 000 dilution). Lane (1) is SR. In SR ~75% of the protein is the Ca^{2+}-ATPase and a major band at 115 kDa, corresponding to the Ca^{2+}-ATPase is clear. K616 microsomes are run in lane (2), and do not show a band at

115 kDa. K616SERCA1b microsomes are run in lane (3). There is a band at 115 kDa in this lane, showing that the yeast have expressed the Ca^{2+}-ATPase, SERCA1b.

6.3.5. The effect of Ca^{2+}-ATPase inhibitors on yeast expressing Ca^{2+}-ATPases

Since expression of SERCA1b and HVSERCA in the yeast strain K616 are necessary to recover the growth in low calcium conditions, it was thought that addition of inhibitors of the ATPase would prevent growth. The only prerequisite for studying the effect of inhibitors by such a method is that the effects of the inhibitors should be just on the Ca^{2+}-ATPase. Therefore the inhibitors should have no inhibitory effect on the normal growth of K616 in high calcium conditions in the presence of uracil.

6.3.6. The effect of BHQ on yeast expressing Ca^{2+}-ATPases

Figure 6.11 shows the growth of K616 in the presence of uracil and 50 μM BHQ at high calcium concentrations. As shown the presence of BHQ has no significant effect on growth under these conditions. As expected, K616 failed to grow in EGTA in either the presence or absence of BHQ. Figure 6.11 also shows a similar experiment for K616SERCA1b. Again in the presence of high concentrations of calcium growth was unaffected by the presence of BHQ. Although growth was also seen in the presence of EGTA in the absence of BHQ, this growth was prevented by the presence of BHQ. A similar result was obtained for K616HVSERCA (Figure 6.11), with growth at both high and low calcium concentrations in the absence of BHQ, but growth at low calcium only in the absence of BHQ. These results suggest that BHQ, at 50 μM is able to inhibit both SERCA and HVSERCA.

6.3.7. The effect of Tb on yeast expressing Ca^{2+}-ATPases

Figure 6.12 shows the growth of K616 in the presence of uracil and 5 μM Tb, in high calcium media. The data show that Tb does not affect growth under these conditions. As expected, K616 failed to grow at all in low calcium conditions in the presence or absence of Tb. Figure 6.12 also shows the same analysis for

K616SERCA1b. The growth in high calcium conditions is unaffected by Tb. In the absence of Tb and calcium, growth was seen, as expected, but this growth was inhibited by the inclusion of 5 μM Tb in the media. Figure 6.12 shows the growth of K616SERCA1b with 50 nM Tb. In both high and low calcium conditions this low concentration of Tb has no effect on the yeast growth. Figure 6.12 shows the analysis using K616HVSERCA. In conditions of high calcium, growth was unaffected by the presence of 5 μM Tb, but growth in low calcium conditions was also unaffected by 5 μM Tb. Figure 6.12 shows the growth of K616HVSERCA with 50 μM Tb in the media. Again, both the growth in high and low calcium conditions is unaffected by the presence of this compound. These results suggest that 5 μM Tb is able to inhibit SERCA1b but neither this concentration nor 50 μM Tb inhibited HVSERCA.

6.3.8. The effect of nonylphenol on yeast expressing Ca^{2+}-ATPases

Figure 6.13 shows the growth of K616 in media containing uracil, calcium and 25 μM NP. Inclusion of NP in the media prevents growth of K616 at both high and low calcium conditions. Likewise, as shown in Figure 6.13, growth of K616SERCA1b is prevented in the presence of 25 μM NP, both in high and low calcium conditions. Figure 6.13 shows the growth of K616HVSERCA in the presence NP. Again, the yeast growth both in high calcium and low calcium conditions is affected by NP. Therefore, NP inhibits K616 growth in a non-calcium dependent manner.

6.3.9. Production of the Y18 HVSERCA construct

The HVSERCA cDNA was introduced into the Y18 vector as described (Section 6.2.8). Figure 6.14 shows the initial HVSERCA PCR product, 3.1 kb in size at band (A). This was ligated into Y18. Restriction analysis of the final construct using Nhe I/Pme I gave a band (C) at ~3kb (HVSERCA cDNA) and the higher band (B) at 7 kb represents the Y18 vector.

6.3.10. Expression of SERCA and HVSERCA using the Y18 vector

Expression of SERCA has been shown by immunological procedures (Figure 6.10). However expression levels are low, with probably just enough expression of the pump to complement K616 growth. This has facilitated inhibitor studies (Figures 6.11 - 6.13) but detection of a functional SERCA in the yeast microsomes using the sensitive Ca^{45} uptake and the phosphorylation methods (Taylor & Hattan, 1979; Black, 1999) has not been successful. Centeno *et al.* (1994) described a method to obtain mg amounts of SERCA1a using the yeast expression vector pY18 (Centeno *et al.*, 1994). This SERCA1a construct and the HVSERCA construct were transformed into K616. Figure 6.15 shows complementation of yeast by SERCA1a and HVSERCA. Plate (A) shows growth in the presence of 10 mM calcium. Untransformed K616 does not grow, but those containing the vector do. In low calcium conditions (plate (B)), where a functional Ca^{2+}-ATPase is required for growth, only the yeast transformed with the cDNA for SERCA and HVSERCA grow. This hence shows functional complementation via expression of Ca^{2+}-ATPases. Microsomes of SERCA1a were made using the method described. Figure 6.16 shows the microsomes run on an SDS gel compared to the microsomes from yeast expressing SERCA1b in the P426 vector. The antibodies used were as previously described for detection on nitrocellulose. Lane (1) shows the band at 115 kDa representing SERCA in SR vesicles. Lane (2) shows untransfected K616 microsomes. Lanes (3 – 5) show microsomes from yeast expressing SERCA1a. As can be seen 10 μg of Y18SERCA1a (lane 3) microsomes exhibits a large band corresponding to SERCA1a protein. In contrast (with the same amount of protein) using microsomes of p426SERCA1b, the SERCA1b band cannot be detected (lane 4). Using a higher concentration of protein (250 μg, lane 5) a band corresponding to the Ca^{2+}-ATPase can be seen. Thus the levels of expression of the Ca^{2+}-ATPase in Y18 is much more than in p426.

6.3.11. Production of the Y18 SERCA-GFP construct

The SERCA-GFP cDNA was introduced into the Y18 vector as described (Section 6.2.8). Figure 6.17 shows the restriction analysis of the ligated construct.

This was digested using Nhe I/Pme I, which gave a band (B) at 3.6 kb (SERCA-GFP cDNA) and the higher band (A) at 7kb represents the Y18 vector.

6.3.12. Expression of SERCA-GFP in yeast

The SERCA-GFP construct was successfully created (Chapter 5). Immunofluorescent procedures to detect proteins in yeast are possible, but the rigid cell wall must be removed completely and the remaining spheroplast permeabilised to facilitate antibody perfusion. The yeast must also be immobilised on a surface for this procedure. This is a time consuming process. Simply by introducing GFP (Section 5.2.3) onto the end of SERCA1b, expression may be observed directly Figure 5.15). Additionally successful expression in K616 in low calcium conditions would show that the protein is functional as a Ca^{2+}-ATPase. K616 was transformed with Y18 SERCA-GFP and Figure 6.18 shows the yeast growth. Plate (A) shows growth in high calcium and plate (B) in low calcium conditions. Under low calcium conditions, only K616 expressing SERCA-GFP grows. This demonstrates that the construct is functional. Figure 6.19 shows the expression of the Y18 SERCA-GFP in K616, visualised using the confocal microscope. Control untransfected cells exhibited no fluorescence (data not shown). The transfected cells exhibited GFP fluorescence inside the cell with a localised area of high expression, possibly surrounding the nucleus or corresponding to the vacuole. GFP fluorescence was also verified using a fluorimeter. The emission spectra from 485 to 580 nm were measured using the excitation maximum of GFP at 480 nm. The untransfected K616 yeast cells exhibited no fluorescence over this range. The cells expressing SERCA-GFP exhibited a large emission peak at 520 nm, which corresponds to the spectra of GFP (data not shown). The exact localisation of SERCA in the cell is unclear and could be determined by fractionation of the cells and analysis using fluorescent procedures.

6.4. Discussion

6.4.1. Expression of Ca^{2+}-ATPases in yeast

Complementation of yeast growth by the expression of heterologous proteins is an ideal system for demonstration of the production of the required protein. The yeast K616 are unable to grow in low calcium conditions. Therefore complementation is a direct indication of expression. Expression of both SERCA and HVSERCA using the p426 vector restore growth in low calcium conditions (Figures 6.8 and 6.9). This is the first evidence to show that HVSERCA is a functional Ca^{2+}-ATPase. Previous attempts to express HVSERCA in Cos-7 cells were unsuccessful (Chapter 5) whereas using this expression system HVSERCA complements yeast growth well. The immunoblotting shows that SERCA is present in the yeast (Figure 6.10), although expression levels are low. Indeed sensitive functional assays (Ca^{45} uptake and phosphorylation (Taylor & Hattan, 1979; Black, 1999) did not detect any Ca^{2+}-ATPase activity. The pump may therefore be expressed at levels just sufficient to complement growth. The expression vector pY18 (Centeno *et al.*, 1994) was used to try to improve the levels of expression. Yeast growth was successfully complemented (Figure 6.15) and increased levels of SERCA expression were indeed observed (Figure 6.16).

SERCA-GFP expression has been shown in K616 (Figures 6.18 and 6.19) and along with complementation of yeast growth show that the pump is active and expressed well in all yeast cells. The exact sub-cellular localisation of SERCA-GFP is unclear. In these experiments the pump appears to be localised to a large organelle within the cell and the pattern of localisation is similar to that obtained by Kunze *et al.* (1999) when they expressed a vacuolar protein chitinase-GFP construct. Using GFP as a marker to study intracellular transport of vacuolar and secretory proteins, this group concluded that GFP may actually direct secretory proteins to the vacuole using an unknown vacuolar signal present in the GFP sequence. Thus, it would appear that the SERCA-GFP construct may be expressed in the vacuole, which is the major calcium store in yeast cells, in contrast to mammalian cells where the ER is the major calcium pool. This localisation in K616 would seem correct since expression of SERCA1b restores growth of this mutant and contributes towards calcium sequestration. However, SERCA1b has more homology to Pmr1p located in the

Golgi and components of the secretory pathway (Antebi & Fink, 1992), than to Pmc1p that is located in the vacuole (Rudolph *et al.*, 1989). The term vacuole is used in a purely descriptive sense. In yeast, vacuoles do not represent clearly separated organelles but are part of a membrane system that could include the endoplasmic reticulum and Golgi (Kreutzfeldt & Witt, 1991). Indeed the Golgi in *S. cerevisiae* is not organised in stacks but is scattered through the cytoplasm (Rossanese *et al.*, 1999). Interestingly, fluorescence of SERCA-GFP can also be seen at the cell periphery. It is known that the expression of functional transport proteins in *S.cerevisiae* is difficult due to the problems of traffic jamming. Over-expression of Pma2, a yeast plasma membrane H^+-ATPase (Supply *et al.*, 1993) and a plant plasma membrane H^+-ATPase (Villalba *et al.*, 1992) led to accumulation of intracellular protein, proliferation of the membrane system (probably ER) and failure of the protein to reach the cell surface. Thus the plasma membrane ATPases were not located exclusively at the plasma membrane as would be expected and the true physiological location of Pma2 was not determined (Supply *et al.*, 1993). So, with the mutation of the two calcium pumps and calcineurin in K616 the function of the normal secretory pathway may be altered. In addition to this, over-expression of SERCA to a high level may result in expression of the pump in a membrane system that would not normally be expected. An N-terminal signal peptide and a vacuolar target signal present in the chitinase are sufficient to direct the heterologous chitinase to the yeast vacuole (Kunze *et al.*, 1998) and thus it may be possible to target the Ca^{2+}-ATPase to the vacuole using such sequences. Unfortunately without an antibody the levels of HVSERCA expression could not be determined.

6.4.2. Inhibitor studies in yeast expressing Ca^{2+}-ATPases

Since growth in low calcium media is due to complementation by the Ca^{2+}-ATPases, yeast expressing Ca^{2+}-ATPases are a possible system on which to test the effectiveness of a range of inhibitors. This, of course, requires that the effects of the inhibitors be specific effects on the Ca^{2+}-ATPase; any inhibitors that prevent growth in a non-specific way cannot be tested for using this system.

The results show that BHQ and trilobilide have no effect on the growth of K616 alone (Figures 6.11 and 6.12) but that NP inhibits yeast growth (Figure 6.13). This suggests that NP has non–specific inhibitory effects on yeast growth. BHQ

prevents growth of both K616SERCA1b and K616HVSERCA (Figure 6.11) expressing yeast. Tb affects growth of K616SERCA1b (Figure 6.12) but not K616HVSERCA (Figure 6.12). These results show that whereas BHQ is an inhibitor of both SERCA and HVSERCA, Tb is an inhibitor of just SERCA. The binding site for the sesquiterpene lactones on the Ca^{2+}-ATPase is believed to involve a region around residue 256 in the stalk section above transmembrane α-helix M3 (Figure 3.2). Comparison of the sequence in this region between SERCA and HVSERCA (Figure 6.20) indicates that the residues are highly conserved. The residue Phe-256 is present in the HVSERCA sequence. This is surprising since Tb did not inhibit HVSERCA (Figure 6.12). Comparison of the HVSERCA and SERCA1b cDNA sequences show that regions of highest homology are those corresponding to the transmembrane α-helices. The most divergent sequences in the first third of the HVSERCA cDNA are the regions between the transmembrane α-helices. In particular the region before residue 245 of the S3 segment is very different in SERCA and HVSERCA (Figure 6.20). Zhong *et al.* (1999) investigated the relevance of the S3 segment for Tg affinity and concluded that this was important (Ma *et al.*, 1999). The relevance of this preceding sequence in HVSERCA is currently unknown and this could possibly play a functional role in the sensitivity to Tg.

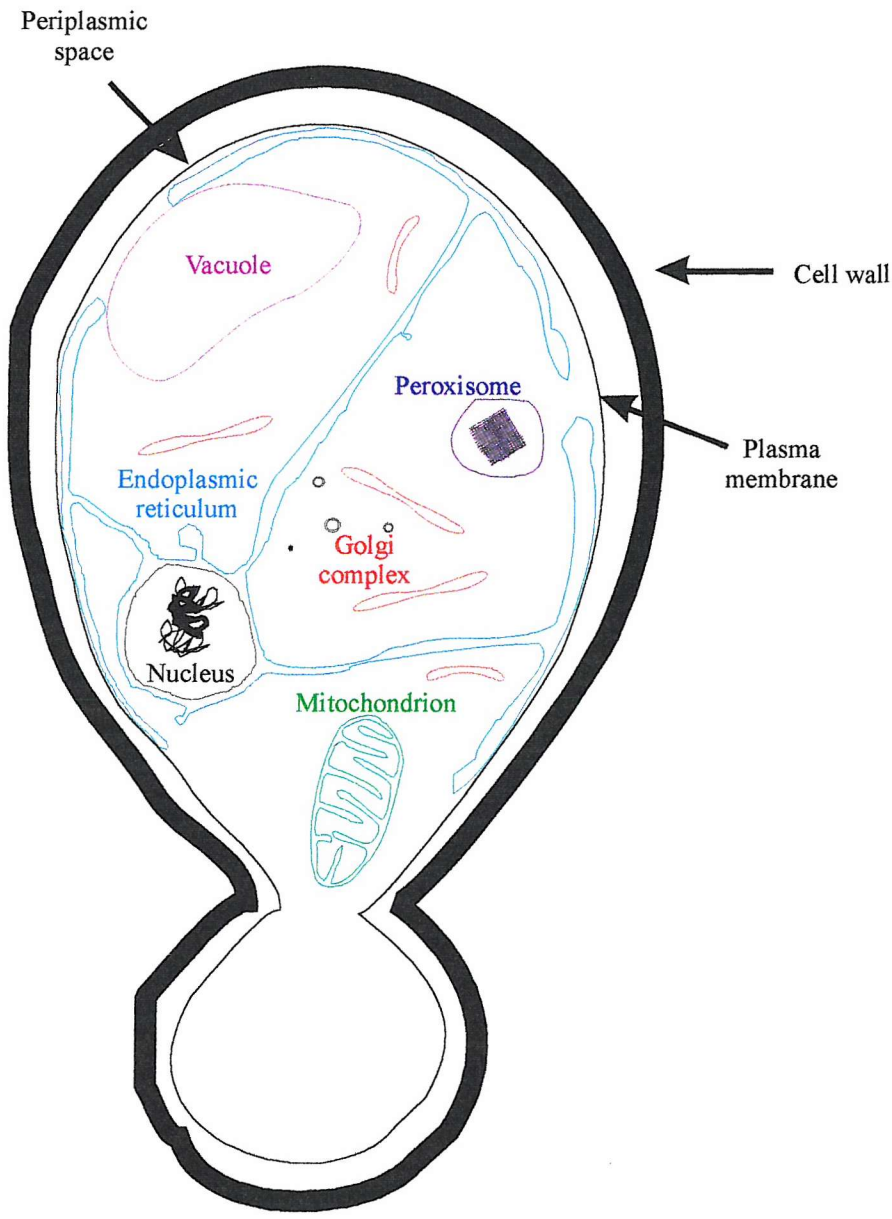

Figure 6.1. Schematic representation of a yeast cell.

Shown are the organelles in the cell, surrounded by the plasma membrane and cell wall. For simplicity the vacuole, Golgi and endoplasmic reticulum are represented as separate organelles but they may form a large membrane system. The Golgi in *S.cerevisiae* is also dispersed throughout the cytoplasm.

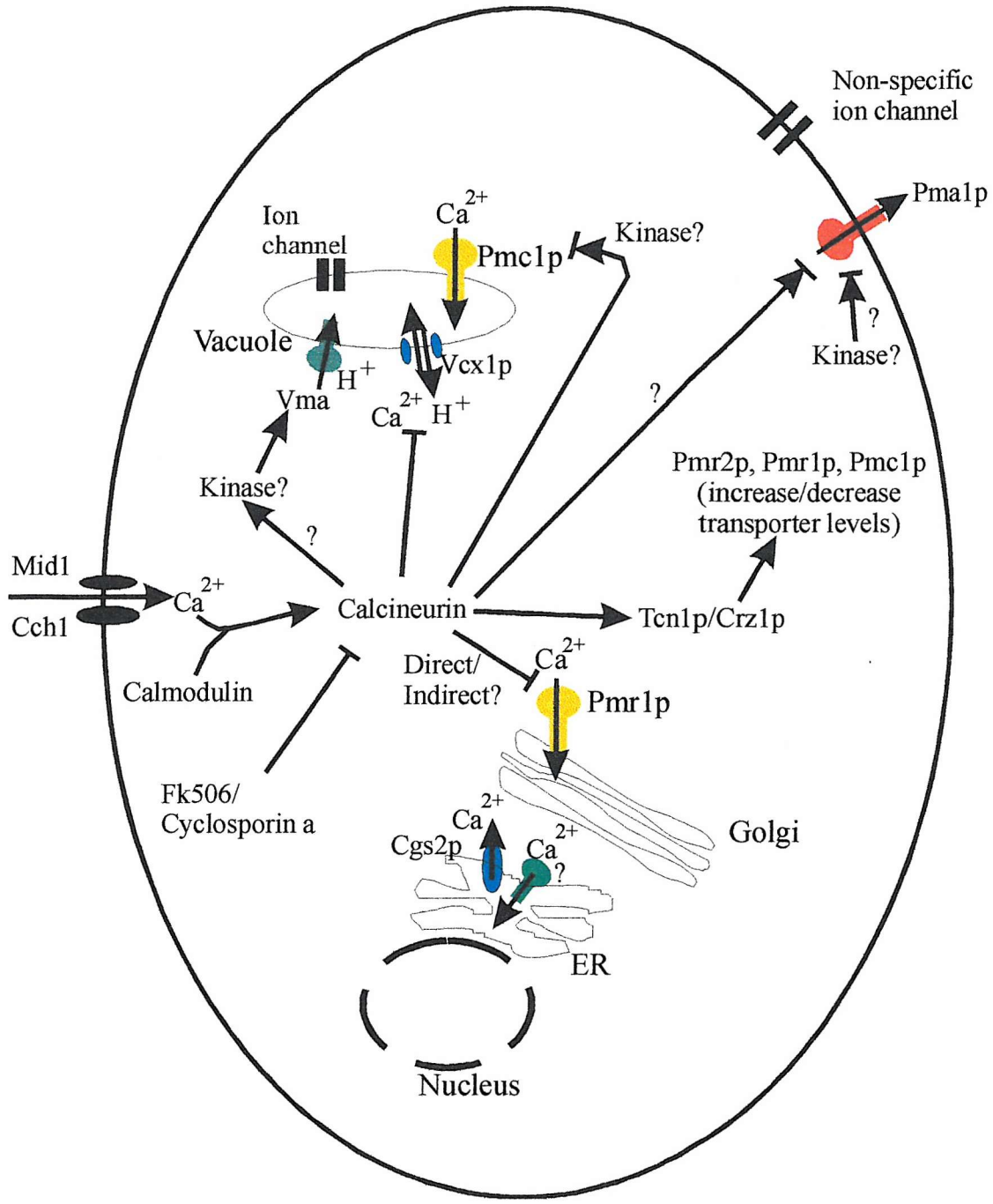

Figure 6.2. Calcium homeostasis in a yeast cell.

The figure represents a yeast cell. Indicated are the proteins proposed to be involved in calcium homeostasis within the cell. ⊥ indicates an inhibitory pathway; ↓ indicates a stimulatory pathway or movement of ions across a membrane.

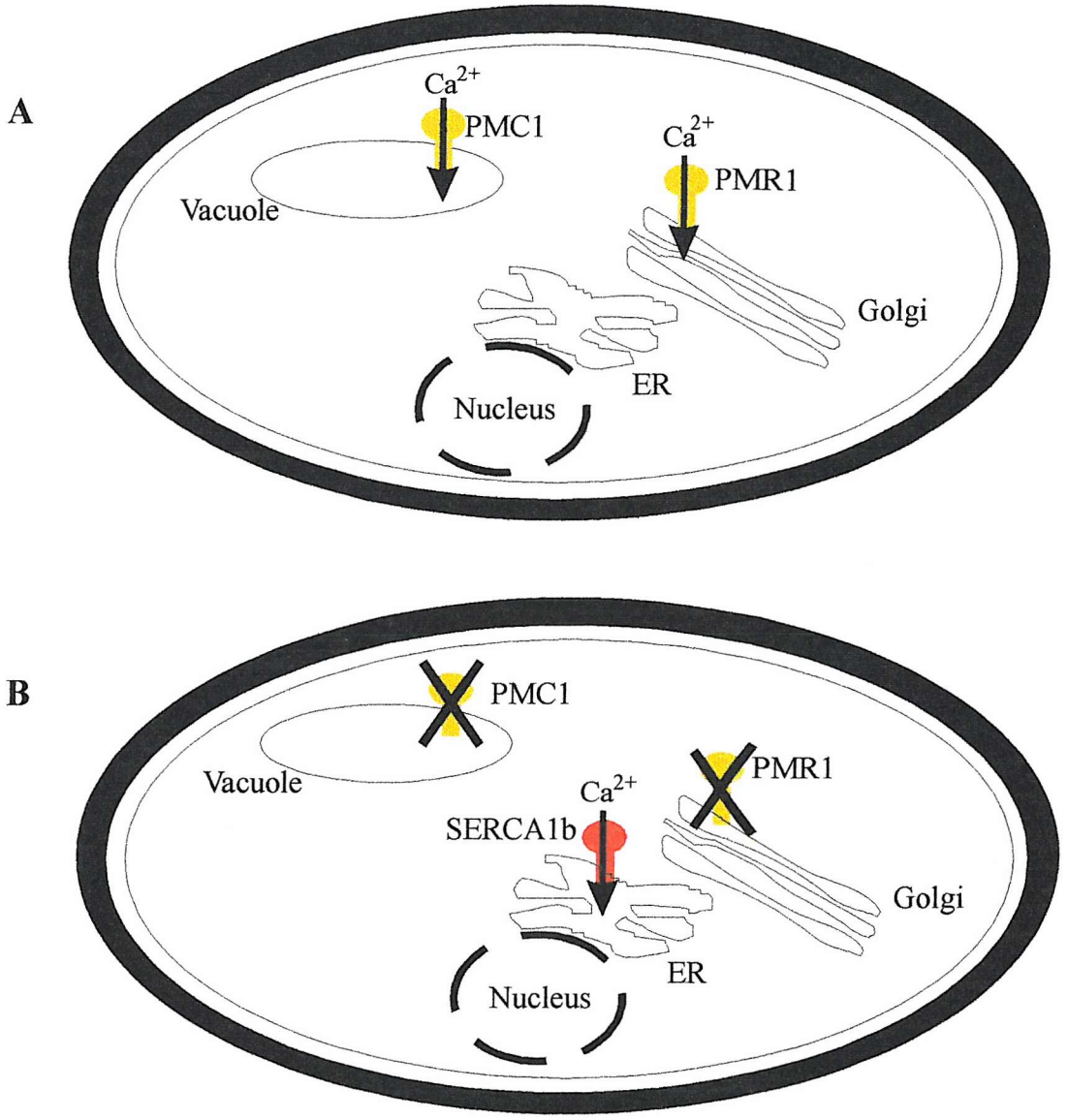

Figure 6.3. Complementation of a yeast cell by expression of SERCA1b.

The figure represents a yeast cell. (A) Pmc1 and Pmr1 are essential for growth of yeast. In (B) *Pmc1* and *Pmr1* have been mutated. This yeast cannot sequester calcium into internal compartments and therefore cannot grow in low calcium. However if the same yeast cell expresses SERCA1b the cell can sequester calcium into an internal compartment, restoring its growth.

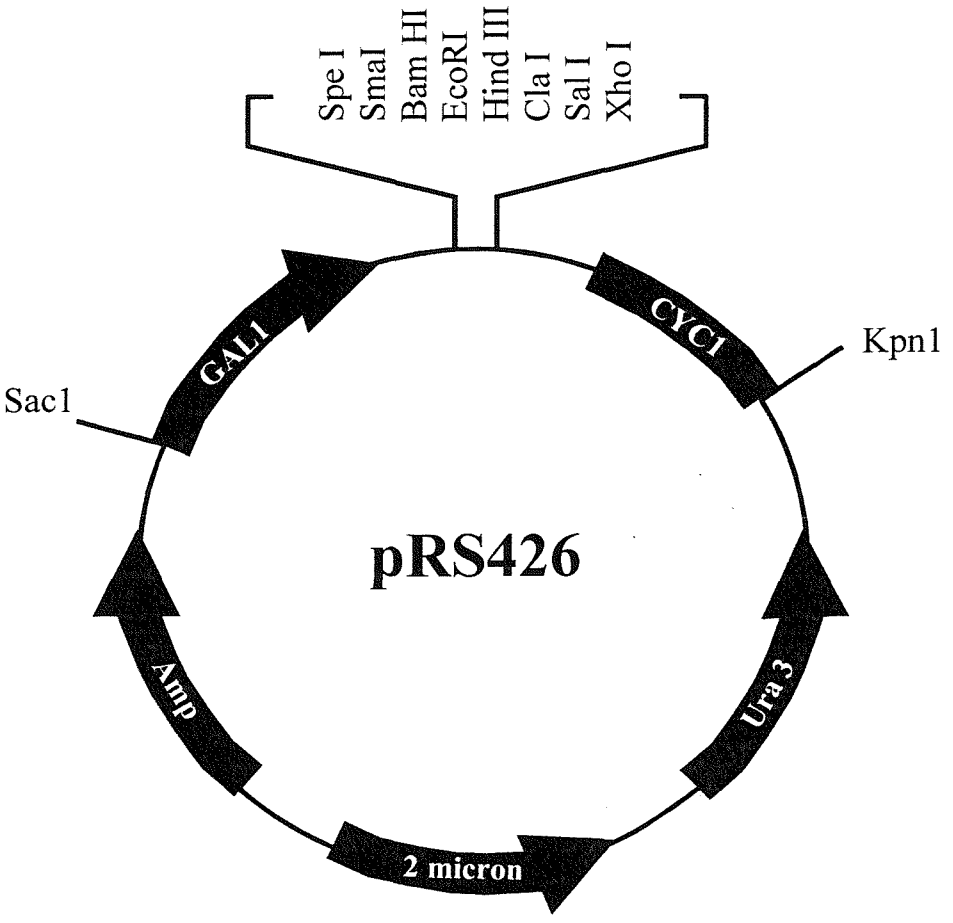

Figure 6.4. A map of the pRS426 yeast expression vector

Indicated are: GAL1, the yeast promoter; CYC1, the yeast terminator; Amp, for bacterial selection; Ura3, for yeast selection; 2 micron, a portion of the 2 micron plasmid from yeast. Adapted from Mumberg *et al.* (1994).

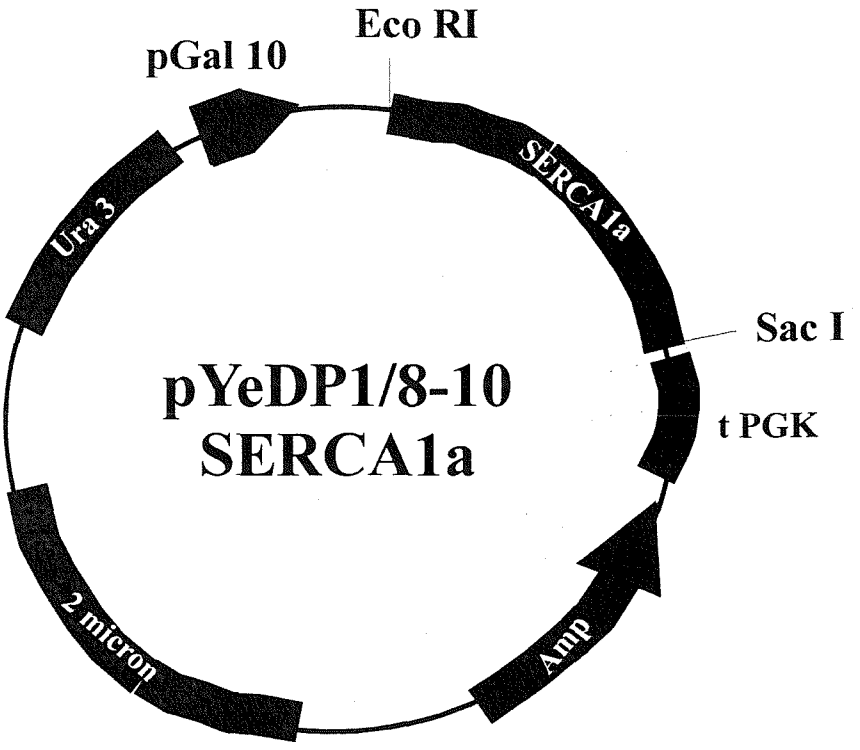

Figure 6.5. A map of the pYeDP1/8-10 vector containing SERCA1a

The SERCA1a cDNA is inserted Eco RI (at base 1) and Sac I (at base3015). The cDNA is under the control of a GAL10 promoter and a PGK (phosphoglycerate kinase) terminator (Centeno *et al,* 1994).

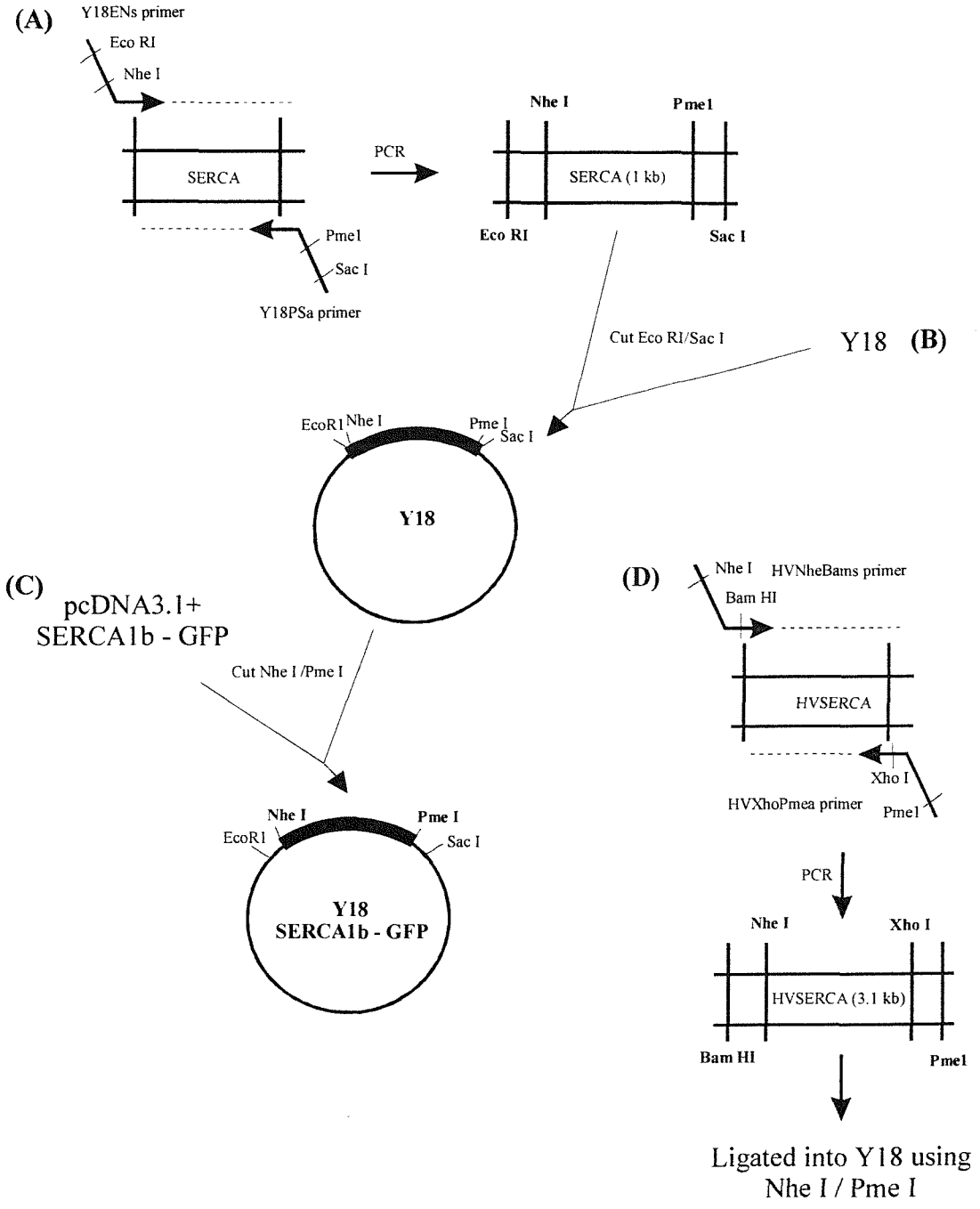

Figure 6.6. Strategy for construction of Y18 SERCA-GFP and Y18 HVSERCA

Initially 1kb of SERCA was amplified to introduce the restriction sites (A). This was cloned into Y18 using the Eco RI and Sac I sites (B) and the SERCA-GFP was subcloned using Nhe I/Pme I (C). HVSERCA was also cloned using these two sites (D).

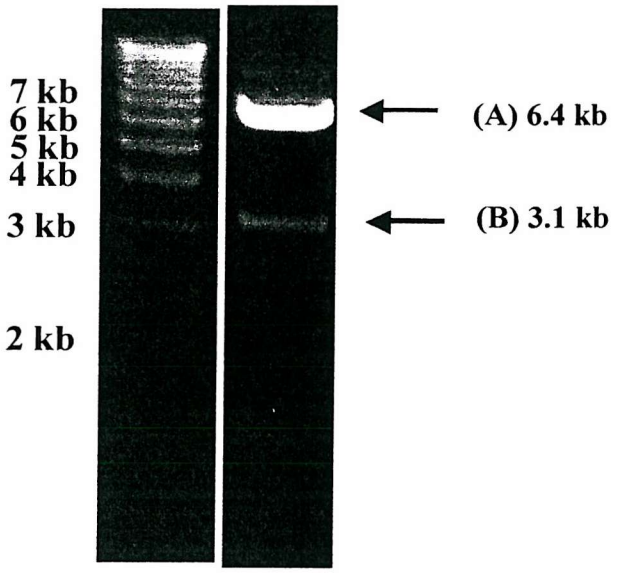

Figure 6.7. Diagnostic agarose gel of the p426 HVSERCA restriction analysis
Products from the double digest of the ligated product p426 and HVSERCA, with Bam HI/Xho I. Band (A) is the p426 vector and band (B) is the HVSERCA insert.

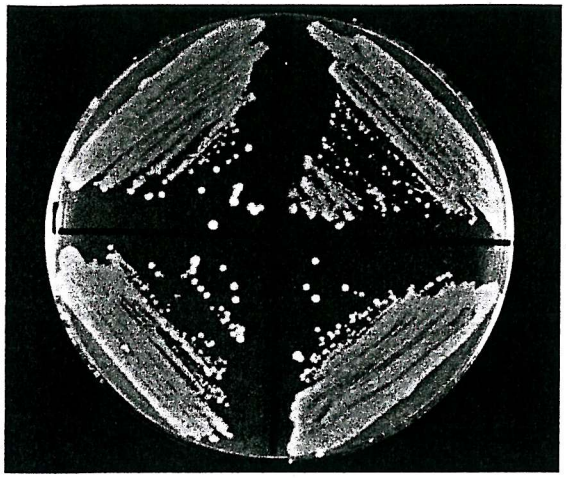

(A) SC + Ura +10 mM $CaCl_2$

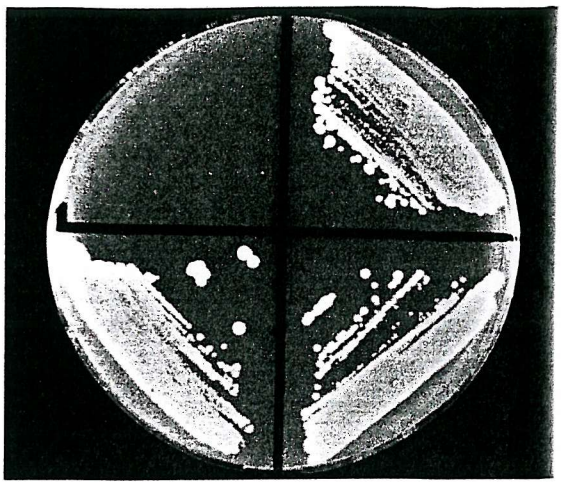

(B) SC - Ura + 10 mM $CaCl_2$

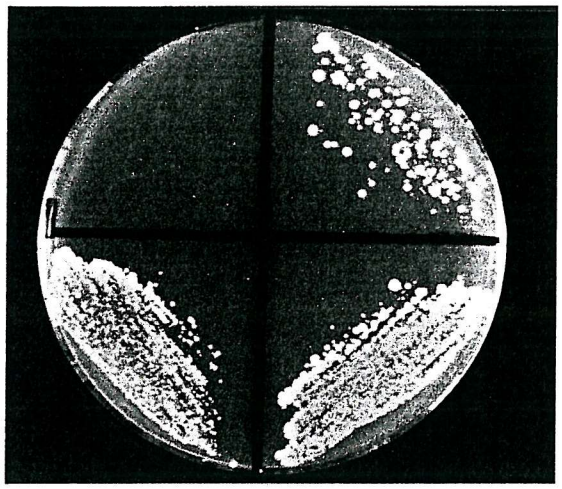

(C) SC - Ura + 10 mM EGTA

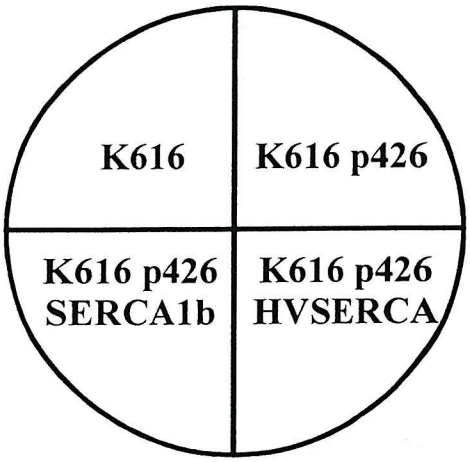

Figure 6.8. Growth analysis of yeast

Plate (A) shows growth of yeast on SC + Ura + 10 mM $CaCl_2$. Plate (B) shows growth of yeast on SC-Ura + 10 mM $CaCl_2$. Plate (C) shows growth of yeast on SC-Ura + 10 mM EGTA. Indicated in the quarters are the untransformed K616 and K616 transformed with p426 vector alone, p426 SERCA1b and p426 HVSERCA.

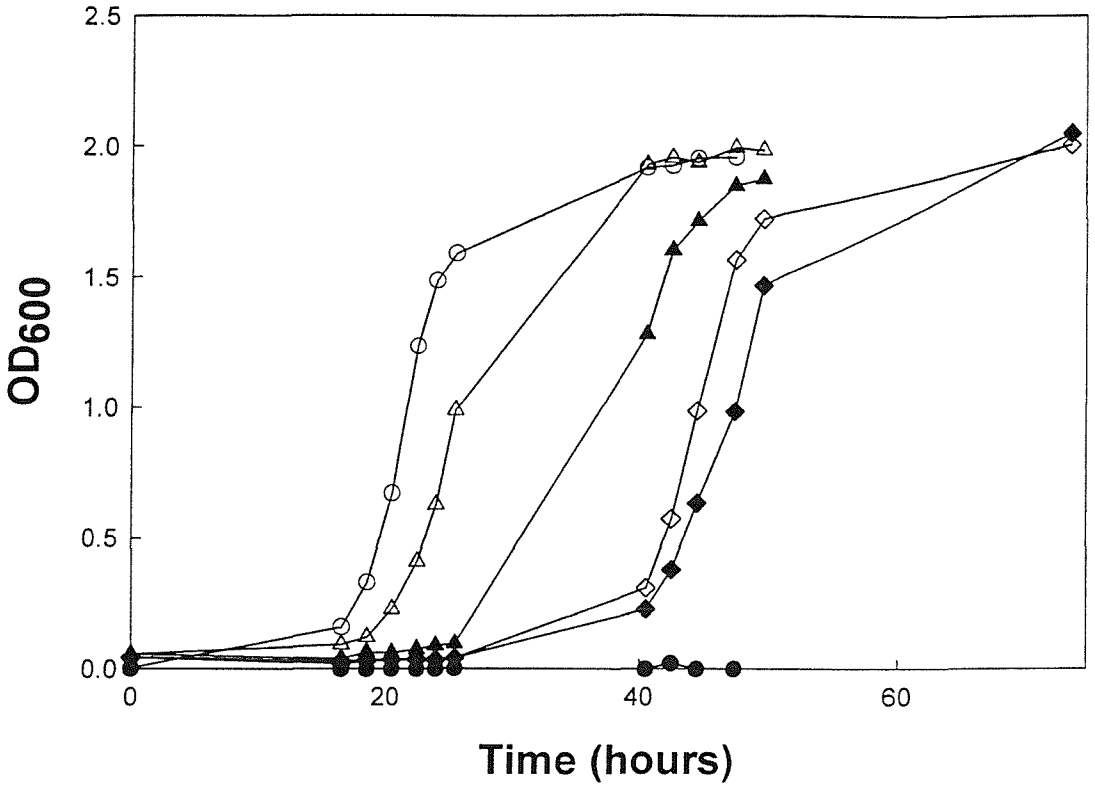

Figure 6.9. Growth analysis of yeast

Untransformed yeast were grown in the presence of uracil and transformed yeast in the absence of uracil. Shown are OD measured at 600 nm as a function of time for: (o), K616 in the presence of 10 mM $CaCl_2$; (•), K616 in the presence of 10 mM EGTA; (Δ), K616 SERCA1b in the presence of 10 mM $CaCl_2$; (▲), K616SERCA1b in the presence of 10 mM EGTA; (◇), K616HVSERCA in the presence of 10 mM $CaCl_2$; (◆), K616HVSERCA in the presence of 10 mM EGTA.

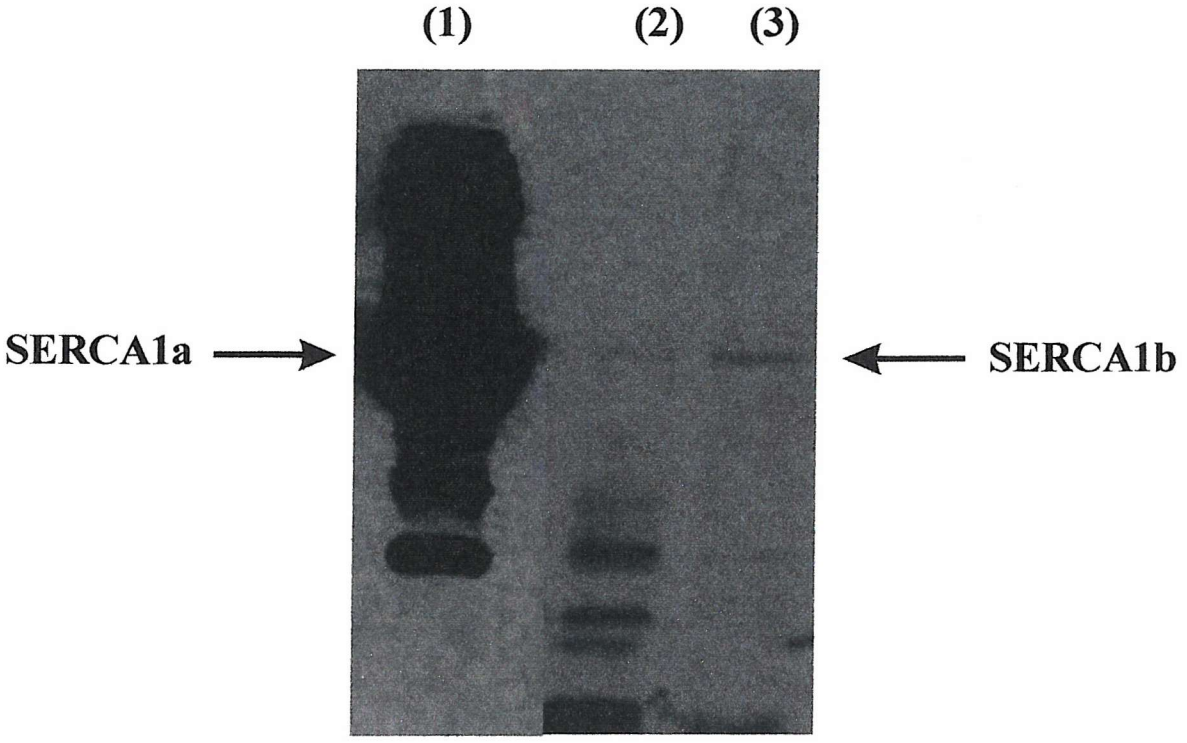

Figure 6.10. Western blot of SR vesicles and yeast microsomes.

A 7.5% SDS gel was transferred onto nitrocellulose. After blocking with BSA the nitrocellulose was probed with antibodies. The primary antibody used was Y1F4 (1:10 dilution), and the secondary antibody, a goat anti-mouse HRP conjugated antibody (Sigma; 1:80000 dilution). Lane (1) 5 μg SR; Lane (2) 10 μg untransformed K616 microsomes; Lane (3) 10 μg K616 p426 SERCA1b microsomes. An enhanced chemiluminescence kit (Amersham) was used for detection.

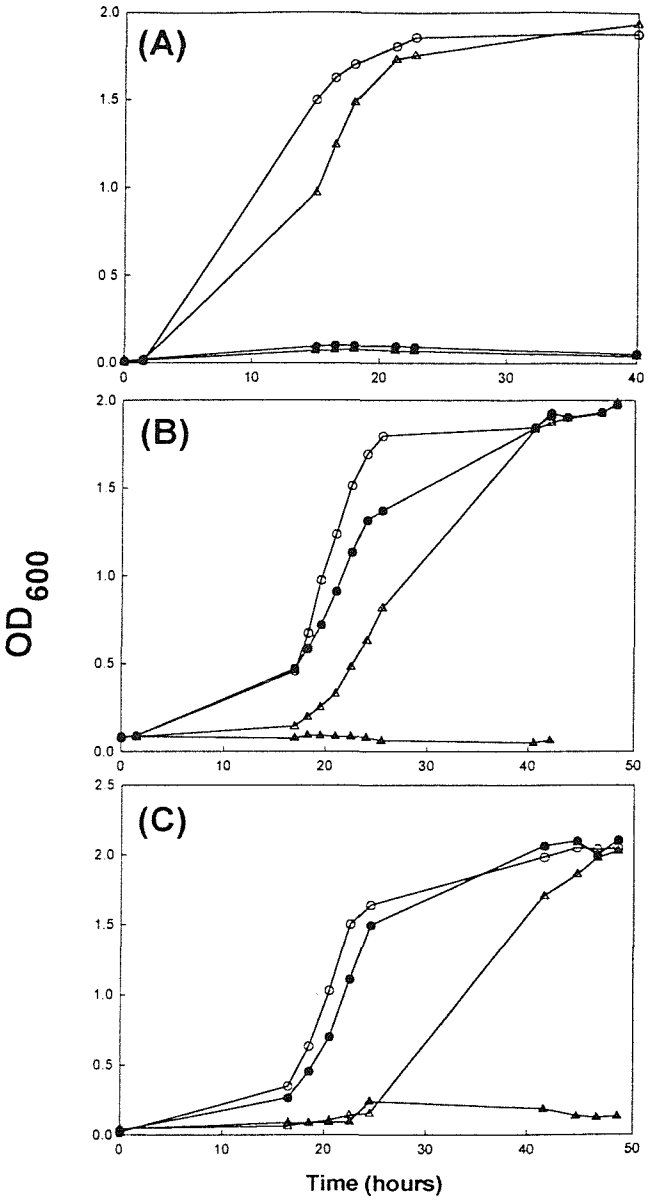

Figure 6.11. The effect of BHQ on yeast growth

Shown are OD measured at 600 nm as a function of time. Graph (A) shows growth of untransformed K616 in the presence of uracil, graph (B) shows growth of K616 SERCA1b and graph (C) shows growth of K616 HVSERCA. The transformed yeast were grown in the absence of uracil. Growth is shown in the presence of: (o) 10 mM $CaCl_2$; (•) 10 mM EGTA; (Δ) 10 mM $CaCl_2$ and 50 μM BHQ; (▲) 10 mM EGTA and 50 μM BHQ.

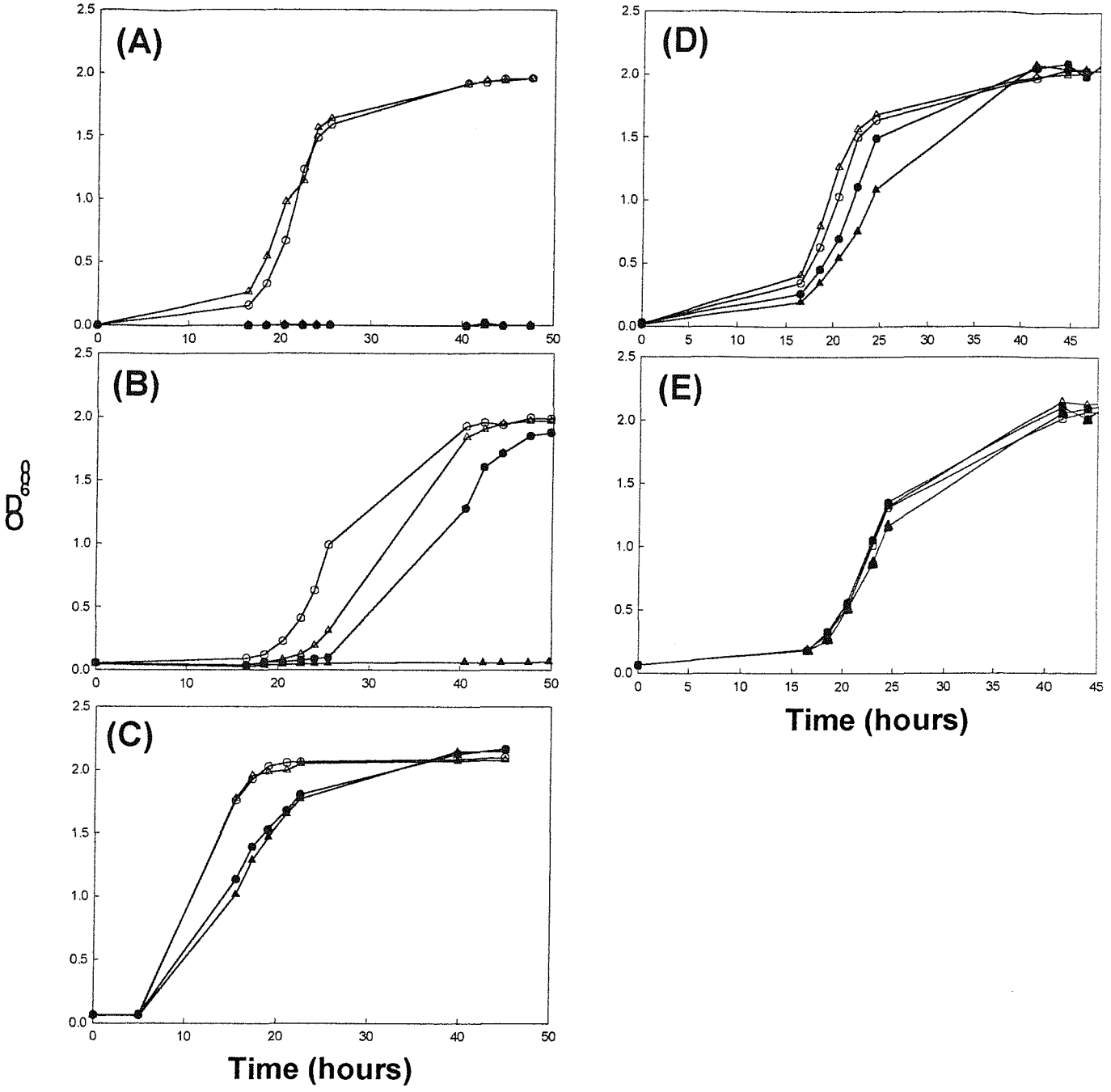

Figure 6.12. The effect of Tb on yeast growth

Shown are OD measured at 600 nm as a function of time for. Graph (A) shows growth of untransformed K616 in the presence of uracil. Graphs (B) and (C) show growth of K616 SERCA1b and graphs (D) and (E) show growth of K616 HVSERCA. The transformed yeast were grown in the absence of uracil. Growth is shown in the presence of: (o) 10 mM $CaCl_2$; (●) 10 mM EGTA; (□) 10 mM $CaCl_2$ + Tb; (□) 10 mM EGTA + Tb. 5 μM Tb was used in (A), (B) and (D), 50 nM Tb was used in (C) and 50 μM Tb in (E).

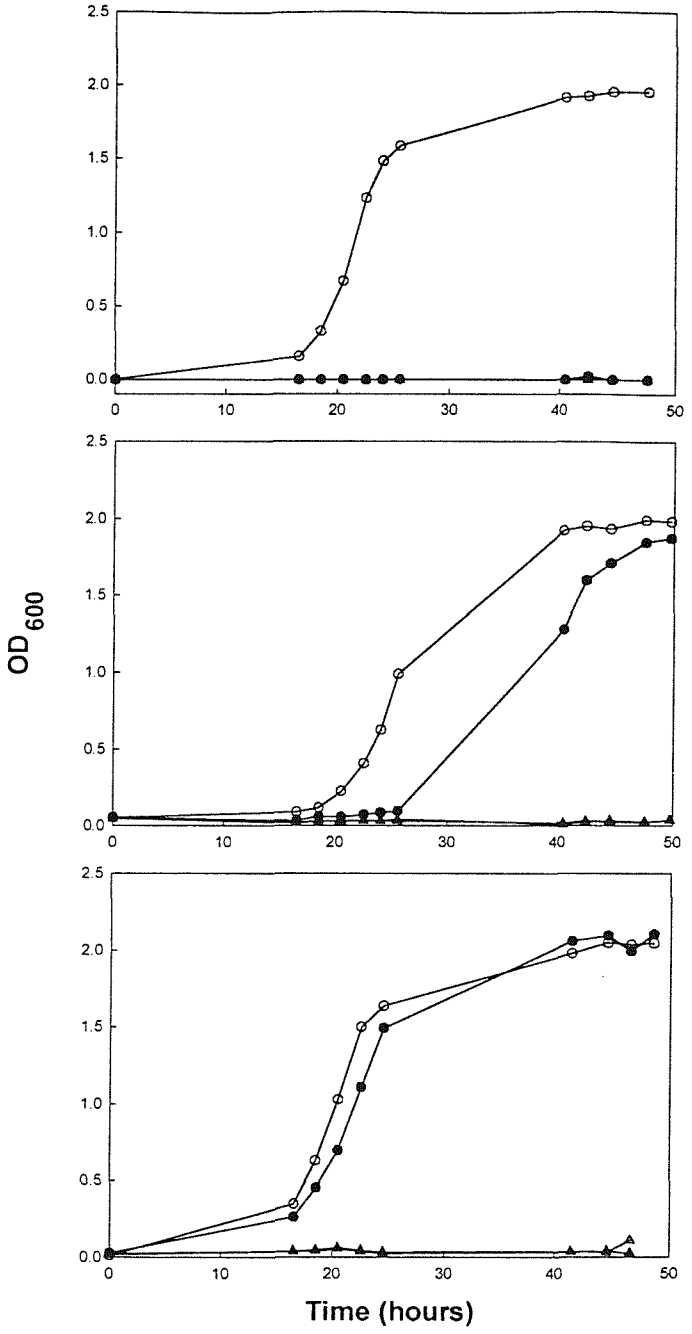

Figure 6.13. The effect of nonylphenol on yeast growth

Shown are OD measured at 600 nm as a function of time. Graph (A) shows growth of untransformed K616 in the presence of uracil, graph (B) shows growth of K616 SERCA1b and graph (C) shows growth of K616 HVSERCA. The transformed yeast were grown in the absence of uracil. Growth is shown in the presence of: (o) 10 mM $CaCl_2$; (●) 10 mM EGTA; (Δ) 10 mM $CaCl_2$ and 25 μM nonylphenol; (▲) 10 mM EGTA and 25 μM nonylphenol.

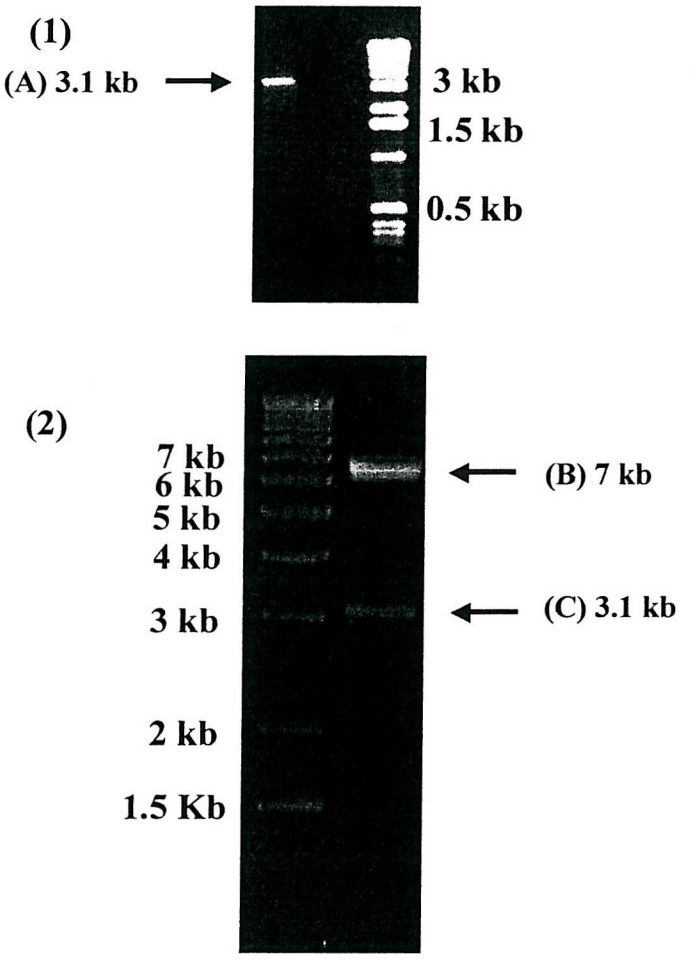

Figure 6.14. Diagnostic agarose gels of HVSERCA and a restriction analysis.
Band (A) on gel (1) shows the DNA PCR product of HVSERCA. Gel (2): Products from the double digest of the ligated product Y18HVSERCA. Band (B) is the Y18 vector and band (C) is the HVSERCA insert.

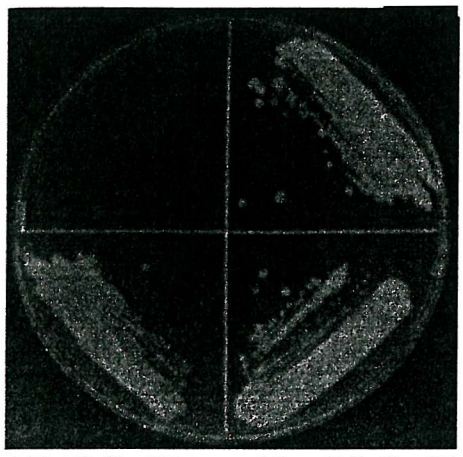

(A) SC - Ura + 10 mM $CaCl_2$

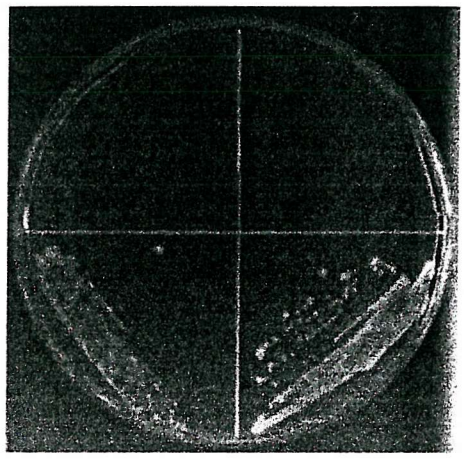

(B) SC - Ura + 10 mM EGTA

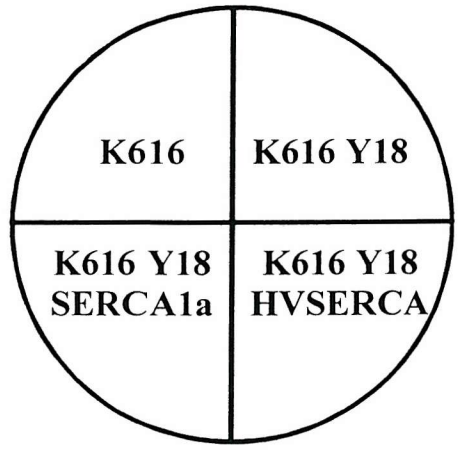

Figure 6.15. Growth analysis of yeast

Plate (A) shows growth of Yeast on SC-Ura, pH 6.2, + 10 mM $CaCl_2$. Plate (B) shows growth of Yeast on SC-Ura, pH 6.2, + 10 mM EGTA. Indicated are untransformed K616, K616 Y18 and K616 yeast expressing the Ca^{2+}-ATPase pumps, SERCA1a and K616 HVSERCA in the plasmid Y18.

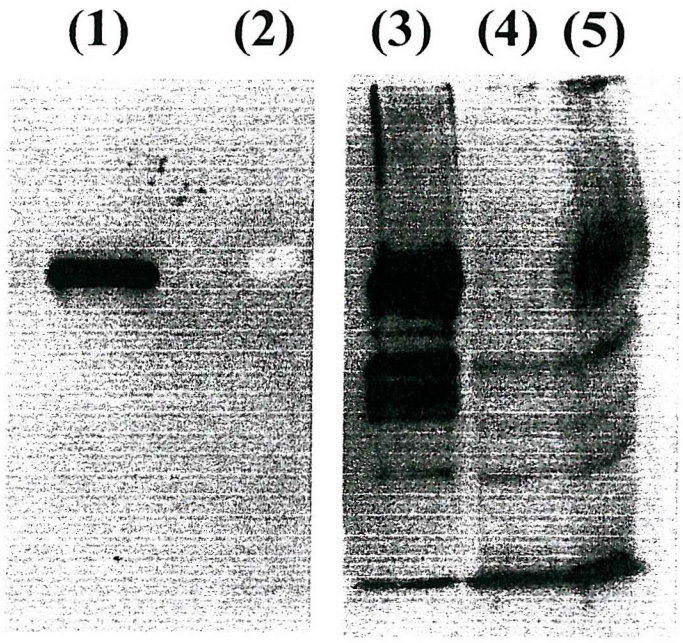

Figure 6.16. Western blot of SR vesicles and yeast microsomes.

A 7.5% SDS gel was transferred onto nitrocellulose. After blocking with BSA the nitrocellulose was probed with antibodies. The primary antibody used was Y1F4 (1:10 dilution), and the secondary antibody, a goat anti-mouse HRP conjugated antibody (Sigma 1:80 000). Lane (1) 100 ng SR; Lane (2) 10 μg untransformed K616 microsomes; Lane (3) 10 μg K616 Y18SERCA1a microsomes; Lane (4) 100 μg K616 p426SERCA1b microsomes; Lane (5) 250 μg K616 p426SERCA1b microsomes. An enhanced chemiluminescence kit (Amersham) was used for detection.

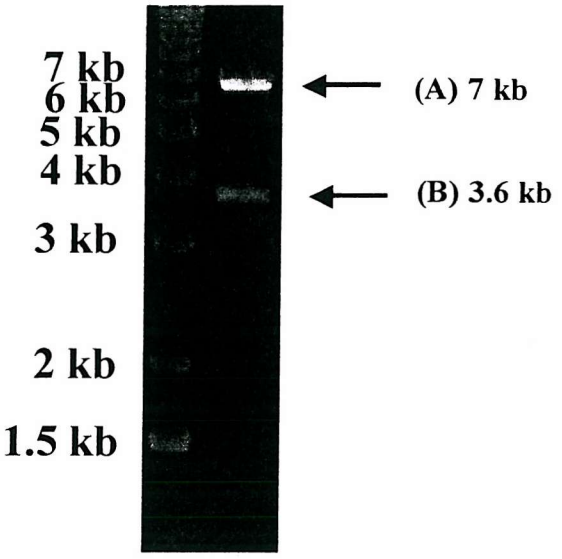

Figure 6.17. Diagnostic agarose gel of the Y18 SERCA-GFP restriction analysis
Products from the double digest of the ligated product Y18 SERCA-GFP, with Nhe1 and Pme1. Band (A) is the Y18 vector and band (B) is the SERCA-GFP insert.

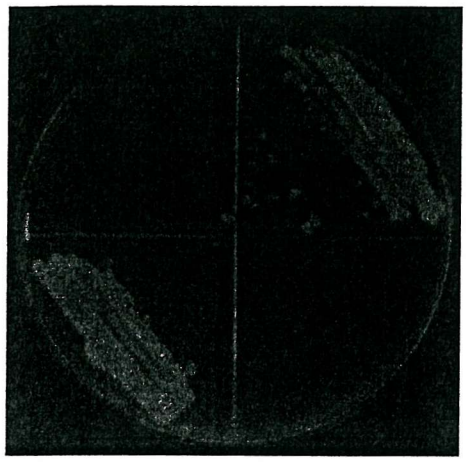

(A) SC - Ura + 10 mM $CaCl_2$

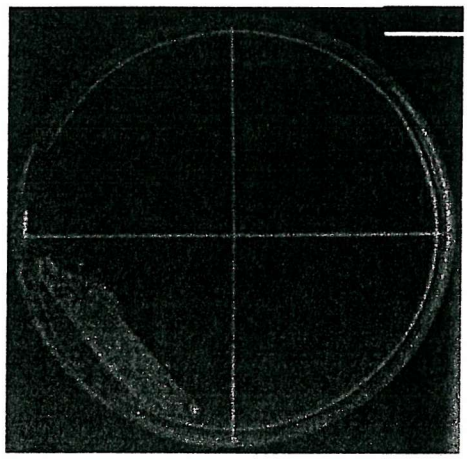

(B) SC - Ura + 10 mM EGTA

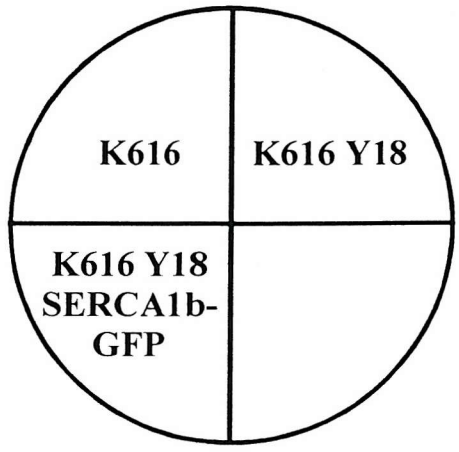

Figure 6.18. Growth analysis of yeast

Plate (A) shows growth of Yeast on SC-Ura, pH 6.2, + 10 mM $CaCl_2$. Plate (B) shows growth of Yeast on SC-Ura, pH 6.2, + 10 mM EGTA. Indicated are untransformed K616, K616 Y18 and K616 yeast expressing the Ca^{2+}-ATPase SERCA-GFP construct in the plasmid Y18.

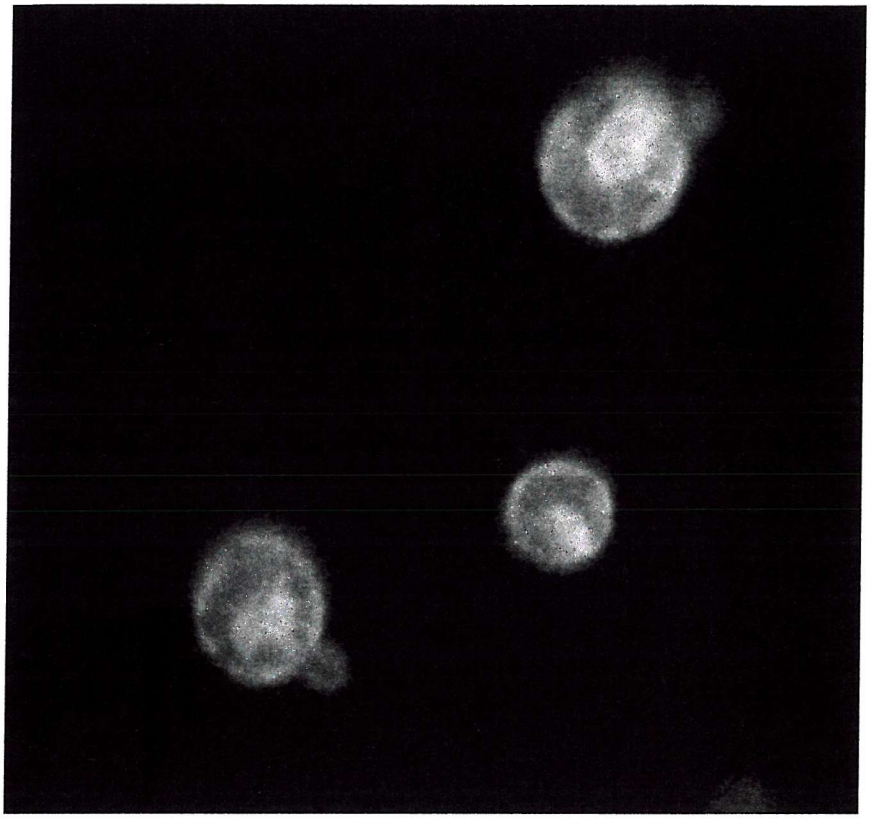

Figure 6.19. K616 yeast cells expressing Y18 SERCA-GFP

Yeast cells were washed with sterile water and mounted onto a glass slide. The cells were then visualised using the confocal microscope. GFP fluorescence can be seen in a large internal organelle and on the cell periphery.

Figure 6.20. Sequence comparison of SERCA1b and HVSERCA cDNA

Shown are the sequences of SERCA1b and HVSERCA from residue number 224 to 288, using the standard one letter abbreviation. The non-conserved residues are shown in red. Phe-256 (F) is thought to be important for binding of thapsigargin and is present in both sequences.

Chapter Seven: Conclusions

The P-type ATPases are a large family of pumps that are involved in the active transport of ions across membranes. They achieve this by utilising the chemical energy acquired from the hydrolysis of the terminal phosphate of ATP. A phosphoryl-aspartyl intermediate of the enzyme is formed after the binding of two calcium ions and ATP during the catalytic cycle, and is subsequently broken down (Moller *et al.*, 1996). It is the conformational change between the E1 and E2 states that is responsible for the active transport of ions (Jencks, 1989). A pair of high affinity cytoplasmic calcium binding sites and a pair of lumenal sites are available for calcium binding in the E1 conformation. Upon phosphorylation the cytoplasmic pair of transport sites transform into low affinity sites exposed to the lumen and calcium is released into the lumen.

These pumps have been grouped into five distinct sets based on analysis of core sequences and according to their substrate specificity as shown in Table 1.1(Axelsen & Palmgren, 1998). The Ca^{2+}-ATPases form group II. The sarco(endo)plasmic reticulum ATPases (SERCAs) belong to subgroup IIA and these function to concentrate calcium in reticular stores from where it is mobilised when required for cell signalling purposes. The SR Ca^{2+}-ATPase is an asymmetrically orientated membrane protein resident in the SR. It is composed of a single 110 kDa polypeptide chain (MacLennan, 1970; Andersen, 1989), with most of the cellular mass on the cytoplasmic side of the membrane. This Ca^{2+}-ATPase was first isolated from skeletal muscle in 1970 by MacLennan (MacLennan, 1970). Since the publication of the sequence of SERCA in 1985 (MacLennan *et al.*, 1985) functional studies, site directed mutagenesis and chemical derivitisation procedures have been used to obtain a variety of information as regards the relationship between structure and function, with respect to calcium binding and translocation. Publication of the 2.6 Å structure in 2000 (Toyoshima *et al.*, 2000) has finally permitted verification and analysis of these studies in light of the crystal structure.

Many compounds inhibit Ca^{2+}-ATPase function but the sites to which they bind are largely unknown. The presence of a single inhibitor binding site with competition for binding of inhibitors could be possible. On the other hand multiple binding sites could exist, that are different for each inhibitor. The experiments in Chapter 3 have shown that inhibition by curcumin is structurally specific.

Bisdesmethoxycurcumin inhibits ATPase activity with the same potency as curcumin (Figure 3.6), showing that the methoxy groups that flank the –OH groups in curcumin are not essential for activity. However, switching the methoxy and the -OH groups, as in compound 5, renders this compound inactive. The importance of -OH groups has also been demonstrated using the compounds deoxytrilobilide and acetyl BHQ (Wictome *et al.*, 1994). Curcumin analogues in which the –OH groups were absent (analogues 2 and 4, Figure 3.8) were unable to inhibit the ATPase highlighting the importance of these groups. Thus the presence of two –OH groups in the right position are essential for inhibitory activity on the Ca^{2+}-ATPase yet the separations between these positions is very different in the different inhibitors. This suggests that all the inhibitors do not bind to the same site on the ATPase. As would be expected from their similar structures BHQ and PHQ compete for binding (Figure 3.13), therefore interacting at the same inhibitory site. In contrast the presence of BHQ actually increases the affinity of the ATPase for curcumin and *vice versa* (Figures 3.6 and 3.11; Table 3.3). Hence, the results in Chapter 3 clearly show that curcumin and BHQ must bind to separate sites on the ATPase. Similar effects were observed with mixtures of BHT, ellagic acid, DES and nonylphenol. Ellagic acid also increases the affinity of the ATPase for curcumin but the presence of 3 μM curcumin had no effect on the apparent affinity for diethylstilbestrol (Table 3.1 and Figure 3.16). This shows that curcumin and diethylstilbestrol must bind to separate sites on the ATPase with the affinity for curcumin being the same for diethylstilbestrol-bound and free ATPase. An increase in affinity for one inhibitor on binding a second inhibitor is consistent with the previous proposal (Wictome *et al.*, 1995) that inhibitors bind to the E1 and E2 conformations of the ATPase with equal affinity but that binding to E2 leads to a conformation change to a new state $E2^{A}I$ ($E2 + I \leftrightarrow E2I \leftrightarrow E2^{A}I$). In terms of this model $E2^{A}I$ would have a higher affinity for the second inhibitor than E2. It is likely that the inhibitors bind in the transmembrane region of the ATPase, due to their hydrophobicity. Residue Phe-256 has been shown to be important in binding thapsigargin (Yu *et al.*, 1998; Ma *et al.*, 1999). Whether other inhibitors bind in the same region or not is unknown. Inhibitors that are less specific than the sesquiterpene lactones may bind to more than one site on the ATPase. This may account for the stimulation observed at low concentrations for some of the compounds studied.

An active Ca^{2+}-ATPase resident in the ER is required to counterbalance the normal leak of calcium out of the ER in unstimulated cells. It was shown in Chapter 4 that addition of Tb and BHQ to QT-6 cells produces a characteristic increase in cytosolic calcium levels. This is due to indirect depletion of cellular stores mediated by inhibition of the reloading mechanism, i.e. the Ca^{2+}-ATPase. Tb induced calcium release was shown to be from the ER using Mn^{2+}. This ion is able to enter the cell across the plasma membrane and quench the calcium indicator calcium crimson. Thus any increases in cytosolic calcium measured by the fluorescence of the dye must be indicative of calcium release from internal stores; following incubation with Mn^{2+}, addition of Tb did indeed result in an increase in calcium crimson fluorescence (Figure 4.6). Furthermore, using XeC as an inhibitor of the IP_3R the pathway calcium leak from the ER (induced by Tb) was shown to be via this IP_3 sensitive calcium channel (Figure 4.3), in agreement with Gafni *et al.* (Gafni *et al.*, 1997). Unexpectedly curcumin, although an inhibitor of ATPase, did not produce the characteristic increase in cytosolic calcium levels. In fact the cytosolic levels of calcium in these resting cells actually decreased on addition of curcumin (Figure 4.3) and moreover curcumin blocked the effect of Tb and BHQ (Figure 4.7). Since the effect of curcumin was the same as XeC (Figure 4.3) it is likely that curcumin blocks the IP_3R. It is noticeable that the structural specificity of the effects of curcumin analogues on the Ca^{2+}-ATPase and the IP_3R are different as curcumin analogue 3 (Figure 4.8) and 5 (data not shown) appear to inhibit the IP_3R, but not Ca^{2+}-ATPase (Section 3.3.2). A further effect of curcumin was shown in studies of the effects of curcumin on accumulation of calcium by SR vesicles (Figure 4.10). BHQ as expected as a typical inhibitor of Ca^{2+}-ATPase activity, decreased the level of calcium uptake by SR vesicles (Figure 4.9). Curcumin however gave an unexpected result, actually increasing the rate of calcium accumulation by SR vesicles (Figure 4.10). This may be explained by either an increase in the uptake rate of calcium into the vesicle by the Ca^{2+}-ATPase or by a decrease in the leak rate in the presence of curcumin. Leak of calcium out of the SR vesicles could be through a channel present in the membrane or through the Ca^{2+}-ATPase itself. By ensuring that other channels are not present in the SR fraction the effect of curcumin on leak through the ATPase was studied (Chapter 4). Leak through the ATPase can be due to passive leak down the concentration gradient or slippage, a process in which calcium is released to the cytosol from the phosphorylated enzyme intermediate, rather than to the lumen of the

SR. Oxalate and P_i can be used to prevent passive leak, but in the presence of oxalate or P_i curcumin still increased calcium uptake (Figure 4.19). Thus the effect of curcumin was shown to be an uncoupling effect, i.e. slippage. Evidence for such a pathway already exists; uptake of calcium by SR vesicles is followed by spontaneous release of some accumulated calcium, even in the presence of ATP and external calcium, conditions under which simple passive leak is inhibited (Inesi & de Meis, 1989; Yu & Inesi, 1995; McWhirter *et al.*, 1987b). The actual time dependencies for passive leak and slippage can be shown to be very different and using simulations of calcium uptake, the uptake in the presence of curcumin was found to match that expected for slippage (Figure 4.9). Thus, curcumin was found to be a novel inhibitor of SERCA, also blocking the IP_3R in ER and decreasing slippage on the Ca^{2-}-ATPase in SR vesicles.

Lockyer (Lockyer *et al.*, 1998) successfully cloned the cDNA of the *Heliothis virescens* insect Ca^{2+}-ATPase (HVSERCA) but did not achieve high-level expression of the pump in Cos-7 cells. The results in Chapter 5 show that the construction of a chimera between SERCA and HVSERCA successfully increased the expression of HVSERCA in Cos-7 cells. Moreover, by introducing the N terminus of SERCA an epitope was introduced which permitted detection of expression levels of the insect pump using a specific antibody. The cDNA of GFP was linked onto the end of the SERCA cDNA sequence and was translated along with SERCA, producing a pump with GFP tagged onto it. This provided a way of directly monitoring SERCA expression in both Cos-7 cells (Figure 5.15) and yeast cells (Figure 6.19), abolishing the need for indirect immunological methods.

Ca^{2+}-ATPase pumps have conserved sequences (Figure 1.6) yet compounds such as the sesquiterpene lactones are specific SERCA inhibitors (Section 3.1.2.). This highlights the possibility of finding an inhibitor that would for example inhibit an insect calcium pump, but not a mammalian pump, which although they share sequence homologies have 30 % of their sequences different. Due to the low levels of expression of HVSERCA in Cos-7 cells inhibitor studies were not previously possible (Lockyer, 1997). Complementation of yeast growth by the expression of heterologous proteins is an ideal system for overexpression of a protein of interest (Chapter 6). The two calcium pumps in *S.cerevisiae* (Pmc1p and Pmr1p) are not expressed in the mutated yeast strain K616 and hence K616 is unable to grow in low calcium conditions. It has been shown previously that expression of Ca^{2+}-ATPases

can complement K616 by contributing towards calcium sequestration into internal stores, sustaining growth (Talla *et al.*, 1998; Liang *et al.*, 1997; Centeno *et al.*, 1994; Degand *et al.*, 1999). Expression of both SERCA and HVSERCA in K616 has been shown in low calcium conditions (Figures 6.8 and 6.9) and is thus a direct indication of expression. This is the first evidence to show that HVSERCA is a functional Ca^{2+}-ATPase. This system provides a simple way to monitor expression of the required protein since in the absence of expression there will be no growth. As the growth in low calcium media is due to complementation by the Ca^{2+}-ATPases, yeast expressing Ca^{2+}-ATPases are a possible system with which to test the effectiveness of a range of Ca^{2+}-ATPase inhibitors. Over-expression of functional ATPase from *H.virescens* in K616 has permitted the first comparative inhibitor studies with SERCA (Figures 6.11, 6.12 and 6.13). The results verify that trilobilide and BHQ both inhibit SERCA. BHQ inhibits growth of K616 expressing HVSERCA but trilobilide has no effect. Thus trilobilide is specific for SERCA. Expression in yeast therefore produces functional SERCA and HVSERCA pumps and additionally permits comparative functional inhibitor studies of these two Ca^{2+}-ATPases.

Appendix One

1. Subroutine necessary for use of the 'two site' model in Sigma Plot

[Variables]	[Constraints]	[Parameters]
x=col(1)	rate2>0	rate2=2
y=col(2)	K2>0	K2=10
	K3>0	K3=0.02

[Equations]

rate1=1

K1=500

et=0.04

b=et+x+(1/K1)

con1=(b*b)-(4*et*x)

con2=(b-(sqrt(con1)))/2

ratestim=(((et-con2)*rate1)+(con2*rate2))/et

ratein=(1/(1+K2*x))+(K3*K2*x)/(1+K2*x)

f=ratestim*ratein

fit f to y

2. Subroutine necessary for use of the 'n site' model in Sigma Plot

[Variables]	[Constraints]	[Parameters]
x=col(1)	K1>0	K1=1
y=col(2)	rate2>0	rate2=1.5
	K2>0	K2=0.9
	n>0	n=3.0

[Equations]

rate1=1

et=0.04

b=et+x+(1/K1)

con1=(b*b)-(4*et*x)

con2=(b-(sqrt(con1)))/2

ratestim=(((et-con2)*rate1)+(con2*rate2))/et

ratein=(1/(1+(K2)*(x)^n))

f=ratestim*ratein

fit f to y

Appendix Two

The oligonucleotides were used for PCR and sequencing.

Name	Sense	Sequence
GFPClaPmea	-	CATCATGTTTAAACATCGATTTACTTG TACAGCTCGTCC
GFPXho1a	-	TGATGACTCGAGTTACTTGTACAGCTC GTC
GFPXhos	+	ATGATGCTCGAGGAACAAAAGCTGAT CTCTG
HV1235s	+	AGATGTCTGTTTCCCGTATG
HV1650s	+	CACACCCCTTAAGCCTTCCC
HV1995s	+	TTGCCGCGCTGCTGGTATCC
HV2200a	-	CGGGTTCCACGCGGGAGAAC
HV3190s	+	TCCATGAACACTCATTGT
HV3292a	-	CTCGAGCGGGGGTGCCGTCCGAAC
HVKpns1bs	+	ACATGCTTTTCTCGGGTACCAATGTCG CCGCCGG
HVNheBams	+	ATGATGGCTAGCGGATCCACCATGGA GGACGCTCACTC
HVXhoa	-	GTGTGCGCTCGAGCGGGGGTGCC
HVXhoPmea	-	CATCATGTTTAAACCTCGAGCGGGGG TGCCGTCCGAAC
HVXhoPmeNSa	-	CATCATGTTTAAACCTCGAGCAGCTTC CACGTCGGCTGGG
S1b115a	-	TGGCCGTATTTCTCTAGATG
S1b450s	+	GGACATCGTCCCCGGGGGAC
S1bAflIIs	+	GATGCCCCTGCCCTTAAGAAGGCCGA G
S1b AflIIa	-	CTACGGGGACGGGAATTCTTCCGGCT C
S1bKpnHVa	-	CCGGCGGCGACATTGGTACCCGAGAA AAGCATGT
S1bNhe1s	+	GATGATGCTAGCGAATTCGAGCTCCC GGG
Y18EcoNhes	+	AATTCCGAATTCGCTAGCGGAGGCCG CGCACTCCAAGAGC
Y18SacPmea	-	CATCATGAGCTCGTTTAAAACGGGCA GGCTCCTCACGATGGCG

Reference List

Adamo, H.P., Grimaldi, M.E. & Arguinzonis, M.I.G. (2000) Biochemistry **39**, 14893-14899

Adams, P., East, J.M., Lee, A.G. & O'Connor, C.D. (1998) Biochem.J. **335**, 131-138

Allen, G., Trinnaman, B.J. & Green, N.M. (1980) Biochem.J. **187**, 591-616

Alvarez, J., Montero, M. & Garcia-Sancho, J. (1991) Biochem.J. **274**, 193-197

Alves, E.W. & de Meis, L. (1986) J.Biol.Chem. **261**, 16854-16859

Andersen, J.P. (1989) Biochim.Biophys.Acta **988**, 47-72

Andersen, J.P. (1995a) Biosci.Rep. **15**, 243-261

Andersen, J.P. (1995b) J.Biol.Chem. **270**, 908-914

Andersen, J.P., Moller, J.V. & Jorgensen, P.L. (1982) J.Biol.Chem. **257**, 8300-8307

Andersen, J.P. & Vilsen, B. (1994) J.Biol.Chem. **269**, 15931-15936

Andersen, J.P. & Vilsen, B. (1995) FEBS Lett. **359**, 101-106

Andersen, J.P., Vilsen, B., Collins, J.H. & Jorgensen, P.L. (1986) J.Membr.Biol. **93**, 85-92

Andreason, G.L. & Evans, G.A. (1988) BioTechniques **6**, 650-660

Antebi, A. & Fink, G.R. (1992) Mol.Biol.Cell **3**, 633-654

Antoniu, B., Kim, D.H., Morii, M. & Ikemoto, N. (1985) Biochim.Biophys.Acta **816**, 9-17

Aravind, L., Galperin, M.Y. & Koonin, E.V. (1998) Trends in Biochem.Sci. **23**, 127-129

Axelsen, K.B. & Palmgren, M.G. (1998) J.Mol.Evol. **46**, 84-101

Baker, K.J., East, J.M. & Lee, A.G. (1994) Biochim.Biophys.Acta **1192**, 53-60

Beeler, T., Gable, K., Zhao, C. & Dunn, T. (1994) J.Biol.Chem. **269**, 7279-7284

Beguin, P., Beggah, A.T., Chibalin, A.V., Burgener-Kairuz, P., Jaisser, F., Matthews, P.M., Rossier, B.C., Cotecchia, S. & Geering, K. (1994) J.Biol.Chem. **269**, 24437-24445

Berridge, M.J. (1993) Nature **361**, 315-325

Berridge, M.J. (1995) Biochem.J. **312**, 1-11

Berridge, M.J., Bootman, M.D. & Lipp, P. (1998) Nature **395**, 645-648

Bezprozvanny, I. & Ehrlich, B.E. (1993) Neuron **10**, 1175-1184

Bezprozvanny, I., Watras, J. & Ehrlich, B.E. (1991) Nature **351**, 751-754

Bezprozvanny, I.B., Ondrias, K., Kaftan, E., Stoyanovsky, D.A. & Ehrlich, B.E. (1993) Mol.Biol.Cell **4**, 347-352

Bigelow, D.J. & Inesi, G. (1992) Biochim.Biophys.Acta **1113**, 323-338

Bigelow, D.J. & Thomas, D.D. (1987) J.Biol.Chem. **262**, 13449-13456

Black, J.P.J. (1999) PhD Thesis, University of Southampton.

Blostein, R., Zhang, R.P., Gottardi, C.J. & Caplan, M.J. (1993) J.Biol.Chem. **268**, 10654-10658

Bonifacino, J.S., Klausner, R.D. & Shah, N. (1991) EMBO J. **10**, 2783-2793

Bonifacino, J.S., Suzuki, C.K. & Klausner, R.D. (1990) Science **247**, 79-82

Botti, R.E. & Ratnoff, O.D. (1964) J.Lab.Clin.Med. **64**, 385-398

Brandl, C.J., Green, N.M., Korczak, B. & MacLennan, D.H. (1986) Cell **44**, 597-607

Brini, M. & Carafoli, E. (2000) Cell.Mol.Life Sci. **57**, 354-370

Burk, S.E., Lytton, J., MacLennan, D.H. & Shull, G.E. (1989) J.Biol.Chem. **264**, 18561-18568

Cameron, A.M., Steiner, J.P., Roskams, J., Ali, S.M., Ronnett, G.V. & Snyder, S.H. (1995) Cell **83**, 463-472

Campbell, A.M., Kessler, P.D., Sagara, Y., Inesi, G. & Fambrough, D.M. (1991) J.Biol.Chem. **266**, 16050-16055

Cao, C.J., Lockwich, T., Scott, T.L., Blumenthal, R. & Shamoo, A.E. (1991) Mol.Cell.Biochem. **103**, 97-111

Carafoli, E. (1994) FASEB J. **8**, 993-1002

Carafoli, E., Garcia, M.E. & Guerini, D. (1996) Experimenta **52**, 1091-1100

Catty, P., de Kerchove d'Exaerde, A. & Goffeau, A. (1997) FEBS Lett. **409**, 325-332

Centeno, F., Deschamps, S., Lompre, A.M., Anger, M., Moutin, M.J., Dupont, Y., Palmgren, M.G., Villalba, J.M., Moller, J.V., Falson, P. & Lemaire, M. (1994) FEBS Lett. **354**, 117-122

Champeil, P., Menguy, T., Soulié, S., Juul, B., Gomez de Gracia, A., Rusconi, F., Falson, P., Denray, L., Henao, F., Lé Maire, M. & Møller, J.V. (1998) Journal of Biological Chemistry **273**, 6619-6631

Chen, S.R.W., Zhang, L. & MacLennan, D.H. (1993) J.Biol.Chem. **268**, 13414-13421

Christensen, S.B., Larsen, I.K. & Rasmussen, U. (1982) J.Org.Chem. **47**, 649-652

Clapham, D.E. (1995) Cell **80**, 259-268

Clapper, D.L., Walseth, T.F., Dargie, P.J. & Lee, H.C. (1987) J.Biol.Chem. **262**, 9561-9568

Clarke, D.M., Loo, T.W., Inesi, G. & MacLennan, D.H. (1989) Nature **339**, 476-478

Clarke, D.M., Loo, T.W. & MacLennan, D.H. (1990) J.Biol.Chem. **265**, 6262-6267

Clarke, D.M., Loo, T.W. & MacLennan, D.H. (1990) J.Biol.Chem. **265**, 17405-17408

Clarke, D.M., Maruyama, K., Loo, T.W., Leberer, E., Inesi, G. & MacLennan, D.H. (1989) J.Biol.Chem. **264**, 11246-11251

Colyer, J., Mata, A.M., Lee, A.G. & East, J.M. (1989) Biochem.J. **262**, 439-447

Corbett, E.F. & Michalak, M. (2000) TIBS **25** , 307-311

Corbett, E.F., Oikawa, K., Francois, P., Tessier, D.C., Kay, C., Bergeron, J.J.M., Thomas, D.Y., Krause, K.H. & Michalak, M. (1999) J.Biol.Chem. **274**, 6203-6211

Csutora, P., Su, Z., Kim, H.Y., Bugrim, A., Cunningham, K.W., Nuccitelli, R., Keizer, J.E., Hanley, M.R., Blalock, J.E. & Marchase, R.B. (1999) Proc.Natl.Acad.Sci.USA **96**, 121-126

Cunningham, K.W. & Fink, G.R. (1994a) J.Exp.Biol. **196**, 157-166

Cunningham, K.W. & Fink, G.R. (1994b) J.Cell Biol. **124**, 351-363

Cunningham, K.W. & Fink, G.R. (1996) Mol.Cell.Biol. **16**, 2226-2237

Cyert, M.S., Kunisawa, R., Kaim, D. & Thorner, J. (1991) Proc.Natl.Acad.Sci.USA **88**, 7376-7380

Daiho, T., Kubota, T. & Kanazawa, T. (1993) Biochemistry **32**, 10021-10026

Daiho, T., Yamasaki, K., Suzuki, H., Saino, T. & Kanazawa, T. (1999) J.Biol.Chem. **274**, 23910-23915

Dalton, K.A. (1998) PhD Thesis, University of Southampton.

Dalton, K.A., East, J.M., Mall, S., Oliver, S., Starling, A.P. & Lee, A.G. (1998) Biochem.J. **329**, 637-646

Dalton, K.A., Mall, S., Pilot, J.D., East, J.M. & Lee, A.G. (1998) Biochem.Soc.Trans. **26**, S234-S234

Dalton, K.A., Pilot, J.D., Mall, S., East, J.M. & Lee, A.G. (1999) Biochem.J. **342**, 431-438

Dasso, L.L. & Taylor, C.W. (1991) Biochem.J. **280**, 791-795

Daston, G.P., Gooch, J.W., Breslin, W.J., Shuey, D.L., Nikiforov, A.I., Fico, T.A. & Gorsuch, J.W. (1997) Repro.Toxicol. **11** , 465-481

Davidson, G.A. & Varhol, R.J. (1995) J.Biol.Chem. **270**, 11731-11734

Davis, T.N., Urdea, M.S., Masiarz, F.R. & Thorner, J. (1986) Cell **47**, 423-431

de Meis,L. (1981) The Sarcoplasmic Reticulum Wiley New York

de Meis, L. (1991) J.Biol.Chem. **266**, 5736-5742

de Meis, L. & Vianna, A.L. (1979) Ann.Rev.Biochem. **48**, 275-292

De Smet, P., Parys, J.B., Callewaert, G., Weidema, A.F., Hill, E., de Smedt, H., Erneux, C., Sorrentino, V. & Missiaen, L. (1999) Cell Calcium **26**, 9-13

Degand, I., Catty, P., Talla, E., Goffeau, A., de Kerchove d'Exaerde, A. & Ghislain, M. (1999) Mol.Microbiol. **31**, 545-556

Delong, L.J. & Blasie, J.K. (1993) Biophys.J. **64**, 1750-1759

Dodds, E.C., Goldberg, L., Lawson, W. & Robinson, R. (1938) Nature **141**, 247-248

Dode, L., De Greef, C., Mountian, I., Attard, M., Town, M.M., Casteels, R. & Wuytack, F. (1998) J.Biol.Chem. **273**, 13982-13994

Dode, L., Wuytack, F., Kools, P.F.J., Baba-Aissa, F., Raeymaekers, L., Brik, F., Van de Ven, W.J.M. & Casteels, R. (1996) Biochem.J. **318**, 689-699

Dohmen, R.J. (1991) Yeast 7, 691-692

Dower, W.J., Miller, J.F. & Ragsdale, C.W. (1988) Nucleic.Acids.Res. **16**, 6127-6145

Doyle, D.A., Cabral, J.M., Pfuetzner, R.A., Kuo, A., Gulbis, J.M., Cohen, S.L., Chait, B.T. & MacKinnon, R. (1998) Science **280**, 69-77

Duggan, P.F. & Martonosi, A. (1970) J.Gen.Physiol. **56**, 147-167

Dunbar, L.A., Aronson, P. & Caplan, M.J. (2000) J.Cell Biol. **148**, 769-778

Dunn, T., Gable, K. & Beeler, T. (1994) J.Biol.Chem. **269**, 7273-7278

East, J.M. & Lee, A.G. (1982) Biochemistry **21**, 4144-4151

East, J.M., Matthews, I., Tunwell, R.E.A., Mata, A.M. & Lee, A.G. (1992) Biochem.Soc.Trans. **20**, 550-554

Ebashi, S. (1991) Ann.Rev.Physiol. **53**, 1-16

Ehrlich, B.E., Kaftan, E., Bezprozvanny, A.S. & Bezprozvanny, I. (1994) TIPS **15**, 145-149

Elzen, G.W., Leonard, B.R., Graves, J.B., Burris, E. & Micinski, S. (1992) J.Econ.Ent. **85**, 2064-2072

Endo, M. (1985) Curr.Top.Memb.Transp. **25**, 181-230

Fagan, M.J. & Saier, M.H. (1994) J.Mol.Evol. **38**, 57-99

Farber, F.E., Melnick, J.L. & Butel, J.S. (1975) Biochim.Biophys.Acta **390**, 298-311

Fasolato, C., Innocenti, B. & Pozzan, T. (1994) TIPS **15**, 77-82

Felgner, P.L., Gadek, T.R., Holm, M., Roman, R., Chan, H.W., Wenz, M., Northrop, J.P., Ringold, G.M. & Danielsen, M. (1987) Proc.Natl.Acad.Sci.USA **84**, 7413-7417

Fersht,A. (1985) Enzyme structure and mechanism. W.H. Freeman, New York.

Fischer, M., Schnell, N., Chattaway, J., Davies, P., Dixon, G. & Sanders, D. (1997) FEBS Lett. **419**, 259-262

Fleischer, S., Ogunbunmi, E.M., Dixon, M.C. & Fleer, E.A.M. (1985) Proc.Natl.Acad.Sci.USA **82**, 7256-7259

Flick, J.S. & Thorner, J. (1993) Mol.Cell.Biol. **13**, 5861-5876

Foletti, D., Guerini, D. & Carafoli, E. (1995) FASEB J. **9**, 670-680

François, J. & Hers, H.-G. (1988) Eur.J.Biochem. **174**, 561-567

Froud, R.J., Earl, C.R.A., East, J.M. & Lee, A.G. (1986a) Biochim.Biophys.Acta **860**, 354-360

Froud, R.J., East, J.M., Jones, O.T. & Lee, A.G. (1986b) Biochemistry **25**, 7544-7552

Furuya, Y., Lundmo, P., Short, A.D., Gill, D.L. & Isaacs, J.T. (1994) Cancer Res. **54**, 6167-6175

Futcher, A.B. (1988) Yeast **4**, 27-40

Gafni, J., Munsch, J.A., Lam, T.H., Catlin, M.C., Costa, L.G., Molinski, T.F. & Pessah, I. (1997) Neuron **19**, 723-733

Galione, A. (1992) Trends in Pharmacol.Sci. **13**, 304-306

Galione, A. & White, A. (1994) TICB **4**, 431-436

Ghosh, T.K., Bian, J., Short, A.D., Rybak, S.L. & Gill, D.L. (1991) J.Biol.Chem. **266**, 24690-14697

Ghosh, T.K., Eis, P.S., Mullaney, J.M., Ebert, C.L. & Gill, D.L. (1988) J.Biol.Chem. **263**, 11075-11079

Giband, M. (1998) Phytoprotec. **79**, 121-126

Gluzman, Y. (1981) Cell **23**, 175-182

Goodey, A.R., Doel, S.M., Piggott, J.R., Watson, M.E.E., Zealey, G.R., Cafferkey, R. & Carter, B.L.A. (1986) Mol.Gen.Genet. **204**, 505-511

Gould, G.W., Colyer, J., East, J.M. & Lee, A.G. (1987b) J.Biol.Chem. **262**, 7676-7679

Gould, G.W., McWhirter, J.M., East, J.M. & Lee, A.G. (1987a) Biochim.Biophys.Acta **904**, 45-54

Graham, R.L. & van der Erb, A.J.A. (1973) Virology **52**, 456-467

Gray, K., Bullock, B., Dickson, R., Raszmann, K., McLachlan, J. & Merlino, G. (1997) Get.Breast Gyn.Cancers **369**, 217-231

Green, N.M. & Stokes, D.L. (1992) Acta Physiol.Scand. **146**, 59-68

Guerini, D., Garcia-Martin, E., Zecca, A., Guidi, F. & Carafoli, E. (1998) Acta Physiol.Scand. **163**, 265-273

Guo, W., Jorgensen, A.O. & Campbell, K.P. (1994) J.Biol.Chem. **269**, 28359-28365

Gustin, M.C., Zhou, X.-L., Martinac, B. & Kung, C. (1988) Science **242**, 762-765

Gutierrez-Merino, C., Munkonge, F., Mata, A.M., East, J.M., Levinson, B.L., Napier, R.M. & Lee, A.G. (1987) Biochim.Biophys.Acta **897**, 207-216

Hakii, H., Fujiki, H., Suganuma, M., Nakayasu, M., Tahira, T., Sugimura, T., Scheuer, P.J. & Christensen, S.B. (1986) J.Cancer.Res.Clin.Oncol. **111**, 177-181

Halachmi, D. & Eilam, Y. (1993) FEBS Lett. **316**, 73-78

Hallam, T.J. & Rink, T.J. (1985) FEBS Lett. **186**, 175-179

Hardie, R.C. & Minke, B. (1993) Trends in Neuro.Sci. **16**, 371-376

Hardwicke, P.M. & Green, N.M. (1974) Eur.J.Biochem. **42**, 183-193

Hasselbach, W. (1964) Prog.Biophys.Biophys.Chem. **14**, 169

Hasselbach, W. & Weber, H.H. (1974) Membrane proteins in transport and phosphorylation (Azzone, G.F., Klingenberg, M.E., Quagliariello, E. & Siliprandi, N., eds.) Amsterdam.

Heckel, D.G., Gahan, L.J., Daly, J.C. & Trowell, S. (1998) Phil.Trans.Roy.Soc.B **353**, 1713-1722

Heckel, D.G., Gahan, L.J., Gould, F., Daly, J.C. & Trowell, S. (1997) Pestic.Sci. **51**, 251-258

Henderson, I.M.J., Khan, Y.M., East, J.M. & Lee, A.G. (1994) Biochem.J. **297**, 615-624

Herskowitz, I. (1988) Microbiol.Rev. **52**, 536-553

Hirota, J., Michikawa, T., Miyawaki, A., Furuichi, T., Okura, I., Mikoshiba, K. (1995) J.Biol.Chem **270**, 19046-19051

Hitzeman, R., Hazie, F.E., Levine, H.L., Goeddel, D.V., Ammerer, G. & Hall, B.D. (1981) Nature **293**, 717-722

Holub, M., Samek, Z., de Groote, R., Herout, V. & Sorm, F. (1973) Collect.Czech.Chem.Comm. **38**, 1551-1562

Horikoshi, Y., Furuno, T., Teshima, R., Sawada, J.-I. & Nakanishi, M. (1994) Biochem.J. **304**, 57-60

Hu, Y.F. & Schilling, W.P. (1995) Biochem.J. **305**, 605-611

Hua, S. & Inesi, G. (1997) Biochemistry **36**, 11865-11872

Huang, M.T., Smart, R.C., Wong, G.Q. & Conney, A.H. (1988) Cancer Res. **48**, 5941-5946

Huang, S. & Squier, T.C. (1998) Biochemistry **37**, 18064-18073

Hughes, P.J., McLellan, H., Lowes, D.A., Khan, S.Z., Bilmen, J.G., Tovey, S.C., Godfrey, R.E., Michell, R.H., Kirk, C.J., Michelangeli, F. (2000) Biochim.Biophys.Res.Comm. **277**, 568-574

Hussain, A., Lewis, D., Sumbilla, C., Lai, L.C., Melera, P.W. & Inesi, G. (1992) Arch.Biochem.Biophys. **296**, 539-546

Iida, H., Nakamura, H., Ono, T., Okumura, M.S. & Anraku, Y. (1994) Mol.Cell.Biol. **14**, 8259-8271

Iida, H., Yagawa, Y. & Anraku, Y. (1990) J.Biol.Chem. **265**, 13391-13399

Inesi, G. & de Meis, L. (1989) J.Biol.Chem. **264**, 5929-5936

Inesi, G., Kurzmack, M., Coan, C. & Lewis, D.E. (1980) J.Biol.Chem. **255**, 3025-3031

Inesi, G., Kurzmack, M. & Verjovski-Almeida, S. (1978) Ann.N.Y.Acad.Sci. **307**, 224-227

Inesi, G., Nakamoto, R., Hymel, L. & Fleischer, S. (1983) J.Biol.Chem. **258**, 14804-14809

Irvine, R.F. (1990) FEBS Lett. **263**, 5-9

Irvine, R.F. (1992) FASEB J. **6**, 3085-3091

Ishii, T., Lemas, M.V. & Takeyasu, K. (1994) Proc.Natl.Acad.Sci.USA **91**, 6103-6107

Ives, E.B., Nichols, J., Wente, S.R. & York, J.D. (2000) J.Biol.Chem. **275**, 36575-36583

Jackson, M.R., Nilsson, T. & Peterson, P.A. (1990) EMBO J. **9**, 3153-3162

Jackson, M.R., Nilsson, T. & Peterson, P.A. (1993) J.Cell Biol. **121**, 317-333

Jencks, W.P. (1989) J.Biol.Chem. **264**, 18855-18858

Jencks, W.P., Yang, T., Peisach, D. & Myung, J. (1993) Biochemistry **32**, 7030-7034

Jiang, S., Chow, S.C., Nicotera, P. & Orrenius, S. (1994) Exp.Cell Res. **212**, 84-92

Jianjie, M. (1993) J.Gen.Physiol. **102**, 1031-1056

Jones, O.T. & Lee, A.G. (1986) Pestic.Biochem.Physiol. **25**, 420-430

Jorgensen, A.O., Kalnins, V.I., Zubrzycka, E. & MacLennan, D.H. (1977) J.Biol.Chem. **74**, 287-298

Joseph, S.K. (1996) Cell.Signal. **8**, 1-7

Kaneko, Y. & Tsukamoto, A. (1994) Cancer Lett. **79**, 147-155

Kargacin, G.J., Ali, Z. & Kargacin, M.E. (1998) Pflugers Arch.Eur.J.Physiol. **436**, 338-342

Khan, A.A., Steiner, J.P., Klein, M.G., Schneider, M.F. & Snyder, S.H. (1992) Science **257**, 815-818

Khan, Y.M., Wictome, M., East, J.M. & Lee, A.G. (1995) Biochemistry **34**, 14385-14393

Klaassen, C.H.W., Vanuem, T.J.F., Demoel, M.P., Swarts, H.G.P. & Depont, J.J.H.H.M. (1993) FEBS Lett. **329**, 277-282

Koenderink, J.B., Hermsen, H.P.H., Swarts, H.G.P., Willems, P.H.G.M. & De Pont, J.J.H.H.M. (2000) Proc.Natl.Acad.Sci.USA **97** , 11209-11214

Koster, J.C., Blanco, G., Mills, P.B. & Mercer, R.W. (1996) J.Biol.Chem. **271**, 2413-2421

Kreutzfeldt, C. & Witt, W. (1991) Biotechnology Handbook 4: *Saccharomyces* (Tuite, M.F. & Oliver, S.G., eds.) Plenum Publishing Corporation,

Kuno, M. & Gardner, P. (1987) Nature **326**, 301-304

Kuno, T., Tanaka, H., Mukai, H., Chang, C.-D., Hiraga, K., Miyakawa, T. & Tanaka, C. (1991) Biochem.Biophys.Res.Comm. **180**, 1159-1163

Kunze, I., Nilsson, C., Adler, K., Manteuffel, R., Horstmann, C. & Kunze, G. (1998) Biochim.Biophys.Acta **1395**, 329-344

Kuo, M.L., Huang, T.S. & Lin, J.K. (1996) Biochim.Biophys.Acta **1317**, 95-100

Kutschabsky, L., Kretschmer, R.G. & Ripperger, H. (1986) Cryst.Res.Technol. **21**, 627-633

Laemmli, U.K. (1970) Nature **227**, 680-685

Lau, K.M., LaSpina, M., Long, J. & Ho, S.M. (2000) Cancer Res. **60**, 3175-3182

Lawson, M.A. & Maxfield, F.R. (1995) Nature **377**, 75-79

Lee, A.G. (1998) Biochim.Biophys.Acta **1376**, 381-390

Lee, A.G., Dalton, K.A., Duggleby, R.C., East, J.M. & Starling, A.P. (1995) Biosci.Rep. **15**, 289-298

Leong, P. & MacLennan, D.H. (1998) J.Biol.Chem. **273**, 7791-7794

Leung, A.T., Kwan, C.Y. & Loh, T. (1994) Biochem.J. **302**, 87-94

Levin, D.E., Fields, O., Kunisawa, R., Bishop, J.M. & Thorner, J. (1990) Cell **62**, 213-224

Levy, D., Gulik, A., Bluzat, A. & Rigaud, J.L. (1992) Biochim.Biophys.Acta **1107**, 283-298

Levy, D., Seigneuret, M., Bluzat, A. & Rigaud, J.L. (1990) J.Biol.Chem. **265**, 19524-19534

Liang, F., Cunningham, K.W., Harper, J.F. & Sze, H. (1997) Proc.Natl.Acad.Sci.USA **94**, 1-6

Lieberman, D.N. & Mody, I. (1994) Nature **369**, 235-239

Liu, J., Farmer, J.D., Lane, W.S., Friedman, J. & Weissman, I. (1991) Cell **66**, 807-815

Liu, Y., Ishii, S., Tokai, M., Tsutsumi, H., Ohki, O., Akada, R., Tanaka, K., Tsuchiya, E., Fukui, S. & Miyakawa, T. (1991) Mol.Gen.Genet. **227**, 52-59

Llopis, J., Chow, S.B., Kass, G.E.N., Gahm, A. & Orrenius, S. (1991) Biochem.J. **277**, 553-556

Lockyer, P.J. (1997) PhD Thesis, University of Southampton.

Lockyer, P.J., Puente, E., Windass, J., Earley, F., East, J.M. & Lee, A.G. (1998) Biochim.Biophys.Acta **1369**, 14-18

Luckie, D.B., Boyd, K.L. & Takeyasu, K. (1991) FEBS Lett. **281**, 231-234

Luckie, D.B., Lemas, V., Boyd, K.L., Fambrough, D.M. & Takeyasu, K. (1992) Biophys.J. **62**, 220-227

Lutsenko, S. & Kaplan, J.H. (1995) Biochemistry **34**, 15607-15613

Lytton, J. & MacLennan, D.H. (1988) J.Biol.Chem. **263**, 15024-15031

Lytton, J., Westlin, M. & Hanley, M.R. (1991) J.Biol.Chem. **266**, 17067-17071

Ma, H., Zhong, L. & Inesi, G. (1999) Biochemistry **38**, 15522-15527

Ma, H.T., Patterson, R.L., van Rossum, D.B., Birnbaumer, L., Mikoshiba, K. & Gill, D.L. (2000) Science **287**, 1647-1651

Mackrill, J.J. (1999) Biochem.J. **337**, 345-361

MacLennan, D.H. (1970) J.Biol.Chem. **245**, 4508-4518

MacLennan, D.H., Brandl, C.J., Korczak, B. & Green, N.M. (1985) Nature **316**, 696-700

Magyar, A. & Varadi, A. (1990) Biochem.Biophys.Res.Comm. **173**, 872-877

Martinez-Azorin, F., Teruel, J.A., Fernandez-Belda, F. & Gomez-Fernandez, J.C. (1992) J.Biol.Chem. **267**, 11923-11929

Maruyama, K., Clarke, D.M., Fujii, J., Inesi, G., Loo, T.W. & MacLennan, D.H. (1989b) J.Biol.Chem. **264**, 13038-13042

Maruyama, K., Clarke, D.M., Fujii, J., Loo, T.W. & MacLennan, D.H. (1989a) Cell Motil.Cytoskeleton. **14**, 26-34

Maruyama, K. & MacLennan, D.H. (1988) Proc.Natl.Acad.Sci.USA **85**, 3314-3318

Maruyama, T., Cui, Z.J., Kanaji, T., Mikoshiba, K. & Kanno, T. (1997b) Biomed.Res.(Tokyo) **18**, 297-302

Maruyama, T., Kanaji, T., Nakade, S., Kanno, T. & Mikoshiba, K. (1997a) J.Biochem. **122**, 498-505

Mata, A.M., Matthews, I., Tunwell, R.E.A., Sharma, R.P., Lee, A.G. & East, J.M. (1992) Biochem.J. **286**, 567-580

Matheos, D.P., Kingsbury, T.J., Ahsan, U.S. & Cunningham, K.W. (1997) Genes Dev. **11**, 3445-3458

Mathieson (1968) Acta Cryst.Ser. **24**, 1456-1461

Matthews, I., Sharma, R.P., Lee, A.G. & East, J.M. (1990) J.Biol.Chem. **265**, 18737-18740

McCaffery, A.R. (1998) Phil.Trans.Roy.Soc.B **353**, 1735-1750

McEnery, M.W. & Pedersen, P.L. (1986) J.Biol.Chem. **261**, 1745-1752

McGrew, S.G., Wolleben, C., Siegl, P., Inui, M. & Fleischer, S. (1989) Biochemistry **28**, 1686-1691

McIntosh, D.B. (1992) J.Biol.Chem. **267**, 22328-22335

McIntosh, D.B. & Woolley, D.G. (1994) J.Biol.Chem. **269**, 21587-21595

McIntosh, D.B., Woolley, D.G., Vilsen, B. & Andersen, J.P. (1996) J.Biol.Chem. **271**, 25778-25789

Mcpherson, P.S. & Campbell, K.P. (1993) J.Biol.Chem. **268**, 13765-13768

McWhirter, J.M., Gould, G.W., East, J.M. & Lee, A.G. (1987a) Biochem.J. **245**, 713-721

McWhirter, J.M., Gould, G.W., East, J.M. & Lee, A.G. (1987b) Biochem.J. **245**, 731-738

Meissner, G. (1986) J.Biol.Chem. **261**, 6300-6306

Meissner, G. (1994) Ann.Rev.Physiol. **56**, 485-508

Meissner, G., Darling, E. & Eveleth, J. (1986) Biochemistry **25**, 236-244

Melgunov, V.I., Jindal, S. & Belikova, M.P. (1988) FEBS Lett. **227**, 157-160

Michalak, M., Dupraz, P. & Shoshan-Barmatz, V. (1988) Biochim.Biophys.Acta **939**, 587-594

Michelangeli, F., Orlowski, S., Champeil, P., East, J.M. & Lee, A.G. (1990) Biochemistry **29**, 3091-3101

Mikos, G.J. & Snow, T.R. (1987) Biochim.Biophys.Acta **927**, 256-260

Mintz, E. & Guillain, F. (1997) Biochim.Biophys.Acta **1318**, 52-70

Miseta, A., Fu, L., Kellermayer, R., Buckley, J. & Bedwell, D.M. (1999a) J.Biol.Chem. **274**, 5939-5947

Miseta, A., Kellermayer, R., Aiello, D.P., Fu, L. & Bedwell, D.M. (1999b) FEBS Lett. **451**, 132-136

Missiaen, L., Parys, J.B. & De Smet, H. (1998) Biochem.J. **329**, 489-495

Mizuno, K., Nakamura, T., Ohshima, T., Tanaka, S. & Matsuo, H. (1989) Biochem.Biophys.Res.Comm. **159**, 305-311

Moller, J.V., Juul, B. & le Maire, M. (1996) Biochim.Biophys.Acta **1286**, 1-51

Monkawa, T., Miyawaki, A., Sugiyama, T., Yoneshima, H.,Yamamoto-Hino, M., Furuichi, T., Saruta, T., Hasagawa, M., Mikoshiba, K. (1995) J.Biol.Chem. **270**, 14700-14704

Mumberg, D., Müller, R. & Funk, M. (1994) Nucleic.Acids.Res. **22**, 5767-5768

Munro, S. & Pelham, H.R.B. (1987) Cell **48**, 899-907

Murakami, S., Isobe, Y., Kijima, H., Nagai, H., Muramatu, M. & Otomo, S. (1991) Planta Med. **57**, 305-308

Myung, J. & Jencks, W.P. (1991) FEBS Lett. **278**, 35-37

Myung, J. & Jencks, W.P. (1994) Biochemistry **33**, 8775-8785

Myung, J. & Jencks, W.P. (1995) Biochemistry **34**, 3077-3083

Nakade, S., Maeda, N. & Mikoshiba, K. (1991) Biochem.J. **277**, 125-131

Nakomoto, R.K. & Inesi, G. (1984) J.Biol.Chem. **259**, 2961-2970

Nayar, R., Schmid, S.L., Hope, M.J. & Cullis, P.R. (1982) Biochim.Biophys.Acta **688**, 169-176

Nishimura, A., Marita, M., Nishimura, Y. & Sagino, Y. (1990) Nucleic.Acids.Res. **18**, 6169

Noller, K.L. & Fish, C.R. (1974) Med.Clin.North Amr. **58**, 793-810

Norregaard, A., Vilsen, B. & Andersen, J.P. (1993) FEBS Lett. **336**, 248-254

Norregaard, A., Vilsen, B. & Andersen, J.P. (1994) J.Biol.Chem. **269**, 26598-26601

Odermatt, A., Kurzydlowski, K. & MacLennan, D.H. (1996) J.Biol.Chem. **271**, 14206-14213

Odom, A.R., Stahlberg, A., Wente, S.R. & York, J.D. (2000) Science **287**, 2026-2029

Ohya, Y., Kawasaki, H., Suzuki, K., Londesborough, J. & Anraku, Y. (1991) J.Biol.Chem. **266**, 12784-12794

Ohya, Y., Ohsumi, Y. & Anraku, Y. (1986) J.Gen.Microbiol. **132**, 979-988

Okorokov, L.A. & Lehle, L. (1998) FEMS Microbiol.Lett. **162**, 83-91

Okorokov, L.A., Tanner, W. & Lehle, L. (1993) Eur.J.Biochem. **216**, 573-577

Paidhurst, M. & Garrett, S. (1997) Mol.Cell.Biol. **17**, 6339-6347

Palmgren, M.G. & Askerlund, P. (1997) FEBS Lett. **400**, 324-328

Palmgren, M.G. & Axelsen, K.B. (1998) Biochim.Biophys.Acta **1365**, 37-45

Parekh, A.B., Terlau, H. & Stühmer, W. (2001) Nature **364**, 814-818

Parker, I. & Ivorra, I. (1991) J.Physiol.(Lond.) **433**, 229-240

Paschen, W., Doutheil, J., Gissel, C. & Treiman, M. (1996) J.Neurochem. **67**, 1735-1743

Patil, A.O., Wilson, S.R., Curtin, D.Y. & Paul, I.C. (1984) J.Chem.Soc.Perkin.Trans.II. 1107-1110

Penniston, J.T. & Enyedi, A. (1998) J.Membr.Biol. **165**, 101-109

Petithory, J.R. & Jencks, W.P. (1988) Biochemistry **27**, 8626-8635

Pinton, P., Pozzan, T. & Rizzuto, R. (1998) EMBO J. **17**, 5298-5308

Portillo, F., de Larrinoa, I.F. & Serrano, R. (1989) FEBS Lett. **247**, 381-385

Pozos, T.C., Sekler, I. & Cyert, M.S. (1996) Mol.Cell.Biol. **16**, 3730-3741

Putney, J.W. (1986) Cell Calcium **7**, 1-12

Putney, J.W. & Pedrosa Ribeiro, C.M. (2000) Cell.Mol.Life Sci. **57**, 1272-1286

Qi, X.M., He, H.L., Zhong, H.Y. & Distelhorst, C.W. (1997) Oncogene **15**, 1207-1212

Randriamampita, C. & Tsien, R.Y. (1993) Nature **364**, 809-814

Rasmussen, U., Christensen, S.B. & Sandberg, F. (1981) Planta Med. **43**, 336-341

Reis, E.M., Kurtenbach, E., Ferreira, A.R., Biselli, P.J., Slayman, C.W. & Verjovski-Almeida, S. (1999) Biochim.Biophys.Acta **1461**, 83-95

Rice, W.J. & MacLennan, D.H. (1996) J.Biol.Chem. **271**, 31412-31419

Romanos, M.A., Scorer, C.A. & Clare, J.J. (1992) Yeast **8**, 423-488

Rossanese, O.W., Soderholm, J., Bevis, B.J., Sears, I.B., O'Connor, J., Williamson, E.K. & Glick, B.S. (1999) J.Cell Biol. **145**, 69-81

Rudolph, H.K., Antebi, A., Fink, G.R., Buckley, C.M., Dormon, T.E., LeVitre, J., Davidow, L.S., Mao, J. & Moir, D.T. (1989) Cell **58**, 133-145

Sagara, Y., Fernandezbelda, F., de Meis, L. & Inesi, G. (1992b) J.Biol.Chem. **267**, 12606-12613

Sagara, Y. & Inesi, G. (1991) J.Biol.Chem. **266**, 13503-13506

Sagara, Y., Wade, J.B. & Inesi, G. (1992a) J.Biol.Chem. **267**, 1286-1292

Saito, A., Seiler, S., Chu, A. & Fleischer, S. (1984) J.Cell Biol. **99**, 875-885

Sambrook, J.F. (1990) Cell **61**, 197-199

Sayers, L.G., Brown, G.R., Michell, R.H., Michalengeli, F. (1993) Biochem.J. **289**, 883-887

Scherer, N.M. & Ferguson, J.E. (1985) Biochem.Biophys.Res.Comm. **128**, 1064-1070

Schonthal, A., Sugarman, J., Brown, J.H., Hanley, M.R. & Feramisco, J.R. (1991) Proc.Natl.Acad.Sci.USA **88**, 7096-7100

Schreuder, M.P., Mooren, T.A., Toschka, H.Y., Verrips, T. & Klis, F.M. (1996) TIBTECH **14**, 115-120

Scott, T.L. (1985) J.Biol.Chem. **260**, 14421-14423

Serrano, R. (1991) Biochim.Biophys.Acta **1062**, 157-164

Serrano, R., Kielland-Brandt, M.C. & Fink, G.R. (1986) Nature **319**, 689-693

Shigekawa, K. & Dower, W.J. (1988) BioTechniques **6**, 742-751

Short, A.D., Bian, J.H., Ghosh, T.K., Waldron, R.T., Rybak, S.L. & Gill, D.L. (1993) Proc.Natl.Acad.Sci.USA **90**, 4986-4990

Shull, G.E., Clarke, D.M. & Gunteski-Hamblin, A.M. (1992) Ann.N.Y.Acad.Sci. **671**, 70-81

Singh, S. & Aggarwal, B.B. (1995) J.Biol.Chem. **270**, 24995-25000

Simberg, D., Hirsch-Lerner, D., Nissim, R. & Barenholz, Y. (2000) J.Liposome res. **10**, 1-13

Skerjanc, I.S., Clarke, D.M., Loo, T.W. & MacLennan, D.H. (1993a) FEBS Lett. **336**, 168-170

Skerjanc, I.S., Toyofuku, T., Richardson, C. & MacLennan, D.H. (1993b) J.Biol.Chem. **268**, 15944-15950

Smith, J.S., Imagawa, T., Ma, J., Fill, M., Campbell, K.P. & Coronado, R. (1988) J.Gen.Physiol. **92**, 1-26

Smith, P.K., Krohn, R.I., Hermanson, G.T., Mallia, A.K., Gartner, F.H., Provenzano, M.D., Fujimoto, E.K., Goeke, N.M., Olson, B.J. & Klenk, D.C. (1985) Anal.Biochem. **150**, 76-85

Sokolove ,P.M., Albuquerque, E.X., Kauffman, F.C., Spande, T.F., Daly, J.W. (1986) FEBS Lett. **203**, 121-126

Sorin, A., Rosas, G. & Rao, R. (1997) J.Biol.Chem. **272**, 9895-9901

Starling, A.P., East, J.M. & Lee, A.G. (1995) Biochem.J. **310**, 875-879

Starling, A.P., Hughes, G., East, J.M. & Lee, A.G. (1994) Biochemistry **33**, 3023-3031

Stathopoulos, A.M. & Cyert, M.S. (1997) Genes Dev. **11**, 3432-3444

Stefanova, H.I., East, J.M. & Lee, A.G. (1991) Biochim.Biophys.Acta **1064**, 321-328

Stepien, P.P., Brouseau, R., Wu, R., Narang, S. & Thomas, D.Y. (1983) Gene **24**, 289-297

Stokes, D.L. & Green, N.M. (2000) Biophys.J. **78**, 1765-1776

Stokes, D.L., Taylor, W.R. & Green, N.M. (1994) FEBS Lett. **346**, 32-38

Stokes, D.L. & Wagenknecht, T. (2000) Eur.J.Biochem. **267**, 5274-5279

Stolz, L.E., Huynh, C.V., Thorner, J. & York, J.D. (1998) Genetics **148**, 1715-1729

Stoner, G.D. & Mukhtar, H. (1995) J.Cellular Biochem., Supplement **22**, 169-180

Strayle, J., Pozzan, T. & Rudolph, H.K. (1999) EMBO J. **18**, 4733-4743

Striggow, F. & Bohnensack.R. (1994) Eur.J.Biochem. **222**, 229-234

Strock, C., Cavagna, M., Peiffer, W.E., Sumbilla, C., Lewis, D. & Inesi, G. (1998) J.Biol.Chem. **273**, 15104-15109

Sullivan, K.M., Lin, D.D., Agnew, W. & Wilson, K.L. (1995) Proc.Natl.Acad.Sci.USA **92**, 8611-8615

Sumbilla, C., Lu, L., Lewis, D.E., Inesi, G., Ishii, T., Takeyasu, K., Feng, Y. & Fambrough, D.M. (1993) J.Biol.Chem. **268**, 21185-21192

Supply, P., Wach, A., Thinessempoux, D. & Goffeau, A. (1993) J.Biol.Chem. **268**, 19744-19752

Takeshima, H., Nishimura, S., Matsumoto, T., Ishida, H., Kangawa, K., Minamino, N., Matsuo, H., Ueda, M., Hanaoka, M., Hirose, T. & Numa, S. (1989) Nature **339**, 439-445

Talla, E., Mendonça, R.L., Degand, I., Goffeau, A. & Ghislain, M. (1998) J.Biol.Chem. **273**, 27831-27840

Tanida, I., Hasegawa, A., Iida, H., Ohya, Y. & Anraku, Y. (1995) J.Biol.Chem. **270**, 10113-10119

Tanida, I., Takita, Y., Hasegawa, A., Ohya, Y. & Anraku, Y. (1996) FEBS Lett. **379**, 38-42

Tanimura, A., Tojyo, Y. & Turner, R.J. (2000) J.Biol.Chem. **275**, 27488-27493

Taylor, C.W. (1998) Biochim.Biophys.Acta **1436**, 19-33

Taylor, C.W. & Traynor, D. (1995) J.Membr.Biol. **145**, 109-118

Taylor, J.S. & Hattan, D. (1979) J.Biol.Chem. **254**, 4402-4407

Thastrup, O., Cullen, P.J., Drbak, B.K., Hanley, M.R. & Dawson, A.P. (1990) Proc.Natl.Acad.Sci.USA **87**, 2466-2470

Thastrup, O., Dawson, A.P., Scharff, O., Foder, B., Cullen, P.J., Drobak, B.K., Bjerrum, P.J., Christensen, S.B. & Hanley, M.R. (1989) Agents Actions **27**, 17-23

Thomas, A.P. & Delaville, F. (1991) Cellular Calcium: A Practical Approach (McCormack, J.G. & Cobbold, P.H., eds.) Oxford University Press, Oxford

Thomas, M.V. (1991) Cellular Calcium: A Practical Approach (McCormack, J.G. & Cobbold, P.H., eds.) Oxford University Press, Oxford

Torok, K., Trinnaman, B.J. & Green, N.M. (1988) Eur.J.Biochem. **173**, 361-367

Towbin, H., Staehelin, T. & Gordon, J. (1979) Proc.Natl.Acad.Sci.USA **76**, 4350-4354

Toyofuku, T., Kurzydlowski, K., Narayanan, N. & MacLennan, D.H. (1994) J.Biol.Chem. **269**, 26492-26496

Toyoshima, C., Nakasako, M., Nomura, H. & Ogawa, H. (2000) Nature **405**, 647-655

Toyoshima, C., Sasabe, H. & Stokes, D.L. (1993) Nature **362**, 469-471

Treiman, M., Caspersen, C. & Christensen, S.B. (2001) Trends in Pharmacol.Sci. **19**, 131-135

Tsien, R.Y. (1998) Ann.Rev.Biochem. **67**, 509-544

Tsien, R.Y., Pozzan, T. & Rink, T.J. (1982) J.Cell Biol. **94**, 325-334

van Rossum, D.B., Patterson, R.L., Ma, H.-T. & Gill, D.L. (2000) J.Biol.Chem. **275**, 28562-28568

Villalba, J.M., Palmgren, M.G. & Berberiàn, G.E. (1992) J.Biol.Chem. **267**, 12341-12349

Vilsen, B. & Andersen, J.P. (1992) FEBS Lett. **306**, 213-218

Vilsen, B. & Andersen, J.P. (1992) FEBS Lett. **306**, 247-250

Vilsen, B., Andersen, J.P., Clarke, D.M. & MacLennan, D.H. (1989) J.Biol.Chem. **264**, 21024-21030

Wakabayashi, S. & Shigekawa, M. (1990) Biochemistry **29**, 7309-7318

Waldron, R.T., Short, A.D. & Gill, D.L. (1995) J.Biol.Chem. **270**, 11955-11961

Weber, A. (1966) Curr.Top.Bioenerg. **1**, 203-254

Weber, A., Herz, R. & Reiss, I. (1964) Fed.Proc. **23**, 896-900

White, S.H. & Wimley, W.C. (1999) Annu.Rev.Biophys.Biomol.Struc. **28**, 319-365

Wictome, M., Holub, M., East, J.M. & Lee, A.G. (1994) Biochem.Biophys.Res.Comm. **199**, 916-921

Wictome, M., Khan, Y.M., East, J.M. & Lee, A.G. (1995) Biochem.J. **310**, 859-868

Wictome, M., Michelangeli, F., Lee, A.G. & East, J.M. (1992) FEBS Lett. **304**, 109-113

Withee, J.L., Sen, R. & Cyert, M.S. (1998) Genetics **149**, 865-878

Wojcikiewicz, R.J.H. & He, Y. (1995) Biochem.Biophys.Res.Comm. **213**, 334-341

Wojcikiewicz, R.J.H. & Luo, S.G. (1998) J.Biol.Chem. **273**, 5670-5677

Wong, W.L., Brostrom, M.A., Kuznetsov, G. & Gmitter-Yellen, D. (1993) Biochem.J. **289**, 71-79

Wu, J., Kamimura, T., Takeo, T., Suga, S., Wakui, M., Maruyama, T. & Mikoshiba, K. (2000) Mol.Pharmacol. **58**, 1368-1374

Xhou, X.H. & Huang, L. (1994) Biochim.Biophys.Acta **1189**, 195-203

Xu, A., Hawkins, C. & Narayanan, N. (1993) J.Biol.Chem. **268**, 8394-8397

Xu, A. & Narayanan, N. (1999) Biochem.Biophys.Res.Comm. **258**, 66-72

Xu, X., Star, R.A., Tortorici, G. & Muallem, S. (269) J.Biol.Chem. 12645-12653

Yamamoto, H., Imamura, Y., Tagaya, M., Fukui, T. & Kawakita, M. (1989) J.Biochem.(Tokyo) **106**, 1121-1125

Yamasaki, K., Daiho, T., Saino, T. & Kanazawa, T. (1997) J.Biol.Chem. **272**, 30627-30636

Yao, Y., Ferrer-Montiel, A.V., Montal, M. & Tsien, R.Y. (1999) Cell **98**, 475-485

Yazawa, M., Nakashima, K.-I. & Yagi, K. (1999) Mol.Cell.Biochem. **190**, 47-54

Yoko-o, T., Matsui, Y., Yagisawa, H., Nojima, H., Uno, I. & Toh-e, A. (1993) Proc.Natl.Acad.Sci.USA **90**, 1804-1808

Yu, M.H., Zhang, L.L., Rishi, A.K., Khadeer, M., Inesi, G. & Hussain, A. (1998) J.Biol.Chem. **273**, 3546

Yu, X. & Inesi, G. (1995) J.Biol.Chem. **270**, 4361-4367

Zaret, K.S. & Sherman, F. (1982) Cell **28**, 563-573

Zhang, P., Toyoshima, C., Yonekura, K., Green, N.M. & Stokes, D.L. (1998) Nature **392**, 835-839

Zhang, Z., Lewis, D., Strock, C. & Inesi, G. (2000) Biochemistry **39**, 8758-8767

Zhang, Z., Sumbilla, C., Lewis, D., Summers, S., Klein, M.G. & Inesi, G. (1995) J.Biol.Chem. **270**, 16283-16290

Zheng, J. & Ramirez, V.D. (2000) Brit.J.Pharmacol. **130**, 1115-1123

Zhong, L. & Inesi, G. (1998) J.Biol.Chem. **273**, 12994-12998

Zhu, X., Jiang, M. & Birnbaumer, L. (1998) J.Biol.Chem. **273**, 133-142

Zhu, X., Jiang, M., Peyton, M., Boulay, G., Hurst, R. & Stefani, E. (1996) Cell **85**, 661-671

Zucchi, R. & Ronca-Testoni, S. (1997) Pharmacol.Rev. **49**, 1-51